Geomorphic response to neotectonic activity in the Jura Mountains and the southern Upper Rhine Graben

Inauguraldissertation

zur

Erlangung der Würde eines Doktors der Philosophie

vorgelegt der

Philosophisch-Naturwissenschaftlichen Fakultät

der Universität Basel

von

Marielle Fraefel

aus

Uzwil und Wartau (SG), Schweiz

Basel, 2008

Genehmigt von der Philosophisch-Naturwissenschaftlichen Fakultät
auf Antrag von

Prof. Stefan M. Schmid (Fakultätsverantwortlicher)
Geologisch-Paläontologisches Institut
Universität Basel

Prof. Alexander L. Densmore (Korreferent)
Department of Geography
Durham University

Basel, 24. Juni 2008

Prof. Hans-Peter Hauri
Dekan der Philosophisch-Naturwissenschaftlichen Fakultät

Abstract

Present-day tectonic activity at the southern end of the Upper Rhine Graben in central Western Europe is evidenced by significant seismicity, which has been documented over hundreds of years. The hazard that is posed by this activity was violently demonstrated in 1356, when an earthquake with an estimated magnitude of $M_L \approx 6.5$ caused extensive damage to the area of Basel in north-western Switzerland. A sound understanding of the regional tectonic deformation field is a prerequisite for the accurate assessment of this hazard. However, long-term deformation rates in this region are very low. Together with the presence of a network of fault families of different age and orientation, which results from the complex tectonic evolution of this area in the Neogene, this makes the characterisation of the regional deformation field and the identification of active faults difficult. Nevertheless, for a better comprehension of the active tectonic processes in general, and for the assessment of the seismic hazard in this region in particular, an improved understanding of the regional tectonic evolution in the recent geological past is indispensable.

This thesis addresses the recent tectonic history of the Basel area by combining seismological data with an investigation of the geomorphological evidence of tectonic activity. The fact that tectonic activity can be recorded and preserved by the landscape provides an additional source of information that has been little used so far. It offers an opportunity to extend the time-scale of observation from the decades covered by (instrumental) seismologic and geodetic records further into the past. Whereas a wide range of geomorphic features can carry signatures of past tectonic events, the focus in this work is laid on fluvial geomorphology.

The fluvial system in the northern Alpine foreland has been affected by a number of large-scale tectonic events since the late Oligocene. Apart from processes related to the Alpine orogeny and the rifting of the Upper Rhine Graben and Bresse Graben, the evolution of the Jura fold-and-thrust belt, the most external element of the Alpine orogen, dramatically influenced the drainage system. Sedimentary and morphological evidence of former river courses allow further constraining the evolution of the drainage system between the Oligocene and the Quaternary.

The tectonic history in the Quaternary was studied using a quantitative geomorphological approach. On the basis of a digital elevation model, geomorphic indices (steepness and concavity index) were determined to characterise the longitudinal profile for a large number of rivers in the area of the southern Upper Rhine Graben and the eastern Jura fold-and-thrust belt. The spatial

distribution of these indices indicates uplift of a region roughly corresponding to the Jura fold-and-thrust belt, as well as subsidence of the interior parts of the Upper Rhine Graben relative to the Tabular Jura. A morphological analysis of Late Quaternary alluvial terraces in the lower Aare valley, northern Switzerland, was carried out using a high-resolution digital elevation model. The results suggest regional northward tilt during the past 20'000 years, compatible with both a general (isostatic) uplift of the Swiss Molasse basin, and continuing convergence due to ongoing Alpine collision.

The geomorphic data revealed no unambiguous evidence of recent tectonic activity on individual faults. Furthermore, no evidence of recent or ongoing thin-skinned deformation in the Mesozoic sedimentary cover could be identified. The study area at the junction of the Upper Rhine Graben and the Jura fold-and-thrust belt is characterised by a pronouncedly diffuse distribution of deformation, typical for regions where strain is accommodated on inherited tectonic structures. The superposition of large-scale regional uplift and small-scale deformation on individual faults, as well as seismic and aseismic movements, results in a distinct heterogeneity of deformation styles in the northern Alpine foreland.

Table of Content

Chapter 4: Neotectonic activity in north-western Switzerland: Evidence from the study of Late Quaternary alluvial terraces of the river Aare

Chapter 5: Seismotectonics and state of stress in north-western Switzerland: Analysis of natural and induced earthquake focal mechanisms

Chapter 1

Introduction

Most of the deformation of the earth's crust is concentrated at lithospheric plate boundaries. However, the interior of these plates is likewise subjected to deformation, although at much lower rates compared to the plate boundaries themselves. The deformation pattern away from plate boundaries is often difficult to resolve, as long-term strain rates are usually too low to be reliably measured. Correspondingly, the return periods of large earthquakes (M > 6) in continental interiors often range from thousands to tens of thousands of years, making the threat they pose difficult to characterise due to limited historical record lengths. Despite these long time spans involved, considerable stresses can build up and lead to devastating earthquakes such as in New Madrid (1812), in the interior of the North American plate (Johnston and Schweig, 1996), and in Bhuj (Gujarat, India) in 2001 (Gupta et al., 2001).

In intraplate tectonic environments, the reactivation of pre-existing structures often plays an important role in the accommodation of tectonic deformation. This fact, combined with generally low deformation rates, frequently leads to diffuse – rather than localized – deformation, and faults rupturing through to the surface are less common compared to other tectonic environments. For this reason, standard neotectonic methods, such as trench analyses or GPS measurements, are often of little help to decipher recent and current tectonic activity and deformation rates of these regions.

In order to characterise the deformation patterns of low deformation-rate tectonic domains, and to advance the assessment of the seismic hazards in these areas, the results from different methods – such as geodetic measurements or seismotectonic analyses – have to be combined and complemented by alternative approaches. One method that has proven particularly useful in the past few years is the study of landforms. Landforms are sensitive to active tectonics, and quantitative investigation of landscape shape can provide information about deformation patterns (Burbank and Anderson, 2001). The use of geomorphic indices allows the objective comparison of landforms.

The geomorphological analysis of fluvial systems is particularly informative. Rivers respond very sensitively to along-channel gradient changes resulting from vertical tectonic deformation. Often,
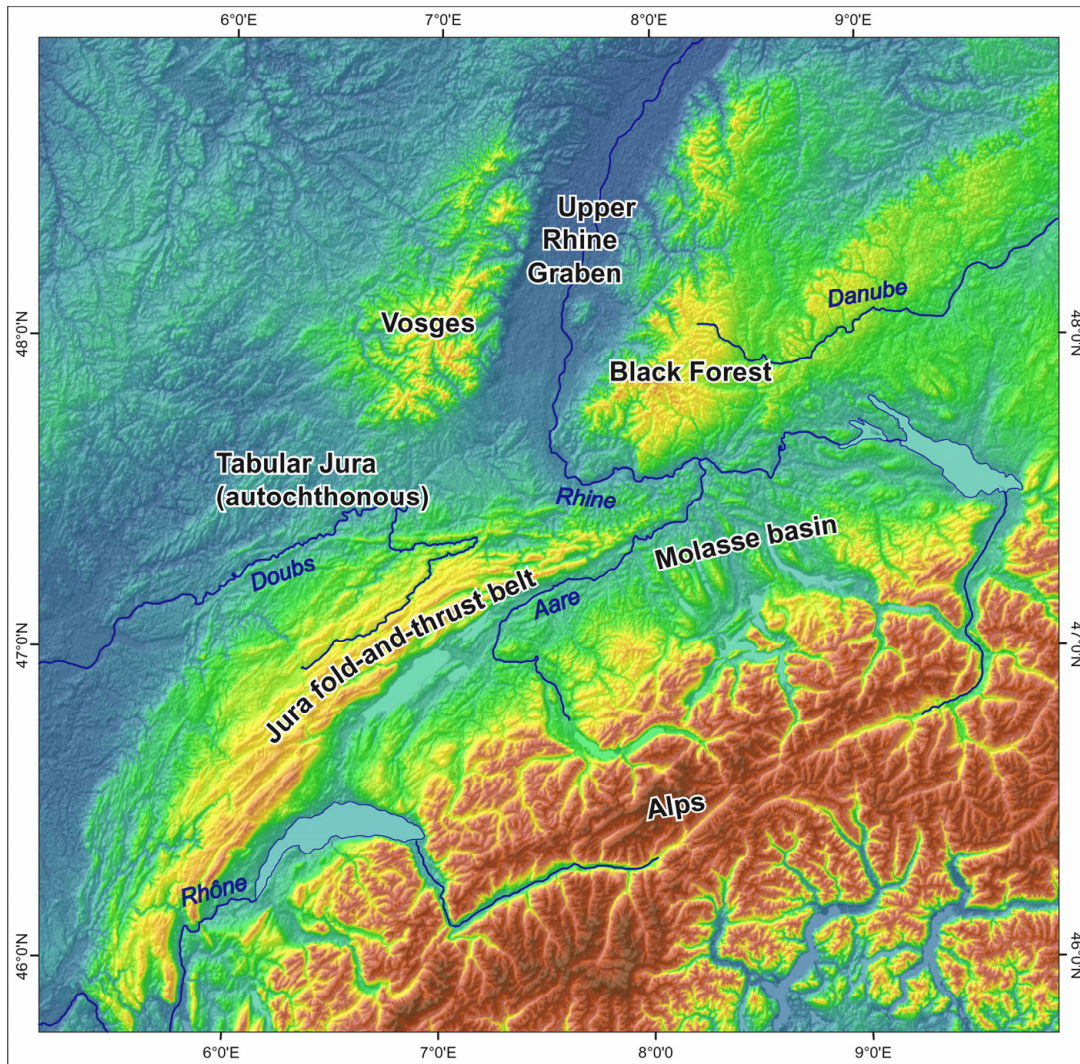
Figure 1: Overview of the topographic and tectonic situation in the study area in central Western Europe (NW Switzerland), based on SRTM data.

these riverbed adjustments leave their marks in the landscape and may still be visible after long periods of time (Holbrook and Schumm, 1999).

This thesis addresses the recent tectonic activity of the Basel area in NW Switzerland. The Basel area is characterised by its location at the touchpoint of the Upper Rhine Graben rift area and the most external parts of the continental collision zone of the Alps (Figure 1). It was here that the largest known earthquake in central Western Europe, a magnitude ~6.5 shock, occurred in 1356 (Meyer et al., 1994). Although the seismic activity of this area is proven, an understanding of the recent and current deformation is difficult to establish, as large earthquakes are rare, and geodetic measurements indicate very low present-day deformation rates of less than 1 mm/a (Schlatter, 2006). In order to better constrain the recent and current regional deformation pattern, and to localise recently active tectonic structures, various geomorphological methods are integrated and

combined with information about the present-day stress field derived from seismological data in this thesis.

In the following, a brief summary of the Cenozoic tectonic evolution of the study area is provided, and the approaches followed in the different chapters are outlined.

1.1 Tectonic evolution of the study area in the Paleogene and Neogene

The Cenozoic tectonic history of the study area in the northern foreland of the Alps was dominated by two main tectonic events: the main phase of the Alpine orogeny (Late Eocene to Miocene), and the formation of the Upper Rhine Graben during the Oligocene. The Upper Rhine Graben forms part of the European Cenozoic Rift System, which extends across the continent from the Mediterranean Sea to the North Sea (Ziegler, 1992; Dèzes et al., 2004). Its orientation and timing of formation indicate an approximately E-W oriented minimum stress during the Oligocene. The rift zone of the Upper Rhine Graben is continued to the northwest by the Lower Rhine Graben, and to the southwest by the Bresse Graben, to which it is linked by the Rhine-Bresse Transfer Zone (Lacombe et al., 1993; Madritsch et al., 2008 (accepted)). The location and orientation of the faults of the Rhine-Bresse Transfer Zone are probably controlled by a ca. WSW-ENE trending, Late Paleozoic basement trough system, which extends from the Bresse Graben in the west to the Lake Constance area in the east, and seems to be transpressionally reactivated in the current stress field (Diebold and Noack, 1996; Ustaszewski, 2004).

At its southern end, the sedimentary infill of the Upper Rhine Graben borders the Lower Triassic to Upper Jurassic sediments of the Jura region (Figure 2). This sedimentary cover was partly detached from its Palaeozoic basement during the latest stages of the Alpine orogeny in the Miocene–Pliocene, forming the Jura fold-and-thrust belt (Laubscher, 1961; Burkhard, 1990). The overall transport direction of the Jura fold-and-thrust belt indicates a major change in the regional stress field from E-W extension to NW-SE compression associated with convergence in the Alps. Time constraints on the beginning of the Jura fold-and-thrust belt formation are provided by sediments that were either included in the folding process (Juranagelfluh and Bois de Raube conglomerates, 14.5 – 9.8 Ma (Kälin, 1997)), or were overridden by external thrusts in the Bresse Graben (Chauve et al., 1988). Due to a general lack of younger sediments, time constraints on the evolution of the Jura fold-and-thrust belt after the Late Miocene are sparse. Folding of Pliocene fluvial gravels in the Ajoie region of eastern France (Giamboni et al., 2004) indicates that contractional deformation continued at least until the Late Pliocene. The deformation style, however, appears to be no longer predominantly controlled by thin-skinned decollement, but by transpressional faulting involving the crystalline basement (Ustaszewski and Schmid, 2007).
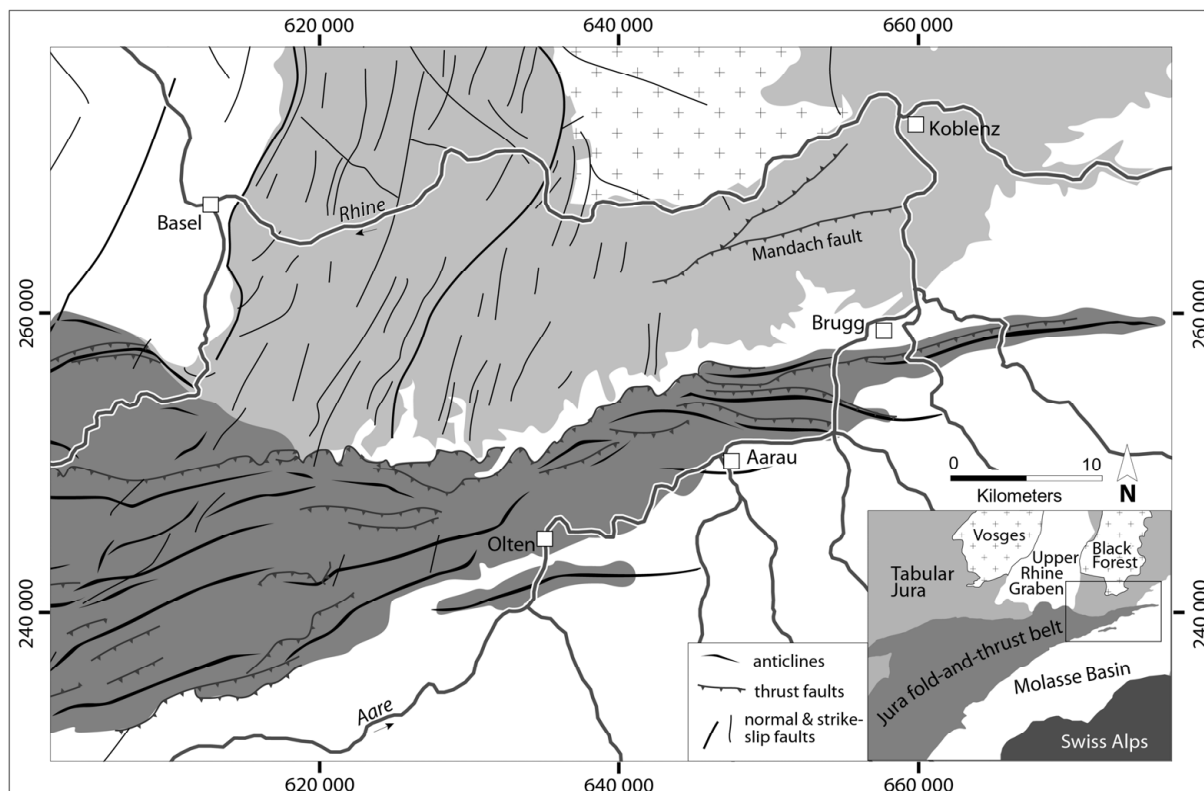
Figure 2: Main tectonic elements and drainage system in north-western Switzerland.

1.2 Quaternary tectonic activity in NW Switzerland

The Quaternary tectonic activity in north-western Switzerland after ca. 5 Ma is not very well resolved. This is mainly the result of a major hiatus in the sedimentary record of the northern Alpine foreland. After the deposition of the youngest preserved Molasse units (Upper Freshwater Molasse, OSM) at around 11-12 Ma (Bolliger, 1998; Rahn and Selbekk, 2007), an overall erosional regime largely prevented the deposition or preservation of younger sediments over wide areas in northern Switzerland. Cederbom et al. (2004) estimated that since ca. 5 Ma, at least 1 km of sediments has been eroded in the northern Alpine foreland, based on fission-track data indicating erosional cooling. Younger sediments are preserved only from the beginning of the Quaternary, when repeated climatic changes with glacials and interglacials led to enhanced erosion in the Alps and the deposition of glacio-fluvial sediments in the northern Alpine foreland (Müller et al., 2002). Few age constraints are available for either the Upper Freshwater Molasse and the Quaternary sediments due to their coarse-grained composition, which makes the preservation of datable fossils unlikely, and the application of dating techniques like optically stimulated luminescence (OSL) difficult.

A complete sequence of Quaternary sediments is found in the Upper Rhine Graben, indicating progressive subsidence during this time period (Bartz, 1974). Outside the Upper Rhine Graben, however, the fluvial Quaternary sediments are very discontinuous (Penck and Brückner, 1909; Wittmann, 1961; Graul, 1962). Nevertheless, they have been investigated in a number of studies dealing with neotectonics in NW Switzerland. For instance, Graf (1993) studied gravels of the Higher Cover Gravels unit (~2 Ma) of Alpine origin that lie north of the topographic high formed by the Mandach thrust fault, suggesting that this north-vergent fault was active in the Pleistocene. A number of studies address the relatively well-preserved late Quaternary terrace systems (Low Terrace Gravels) of the rivers Rhine and Aare (Haldimann et al., 1984; Verderber, 2003), pointing to possible recent tectonic deformation. However, the young age (ca. 20 ka) of these sediments (Bitterli et al., 2000), in combination with the low tectonic deformation rates, has so far not allowed for a characterisation of the regional deformation pattern or for the delineation of active structures based on deformation features of these deposits.

1.3 Seismological and geodetic evidence

Present-day tectonic activity in the area of the Upper Rhine Graben and the eastern Jura mountains is mainly manifest from the earthquake record and geodetic measurements. Although seismicity has been monitored in all of the tectonic units in this region, it is clearly concentrated at the eastern border of the Upper Rhine Graben and in the Jura mountains to the south of it (Bonjer, 1997). The majority of the focal mechanisms indicate strike-slip deformation; pure and oblique normal faulting also occur. Thrust faulting events are rare. Due to the uncertainty of the hypocentre locations, and the large number of pre-existing faults in the area, seismic activity can usually not be attributed to a particular fault. This is also true for the largest earthquake known in this area, the 1356 Basel event (Meyer et al., 1994). The regional stress field in the northern Alpine foreland has been investigated using focal mechanisms (Kastrup et al., 2004) and borehole breakouts (Becker, 2000), yielding a maximum horizontal stress axis orientation of NW-SE in the crystalline basement, and NNW-SSE to N-S in the sedimentary cover of the Jura mountains.

Geodetic constraints on the present-day deformation pattern mainly come from precise-levelling measurement campaigns. Precise levelling has been carried out in Switzerland for a period of ca. 100 years. The results suggest uplift in the area of the Folded Jura relative to the Tabular Jura, and a tendency to regional uplift of the southern parts of the Alpine foreland compared to the northern parts (Müller et al., 2002; Schlatter, 2006). Geodetic measurements across the eastern Main Boundary Fault of the Upper Rhine Graben point to ongoing subsidence of the Graben relative to the Graben shoulder (Zippelt and Dierks, 2007), an observation that is

confirmed by morphological studies in the Freiburg area (Niviere et al., 2008). However, the measurement uncertainties are still very large compared to the deformation rates, and a consistent deformation pattern cannot be distinguished. Likewise, the record of GPS measurements of this area covers ca. 20 years only, and does not yet yield horizontal deformation values above the measurement uncertainties (Rózsa et al., 2005). However, it does allow constraining the horizontal deformation rates to below 1 mm/a.

1.4 Open questions and approach of this study

Despite in-depth analysis of data from different sources, the tectonic deformation pattern in the boundary area of the Jura fold-and-thrust belt, the Tabular Jura, and the Upper Rhine Graben is not yet well understood. In particular, the question as to whether the observed vertical deformations can be attributed to regional uplift or local tectonic processes remains open.

In an attempt to extend the time-scale of observation from the decades covered by instrumental seismology and geodetic measurements into Late Quaternary times, this thesis applies a geomorphological approach to study the effect of tectonic deformation on the landscape in north-western Switzerland. While investigating the shape of different landforms has always been an important part of neotectonic studies, the technological advancements of the past decades have revolutionised this field. GPS measurements, precise levelling data over long time periods, radar interferometry, and laser altimetry now allow the quantitative characterisation and comparison of landforms, especially in combination with geographic information systems (GIS). By integrating this information with knowledge about the different landscape-shaping processes, the effects of tectonic activity may be distinguished from other influences on the landscape (such as resistance to erosion) and further the understanding of the recent tectonic deformation pattern.

1.5 Thesis organisation

In this thesis, the interactions between tectonic activity and the fluvial system in NW Switzerland are investigated on different time scales.

On the largest temporal and spatial scale covered here, the response of the drainage system to the evolution of the Jura fold-and-thrust belt and the Upper Rhine Graben is studied (**Chapter 2**). In the Miocene and Pliocene, the evolution of the Jura fold-and-thrust belt created a new watershed that had a dramatic impact on the drainage system of the northern Alpine foreland. The sediments deposited by different rivers during that period are used to determine the flow patterns at different

times. This information is complemented by the analysis of fluvial landforms, in particular wind and water gaps created by rivers cutting through growing anticlines, and incised river channels in general. Chapter 2 presents a synthesis of a large number of previous studies, embeds new morphological data into the existing concept, and proposes a new interpretation of the drainage system evolution of this tectonically complex area from the Oligocene to the Quaternary. *This chapter has been submitted to the Swiss Journal of Geosciences, with P.A. Ziegler as first author and M. Fraefel as second author. The first author proposed the concept of the study, carried out most of the literature review and wrote the manuscript. The second author provided all illustrations and substantially contributed to the manuscript with discussions and revisions.*

Because rivers respond to vertical deformation, systematic mapping of river gradients – for individual rivers as well as groups of rivers – allows the delineation of zones of varying uplift. This effect of tectonic activity on the drainage system is studied in **Chapter 3**. 50 rivers are analysed in the boundary area of the tectonic units of the Jura fold-and-thrust belt, the Tabular Jura and the Upper Rhine Graben. Geomorphic indices (steepness index and concavity index) are determined to make quantitative comparison of river characteristics possible. These studies are combined with geological field investigations in order to distinguish tectonic from lithologic influences on river gradients. *This chapter represents a manuscript in preparation for submission, with M. Fraefel as first author and A.L. Densmore as second author. The first author developed the concept of the study and performed all necessary DEM (digital elevation model) analyses, data processing and field investigations herself. She also wrote the manuscript. The second author provided scientific advice and support with the interpretation of the results and the writing.*

Chapter 4 presents a morphological study of the alluvial terraces of one of the largest rivers in northern Switzerland. By incision, the river Aare has formed a fluvial terrace system in the course of the Quaternary. The youngest and lowest unit of these deposits is relatively well preserved (Niederterrasse, or Low Terrace Gravels). The terrace treads represent former river bed positions, acting as "markers" for tectonic deformation. Using the altitude information from a high-resolution (2 m) digital elevation model, the occurrence and 3D orientation of the terrace surfaces are analysed for signs of tectonic activity in the time period spanning the last ca. 20 ka since the deposition of the Low Terrace Gravels.

To characterise the present-day state of stress in the lithosphere of the study area and determine on which fault sets deformation most probably occurs, the seismological record in the wider study area is investigated (**Chapter 5**). Focal mechanisms from a set of 115 earthquakes between 1961 and 2006 are analysed using the Right-Dihedra method and compared to a series of earthquakes that were induced by the stimulation of a geothermal reservoir in 2006/2007. Apart from the investigation of the mean regional stress field, different subsets of the data set are analysed individually in order to find spatial stress field variations.

References

Bartz, J., 1974. Die Mächtigkeit des Quartärs im Oberrheingraben. Approaches to Taphrogenesis; The Rhinegraben; geologic history and neotectonic activity: 78-87.

Becker, A., 2000. The Jura Mountains - An active foreland fold-and-thrust belt? Tectonophysics, 321(4): 381-406.

Bitterli, T., Graf, H.R., Matousek, F. and Wanner, M., 2000. Geologischer Atlas der Schweiz: Zurzach (Blatt 1050), Erläuterungen. Bundesamt f. Wasser u. Geologie. Bern, Switzerland.

Bolliger, T., 1998. Age and geographic distribution of the youngest Upper Freshwater Molasse (OSM) of eastern Switzerland. Eclogae Geologicae Helvetiae, 91: 321-332.

Bonjer, K.P., 1997. Seismicity pattern and style of seismic faulting at the eastern borderfault of the southern Rhine Graben. Tectonophysics, 275(1-3): 41-69.

Burbank, D.W. and Anderson, R.S., 2001. Tectonic Geomorphology. Blackwell Science.

Burkhard, M., 1990. Aspects of the large-scale Miocene deformation in the most external part of the Swiss Alps (Subalpine Molasse to Jura fold belt). Eclogae Geologicae Helvetiae, 83(3): 559-583.

Cederbom, C.E., Sinclair, H.D., Schlunegger, F. and Rahn, M.K., 2004. Climate-induced rebound and exhumation of the European Alps. Geology, 32(8): 709-712.

Chauve, P., Martin, J., Petitjean, E. and Sequeiros, F., 1988. Le chevauchement du Jura sur la Bresse. Données nouvelles et réinterpretation des sondages. Bull. Soc. géol. France, 8(4): 861-870.

Dèzes, P., Schmid, S.M. and Ziegler, P.A., 2004. Evolution of the European Cenozoic rift system; interaction of the Alpine and Pyrenean orogens with their foreland lithosphere. Tectonophysics, 389(1-2): 1-33.

Diebold, P. and Noack, T., 1996. Late Palaeozoic troughs and Tertiary structures in the eastern Folded Jura. In: O.A. Pfiffner, P. Lehner, P. Heitzmann, S. Mueller and A. Steck (Editors), Deep structure of the Swiss Alps; results of NRP 20. Birkhäuser, Basel, Switzerland, pp. 59-63.

Giamboni, M., Ustaszewski, K., Schmid, S.M., Schumacher, M.E. and Wetzel, A., 2004. Plio-Pleistocene transpressional reactivation of Paleozoic and Paleogene structures in the Rhine-Bresse transform zone (northern Switzerland and eastern France). International Journal of Earth Sciences, 93(2): 207-223.

Graf, H.R., 1993. Die Deckenschotter der zentralen Nordschweiz. PhD Thesis, ETH Zürich, Zürich.

Graul, H., 1962. Geomorphologische Studien zum Jungquartär des nördlichen Alpenvorlandes. Teil 1: Das Schweizer Mittelland. Heidelberger Geographische Arbeiten, Heft 9.

Gupta, H.K. et al., 2001. Bhuj earthquake of 26 January, 2001. Journal of the Geological Society of India, 57(3): 275-278.

Haldimann, P., Naef, H. and Schmassmann, H., 1984. Fluviatile Erosions- und Akkumulationsformen als Indizien jungpleistozäner und holozäner Bewegungen in der Nordschweiz und angrenzenden Gebieten. Nagra Technischer Bericht, 84-16.

Holbrook, J. and Schumm, S.A., 1999. Geomorphic and sedimentary response of rivers to tectonic deformation: a brief review and critique of a tool for recognizing subtle epeirogenic deformation in modern and ancient settings. Tectonophysics, 305: 287-306.

Johnston, A.C. and Schweig, E.S., 1996. The enigma of the New Madrid earthquakes of 1811-1812. Annual Review of Earth and Planetary Sciences, 24: 339-384.

Kälin, D., 1997. Litho- und Biostratigraphie der mittel- bis obermiozänen Bois de Raube-Formation (Nordwestschweiz). Eclogae Geologicae Helvetiae, 90(1): 97-114.

Kastrup, U. et al., 2004. Stress field variations in the Swiss Alps and the northern Alpine foreland derived from inversion of fault plane solutions. Journal of Geophysical Research-Solid Earth, 109(B1).

Lacombe, O., Angelier, J., Byrne, D. and Dupin, J.M., 1993. Eocene-Oligocene Tectonics and Kinematics of the Rhine-Saone Continental Transform Zone (Eastern France). Tectonics, 12(4): 874-888.

Laubscher, H., 1961. Die Fernschubhypothese der Jurafaltung. Eclogae geologicae Helvetiae, 54: 221-282.

Madritsch, H., Schmid, S.M. and Fabbri, O., 2008 (accepted). Interactions of thin- and thick-skinned tectonics along the northwestern front of the Jura fold-and-thrust-belt (Eastern France). Tectonics.

Meyer, B., Lacassin, R., Brulhet, J. and Mouroux, B., 1994. The Basel 1356 earthquake: which fault produced it? Terra Nova, 6: 54-63.

Müller, W.H., Naef, H. and Graf, H.R., 2002. Geologische Entwicklung der Nordschweiz, Neotektonik und Langzeitszenarien Zürcher Weinland. Nagra Technischer Bericht, 99-08.

Niviere, B. et al., 2008. Active tectonics of the southeastern Upper Rhine graben, Freiburg area (Germany). Quaternary Science Reviews, 27(5-6): 541-555.

Penck, A. and Brückner, E., 1909. Die Alpen im Eiszeitalter. Band 2: Die Eiszeiten in den nördlichen Westalpen.

Rahn, M.K. and Selbekk, R., 2007. Absolute dating of the youngest sediments of the Swiss Molasse basin by apatite fission track analysis. Swiss Journal of Geosciences, 100(3): 371-381.

Rózsa, S. et al., 2005. Determination of displacements in the upper Rhine graben Area from GPS and leveling data. International Journal of Earth Sciences, 94(4): 538-549.

Schlatter, A., 2006. Das neue Landeshöhennetz der Schweiz LHN95. PhD Thesis, Diss Nr. 16840, ETH Zürich, Zürich.

Ustaszewski, K. and Schmid, S.M., 2007. Latest Pliocene to recent thick-skinned tectonics at the Upper Rhine Graben - Jura Mountains junction. Swiss Journal of Geosciences, 100(2): 293-312.

Ustaszewski, K.M., 2004. Reactivation of pre-existing crustal discontinuities: the southern Upper Rhine Graben and the northern Jura Mountains: a natural laboratory PhD Thesis, University of Basel.

Verderber, R., 2003. Quartärgeologie im Hochrheingebiet zwischen Schaffhausen und Basel. Zeitschrift der Deutschen Gesellschaft für Geowissenschaften, 154(2-3): 369-406.

Wittmann, O., 1961. Die Niederterrassenfelder im Umkreis von Basel und ihre kartographische Darstellung. Basler Beiträge zur Geographie und Ethnologie, 3.

Ziegler, P.A., 1992. European Cenozoic rift system. Tectonophysics, 208(1-3): 91-111.

Zippelt, K. and Dierks, O., 2007. Auswertung von wiederholten Präzisionsnivellements im südlichen Schwarzwald, Bodenseeraum sowie in angrenzenden schweizerischen Landesteilen. Nagra Arbeitsbericht NAB 07-27.

Chapter 2

Response of drainage systems to Neogene evolution of the Jura fold-thrust belt and Upper Rhine Graben

Peter A. Ziegler and Marielle Fraefel

submitted to Swiss Journal of Geosciences

Abstract

The eastern Jura Mountains consist of the Jura fold-thrust belt and the autochthonous Tabular Jura and Vesoul-Montbéliard Platform. They are drained by the river Rhine, which flows into the North Sea, and the river Doubs, which flows into the Mediterranean. The internal drainage systems of the Jura fold-thrust belt consist of rivers flowing in synclinal valleys that are linked by river segments cutting orthogonally through anticlines. The latter appear to employ parts of the antecedent Jura Nagelfluh drainage system that had developed in response to Late Burdigalian uplift of the Vosges-Back Forest Arch, prior to Late Miocene-Pliocene deformation of the Jura fold-thrust belt.

The following stages are recognized in the evolution of the Jura Mountain drainage systems: 1) middle to late Tortonian (10-7.2 Ma) folding-related overpowering and partial reversal of the south-directed Jura Nagelfluh drainage system, 2) Messinian to early Pliocene (7.2-4.2 Ma) Aare-Danube and proto-Doubs stage, 3) early to middle Pliocene (4.2-2.9 Ma) Aare-Doubs stage, 4) late Pliocene to early Quaternary (2.9-1.7 Ma) Aare-Rhine and Doubs stage and 5) Quaternary (1.7-0 Ma) Alpine-Rhine and Doubs stage.

Development of the thin-skinned Jura fold-thrust belt controlled the first three stages of this drainage system evolution, whilst the last two stages were essentially governed by the subsidence of the Upper Rhine Graben, which resumed during the late Pliocene. Late Pliocene and Quaternary deep incision of the Aare-Rhine/Alpine-Rhine and its tributaries in the Jura Mountains and Black Forest is mainly attributed to lowering of the erosional base level in the continuously subsiding Upper Rhine Graben. Incision of the Doubs and Dessoubre canyons reflects uplift of the Franches-Montagnes and Franche-Comté in response to thick-skinned deformation of the Jura fold-thrust belt, which had commenced around 3 Ma.

Geodetic data indicate that uplift of the Jura Mountains, relative to the Tabular Jura, presently continues at very low strain rates whilst the Upper Rhine Graben subsides very slowly and the Black Forest is relatively stable.

2.1 Introduction

The Jura fold-thrust belt (JFTB), forming the core of the Jura Mountains, is the youngest and most external element of the Central Alpine orogenic system. It has accounted for up to 30 km of essentially thin-skinned shortening since late Miocene times (Laubscher, 1961; 1992; Philippe et al., 1996; Affolter and Gratier, 2004) and is still seismotectonically active (Becker, 2000; Lacombe and Mouthereau, 2002; Edel et al., 2006). The JFTB is flanked to the SE by the flexural Swiss Molasse foreland basin of the Alps whilst its most external elements encroach on the Bresse and Upper Rhine grabens (Figure 1; Chauve et al., 1980; Dèzes et al., 2004).

Evolution of the JFTB combined with the development of the Upper Rhine Graben (URG) and the Bresse Graben, exerted strong control on the location of the repeatedly shifting watersheds between the rivers Danube, Doubs and Rhine, which flow into the Black Sea, the Mediterranean and the North Sea, respectively. Numerous studies have addressed the evolution of the headwaters of these major drainage systems and the underlying tectonic processes (Liniger, 1966; 1967; Hofmann, 1996; Petit et al., 1996; Villinger, 1998; Kuhlemann and Kempf, 2002; Müller et al., 2002; Berger et al., 2005a; Ziegler and Dèzes, 2007), or have analyzed neotectonic deformation controlling drainage pattern changes at the boundary between the Jura Mountains and the URG (Giamboni et al., 2004a; Giamboni et al., 2004b; Braillard, 2006). However, only few studies have addressed the development of drainage systems within the JFTB (Heim, 1919; Liniger, 1953; 1966; Laubscher, 1967).

In an effort to further constrain the evolution of the JFTB and its drainage systems, this paper builds on a literature review, including the pioneering work of Liniger (1953; 1966; 1967) and Laubscher (1981; 1986; 1992), and presents a morphotectonic analysis of the drainage system. In particular, we studied the distribution of water and wind gaps (Figure 2), considered as vestiges of antecedent rivers, and classified the different river segments, according to their history (Figure 3). In this context it is important to note that the pre-orogenic sedimentary record of the JFTB and its surroundings ends in Serravallian to early Tortonian times. On the other hand, its late syn-deformational sedimentary record is restricted to its northern deformation front where it commences in the late Early Pliocene (Berger et al., 2005a; Berger et al., 2005b). As sediments of mid-Tortonian to mid-Quaternary age are missing within the JFTB, we had to use geomorphologic criteria to further constrain its structural evolution and the development of its
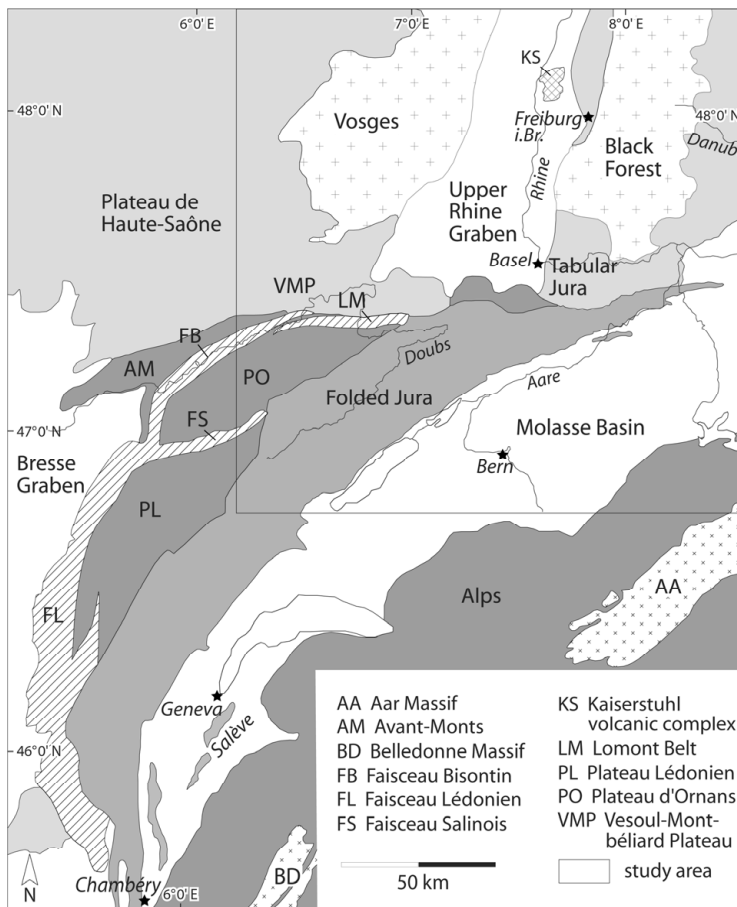
Figure 1: Tectonic map of NW Switzerland and adjacent areas (after Ustaszewski (2004) and Chauve et al. (1980)).

drainage systems. In addition, we compared indications for neotectonic activity with the results of geodetic surveys.

2.2 Geological and topographic setting of the area addressed

The main morpho-tectonic units of the Eastern Jura Mountains and their French and German foreland comprise the JFTB, which was activated during the Late Miocene, the Tabular Jura on the southern slopes of Black Forest basement arch, the Upper Rhine Graben (URG) into which the Mulhouse High projects, and on the southern slopes of the Vosges basement arch the Vesoul-Montbéliard Plateau, which grades NW-ward into the Haute Plateau de Saône (Figures 1 and 2). The JFTB and the undeformed Tabular Jura underlie the high topography of the Eastern Jura Mountains. The width of the essentially thin-skinned JFTB decreases from 60 km in its western parts to zero at its eastern termination. In its western, widest parts the JFTB accounts for 25-30 km shortening. This value decreases eastward to 13 km and 7 km in the Delémont and Aarau
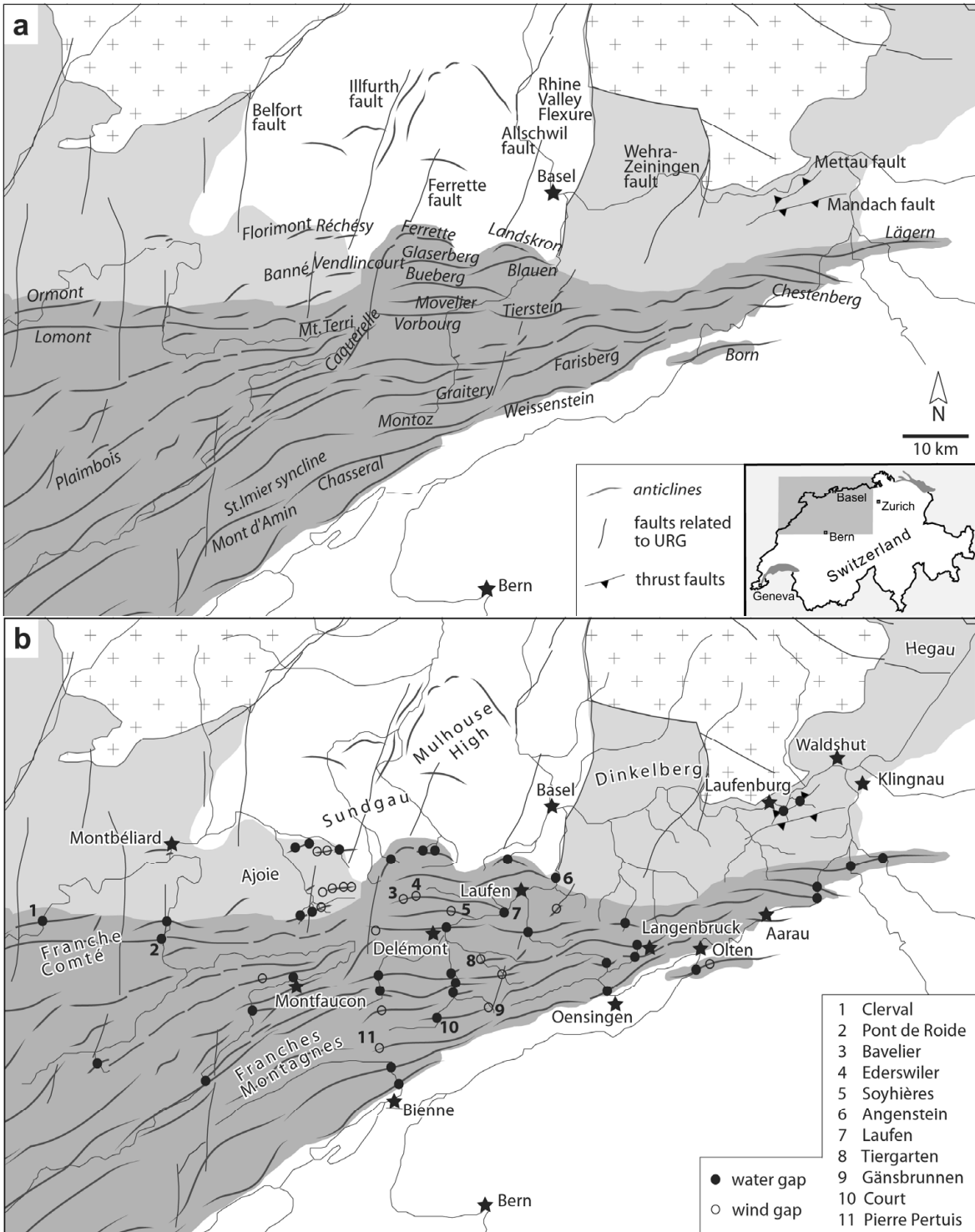
Figure 2a: Main tectonic elements of the study area. Crosses: outcropping basement, light grey: Tabular Jura and equivalents, dark grey: Jura fold-thrust belt, white: Cenozoic sedimentary basins.

Figure 2b: Prominent water and wind gaps of the study area. Same legend as 2a.

transects, respectively, and to 1 km in the Lägern anticline (Philippe et al., 1996; Affolter and Gratier, 2004).

East of the city of Olten, the JFTB consists of a 5-8 km wide stack of thrust sheets and thrusted anticlines, tapering to zero at the eastern end of the Lägern anticline, and attains elevations of up to 950 m (Figure 2). West of Olten, the JFTB broadens to 38 km, advances to the southern margin of the URG and is dominated by flexural-slip and thrust-faulted anticlines and broad synclines. Synclinal valleys and anticlinal ridges dominate the morphology of this province. Ridges attain elevations of up to 1300 m along the southern, internal margin of this province, and decrease in its northern, external parts to 800 m and less. This valley-and-ridge province grades westward into the undulating and gently north-sloping up to 1000 m high plateau of the Franches-Montagnes and Franche-Comté. This plateau is flanked to the south by the deep, synclinal St. Imier valley and the 1500 m high Mont d'Amin-Chasseral anticline, and to the north by the frontal Lomont and Ormont anticlines, thus accounting for a total fold-belt width of 60 km. Main topographic features of the Franches-Montagnes and Franche-Comté are the deeply incised canyons of the rivers Doubs and Dessoubre (Figure 3).

In the foreland of the JFTB, to the east of Basel, monoclinally south-dipping Jurassic and Triassic sediments underlie the Tabular Jura. These are progressively eroded as they rise towards the Black Forest in which the crystalline basement is exposed. The western part of this monocline is transected by an array of mainly NNE-SSW striking normal faults that form part of the URG extensional system, whereas its eastern part is disrupted by the Mandach and Mettau thrusts (Müller et al., 2002; Laubscher, 2003; Diebold et al., 2006). Similar to the Tabular Jura, the rather low lying Vesoul-Montbéliard Plateau, which flanks the Vosges to the south, is also underlain by gently south-dipping Triassic and Jurassic sediments transected by N-S to NNE-SSW striking normal faults. The URG consists of several rotational fault blocks that are delimited by NNE-SSW striking, west-dipping normal faults, such as the Allschwil, Ferrette and Illfurth faults (Giamboni et al., 2004b; Ustaszewski, 2004; Hinsken et al., 2007). The Rhine Valley Flexure marks the eastern margin of the morphologically expressed URG and bounds the Tabular Jura to the west (Figure 2).

The evolution of these tectonic elements had a strong bearing on the development of the drainage systems in the study area. In the following section we address the configuration of the present-day drainage systems of the Jura Mountains before discussing their step-wise evolution in sections 4 to 8.

2.3 Morphotectonic analysis of the modern drainage systems of the Jura Mountains

The modern drainage systems of the Eastern Jura Mountains consists of (i) rivers draining southward into the river Aare, which flows NE along the southern margin of the Jura Mountains

and joins the Rhine near Waldshut, (ii) rivers flowing north into the Rhine, which debouches into the North Sea, and (iii) the river Doubs, which flows into the Saône and ultimately joins the river Rhône, which flows into the western Mediterranean (Figure 3).

A large number of tributaries to these rivers, as well as the Aare and Doubs rivers themselves, cut more or less perpendicularly through anticlines and in some cases through thrust-controlled structures. We systematically mapped these breaches and assigned them to water gaps, if a major river occupies the gap today, or to wind gaps, if a well developed breach is not occupied by a significant river. These gaps (Klusen) are interpreted as evidence of antecedent river courses that predate development of the JFTB.

The distribution of these features is summarized in Figure 2b. Important water gaps occur particularly in the valley-and-ridge province of the JFTB, which is characterized by a trellis-type drainage pattern consisting of synclinal river valleys, linked by water gaps. Interestingly, the external Glaserberg and Blauen Anticlines of the valley-and-ridge province are not cut by wind or water gaps, whilst the frontal Florimont, Réchesy, Banné, Vendlincourt, Ferrette and Landskron anticlines are breached by gaps related to northward flowing rivers. The rivers Doubs and Dessoubre of the Franches-Montagnes and Franche-Comté are prominent examples of entrenched meandering streams that wind through synclinal valleys and a number of water gaps.

In the Tabular Jura, a dendritic drainage pattern dominates. However, some of the long, north-directed valleys of Rhine tributaries (e.g. Frenke) are aligned with NNE-SSW striking Rhine Graben-related faults. In the easternmost Jura Mountains, the external Mettau thrust is cut by water gaps whilst the Mandach thrust element to the south forms a prominent local drainage divide.

Based on the distribution of water and wind gaps, and in the context of the tectonic evolution of the study area, we have classified the rivers of the Jura Mountain drainage systems (Figure 3), according to their history, into different categories, applying the classification schemes of Skinner and Porter (1995) and Twidale (2004). Accordingly, we assigned the rivers or river segments of the study area to one of the following groups:

Consequent: Rivers following the slope of a newly uplifted land mass

Insequent: Dendritic pattern of tributaries developing by random headward erosion little influenced by the structure and lithology of incised strata

Antecedent: Rivers maintaining their initial course across a land mass or fold that is uplifted across their path, rather than flowing around it

Subsequent: Rivers flowing in structurally controlled valleys that developed in response to folding of an area initially drained by consequent rivers
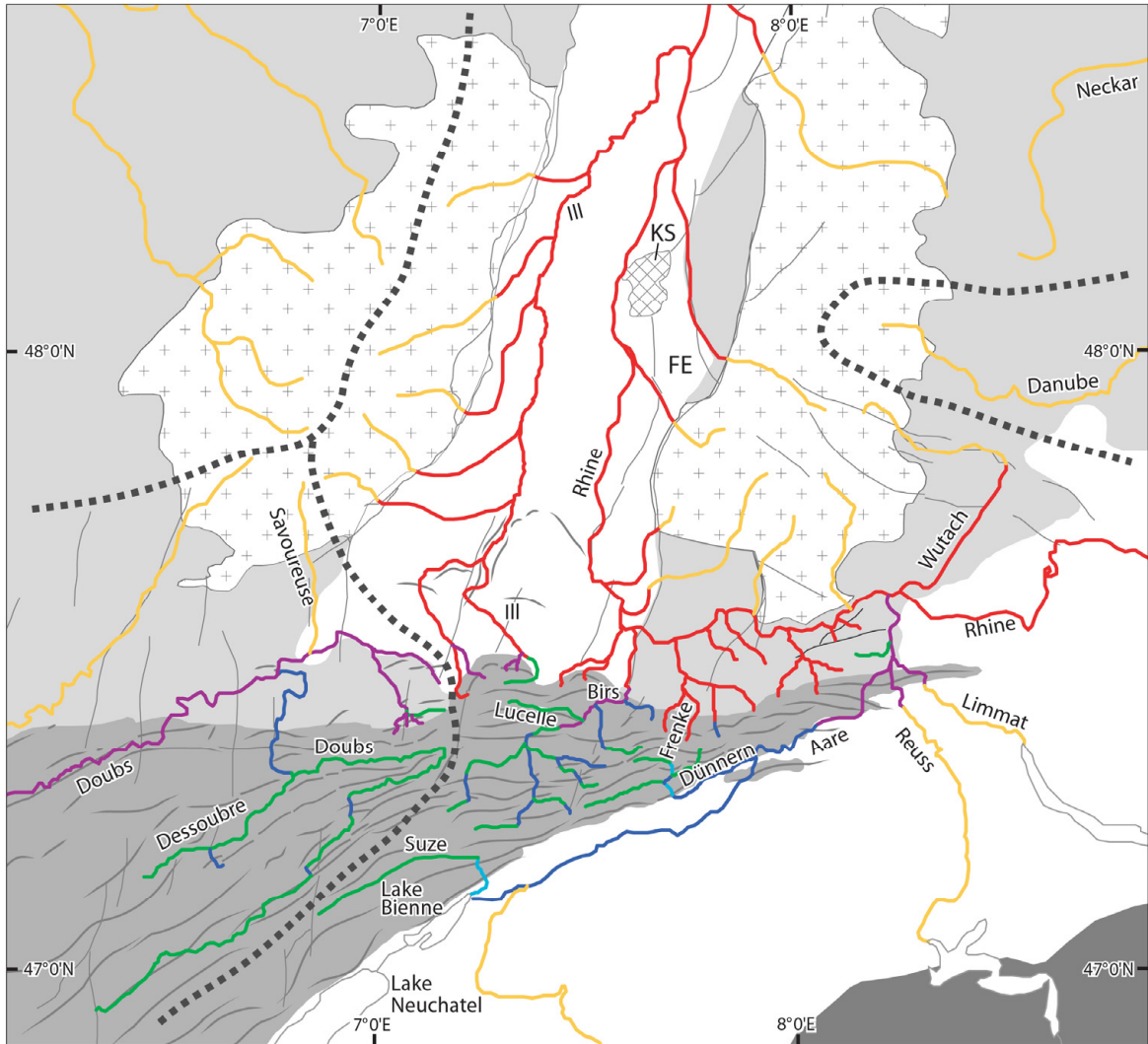
Figure 3: Modern drainage system of the study area. Dashed lines: drainage divides. Yellow: consequent rivers related to Burdigalian uplift of Vosges-Black Forest Arch and to Alpine fans in the Molasse Basin. Rivers related to Jura folding and uplift of the Molasse Basin: subsequent (green), resequent (light blue), obsequent (dark blue), antecedent to late Jura folding (purple). Insequent rivers related to Pliocene-Quaternary subsidence of the URG (red). Abbreviations: FE Freiburg Emabayment, KS Kaiserstuhl volcanic complex. For discussion see sections 4 to 8.

Resequent:	Rivers flowing after folding of an area in the same direction as the initial consequent drainage system, employing segments of antecedent rivers
Obsequent:	Rivers flowing after folding of an area in a direction opposite to the initial consequent drainage system, involving reversal of antecedent river segments
Superposed:	Rivers incised in strata that do not control their course that was inherited from the configuration of overlying strata or landforms

A step-wise reconstruction of tectonic processes, which controlled the development of this drainage system starting in Oligocene times, is presented in the following sections.

_____

2.4 Oligocene to early Miocene Rhine Graben stage of the Jura domain

During the Oligocene and early Aquitanian, intermittent communications were established between the flexural Molasse Basin and the rifted URG via the Rauracian Depression that crossed the area of the future Eastern Jura Mountains in the SW prolongation of the URG (Kuhlemann and Kempf, 2002; Berger et al., 2005a). The axial parts of this shallow depression coincide with the valley-and-ridge province of the Jura Mountains and were controlled by tensional fault systems that extend from the URG SW-ward (Laubscher, 1981; 1998; 2003). In this area, the middle and late Aquitanian corresponds to an erosional hiatus, which has been variably attributed to the development of an Alpine flexural forebulge (Laubscher, 1992; 2001) or to the build-up of intraplate compressional stresses causing transpressional reactivation of pre-existing basement discontinuities (Laubscher, 2003; Ziegler and Dèzes, 2007). In response to these deformations, the upper Aquitanian conglomeratic "older Jura Nagelfluh" was shed SE-ward from the Black Forest into the area of the Tabular Jura (Diebold et al., 2006) and the Hegau (Schreiner, 1965; Müller et al., 2002). These depositional areas formed part of the northern margin of the continuously subsiding Molasse Basin in which fluvial clastics derived from the Alps were transported ENE-ward since the late Oligocene (Untere Süsswassermolasse, USM). During the late Burdigalian high-stand in sea level, the Molasse Basin was invaded by seas, which entered it from the SW and E. At the same time much of the area of the future Jura Mountains was overstepped by transgressions advancing from the Molasse Basin, controlling the deposition of brackish-marine series (Obere Meeresmolasse, OMM) (Kuhlemann and Kempf, 2002; Berger et al., 2005a; Bieg, 2005).

2.5 Late Burdigalian uplift of the Vosges-Black Forest Arch

At about 18 Ma lithospheric folding controlled rapid uplift of the Vosges-Black Forest Arch, which at the level of the Moho discontinuity extends from the Massif Central to the Bohemian Massif. In the process of this, the southern parts of the URG were uplifted and its border faults transpressionally reactivated (Dèzes et al., 2004; Rotstein et al., 2005a; Ziegler and Dèzes, 2007). At the same time a regional erosional unconformity developed in the Molasse Basin that preceded the OMM transgression (Kempf et al., 1999; Kuhlemann and Kempf, 2002). These deformations reflect the build-up of intraplate compressional stresses in the foreland of the Alps at the onset of imbrication of their external crystalline massifs (Fügenschuh and Schmid, 2003; Dèzes et al., 2004).
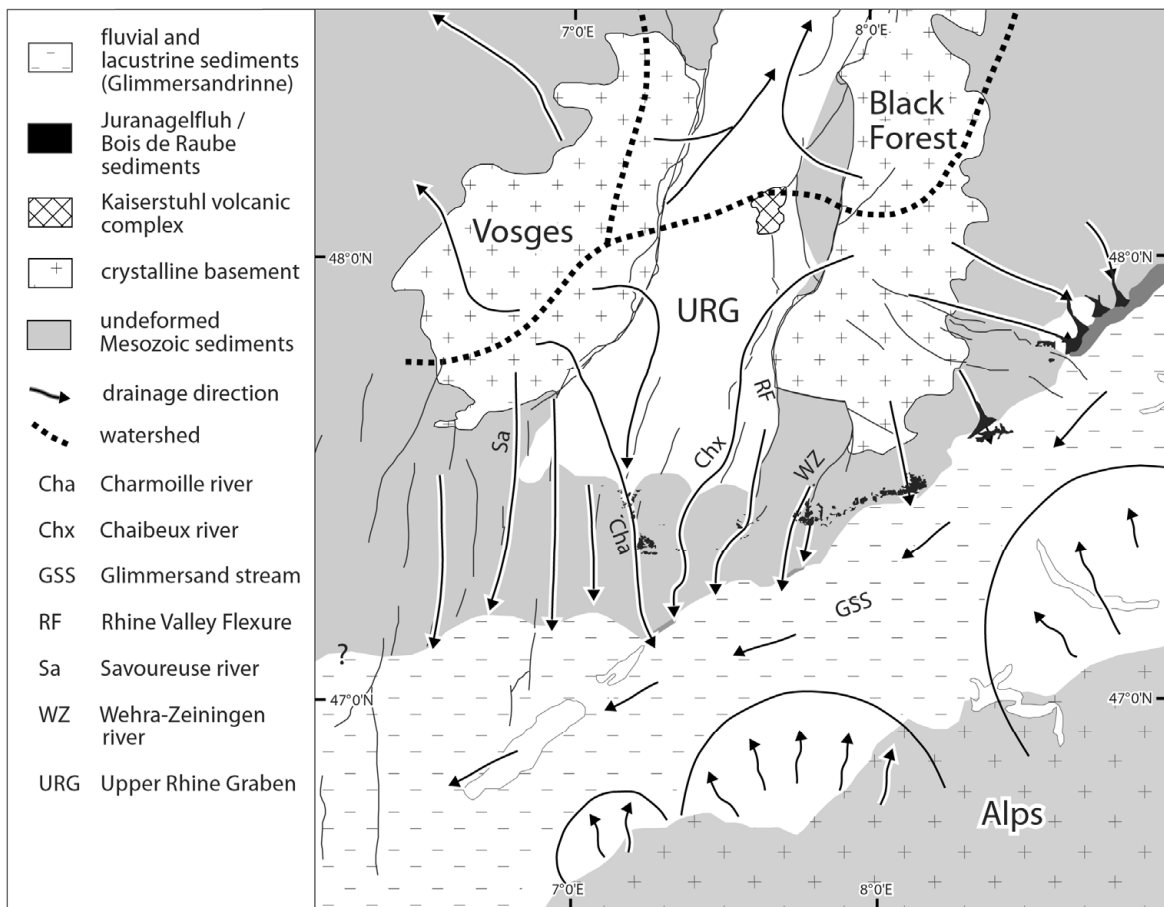
Figure 4: Serravallian to early Tortonian (Jura Nagelfluh stage, 13.6-10 Ma, no palinspastic restoration). The SW flowing Glimmersand stream drains the Molasse Basin whilst from a watershed near the Kaiserstuhl the proto-Rhine flows N in the Upper Rhine Graben.

During the late Burdigalian the WSW-directed estuarine "Glimmersand" stream developed in the Molasse Basin in a depression that straddled its present-day northern margin. This depression was flanked to the south by alluvial fans, which originated in the Alps, whilst to the north it was flanked by the Vosges-Black Forest Arch and its extension into the Bohemian Massif. This fluvial to lacustrine drainage system (Obere Süsswassermolasse, OSM) persisted, despite falling sea levels, during Langhian and Serravallian times and probably even during the earlier parts of the Tortonian (Figure 4; Hofmann, 1960; 1996; Kuhlemann and Kempf, 2002; Berger et al., 2005a; Bieg, 2005). Compared to the late Oligocene-early Miocene ENE directed drainage system of the Molasse Basin, the late Burdigalian development of the WSW directed Glimmersand systems reflects a reversal of its drainage pattern (Kuhlemann and Kempf, 2002). This suggests that during the late Burdigalian to Serravallian early uplift phases of the Central Alpine External Massifs the western parts of the Molasse Basin subsided faster than its eastern parts.

Late Burdigalian uplift of the Vosges-Black Forest Arch caused the development of a S- and SE-directed consequent drainage system on its southern flank that debouched into the Glimmersand depression. In the domain of the future Eastern Jura Mountains and the Hegau, related rivers initially truncated the OMM and locally incised into Jurassic carbonates, forming up to 100 m deep valleys, and later controlled the deposition of the Vosges-derived "Bois de Raube" and the Black Forest-derived "Jura Nagelfluh" formations (Figure 4; Liniger 1953; 1966; 1967; Hofmann, 1996; Kälin, 1997; Berger et al., 2005a). In the Jura Mountain valley-and-ridge province, remnants of the Bois de Raube and the Jura Nagelfluh formations are preserved in the broad Delémont and Laufen synclines, attain thicknesses of up to 130 m, span Serravallian to early Tortonian times (14.5-9.8 Ma) and consist of predominantly coarse fluvial conglomerates and minor sands and marls (Kälin, 1997; Kemna and Becker-Haumann, 2003; Braillard, 2006). In the Tabular Jura, the so-called "younger Jura Nagelfluh" is preserved near the thrust front as a coherent, up to 200 m thick sequence of lacustrine marls and freshwater carbonates that contains intercalations of fluvial sands and conglomeratic layers. This sequence dips 3-4° to the south, rests unconformably on truncated OMM and Late Jurassic series, spans Serravallian to earliest Tortonian times and grades southward into the Glimmersand facies of the OSM (Berger et al., 2005b; Diebold et al., 2006). In the Hegau, remnants of the "younger Jura Nagelfluh" range in age from late Burdigalian to late Serravallian (17.5-12 Ma) and similarly grade SE-ward into the OSM Glimmersand, which probably extends into the early Tortonian (Hofmann, 1960; Hofmann, 1969; 1996; Kuhlemann and Kempf, 2002; Müller et al., 2002; Bieg, 2005; Rahn and Selbekk, 2007).

Additional remnants of the Bois de Raube and Jura Nagelfluh formations have been reported from the more internal parts of the Jura Mountain valley-and-ridge province to the SW and S of the Delémont and Laufen synclines (e.g. Montfaucon, Bellelay, Mt. Raimeux, Vermes, Schelten Pass). Moreover, scattered remnants of the probably time-equivalent "Höhenschotter" have an even wider distribution and occur as far south as the Pierre Pertuis wind gap (Liniger, 1953). Therefore, the underlying south-directed drainage system probably extended across the entire area of the future Jura Mountains and linked up with that of the Glimmersand Depression along the northern margin of the Molasse Basin (Liniger, 1966; Hofmann, 1969; 1996; Kälin, 1997; Berger et al., 2005a). The conglomeratic fans of the Jura Nagelfluh and Bois de Raube formations were apparently channelled by fault systems that extended southward from the Rhine Graben into the area of the future Jura Mountains, such as the Wehratal-Zeiningen fault, the Rhine Valley Flexure and the Allschwil, Ferrette-Caquerelle, Illfurth and Belfort faults (Figures 2 & 4; Liniger, 1966; Kälin, 1997; Laubscher 2001; Kemna and Becker-Haumann, 2003). Similarly, the "younger Jura Nagelfluh" fans of the Hegau were apparently channelled by reactivated basement faults of the

Hegau-Bodensee Graben (Schreiner, 1965; Hofmann, 1996; Müller et al., 2002). By contrast, the "younger Jura Nagelfluh" of the Tabular Jura, with a clearly erosional base, was apparently deposited on a near-planar S- to SE-dipping surface against which it on-lapped northward (Diebold et al., 2006).

As the top of the Jura Nagelfluh and its equivalents is everywhere erosional, their youngest parts are missing and may have extended into the middle or even the late Tortonian (10–7.2 Ma), particularly in the external parts of the Jura Mountains. The size of clasts contained in the Jura Nagelfluh and Bois de Raube formations (Kälin, 1997; Kemna and Becker-Haumann, 2003), and their incision into Oligocene sediments and Jurassic carbonates (Liniger, 1966; 1967), are indicative of clastic transport by relatively high-energy rivers. Deep truncation to total removal of the Jura Nagelfluh and its equivalents in the more internal parts of the valley-and-ridge province of the Jura Mountains renders it impossible to reconstruct details of the underlying drainage system. Yet, circumstantial evidence for the configuration of this drainage system is provided by the distribution of wind and water gaps, which were incised by Jura Nagelfluh streams into anticlines that started to grow during the early deformation phases of the JFTB (Liniger, 1953).

2.6 Late Miocene to early Pliocene folding phase of the Jura Mountains

As the Jura Nagelfluh and its equivalents are clearly involved in the structures of the Eastern JFTB (Liniger, 1966; Laubscher, 1998; 2001; Diebold et al., 2006), and as there is no evidence for their syn-depositional deformation (Kälin, 1997), it is unlikely that the main parts of the JFTB were activated before the middle Tortonian (10-9 Ma). Nevertheless, in the southernmost parts of the JFTB, which branch off from the Subalpine Chains near Chambéry, thrusting had commenced already during the Burdigalian (Deville et al., 1994).

Shortening in the essentially thin-skinned JFTB is kinematically linked to the Alps by thrust faults which ramp up through the upper crust at the northern margin of their external Aare, Aiguilles Rouges and Belledonne massifs, extend as sole-thrusts in Triassic sediments across the Molasse Basin and ramp up in the Jura Mountains in multiple splays through Triassic and Jurassic series. In the hanging wall of these sole-thrusts the sedimentary fill of the Molasse Basin was passively translated NW-ward, uplifted and tilted to the NE (Laubscher, 1961; Guellec et al., 1990; Laubscher, 1992; Burkhard and Sommaruga, 1998; Affolter and Gratier, 2004). Uplift and erosional unroofing of the external Alpine massifs accelerated around 10 Ma (Fügenschuh and Schmid, 2003) and, thus, is compatible with an intra-Tortonian onset of the main deformation phase of the JFTB.
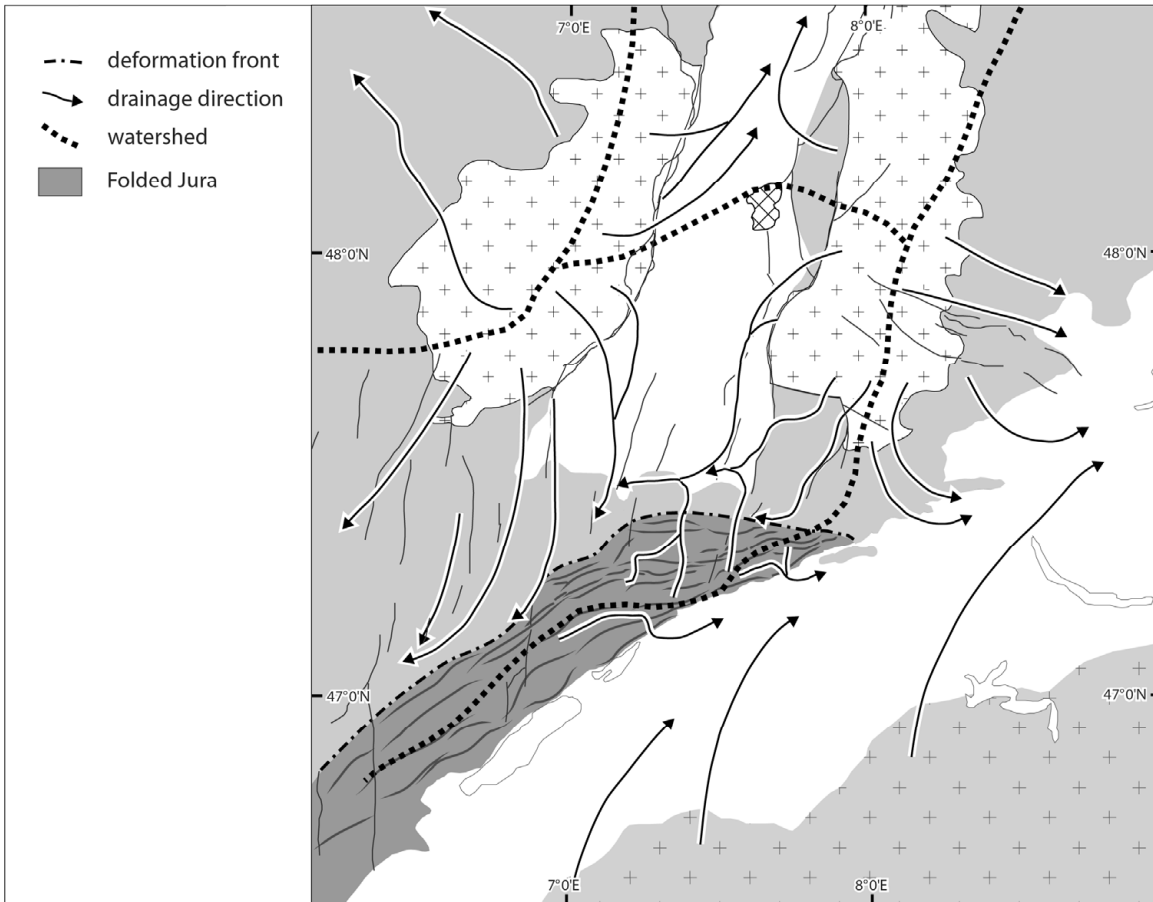
Figure 5: Middle to late Tortonian (early folding phases of the Jura Mountains, 10-7.2 Ma, no palinspastic restoration). The drainage direction of the Molasse Basin has changed to NE; a new watershed has formed in the Jura fold-and-thrust belt.

2.6.1 Drainage reversal in the Molasse Basin

In the course of the middle Tortonian (10-9 Ma), the WSW-directed Glimmersand drainage system was abandoned owing to uplift and NE-ward tilting of the western parts of the Swiss Molasse Basin during the early folding phases of the Jura Mountains. With this, a new ENE-directed drainage system began to develop that can be regarded as the precursor of the Aare-Danube system (Figure 5; Hofmann, 1960; 1996; Müller et al., 2002; Kuhlemann and Kempf, 2002; Berger et al., 2005a). In this context it is important to note that the preserved sedimentary record of the Swiss Molasse Basin ends in the Serravallian, and that about 700 m of sediments have been eroded from its eastern parts and over 2000 m from its western parts. Correspondingly, the timing of this drainage reversal is poorly constrained in Switzerland and has been inferred from the middle Tortonian NE- and E-ward deflection of Alpine alluvial fans in the Bavarian and Upper Austrian Molasse Basin (Kuhlemann and Kempf, 2002; Müller et al., 2002; Berger et al., 2005a; Berger et al., 2005b).
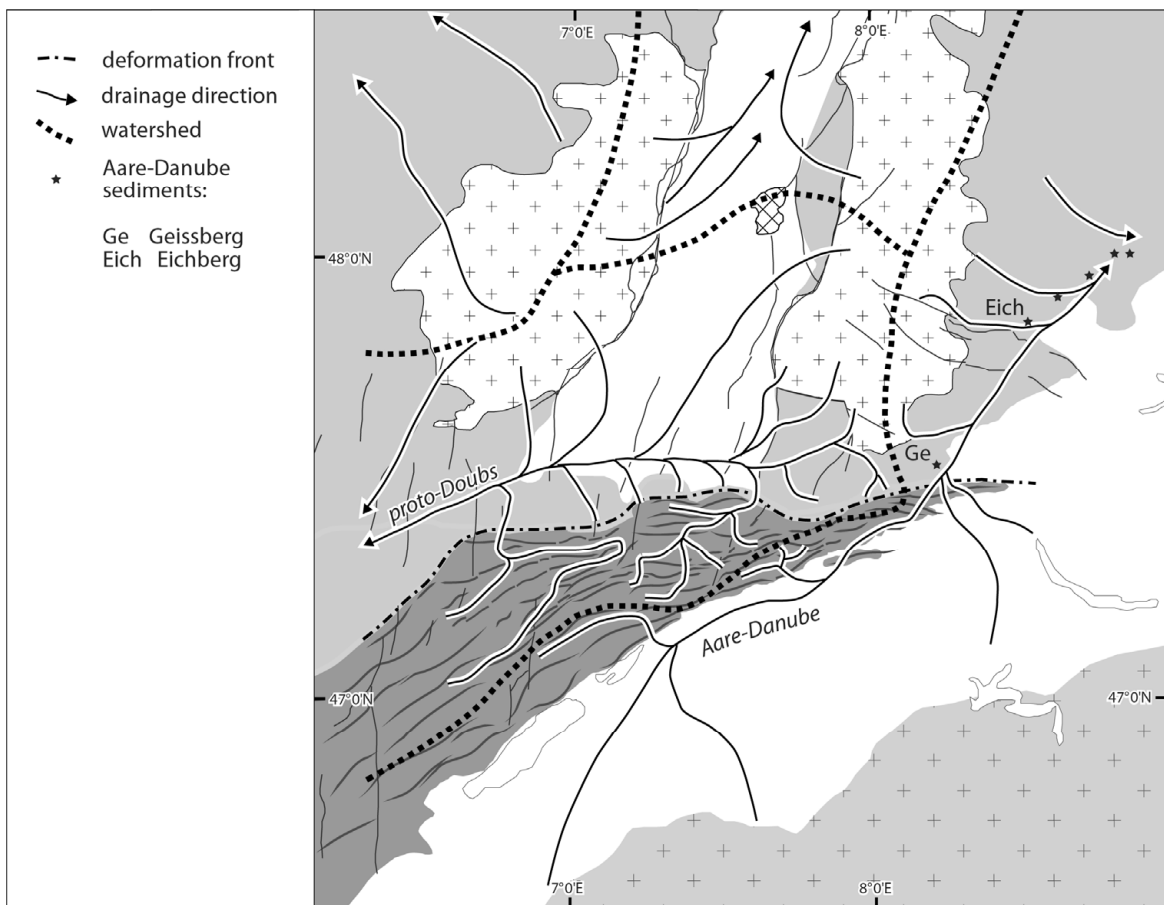
Figure 6: Messinian to early Pliocene (Aare-Danube and proto-Doubs stage, 7.2-4.2 Ma, no palinspastic restoration). Sediments attributed to the river Aare-Danube occur on the SE flank of the Black Forest. The headwaters of the proto-Doubs extends into the foreland of the Jura fold-and-thrust belt.

The ENE-flowing former Aare-Danube River is documented by undated relics of epidote-bearing quartz gravels occurring in the lower Aare valley (Geissberg near Villigen), on the eastern flank of the Black Forest (Eichberg near Blumberg) and in the upper Danube valley (Figure 6). This river presumably came into existence during the late Tortonian (8-7.2 Ma) or in the course of the Messinian (7.2-5.3 Ma) and persisted until the early Pliocene (4.2 Ma) (Hofmann, 1996; Villinger, 1998; Müller et al., 2002; Villinger, 2003; Berger et al., 2005a; Berger et al., 2005b; Sissingh, 2006).

2.6.2 Drainage reversal in the valley-and-ridge province

The occurrence of water and wind gaps is largely limited to the valley-and-ridge province of the Eastern Jura Mountains, which is characterized by major, thrust-related flexural-slip folds and large synclinal depressions. Nearly linear chains of water and wind gaps cutting across adjacent anticlines are interpreted as marking branches of the antecedent south-directed Jura Nagelfluh

drainage system, which had begun to incise into growing anticlines during the middle and late Tortonian (Liniger, 1953). For example, water and wind gaps seem to be aligned in the southward prolongation of the Wehratal-Zeiningen fault system and the Rhine Valley Flexure (Figure 2). Similarly, N-S and NNE-SSW aligned wind and water gaps indicate the course of former southward flowing rivers in the prolongation of the Allschwil and Ferrette faults, corresponding to the Chaibeux Jura Nagelfluh river and the Charmoille Bois de Raube river as defined by Liniger (1953) (Figure 4). Locally river incision was apparently accompanied by the development of doubly plunging anticlines (Simpson, 2004b; a) as seen at Soyhières and Tiergarten.

In the course of the evolution of the JFTB, involving rapid and perhaps not strictly in-sequence NW-ward fold and thrust propagation (see analogue model of Philippe et al., 1996), the southward flowing consequent Jura Nagelfluh drainage system was gradually overpowered and partly reversed. This led to the development of new drainage systems consisting of subsequent and obsequent segments (e.g. river Birs), or subsequent and resequent segments (e.g. river Dünnern; Figure 3). Unfortunately the exact timing of the different steps in this drainage reorganization cannot be further constrained for want of a corresponding sedimentary record. As folding continued, some earlier formed water gaps were employed by the new drainage systems, which accounted for their further incision into growing anticlines, whilst others were abandoned and uplifted and now form wind gaps. This drainage reorganization also explains why some present-day creeks with small drainage areas, corresponding to low discharge, employ large gaps that they cannot have incised on their own (e.g. Soyhières, Tiergarten, Gänsbrunnen gaps; Figure 2).

These new drainage systems also interacted with anticlinal structures that started to develop in the younger, more external parts of the Jura Mountains. Of special interest are anticlines that lack wind and water gaps. These were either not transected by antecedent rivers during the initial stage of their evolution or they developed only after such rivers had been abandoned. For instance, the external Bueberg, Glaserberg and Blauen anticlines are not breached by water gaps, apart from the Laufen gap through the eastern end of the Bueberg structure (Figure 2). These anticlines probably began to develop during a later stage (late Tortonian-Messinian?), after the Jura Nagelfluh drainage system had been abandoned and the northward flowing river Birs had been established. Correspondingly, it is likely that it was the river Birs that cut the Laufen and Angenstein gaps through the eastern, plunging ends of the Bueberg and Blauen anticlines, respectively. Incision of two partial wind gaps in the western part of the Bueberg anticline presumably commenced during this drainage system reorganization and continued subsequently in

response to headward erosion by the subsequent river La Lucelle that flows eastward between the Bueberg and Glaserberg anticlines.

The fact that even the most internal anticlines of the JFTB are locally breached by water gaps, such as near Bienne and Oensingen (Figure 2), supports the hypothesis that antecedent rivers once crossed the entire Jura Mountain domain and probably built out fans on the floodplain of the Glimmersand Depression, as already inferred above from the distribution of the Jura Nagelfluh, Bois de Raube and equivalent sediments (Figure 4). On the other hand, an embayment of the Glimmersand Depression may have extended between Bienne and Oensingen across the area of the Montoz and Weissenstein anticlines, which are not cut by water gaps, whilst the Graitery anticline to the north is transected by the Court water gap and the Gänsbrunnen wind gap. This interpretation is compatible with the occurrence of Glimmersand intercalations in the Tortonian (Serravallian?) lacustrine carbonates of the Court syncline, which separates the Graitery and Montoz-Weissenstein anticlines, as well as in those of the St. Imier syncline (Hofmann, 1969).

2.6.3 Franches-Montagnes and Franche-Comté

During the middle and late Tortonian, the deformation front of the JFTB apparently advanced across the Franches-Montagnes and reached the Faisceau Salinois by early Pliocene times. This narrow deformation belt links up to the NE with the Mont Terri anticline and the SW with the Lédonien thrust sheet (Figures 1 & 2). The latter overrode the eastern margin of the Bresse Graben at the Miocene-Pliocene transition (Chauve et al., 1980; Chauve et al., 1988; Guellec et al., 1990; Roure et al., 1994). Moreover, it is likely that the Lomont anticline, which lies on trend with the Mont Terri, Bueberg and Glaserberg anticlines, was activated during the Messinian to early Pliocene whilst deformation of the Faisceau Bisontin may have begun during the early Pliocene (Figures 5 & 6).

In this area several prominent water gaps occur that can be linked to roughly NNE-SSW trending faults, which extend from the URG and the Vosges into the Jura domain, such as the Illfurth and Belfort faults, and probably exerted controls on the antecedent late Miocene drainage system (Figures 2 & 4). Several water gaps of the rivers Doubs and Dessoubre are located in the southward prolongation of the river Savoureuse, which now flows from the Vosges Mountains into the Doubs (Figure 3); however, it might once have been part of a longer river that flowed southward towards the Molasse Basin, following Vosgian fracture systems. Thus we assume that the upper reaches of the river Doubs developed during the late Tortonian to early Pliocene deformation of the JFTB, consequently employing synclinal valleys and obsequently using water

gaps initially cut through rising anticlines by southward-flowing consequent Vosgian rivers. From Montbéliard the meandering proto-Doubs flowed SW-ward towards the Bresse Graben in a gentle depression that was flanked to the SE by the Faisceau Bisontin, which marks the boundary between the Ornans Plateau, the Avant-Monts Zone and the Montbéliard Plateau (Figure 1; Madritsch et al., 2008 (accepted)).

2.6.4 Eastern thrust belt

In the thrust-dominated easternmost Jura Mountains, water gaps occur only where the river Aare, and its tributaries Reuss and Limmat, incised into the evolving fold-thrust belt (Figure 2). South of the city of Olten the doubly plunging Born anticline is transected at its culmination by the river Aare, and thus conforms to the erosion-induced anticlinal growth model (Simpson, 2004a,b; see Ziegler & Dèzes, 2007). Yet, the thrust stack immediately to the north of Olten is not breached by water or wind gaps. Therefore we postulate that antecedent rivers originating in the Black Forest were not able to cut water gaps in this area. This is compatible with the fact that in this part of the Jura Mountains the "younger Jura Nagelfluh" deposits display a distinctly lacustrine affinity (Diebold et al., 2006) that does not imply the presence of persisting high-energy streams. Based on these considerations, and assuming that the thin-skinned Born anticline is not a late out-of-sequence structure, we postulate that deformation of the easternmost parts of the Jura Mountains commenced only after the Aare-Danube and its tributary rivers Reuss and Limmat had been established, perhaps as early as during the late Tortonian (8.0-7.2 Ma) or more likely in the course of the Messinian (7.2-5.3 Ma). This would account for the development of the water gaps that these rivers carved through the eastern-most elements of the JFTB. It is noteworthy that the Aare-Danube drainage system essentially employed the Glimmersand drainage system in an obsequent mode (Figures 5 and 6).

2.7 Pliocene and Quaternary reorganization of drainage systems in the foreland of the Jura Mountains

During the late early Pliocene (4.2 Ma) the palaeo-Aare river was deflected into a western direction at the eastern end of the JFTB near Waldshut and began to flow along the southern flank of the Black Forest in an isoclinal valley of the Tabular Jura towards the Sundgau and via the Franche-Comté, the Bresse Graben and the Rhône Valley into the Mediterranean (Figure 7; Liniger, 1966; 1967; Hofmann, 1996; Villinger, 1998; Laubscher, 2001; Sissingh, 2006). This Aare-Doubs deposited gravels dominated by Alpine clasts in the Sundgau, on the Vesoul-
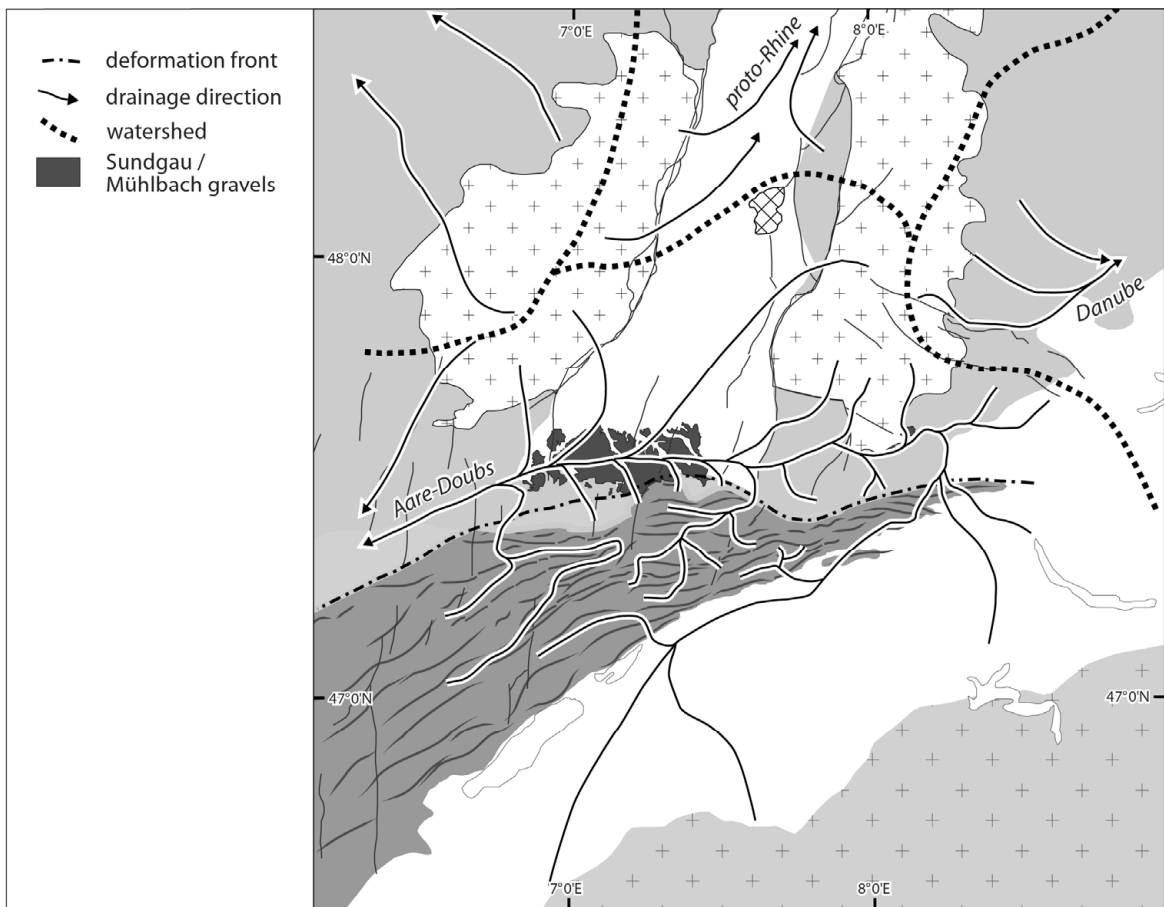
Figure 7: Mid-Pliocene (Aare-Doubs stage, 4.2-2.9 Ma, no palinspastic restoration). In response to headward erosion of the proto-Doubs, the river Aare is deflected to the W. The river Aare-Doubs deposited the Sundgau Gravels.

Montbéliard Plateau and Forêt de Chaux as well as in the Bresse Graben. In the Forêt de Chauxand Bresse Graben these gravels are known as "Cailloutis de Desnes" and are dated as 4.2-2.9 Ma (Petit et al., 1996; Fejfar et al., 1998). These gravels were uplifted and eroded throughout the Besançon zone, which represents the NW-most segment of the JFTB (Madritsch et al., 2008 (accepted)), but are preserved in the Sundgau area. These "Sundgau Gravels" were deposited on a nearly planar, relatively wide surface by a shallow braided stream system, characterized by shifting channels, and form an up to 30 m thick layer (Giamboni et al., 2004a; Giamboni et al., 2004b). The base of these gravels is erosional and there is evidence for reworking of the underlying Bois de Raube formation (Liniger, 1967; Braillard, 2006).

Deflection of the river Aare towards the west is attributed to its capture by the proto-Doubs drainage system, which had developed in front of the evolving JFTB during the late Tortonian and Messinian and collected the consequent Vosges and Black Forest and the new obsequent Jura rivers. By early Pliocene times, the headwaters of the proto-Doubs drainage systems, which had

its base level in the subsiding Bresse Graben (Ziegler and Dèzes, 2007), extended into the foreland of the Eastern Jura thrust belt and started to interfere with the Aare-Danube drainage system, ultimately capturing the river Aare around 4.2 Ma (Figure 6; Liniger, 1966; Hofmann, 1996; Villinger, 1998; Sissingh, 2006). With this, the water and sediment load of the newly established Aare-Doubs increased sharply (Figure 7).

During these times the proto-Rhine flowed northward from a watershed near the Kaiserstuhl into the continuously subsiding northern parts of the transtensional URG (Hagedorn, 2004; Haimberger et al., 2005; Lopes Cardozo and Behrmann, 2006; Hagedorn and Boenigk, 2008). Rivers originating on the southern slopes of the Black Forest Massif, corresponding to the headwaters of the S-flowing consequent Jura Nagelfluh drainage system now debouched into the westward flowing Aare-Doubs (Villinger, 1999). Similarly, the obsequent drainage system of the Tabular Jura in front of the Jura thrust belt and the combined subsequent and obsequent drainage system of the Jura valley-and-ridge province formed tributaries of the Aare-Doubs. This is compatible with the compositional spectrum of the Sundgau Gravel components (Liniger, 1967).

The Aare-Doubs drainage system persisted until about 2.9 Ma (Fejfar et al., 1998) when the river Aare was deflected into the URG at Basel and joined the northward flowing proto-Rhine, thus forming the Aare-Rhine (Figure 8; Liniger, 1966; Villinger, 1998; Laubscher, 2001; Giamboni et al., 2004a,b). In the sedimentary record of the URG, this is reflected by a massif influx of Alpine heavy minerals, commencing towards the end of the late Pliocene (Hagedorn, 2004; Hagedorn and Boenigk, 2008; Rolf et al., 2008). In the Lower Rhine Graben, however, the first occurrence of Alpine heavy minerals has been reported from the Oebel Beds of the Waalre-1 Formation, which clearly pre-dates the Pliocene-Quaternary boundary (Gauss-Matuyama magnetic reversal at 2.58 Ma; Kemna, 2008) and has been tentatively assigned an age of 2.8-2.58 Ma (Westerhoff et al., 2008).

Owing to the late Pliocene diversion of the river Aare into the URG, the water and sediment load of the river Doubs decreased sharply. Deflection of the Aare into the Rhine drainage system was induced by transtensional subsidence of the southern parts of the URG, which resumed during the late Pliocene and continues to the present, as evidenced by the occurrence of up to 240 m of upper Pliocene and Quaternary sediment in the fault-controlled Geiswasser Basin adjacent to the Kaiserstuhl (Bartz, 1974; Dèzes et al., 2004; Lang et al., 2005; Ziegler and Dèzes, 2007). LatePliocene and Quaternary subsidence of the URG was accompanied by a gradual lowering of its alluvial plain, and with this, a lowering of the erosional base level of the Aare-Rhine. Outside the graben this led to the progressive incision of the Aare-Rhine and its tributaries, such as the Klettgau-Rhine. As a result, around 1.7 Ma, the latter captured the Alpine headwaters of the river
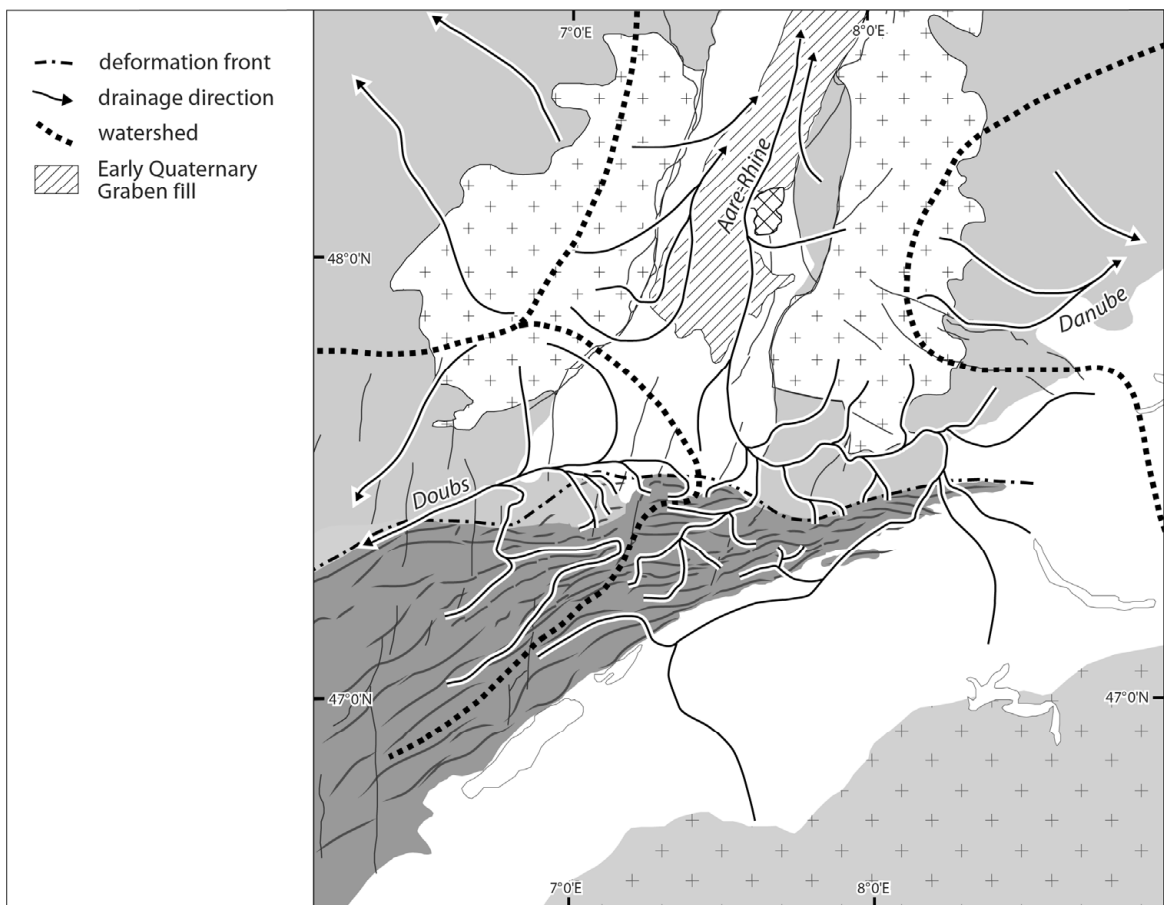
Figure 8: Late Pliocene to early Quaternary (Aare-Rhine and Doubs stage, 2.9-1.7 Ma, no palinspastic restoration). The river Aare is deflected into the Upper Rhine Graben. Headward erosion of Aare tributaries intensified in response to lowering of the base level in the subsiding Upper Rhine Graben.

Rhine in the area of Lake Constance in response to headward erosion, assisted by the run-off ofglacial melt waters during the Donau/Günz glacial stages (Figure 9; Villinger, 2003). With this, the water and sedimentary load of the newly formed Alpine Rhine increased strongly (Hofmann, 1996; Villinger, 1998; Müller et al., 2002; Villinger, 2003; Hagedorn, 2004; Hagedorn and Boenigk, 2008).

During the Quaternary the Alpine Rhine and its tributaries in the Jura Mountains and the Black Forest continued to incise in response to progressive lowering of their erosional base level in the continuously subsiding URG, and possibly to gentle uplift of the Black Forest. This is evidenced by distinct cut-and-fill terrace systems of the Alpine Rhine upstream from Basel and along the lower reaches of the river Aare (Haldimann et al., 1984; Verderber, 1992; Müller et al., 2002; Verderber, 2003). On the eastern flank of the Black Forest, continuing river incision resulted in the capture of the Feldberg-Danube by the river Wutach, a tributary of the Rhine, between 19-20 ka (Hofmann, 1996; Villinger, 2003).
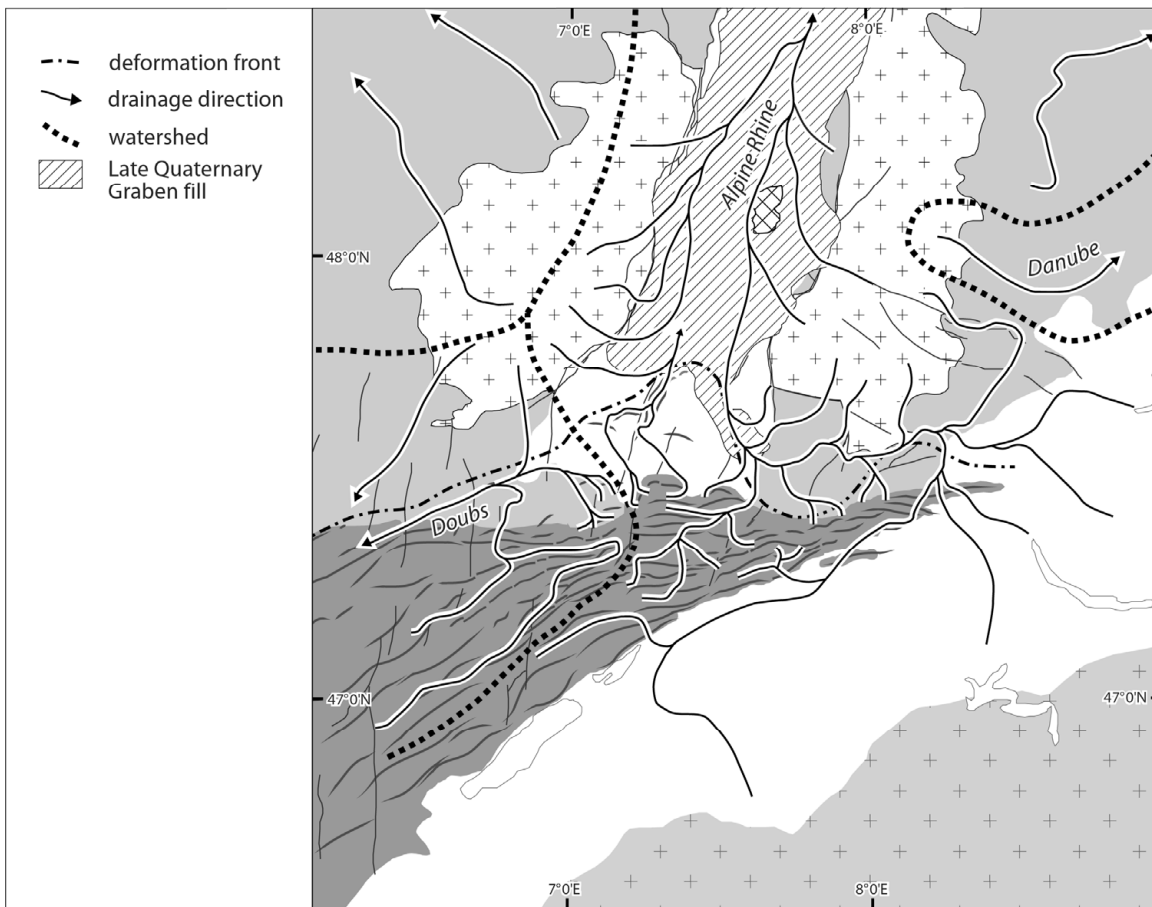
Figure 9: Late Quaternary (Alpine Rhine and Doubs stage, 1.7-0 Ma). Capture of the Alpine Rhine and the headwaters of the Danube by tributaries of the river Aare.

2.8 Evidence for Pliocene and Quaternary tectonic activity

In the foreland of the Eastern Jura thrust belt, the thin-skinned Mandach and Mettau thrusts (Figure 2a; Bitterli and Matousek, 1991; Diebold et al., 2006) probably developed during the Quaternary. This is suggested by the occurrence of remnants of "Höhere Deckenschotter" gravels (2.6-1.6 Ma) N of the Mandach thrust that were deposited by a northward flowing river, the course of which was apparently blocked by the development of the Mandach thrust (Müller et al., 2002). Moreover, the Etzgerbach and Sulzerbach rivers originate on the northern flank of the Mandach structure, which is not breached by gaps, and cut through the Mettau thrust in water gaps (Figure 2b). Therefore, these creeks probably developed on the northern slope of the Mandach structure prior to activation of the Mettau thrust. Furthermore, minor compressional structures observed in the projection of the Mandach thrust and at Klingnau in the lower Aare Valley may have been active during the Quaternary (Haldimann et al., 1984; Müller et al., 2002).

Upstream from Basel, small remnants of the Sundgau Gravel equivalent Mühlbach Series are preserved between Laufenburg and Waldshut (Hofmann, 1996; Verderber, 2003). These deeply weathered gravels are characterized by the same heavy mineral spectrum as the Pliocene Sundgau Gravels (4.2-2.9 Ma). Moreover, sediment-petrographically they differ profoundly from the garnet-rich "Höhere Deckenschotter" gravels (Hofmann, 1996) that range in age between 2.6 and 1.6 Ma (Müller et al., 2002; Villinger, 2003). In view of this, and as the Mühlbach Series is characterized by normal magnetisation (Fromm, 1989), it was probably deposited during the Pliocene Gauss epoch (3.580-2.588 Ma) rather than during the early Quaternary Olduvai epoch (1.95-1.77-Ma), as postulated by Verderber (2003).

In the Rhine Valley upstream from Basel the distribution of remnants of Sundgau Gravel equivalent deposits (4.2-2.9 Ma) and of older river terraces ("Deckenschotter", 2.6-0.78 Ma) is generally too limited to record potential tectonic activity along fault systems extending from the Black Forest into the Tabular Jura. Nevertheless, scattered remnants of the Deckenschotter suggest a subtle gradient increase across the Rhine Valley flexure, indicative of its tensional reactivation (Kock et al., in prep.). The uniform gradients of the well-preserved younger Rhine river terraces ("Hoch- and Niederterrassen") suggests that during the last 0.78 Ma the fault systems of the Black Forest and Tabular Jura were essentially quiescent, perhaps with exception of the Rhine Valley flexure across which Niederterrasse gradients increase gently (Haldimann et al., 1984; Verderber, 1992; 2003).

In the Sundgau, by contrast, the Pliocene Sundgau Gravels are still well preserved in front of the valley-and-ridge province of the Jura Mountains where they were deposited on a wide floodplain. In the Bresse Graben their equivalents (Desnes Gravels) attain thicknesses of up to 300m (Petit et al., 1996; Giamboni et al., 2004a), thus attesting to its tensional reactivation (Dèzes et al., 2004). In the Sundgau and Ajoie, the Sundgau Gravels are involved in the frontal folds of the Jura Mountains. Moreover, there is evidence for Quaternary changes in drainage patterns and anomalies in river gradients, as well as for the deformation of terraces, indicating late stage compressional deformation of the Mulhouse High (Niviere and Winter, 2000; Giamboni et al., 2004a; Giamboni et al., 2004b; Carretier et al., 2006) and the Ajoie (Braillard, 2006). Deformation of the Mulhouse High and its Sundgau Gravel cover involved the development of several gentle folds (Giamboni et al., 2004a) and sinistral reactivation of the Paleogene URG-related Illfurth fault (Figure 2a; Le Carlier de Veslud et al., 2005; Rotstein et al., 2005b; Ustaszewski and Schmid, 2007). The frontal Florimont and Réchésy folds of the Ajoie, which also involve the Sundgau Gravels, are associated with compressionally reactivated WSW-ENE striking Permo-Carboniferous basement faults and, thus, are thick skinned (Giamboni et al.,

2004a; Ustaszewski et al., 2005). It is unknown whether this also applies to the Banné and Vendlincourt anticlines to the south that may have developed during the Pliocene and Quaternary (Braillard, 2006). Further to the east, the thin-skinned frontal Ferrette and Landskron folds, which are associated with the Paleogene Ferrette and Allschwil faults of the URG, respectively, probably began to develop prior to the deposition of the Sundgau Gravels (Ustaszewski and Schmid, 2006) and presumably continued to grow during the late Pliocene and Quaternary compressional deformation of the Mulhouse High.

These young anticlines are all characterized by minor wind and/or water gaps (e.g. gaps in the Ferrette anticline at Durlinsdorf and Ferrette; Figure 2b). Moreover, they are located to the north of the Blauen, Glaserberg and Mont Terri anticlines, which are devoid of wind and water gaps. Thus, development of these gaps must be attributed to rivers that originated in the earlier elevated ranges of the Jura Mountains to the south, and that incised into the evolving frontal anticlines during their Pliocene and Quaternary development (Giamboni et al., 2004a; Braillard, 2006).

Regarding the Pliocene and Quaternary evolution of the Franches-Montagnes and the adjacent parts of the Franche-Comté, the relatively high sinuosity of the rivers Doubs and Dessoubre indicates that they developed as low gradient rivers prior to their incision by 300-400 m into the gently undulating relief of this plateau, which apparently was nearly peneplained after its mid-Tortonian to end-Messinian main deformation. The indicated timing of the main deformation of the Franches-Montagnes and the Franche-Comté is compatible with (i) the fact that deformation of the internal Mont d'Amin anticline (Figure 2a) had ceased by early Pliocene times, as evidenced by a geopetal karst fill dated as MN15 (4.1-3.6 Ma; Bolliger et al., 1993), and (ii) that the Lédonien thrust sheet (Figure 1) had overridden the eastern margin of the Bresse Graben at the Miocene-Pliocene transition but became inactive thereafter (ca. 5.3 Ma; Chauve et al., 1988; Guellec et al., 1990; Roure et al., 1994). Mid-Pliocene to Quaternary (ca. 4-0 Ma) uplift of the Franches-Montagnes and Franche-Comté, causing deep incision of the rivers Doubs and Dessoubre, is attributed to late-stage thick-skinned deformation of the Jura Mountains, involving the inversion of Permo-Carboniferous troughs, as indicated by reflection-seismic data and seismic activity (Roure et al., 1994; Philippe et al., 1996; Becker, 2000; Lacombe and Mouthereau, 2002; Pfiffner, 2006; Ustaszewski and Schmid, 2007).

During the Pliocene and Quaternary, compressional deformation of the Bisontin belt continued and ultimately also affected the Avant-Monts domain to the NW (Figure 1). The Clerval water gap through the Ormont anticline (Figure 2b) speaks for the antecedence of the river Doubs with respect to the development of the Bisontin belt. Growth of the Bisontin bundle of

_____

folds, as well as of the Lomont Anticline had confined the deposition of the Sundgau Gravels and their equivalents to the Montbéliard Plateau and Avant-Monts domain (Figure 7; Madritsch et al., 2008 (accepted)).

2.9 Geodetic constraints on neotectonics

Precision levelling data (Müller et al., 2002) indicate that the thrust belt of the Eastern Jura Mountains currently rises at rates of 0.25–0.35 mm/a, whilst the Swiss Tabular Jura appears to be stable and the Dinkelberg Block to the north subsides gently with respect to a reference point at Laufenburg. Assuming for the Jura thrust belt a basal 30° ramp, its uplift rate can be translated into ongoing horizontal displacement rates of 0.5–0.7mm/a (Müller et al., 2002). The Swiss GPS Reference Network LU95, however, has not yet detected corresponding horizontal displacements (Brockmann et al., 2005). Furthermore, precision levelling shows that adjacent to the Freiburg embayment the alluvial plain of the URG subsides relative to the Black Forest at rates of 0.5-0.6 mm/a, with the fault systems of the Freiburg embayment being tectonically and seismically active (Behrmann et al., 2003; Rózsa et al., 2005). Moreover, precision levelling data indicate that the valley-and-ridge province and the Franches-Montagnes gently subside with respect to the Laufenburg reference point, possibly in response to strike-slip reactivation of URG-related basement-involving fault systems that extend beneath these areas (Schlatter et al., 2005). This is compatible with the fault-plane solutions of earthquakes occurring in the area of the Eastern Jura Mountains (Deichmann et al., 2000; Müller et al., 2002). Yet, repeated levelling surveys, carried out during the last 30 years near the city of Basel, have not detected any movements on the Rhine Valley Flexure (Schlatter et al., 2005), even though it has a distinct morphological expression. Considering that the terraces of the Rhine do not give clear evidence for late Quaternary tectonic activity (Wittmann, 1961; Haldimann et al., 1984; Villinger, 2003), this may mean that either stresses are currently building up on this important fault, or that tectonic deformation is partitioned over a number of faults and thus, is difficult to detect.

GPS data acquired during the last 17 years show only minor differential horizontal displacements for campaign stations located within the JFTB; these are at best close to the level of significance (Brockmann et al., 2005) but do not reflect a consistent deformation pattern. On the other hand, data derived from the European network of continuously operating GPS reference stations indicate sinistral transtensional displacement rates of up to 0.76 mm/a between the flanks of the URG and similar transpressional to compressional displacement rates across the Bresse-URG transfer zone (Tesauro et al., 2005).

2.10 Summary

Thin-skinned deformation of the JFTB commenced probably around 10-9 Ma during the middle Tortonian and continued during the Pliocene when thick-skinned deformation became increasingly important (Becker, 2000; Ustaszewski and Schmid, 2007). During the Tortonian initial deformation pulses the pre-existing south-directed consequent drainage system that had developed in response to late Burdigalian (ca. 18 Ma) uplift of the Vosges-Black Forest Arch (Figure 4) was gradually overpowered. With this, development of the modern drainage systems of the JFTB and its fore- and hinterlands commenced, as outlined below:

1) During the initial deformation stage of the JFTB, spanning approximately middle and late Tortonian times (10-7.2 Ma), the deformation front propagated NW-ward across the Franches-Montagnes into the upper reaches of the river Doubs and across the Delémont Basin to the Les Vorbourgs, Movelier and Thierstein anticlines, but probably not much beyond the Langenbruck area into the eastern thrust belt (Figures 2 and 5). During this stage, development of major water and wind gaps commenced in the valley-and-ridge province, owing to incision of the S-directed consequent Jura Nagelfluh drainage system into the rising anticlines. As folding progressed, this drainage system was gradually overpowered and new subsequent drainage systems developed, which were linked by resequently and obsequently employed segments of the antecedent Jura Nagelfluh river system, thus accounting for further incision of major water gaps. Contemporaneous uplift, ENE-ward tilting and erosion of the Swiss Molasse Basin in response to thin-skinned shortening in the JFTB, controlled the abandonment of the WSW-directed Glimmersand drainage system and the gradual development of an ENE-directed precursor of the Aare-Danube drainage system.

2) During the second stage, spanning approximately Messinian and early Pliocene times (7.2-4.2 Ma), the deformation front of the JFTB propagated into the Franche-Comté and Sundgau, activating the Lomont, Mt. Terri, Bueberg, Glaserberg and Blauen anticlines, as well as into the eastern thrust belt (Figures 2 & 6). During this stage, the combined subsequent and resequent Suze and Dünnern drainage systems of the internal Jura Mountains debouched S-ward via water gaps into the ENE-ward flowing river Aare-Danube (Figure 3). By this time, the Aare-Danube and its tributary rivers Reuss and Limmat had cut water gaps through the rising Born, Chestenberg and Lägern anticlines. On the other hand, the combined subsequent and obsequent Birs drainage system of the valley-and-ridge province flowed N-ward, cutting the Laufen and Angenstein gaps, and

joined the consequent Black Forest rivers at the southern end of the URG, thus forming the headwaters of the evolving SW-ward flowing proto-Doubs river. Moreover, the combined subsequent and obsequent upper reaches of the river Doubs probably developed during this stage, employing water gaps that initially were carved through evolving anticlines by the S-ward flowing river Savoureuse.

3) The third stage in the evolution of the Jura Mountain drainage systems commenced with the late early Pliocene (4.2 Ma) capture of the river Aare by the proto-Doubs drainage system at the eastern end of the JFTB. As evidenced by the Sundgau and Desnes Gravels (4.2-2.9 Ma), this new Aare-Doubs flowed in the foreland of the Jura Mountains SW-ward into the tensionally subsiding Bresse Graben where it found its erosional base level (Figure 7). During the deposition of the Sundgau Gravels shortening persisted in the eastern Jura thrust belt and in front of the valley-and-ridge province, where the thin-skinned Landskron and Ferrette anticlines, as well as the Vendlincourt and Banné anticlines continued to grow. These evolving structures were transected by N-ward flowing rivers, which originated on the flanks of earlier-formed anticlinal ridges of the Jura Mountains to the south, thus causing the development of water/wind gaps. At the same time the deformation front advanced further into the Franche-Comté and uplift of the Franches-Montagnes and Franche-Comté commenced, controlling incision of the meandering rivers Doubs and Dessoubre.

4) The fourth stage in the evolution of the Jura Mountain drainage systems commenced in the late Pliocene (2.9 Ma) with the deflection of the river Aare into the URG, the southern parts of which resumed subsiding in a transtensional stress regime. This provided the combined Aare-Rhine with a new erosional base level (Figure 8). Continued subsidence of the URG caused incision of the river Aare and its tributaries in the Jura Mountains and in the gently rising Black Forest upstream from Basel. During the late Pliocene and early Quaternary (2.9-1.7 Ma), shortening persisted in the JFTB, as evidenced in the Sundgau and Ajoie by folding of the Sundgau Gravels, that was controlled by dextral transpressional reactivation of ENE striking Permo-Carboniferous basement faults (Florimont and Réchésy anticlines) and by sinistral reactivation of SSW trending URG-related basement faults (Mulhouse High) (Becker, 2000; Ustaszewski and Schmid, 2006; 2007).

5) The final, Quaternary (1.7-0 Ma) evolutionary stage of the Jura Mountain drainage systems was dominated by continued subsidence of the URG, involving further lowering of the erosional base level of the river Aare-Rhine. The latter captured the Alpine

headwaters of the river Rhine in the area of Lake Constance around 1.7 Ma, and the Feldberg-Danube on the eastern flank of the Black Forest around 19-20 ka (Figure 9). With this the water and sediment load of the newly formed Alpine Rhine increased significantly. Continued compressional deformation of the JFTB, though at low strain rates, is evidenced by (1) the development of the thin-skinned Mandach and Mettau thrusts in the eastern parts of the Tabular Jura sometime after 1.6 Ma, (2) further deformation of the Mulhouse High, and (3) changes in the drainage pattern of the Sundgau and Ajoie – controlled by both structure and headward erosion – that had repercussions on the location of the watersheds between the rivers Rhine, Ill and Doubs.

Present-day tectonic activity in the domain of the Jura Mountains is evidenced by their seismic record and geodetic measurements. Seismicity testifies to on-going reactivation of pre-existing crustal discontinuities under the prevailing NW-directed compressional stress field (Becker, 2000; Deichmann et al., 2000; Lacombe and Mouthereau, 2002; Müller et al., 2002). Repeated precision levelling, covering time spans of 25 to 60 years, indicates that the thrust belt of the Eastern Jura Mountains is currently being uplifted at rates of 0.25-0.35 mm/a, the valley-and-ridge province and the Franches-Montagnes subside gently, while the alluvial plain of the URG subsides at rates of 0.5-0.6 mm/a and the Black Forest is apparently relatively stable with respect to a reference point at Laufenburg. In the Eastern JFTB no appreciable shortening can be deduced from GPS data, which cover a time span of 17 years (Müller et al., 2002; Brockmann et al., 2005; Schlatter et al., 2005).

2.11 Conclusions

We distinguish five stages in the development of the modern drainage systems of the Jura Mountains, taking into account the distribution of water/wind gaps, which we consider as evidence of former river courses. These stages are intimately related to the evolution of the JFTB and the URG. The timing and scope of the underlying deformation stages of the JFTB are, however, poorly constrained, owing to the general lack of a syn-deformational sedimentary record within the Jura Mountains and to the limitation of stratigraphic controls in their foreland to Mid-Pliocene and younger times. Consequently, the timing of the five evolutionary stages of the Jura Mountain drainage systems, as summarized above, must be considered as tentative. In this respect, special attention has to be paid to the Pliocene and Quaternary deformation of the Jura Mountains and their surroundings.

Compared to the thin-skinned deformation of the JFTB that had commenced around 9-10 Ma, its thick-skinned transpressional to strike-slip deformation apparently played an increasingly important role from about 3 Ma onward, controlling folding of the Sundgau Gravel. This is evidenced by reflection-seismic data (Ustaszewski & Schmid, 2006), seismicity and geomorphologic features indicating late-stage broad uplift of the Franches-Montagnes and Franche-Comté that controlled deep incision of the rivers Doubs and Dessoubre. This Pliocene-Quaternary phase of thick-skinned deformation of the JFTB, which involved reactivation of ENE striking Permo-Carboniferous troughs and fault systems (Roure et al., 1994; Philippe et al., 1996; Ustaszewski and Schmid, 2007; Madritsch et al., 2008 (accepted)), reflects an increase in the magnitude of NW-directed compressional intraplate stresses in the Alpine foreland. From about 2.9 Ma onward, these stresses governed the renewed transtensional subsidence of the southern parts of the URG, continued subsidence of its northern parts (Dèzes et al., 2004) and probably also moderate uplift of the seismically still active Vosges-Black Forest Arch (Edel et al., 2006). Beyond the area of the URG, these stresses controlled the late Pliocene–early Quaternary accelerated tensional subsidence of the Lower Rhine Graben, and by lithospheric folding, accelerated subsidence of the North Sea-North German Basin (for refs. see Dèzes et al., 2004; Ziegler and Dèzes, 2007).

In the Tabular Jura, the 3-4° southern dip of the Jura Nagelfluh (Diebold et al., 2006) reflects gentle post-early Tortonian uplift of the Black Forest. Late-stage uplift of the Black Forest Arch is furthermore supported by the occurrence of gravels attributed to the Messinian to early Pliocene Aare-Danube at 600 m above MSL in the lower Aare valley (Geissberg), and downstream at 900 m above MSL on the eastern flank of the Black Forest (Eichberg near Blumberg) (Figure 6; Hofmann, 1996; Müller et al., 2002). It is, however, uncertain whether this late-stage uplift of the Black Forest contributed to the westward deflection of the river Aare from its previous easterly course around 4.2 Ma, as postulated by Hofmann (1996), or whether it post-dates this drainage system reorganization.

Present-day seismicity seems to concentrate on fault systems that extend SSW-ward from the URG and to ENE trending fault systems that outline Permo-Carboniferous troughs (Ustaszewski, 2004; Ustaszewski et al., 2005; Ustaszewski and Schmid, 2007). Late Pliocene to present-day thick-skinned deformation of the Jura Mountains probably involves the activation of an intra-crustal detachment horizon that extends from the Alps beneath the Molasse Basin into the Jura domain (Mosar, 1999; Lacombe and Mouthereau, 2002; Edel et al., 2006; Pfiffner, 2006; Ustaszewski and Schmid, 2007). The geodetic record, combined with geomorphologic evidence, indicates that the Eastern JFTB, which has accounted for up to 30 km of thin-skinned shortening

in its western parts during the last 9-10 million years (Philippe et al., 1996; Affolter and Gratier, 2004), is currently tectonically still active but deforms at very low horizontal displacement rates of less than 1 mm/a.

Acknowledgements

References

Affolter, T. and Gratier, J.P., 2004. Map view retrodeformation of an arcuate fold-and-thrust belt: The Jura case. Journal of Geophysical Research-Solid Earth, 109(B3).

Bartz, J., 1974. Die Mächtigkeit des Quartärs im Oberrheingraben. Approaches to Taphrogenesis; The Rhinegraben; geologic history and neotectonic activity: 78-87.

Becker, A., 2000. The Jura Mountains - An active foreland fold-and-thrust belt? Tectonophysics, 321(4): 381-406.

Behrmann, J.H., Hermann, O., Horstmann, M., Tanner, D.C. and Bertrand, G., 2003. Anatomy and kinematics of oblique continental rifting revealed: A three-dimensional case study of the southeast Upper Rhine graben (Germany). Aapg Bulletin, 87(7): 1105-1121.

Berger, J.-P. et al., 2005a. Paleogeography of the Upper Rhine Graben (URG) and the Swiss Molasse Basin (SMB) from Eocene to Pliocene. International Journal of Earth Sciences, 94(4): 697-710.

Berger, J.-P. et al., 2005b. Eocene-Pliocene time scale and stratigraphy of the Upper Rhine Graben (URG) and the Swiss Molasse Basin (SMB). International Journal of Earth Sciences, 94(4): 771-731.

Bieg, U., 2005. Palaeooceanographic modelling in global and regional scale: An example from the Burdigalian Seaway Upper Marine Molasse (Early Miocene). PhD Thesis, University of Tübingen.

Bitterli, T. and Matousek, F., 1991. Die Tektonik des östlichen Aargauer Tafeljuras. Mitteilungen der Aargauischen Naturforschenden Gesellschaft, 33: 5-30.

Bolliger, T., Engesser, B. and Weidmann, M., 1993. Première découverte de mammifères pliocènes dans le Jura neuchâtelois. Eclogae geologicae Helvetiae, 86(3): 1031-1068.

Braillard, L., 2006. Morphogenèse des vallées sèches du Jura tabulaire d'Ajoie (Suisse): rôle de la fracturation et étude des remplissages quaternaires. PhD Thesis, University of Fribourg (GeoFocus 14).

Brockmann, E., Ineichen, D., Marti, U. and Schlatter, H., 2005. Results of the 3rd observation of the Swiss GPS Reference Network LV95 and status of the Swiss Combined Geodetic Network CH-CGN. In: J.A. Torres and H. Hornik (Editors), Subcommission of the European Reference Frame (EUREF), Vienna 2005. EUREF Publ. 15 (in prep.).

Burkhard, M. and Sommaruga, A., 1998. Evolution of the western Swiss Molasse Basin; structural relations with the Alps and the Jura Belt. In: A. Mascle, C. Puigdefàbregas, H.P. Luterbacher and M. Fernàndez (Editors), Cenozoic foreland basins of Western Europe. Geological Society Special Publications.

Carretier, S., Niviere, B., Giamboni, M. and Winter, T., 2006. Do river profiles record along-stream variations of low uplift rate? Journal of Geophysical Research-Earth Surface, 111(F2).

Chauve, P., Enay, R., Fluck, P. and Sittler, C., 1980. L'Est de la France (Vosges, Fossé Rhénan, Bresse, Jura). Annales scientifiques de l'Université de Besançon, Géologie, 4(1): 3-80.

Chauve, P., Martin, J., Petitjean, E. and Sequeiros, F., 1988. Le chevauchement du Jura sur la Bresse. Données nouvelles et réinterpretation des sondages. Bull. Soc. géol. France, 8(4): 861-870.

Deichmann, N., Dolfin, D.B. and Kastrup, U., 2000. Seismizität der Nord- und Zentralschweiz. Nagra Technischer Bericht, 00-05.

Deville, E. et al., 1994. Thrust propagation and syntectonic sedimentation in the Savoy Tertiary Molasse Basin (Alpine Foreland). In: A. Mascle (Editor), Hydrocarbon and Petroleum Geology of France. European Association of Petroleum Geoscientists Special Publication 4, pp. 269-280.

Dèzes, P., Schmid, S.M. and Ziegler, P.A., 2004. Evolution of the European Cenozoic rift system; interaction of the Alpine and Pyrenean orogens with their foreland lithosphere. Tectonophysics, 389(1-2): 1-33.

Diebold, P., Bitterli-Brunner, P. and Naef, H., 2006. Frick: Geologischer Atlas der Schweiz. Erläuterungen.

Edel, J.-B., Whitechurch, H. and Diraison, M., 2006. Seismicity wedge beneath the Upper Rhine Graben due to backwards Alpine push? Tectonophysics, 428(1-4): 49-64.

Fejfar, O., Heinrich, W.-D. and Lindsay, E.H., 1998. Updating the Neogene rodent biochronology in Europe. Mededelingen Nederlands Instituut voor Toegepaste Geowetenschappen TNO, 60: 533-553.

Fromm, K., 1989. Paläomagnetische Untersuchungen zur Quartärstratigraphie im Südschwarzwald bei Schadenbirndorf. Geowissenschaftliche Gemeinschaftsaufgaben, Niedersächsisches Landesamt für Bodenforschung, Hannover: 16 p.

Fügenschuh, B. and Schmid, S.M., 2003. Late stages of deformation and exhumation of an orogen constrained by fission-track data; a case study in the Western Alps. Geological Society of America Bulletin, 115(11): 1425-1440.

Giamboni, M., Ustaszewski, K., Schmid, S.M., Schumacher, M.E. and Wetzel, A., 2004a. Plio-Pleistocene transpressional reactivation of Paleozoic and Paleogene structures in the Rhine-Bresse transform zone (northern Switzerland and eastern France). International Journal of Earth Sciences, 93(2): 207-223.

Giamboni, M., Wetzel, A., Niviere, B. and Schumacher, M., 2004b. Plio-Pleistocene folding in the southern Rhinegraben recorded by the evolution of the drainage network (Sundgau area; northwestern Switzerland and France). Eclogae Geologicae Helvetiae, 97(1): 17-31.

Guellec, S., Mugnier, J.-L., Tardy, M. and Roure, F., 1990. Neogene evolution of the western Alpine Foreland in the light of ECORS data and balanced cross-section. Mémoires de la Société Géologique de France, Nouvelle Serie, 156: 165-184.

Hagedorn, E.-M., 2004. Sedimentpetrographie und Lithofazies der jungtertiären und quartären Sedimente im Oberrheingebiet. PhD Thesis, University of Cologne.

Hagedorn, E.-M. and Boenigk, W., 2008. The Pliocene and Quaternary sedimentary and fluvial history in the Upper Rhine Graben based on heavy mineral analyses. Netherlands Journal of Geosciences (Geologie en Mijnbouw), 87(1).

Haimberger, R., Hoppe, A. and Schäfer, A., 2005. High-resolution seismic survey on the Rhine River in the northern Upper Rhine Graben. International Journal of Earth Sciences, 94(4): 657-668.

Haldimann, P., Naef, H. and Schmassmann, H., 1984. Fluviatile Erosions- und Akkumulationsformen als Indizien jungpleistozäner und holozäner Bewegungen in der Nordschweiz und angrenzenden Gebieten. Nagra Technischer Bericht, 84-16.

Heim, A., 1919. Geologie der Schweiz. Band 1, Molasseland und Juragebirge. C.H. Tauchnitz, Leipzig, 704 pp.

Hinsken, S., Ustaszewski, K. and Wetzel, A., 2007. Graben width controlling syn-rift sedimentation: the Palaeogene southern Upper Rhine Graben as an example. International Journal of Earth Sciences, 96(6): 979-1002.

Hofmann, F., 1960. Beitrag zur Kenntnis der Glimmersandsedimentation in der oberen Süsswassermolasse der Nord- und Nordostschweiz. Eclogae Geologicae Helvetiae, 53(1): 1-25.

Hofmann, F., 1969. Neue Befunde über die westliche Fortsetzung des beckenaxialen Glimmersand-Stromsystems in der oberen Süsswassermolasse des schweizerischen Alpenvorlandes. Eclogae Geologicae Helvetiae, 62(1): 279-284.

Hofmann, F., 1996. Zur plio-pleistozänen Landschaftsgeschichte im Gebiet Hochrhein-Wutach-Randen-Donau: Geomorphologische Überlegungen und sedimentpetrographische Befunde. Eclogae geologicae Helvetiae, 89(3): 1023-1041.

Kälin, D., 1997. Litho- und Biostratigraphie der mittel- bis obermiozänen Bois de Raube-Formation (Nordwestschweiz). Eclogae Geologicae Helvetiae, 90(1): 97-114.

Kemna, H.A., 2008. A Revised Stratigraphy for the Pliocene and Lower Pleistocene Deposits of the Lower Rhine Embayment. Netherlands Journal of Geosciences (Geologie en Mijnbouw), 87(1): 91-105.

Kemna, H.A. and Becker-Haumann, R., 2003. Die Wanderblock-Bildungen im Schweizer Juragebirge südlich von Basel: Neue Daten zu einem alten Problem. Eclogae geologicae Helvetiae, 96(1): 71-83.

Kempf, O., Matter, A., Burbank, D.W. and Mange, M., 1999. Depositional and structural evolution of a foreland basin margin in a magnetostratigraphic framework: the eastern Swiss Molasse Basin. International Journal of Earth Sciences, 88(2): 253–275.

Kock, S., Schmid, S.M., Fraefel, M. and Wetzel, A., in prep. Neotectonic activity in the area of Basel inferred from morphological analysis of fluvial terraces of the Rhine River.

Kuhlemann, J. and Kempf, O., 2002. Post-Eocene evolution of the North Alpine foreland basin and its response to Alpine tectonics. Sedimentary Geology, 152(1-2): 45-78.

Lacombe, O. and Mouthereau, F., 2002. Basement-involved shortening and deep detachment tectonics in forelands of orogens: Insights from recent collision belts (Taiwan, Western Alps, Pyrenees). Tectonics, 21(4).

Lang, U., Gudera, T., Elsass, P. and Wirsing, G., 2005. Numerical modelling of chloride propagation in the quaternary aquifer of the southern Upper Rhine Graben. International Journal of Earth Sciences, 94(4): 550-564.

Laubscher, H., 1961. Die Fernschubhypothese der Jurafaltung. Eclogae geologicae Helvetiae, 54: 221-282.

Laubscher, H., 1967. Exkursion Nr. 14, Basel-Delémont-Biel. Geologischer Führer der Schweiz.

Laubscher, H., 1981. The 3D propagation of decollement in the Jura. In: K.R. McClay and N.J. Price (Editors), Thrust and nappe tectonics; International conference. Special Publication - Geological Society of London, pp. 311-318.

Laubscher, H., 1986. The eastern Jura: relations between thin-skinned and basement tectonics, local and regional. Geologische Rundschau, 75: 535-553.

Laubscher, H., 1992. Jura kinematics and the Molasse Basin. Eclogae geologicae Helvetiae, 85(3): 653-675.

Laubscher, H., 1998. Der Ostrand des Laufenbeckens und der Knoten von Grellingen; die verwickelte Begegnung von Rheingraben und Jura. Eclogae Geologicae Helvetiae, 91(2): 275-291.

Laubscher, H., 2001. Plate interactions at the southern end of the Rhine graben. Tectonophysics, 343(1-2): 1-19.

Laubscher, H., 2003. The Miocene dislocations in the northern foreland of the Alps: Oblique subduction and its consequences (Basel area, Switzerland-Germany). Jahresberichte und Mitteilungen des Oberrheinischen Geologischen Vereins, Neue Folge, 85: 423-439.

Le Carlier de Veslud, C., Bourgeois, O., Diraison, M. and Ford, M., 2005. 3D stratigraphic and structural synthesis of the Dannemarie basin (Upper Rhine Graben). Bulletin de la Société Géologique de France, 176: 433-442.

Liniger, H., 1953. Zur Geschichte und Geomorphologie des nordschweizerischen Juragebirges. Geographica Helvetica, 8(4): 289-303.

Liniger, H., 1966. Das Plio-Altpleistozäne Flussnetz der Nordschweiz. Regio Basiliensis, 7(2).

Liniger, H., 1967. Pliozän und Tektonik des Juragebirges. Eclogae geologicae Helvetiae, 60(2): 407-490.

Lopes Cardozo, G.G.O. and Behrmann, J.H., 2006. Kinematic analysis of the Upper Rhine Graben boundary fault system. Journal of Structural Geology, 28(6): 1028-1039.

Madritsch, H., Schmid, S.M. and Fabbri, O., 2008 (accepted). Interactions of thin- and thick-skinned tectonics along the northwestern front of the Jura fold-and-thrust-belt (Eastern France). Tectonics.

Madritsch, H., Schmid, S.M. and Fabbri, O., submitted. Interactions of thin- and thick-skinned tectonics along the northwestern front of the Jura fold-and-thrust-belt (Eastern France). . Tectonics.

Mosar, J., 1999. Present-day and future tectonic underplating in the western Swiss Alps: reconciliation of basement/wrench-faulting and decollement folding of the Jura and Molasse basin in the Alpine foreland. Earth and Planetary Science Letters, 173(3): 143-155.

Müller, W.H., Naef, H. and Graf, H.R., 2002. Geologische Entwicklung der Nordschweiz, Neotektonik und Langzeitszenarien Zürcher Weinland. Nagra Technischer Bericht, 99-08.

Niviere, B. and Winter, T., 2000. Pleistocene northwards fold propagation of the Jura within the southern Upper Rhine Graben: seismotectonic implications. Global and Planetary Change, 27(1-4): 263-288.

Petit, C., Campy, M., Chaline, J. and Bonvalot, J., 1996. Major palaeohydrographic changes in Alpine foreland during the Pliocene - Pleistocene, pp. 131-143.

Pfiffner, O.A., 2006. Thick-skinned and thin-skinned styles of continental contraction. Special Paper - Geological Society of America, 414: 153-177.

Philippe, Y., Colletta, B., Deville, E. and Mascle, A., 1996. The Jura fold-and-thrust belt: a kinematic model based on map-balancing. In: Peri-Tethys memoir 2; Structure and prospects of Alpine basins and forelands, Eds: Ziegler, Horvath / Memoires du Museum National d'Histoire Naturelle, 170: 235-261.

Rahn, M.K. and Selbekk, R., 2007. Absolute dating of the youngest sediments of the Swiss Molasse basin by apatite fission track analysis. Swiss Journal of Geosciences, 100(3): 371-381.

Rolf, C., Hambach, U. and Weidenfeller, M., 2008. Rock and palaeomagnetic evidence for the Plio-Pleistocene palaeoclimatic change recorded in Upper Rhine Graben sediments (Core Ludwigshafen-Parkinsel) Netherlands Journal of Geosciences (Geologie en Mijnbouw), 87(1): 41-50.

Rotstein, Y., Behrmann, J.H., Lutz, M., Wirsing, G. and Luz, A., 2005a. Tectonic implications of transpression and transtension: Upper Rhine Graben. Tectonics, 24(6).

Rotstein, Y., Schaming, M. and Rousse, S., 2005b. Structure and Tertiary tectonic history of the Mulhouse High, Upper Rhine Graben: Block faulting modified by changes in the Alpine stress regime. Tectonics, 24(1).

Roure, F., Brun, J.-P., Colletta, B. and Vially, R., 1994. Multiphase extensional structures, fault reactivation, and petroleum plays in the Alpine foreland Basin of southeastern France. In: Mascle, A (Ed.), Hydrocarbon and Petroleum Geology of France, Europ. Assoc. Petrol. Geosci., Spec. Publ., 4: 245-268.

Rózsa, S. et al., 2005. Determination of displacements in the upper Rhine graben Area from GPS and leveling data. International Journal of Earth Sciences, 94(4): 538-549.

Schlatter, A., Schneider, D., Geiger, A. and Kahle, H.-G., 2005. Recent vertical movements from precise levelling in the vicinity of the city of Basel, Switzerland. Int Journ Earth Sciences, 94(4): 507-514.

Schreiner, A., 1965. Die Juranagelfluh im Hegau. Jahresheft Geologisches Landesamt Baden-Württemberg, 7(303-354).

Simpson, G., 2004a. A dynamic model to investigate coupling between erosion, deposition, and three-dimensional (thin-plate) deformation. Journal of Geophysical Research-Earth Surface, 109(F2).

Simpson, G., 2004b. Role of river incision in enhancing deformation. Geology, 32(4): 341-344.

Sissingh, W., 2006. Syn-kinematic palaeogeographic evolution of the West European Platform: correlation with Alpine plate collision and foreland deformation. Netherlands Journal of Geosciences-Geologie En Mijnbouw, 85(2): 131-180.

Skinner, B.J. and Porter, S.C., 1995. The Dynamic Earth, An Introduction to Physical Geology, New York, 567 pp.

Tesauro, M., Hollenstein, C., Egli, R., Geiger, A. and Kahle, H.G., 2005. Continuous GPS and broad-scale deformation across the Rhine Graben and the Alps. International Journal of Earth Sciences, 94(4): 525-537.

Twidale, C.R., 2004. River patterns and their meaning. Earth-Science Reviews, 67(3-4): 159-218.

Ustaszewski, K. and Schmid, S.M., 2006. Control of preexisting faults on geometry and kinematics in the northernmost part of the Jura fold-and-thrust belt. Tectonics, 25(5).

Ustaszewski, K. and Schmid, S.M., 2007. Latest Pliocene to recent thick-skinned tectonics at the Upper Rhine Graben - Jura Mountains junction. Swiss Journal of Geosciences, 100(2): 293-312.

Ustaszewski, K., Schumacher, M.E., Schmid, S.M. and Nieuwland, D., 2005. Fault reactivation in brittle-viscous wrench systems - Dynamically scaled analogue models and application to the Rhine-Bresse transfer zone. Quaternary Science Reviews, 24: 365-382.

Ustaszewski, K.M., 2004. Reactivation of pre-existing crustal discontinuities: the southern Upper Rhine Graben and the northern Jura Mountains: a natural laboratory PhD Thesis, University of Basel.

Verderber, R., 1992. Quartärgeologische Untersuchungen im Hochrheingebiet zwischen Schaffhausen und Basel. PhD Thesis, University of Freiburg i.Br.

Verderber, R., 2003. Quartärgeologie im Hochrheingebiet zwischen Schaffhausen und Basel. Zeitschrift der Deutschen Gesellschaft für Geowissenschaften, 154(2-3): 369-406.

Villinger, E., 1998. Zur Flussgeschichte von Rhein und Donau in Südwestdeutschland. Jahresberichte und Mitteilungen des Oberrheinischen Geologischen Vereins, Neue Folge, 80: 361-398.

Villinger, E., 1999. Freiburg im Breisgau - Geologie und Stadtgeschichte. Informationen LGRB, 12.

Villinger, E., 2003. Zur Paläogeographie von Alpenrhein und oberer Donau. Zeitschrift der Deutschen Gesellschaft für Geowissenschaften, 154(2-3): 193-253.

Westerhoff, W.E., Kemna, H.A. and Boenigk, W., 2008. The confluence area of Rhine, Meuse, and Belgian rivers: Late Pliocene and Early Pleistocene fluvial history of the northern Lower Rhine Embayment Netherlands Journal of Geosciences (Geologie en Mijnbouw), 87(1): 107-125.

Wittmann, O., 1961. Die Niederterrassenfelder im Umkreis von Basel und ihre kartographische Darstellung. Basler Beiträge zur Geographie und Ethnologie, 3.

Ziegler, P.A. and Dèzes, P., 2007. Cenozoic uplift of Variscan Massifs in the Alpine foreland: Timing and controlling mechanisms. Global and Planetary Change, 58: 237-269.

Chapter 3

Quaternary tectonic activity in the eastern Jura Mountains: Implications from stream gradient analysis

Abstract

A complicated tectonic setting characterises the area at the southern end of the Upper Rhine Graben in the northern foreland of the Central Alps. While the recorded seismicity and geodetic measurements demonstrate ongoing tectonic activity near the eastern Main Border Fault of the Upper Rhine Graben and in the Jura mountains, these data do not allow constraining the regional deformation pattern or determining individual active faults due to low deformation rates of less than 1 mm/a.

In this study, we investigate the effect of differential vertical deformation on the fluvial system at the boundary of the Jura mountains, consisting of the Jura fold-and-thrust belt and the Tabular Jura, and the Upper Rhine Graben. To this aim, we analyse the gradient distribution in the longitudinal profiles of 50 rivers in this area, based on a digital elevation model with a spatial resolution of 25 m. For each river, the shape of the longitudinal profile is characterised by calculating two geomorphic indices, the steepness and concavity index. In addition, the steepness index is determined for river segments, enabling us to detect alongstream changes. From the distribution of the steepness indices we deduce, relative to the Tabular Jura, uplift of a region roughly corresponding to the Jura fold-and-thrust belt, as well as subsidence of the interior parts of the Upper Rhine Graben.

3.1 Introduction

The border region of Switzerland, France and Germany in the vicinity of Basel is characterised by the adjoining tectonic units of the Upper Rhine Graben and the Jura fold-and-thrust belt. The Upper Rhine Graben represents a part of the European Cenozoic Rift System, which extends from the Mediterranean Sea to the North Sea (Ziegler, 1992). The thin-skinned Jura fold-and-thrust belt developed after the main rifting phase in the Miocene and forms the most external element of the Central Alpine orogen (Burkhard, 1990). While the evolution of these partly overlapping and

interfering structures is quite well understood on a large timescale (Burkhard and Sommaruga, 1998; Dèzes et al., 2004), the youngest (Late Miocene to Quaternary) tectonic development of the region remains less well constrained. In particular, the question of if and where shortening, or tectonic activity in general, persists today in the Jura fold-and-thrust belt is difficult to answer. This is mainly due to a major hiatus in the sedimentary record between the Middle Miocene (Early Tortonian) and the Middle Pliocene, and the difficulties associated with dating the existing Miocene as well as the Plio-/Pleistocene fluvial sediments. However, knowledge about where deformation is concentrated and which faults are likely reactivated in the current stress field is crucial to better define the earthquake hazard. It is evident from the Basel earthquake of 1356, the largest earthquake north of the Alps in historic times (Mayer-Rosa and Cadiot, 1979), that this hazard is substantial. Seismologic and geodetic measurements indicate ongoing tectonic activity, but do not describe the deformation pattern in much detail due to their relatively short observation periods (Müller et al., 2002).

In this study, we apply geomorphological methods to complement existing geological, seismological and geodetic information. The fact that tectonic deformation can be accumulated and preserved in the shape of the landscape provides an additional source of information and offers an opportunity to extend the time-scale of observation from the few decades covered by seismologic and geodetic records further into the past. A wide variety of geomorphic features, such as mountain front morphology, valley shapes, or drainage patterns, can reveal information about past tectonic events (Burbank and Anderson, 2001; Keller and Pinter, 2002). In this study we concentrate on the characteristics of river channels and, in particular, river gradients. A number of recent studies have successfully used stream gradient analysis to detect differential vertical deformation (Merritts and Vincent, 1989; Lague et al., 2000; Snyder et al., 2000; Kirby et al., 2003; Hodges et al., 2004). Our aim is to apply these methods in an attempt to better define the recent regional tectonic deformation pattern in NW Switzerland, an essential step towards assessing the seismic hazard in this densely populated area.

3.1.1 Geographic and tectonic setting

The study area in the eastern Jura mountains of northwestern Switzerland covers about 2500 km^2 and comprises part of the tectonic units of the Folded Jura, the Tabular Jura and the Upper Rhine Graben (Figure 1). The Upper Rhine Graben forms a part of the Western European Cenozoic rift system, together with the Lower Rhine Graben and the Bresse Graben, to which it is linked by the Rhine-Bresse Transfer Zone (Ziegler, 1992; Dèzes et al., 2004). At its southern end, the Tertiary sedimentary fill of the Upper Rhine Graben is bordered by Mesozoic sediments, ranging from the
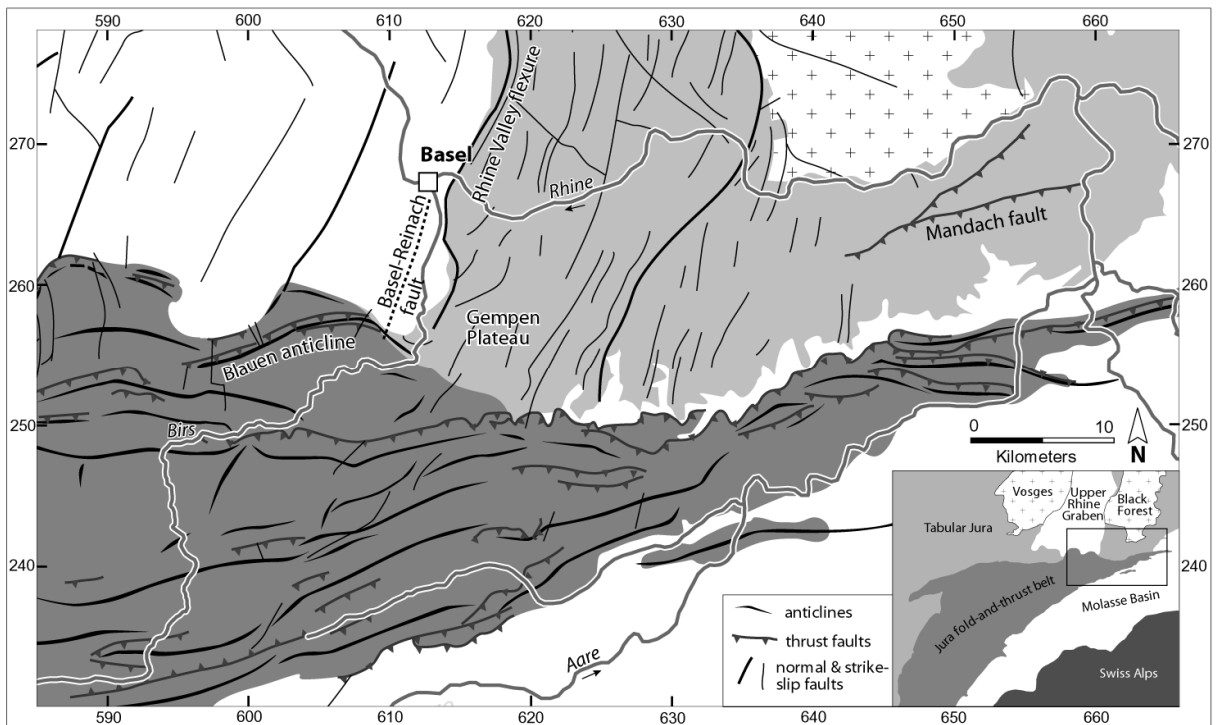
Fig. 1: Main tectonic elements of the study area. Black rectangle shows extent of Figures 4, 6, 7, and 10.

Lower Triassic to the Upper Jurassic. The Triassic sequences include sandstones, dolomites, (bioclastic) limestones and evaporites, whereas in the Jurassic marls, clays and (oolitic) limestones predominate (Meyer, 2001; Diebold et al., 2006). The thickness of distinct lithological units varies from ca. 20 m to ca. 100 m. In the autochthonous Tabular Jura, the sedimentary layers are still more or less horizontal, which gives the landscape its table-like appearance. In the Folded Jura, the sedimentary cover was detached from the basement on highly incompetent Triassic evaporites, creating anticlines and synclines that still define the ridges and valleys of this region today. It is commonly interpreted as a text-book example of a thin-skinned foreland fold-and-thrust belt (Jordan, 1992; Burkhard and Sommaruga, 1998).

The highest ridges of the Folded Jura define the drainage divide between the river Rhine in the north and, in the south, the river Aare, which drains into the Rhine at the eastern termination of the Jura fold-and-thrust belt (Figure 1). The Upper Rhine Graben constitutes the regional base level of all rivers in this analysis.

3.1.2 Tectonic evolution since Oligocene times

The Neogene stress regime in the Northern Alpine foreland has been subject to important changes, which have led to a complex tectonic setting with multiple fault sets of different orientations. Rifting of the Upper Rhine Graben started in the Late Eocene in a stress field

_____

compatible with E-W extension (Dèzes et al., 2004). Contemporaneously, rifting occurred in the Bresse Graben, linked to the Upper Rhine Graben by the Rhine-Bresse Transfer Zone, which acted as a zone of left-lateral transtension (Lacombe et al., 1993; Ustaszewski et al., 2005; Madritsch et al., 2008). The formation of this transfer zone was controlled by pre-existing, ~ENE-WSW trending basement faults related to a Permo-Carboniferous trough system.

In the Miocene, the regional stress field underwent a major change from E-W extension to NW-SE shortening associated with convergence in the Alps. The stresses emanating from the Alpine arc subsequently led to the detachment of the sedimentary cover on a Triassic decollement horizon and the formation of the Jura fold-and-thrust belt (Laubscher, 1961). Constraints on the timing of Jura deformation are given by the (late) Middle Miocene Bois de Raube and Juranagelfluh fluvial sediments (Kälin, 1997), originating from the Vosges and Black Forest mountains, respectively. These conglomerates were affected by folding in the region W of Basel (Giamboni et al., 2004a) and overridden by external thrusts in the Bresse graben and thus predate the beginning of folding (Chauve et al., 1988). Complex interactions between tectonic activity in the Jura fold-and-thrust belt and the southern Upper Rhine Graben are demonstrated by the fact that the Mesozoic of the frontal part of the fold-and-thrust belt was thrusted onto Rhine Graben sediments (Dèzes et al., 2004), while at the same time Rhine Graben-related faults can be followed further south and into the Folded Jura (Figure 1; (Laubscher, 2001; Ustaszewski and Schmid, 2006). In addition, the position of Permo-Carboniferous faults in the crystalline basement predetermined the location of thrust faults that developed in the Jura belt during the Miocene (Laubscher, 1986; Noack, 1995). Since the Late Pliocene, compressional reactivation of these basement faults has appeared to control folding in the sedimentary cover, which is very probably ongoing at present (Ustaszewski and Schmid, 2006). This "thick-skinned" deformation style is also documented by folded Pliocene fluvial gravels in the Ajoie region of eastern France (Giamboni et al., 2004a). No sediments have been preserved in the region from the timespan between ~10 and 5 Ma.

3.1.3 Previous geomorphological studies on neotectonics in the eastern Jura mountains – Upper Rhine Graben area

A number of studies have used geomorphologic approaches to analyse recent or active tectonic deformation in the area of the eastern Jura mountains and the Upper Rhine Graben. Giamboni et al. (2004b) inferred ongoing subsidence of the Upper Rhine Graben as well as local uplift at the front of the Folded Jura from the analysis of deformed sedimentary terraces and changes in drainage patterns. Graf (1993) studied Late Pliocene gravels (~2 Ma) of Alpine origin that lie

north of the topographic high formed by the Mandach thrust fault, suggesting that this north-vergent fault was active in the Pleistocene. Due to their relatively continuous distribution, a number of studies have addressed the Late Quaternary cut-and-fill terrace systems of the rivers Rhine and Aare (Penck and Brückner, 1909; Wittmann, 1961; Graul, 1962). Haldimann et al. (1984) studied the lower Aare river pattern and terrace systems, as well as the morphology of the bedrock channel below the Quaternary valley fill, between Aarau and the confluence with the Rhine; they suggested a regional tilt to the north in Late Pleistocene and Holocene times. From an investigation of the present-day position of the Rhine terraces between Basel and Schaffhausen, Verderber (2003) inferred possible vertical tectonic dislocations in the vicinity of the Upper Rhine Graben. Together, these analyses demonstrate that evidence of recent tectonic activity can be found at several locations in NW Switzerland, but they do not allow conclusions to be drawn about the general deformation pattern, mainly because detailed information from the Jura fold-and-thrust belt itself is missing.

3.1.4 Seismotectonic and geodetic constraints on present-day tectonic activity

Information on present-day tectonic activity in the study area mainly comes from seismologic and geodetic data, which both indicate continuing tectonic deformation (Müller et al., 2002). The occurrence of large earthquakes in historical times, such as the 1356 event in Basel with a magnitude M_W between 6.2 (Lambert et al., 2004) and 6.9 (Fäh et al., 2003), demonstrates the ongoing tectonic activity and the potential for destructive earthquakes in this intraplate region. Fault plane solutions indicate mainly strike-slip and normal-faulting deformation in the area around Basel, where many earthquakes are large enough for calculating a fault plane solution. However, there seems to be a change in the predominant faulting style from strike-slip and normal to reverse going further west (Figure 2; see also discussion in Chapter 5). Stress inversion of a large number of fault plane solutions in NW Switzerland yields a maximum horizontal stress direction of approximately SE-NW in the basement (Kastrup et al., 2004), while surficial in-situ stress measurements (from a combination of different borehole measurement techniques) carried out in the Jura fold-and-thrust belt point to a ca. NNW-SSE directed maximum horizontal stress orientation (Becker, 2000). This is in agreement with an observed orientation change of borehole breakouts in a borehole that crosses the Triassic detachment horizon (Müller et al., 1987), implying a decoupling of the stress field at this boundary. However, this is no proof for ongoing decollement processes, as the detachment horizon may be too shallow today to deform in plastic style (Ustaszewski and Schmid, 2007), due to uplift and erosion of at least 1 km of sediments in the past 5 Ma in the Alpine foreland (Cederbom et al., 2004).
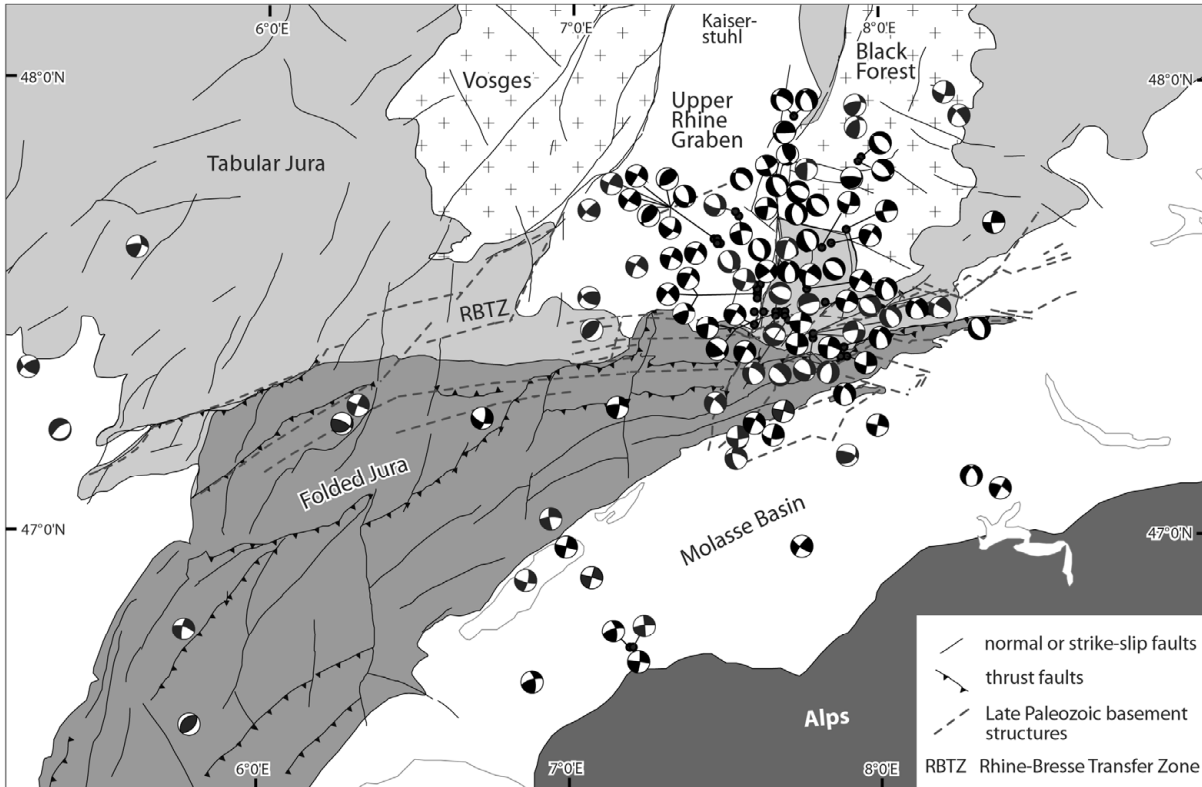
Figure 2. Fault plane solutions in the wider study area (Jura mountains, southern Upper Rhine Graben, Rhine-Bresse Transfer Zone). Sources: See Chapter 5.

Despite the observed earthquake activity and a relatively dense seismic network, it remains difficult to assign the seismicity to individual faults. Active faults have been postulated to belong to the Permo-Carboniferous trough system in the crystalline basement (Meyer et al., 1994; Ustaszewski and Schmid, 2006), and activity cannot be excluded on the Upper Rhine Graben fault system. The most pronounced structure of this NNE-SSW oriented fault system in the study area is the so-called Rhine Valley flexure (Figure 1), which represents the southward extension of the eastern Main Border Fault of the Upper Rhine Graben. In addition, Ferry et al. (2005) suggested recent normal faulting activity on an ESE-dipping fault – the so-called Basel-Reinach fault (Figure 1) – based on the interpretation of trench investigations south of the city of Basel.

Precise levelling measurements over decadal time scales appear to provide some evidence for differential relative uplift in NW Switzerland (Schlatter, 2006), although this is fairly equivocal due to the low measurement point density. However, levelling points in the Folded Jura seem to be uplifted with reference to stations in the Tabular Jura. Maximum rates of this relative movement are ca. 0.25 mm/a, i.e. close to the level of uncertainty (Schlatter, 2007; Zippelt and Dierks, 2007). Significant subsidence of ca. 0.6 (± 0.15) mm/a was found in the Upper Rhine Graben south of Freiburg, relative to a reference point at the Tabular Jura – Black Forest

boundary (Zippelt and Dierks, 2007). In contrast, levelling measurements carried out across the eastern Main Border Fault of the Upper Rhine Graben in the vicinity of Basel, covering a time span of ca. 30 years, could not detect any differential vertical movement above uncertainty (Schlatter et al., 2005). GPS measurements, which have been carried out for a maximum of ca. 20 years, show displacements that are still within uncertainty of the measurement (Rózsa et al., 2005).

3.2 Geomorphological indicators of tectonic activity

The shape of the landscape in a tectonically active setting is the result of the competing forces of tectonic and surface processes. Tectonic deformation leaves a signal in the shape of the surface, which is then subjected to erosional and sedimentary processes. A fingerprint of differential uplift can be observed at the surface if the tectonic event was recent enough (or ongoing) in order to not be erased by erosion and sedimentation. This approach has also been used quantitatively in the study of hillslope distributions (using digital elevation models) to trace tectonically active structures (Wobus et al., 2006b). However, a young tectonic signal is often not easy to detect in the distribution of hillslope gradients: In areas with high uplift rates, hillslopes have a threshold steepness above which the slope morphology is controlled by landsliding processes (Montgomery and Brandon, 2002), whereas in areas with low deformation rates the hillslope distribution is often dominated by older (and possibly inactive) structures (like inherited folds) and other factors, such as resistance to erosion.

Because of their higher erosive power, rivers are less subject to threshold gradients and to the influence of varying erodibility. For this reason, they tend to develop a characteristic longitudinal profile where the river gradient continuously decreases with downstream increasing discharge ('concave up'), all else being equal, as documented in numerous studies (e.g., Mackin (1948); Hack (1957). This observation can be explained by a model of stream incision in which the erosive power of a stream is a function of the discharge and the slope at any point in the river (Leopold et al., 1964; Howard and Kerby, 1983; Tucker and Slingerland, 1996; Whipple and Tucker, 1999). A number of variations on this general model have been proposed; for a review, see Whipple (2004).

Rivers are very sensitive to tectonically induced changes (e.g., varying uplift rates) along their courses. In steady-state conditions, where rock uplift is balanced by river incision, the form of the river profile may contain information on spatial variations in rock uplift rate (Whipple and Tucker, 1999; Snyder et al., 2000; Kirby and Whipple, 2001; 2002). Alternatively, in transient

conditions when rock uplift and incision rates are not in equilibrium, departures from the expected longitudinal river profile can be used to suggest recent or ongoing tectonic activity (Burbank and Anderson, 2001; Kirby et al., 2007; Oskin and Burbank, 2007). The fact that rivers are sensitive to tectonic forcing and hence are capable of recording spatial variations in rock uplift rates in their longitudinal profiles has been demonstrated in experimental studies (Ouchi, 1985) as well as in studies on rivers in tectonic settings with known uplift rates (Merritts and Vincent, 1989; Kirby and Whipple, 2001; Duvall et al., 2004).

To quantify departures from the equilibrium profile, we use the observation that stream gradient and upstream drainage area at every point along the river can be described by a power-law function (e.g., Hack, 1973; Flint, 1974; Howard and Kerby, 1983)(Hack, 1973; Flint, 1974; Howard and Kerby, 1983):

$$S = k\,A^{-\theta} \qquad\qquad\qquad [1]$$

where S is the slope, A is the upstream drainage area, while k and θ are constants. Drainage area is typically assumed to be a proxy for discharge. Although this may not always be the case (Huang and Niemann, 2006), it is often a reasonable assumption for the largest part of many rivers, apart from their uppermost reaches.

It follows that

$$\log S = k_s - \theta \log A \qquad\qquad\qquad [2]$$

with $k_s = \log(k)$. This relationship plots as a linear correlation between slope and drainage area in double-logarithmic diagrams (Figure 3), downstream of some critical drainage area A_{cr} which is commonly interpreted as the transition from hillslope or debris-flow to fluvial processes (Dietrich et al., 1993; Stock and Dietrich, 2003). The constants k_s and θ represent the increment and slope of this straight line and are referred to as steepness index and concavity index, respectively. They can be calculated by a linear regression and used to compare the complete longitudinal profiles of different rivers as well as different segments of a single river. The value of θ mainly reflects the characteristics of basin hydrology and the dominant erosion process, while k_s is influenced by rock strength, channel bed material, runoff, and sediment load (Whipple and Tucker, 1999; Snyder et al., 2000). For an in-depth description of this method, as well as for field examples, see Snyder et al. (2000), Kirby et al. (2003), and Wobus et al. (2006a).
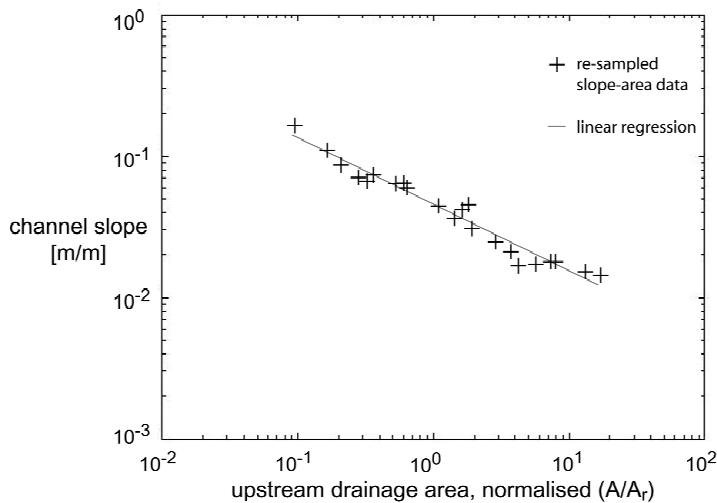
Figure 3. Linear double-logarithmic relation between slope and catchment area for the Etzgerbach (river 38, Table 1). Slope and area values are re-sampled using a moving window over a constant vertical interval of 10 m; area values are normalised by the median catchment size A_r.

While river longitudinal profiles and the concept of stream gradients decreasing downstream have been used to infer tectonic deformation for many years (Hack, 1973; Merritts and Vincent, 1989), slope-area investigations have only recently gained importance due to the increasing availability and higher accuracy of digital elevation models with a reasonable resolution (for a notable exception see Howard and Kerby (1983)). A major advantage of this approch is that changes in channel slope that may occur at river confluences, due to the corresponding increase in runoff, are not considered in the analysis, in contrast to studies that compare channel slope and river length. Whereas a number of analyses have been carried out in the Himalayas and California, where high (relative) uplift rates prevail, only few studies have investigated slope-area relations in intraplate, low-deformation rate settings (e.g., Marple and Talwani, 2000).

Small-scale erodibility variations along the river course due to lithological changes in a geologically complex area could be expected to introduce a large amount of non-tectonic disturbances into the slope-area distribution. However, if the steepness and concavity indices are calculated over the whole length of the rivers, and if the widths of the different lithologies that are crossed by the river are very short compared to the total length of the river, we can assume that most of these variations will be averaged out in the regression. To determine if this assumption is valid also for the analysis of river segments, we combined our slope-area investigations with the available lithological information from geological maps and field observations.

Another possible factor causing deviations from equilibrium conditions are past climatic changes. The northern Alpine foreland has experienced approximately 26 changes from a cool to a warm climate and back during the last 2.6 Ma (Müller et al., 2002). The influence of these

variations on river profiles has been recently investigated by Carretier et al. (2006), who modelled the effect of different climatic variations on river profiles featuring knickpoints in the southern Upper Rhine Graben. They showed that a) the amplitudes of the climatically-induced model knickpoints were much smaller than those observed in the field, and b) the response time of the system to climatic oscillations is greater than the oscillation wavelength. From this we conclude that the effect of climatic changes on the shape of the river profiles we see today is negligible in the study area.

3.3 Methodology

We examined 50 rivers in the eastern Jura mountains and the adjoining southern Upper Rhine Graben (Figure 4), focussing on spatial patterns in the steepness and concavity index distributions. Our analysis is based on the information in a (mainly) contour-line derived digital elevation model (DEM) with a cell size of 25 m and a mean vertical accuracy of 2 m (DTM25, Swisstopo). After removing internal hydrological sinks (i.e., artefacts resulting from inaccuracies in the data) the flow paths were constructed using built-in flow-direction, flow-accumulation and flow-length procedures in a GIS (Geographic Information system). Rivers were selected for our analysis if they had a minimum length of 3 km and if their courses showed no significant anthropogenic influence, such as dams or diversion, which are common due to the intensive use of the area. Trunk streams were defined following the maximum flowlength (distance to the drainage divide) from a chosen starting point. For each river, an individual point dataset was created containing altitude, upstream drainage area and distance to the drainage divide, with points every 25 to 35 m. The starting point of each river was set at a minimum drainage area of 100 cells (62500 m^2).

To assess the quality of these automatically derived data, they were compared with the plan-view river courses on 1:25000 topographic maps and, in a few cases, with longitudinal profiles determined from the contour lines on 1:10'000 topographic maps (Figure 5). Field investigations yielded additional information on the accuracy of the data. Fit to the map-view river course was generally very good, while the longitudinal profile derived from the DEM in some cases did not fully capture the incision of very small channels (see Figure 5). A significant difference between the automatically derived river course and the one given by the topographic map occurred in one case (river No 41). For river No 19 the procedure did not yield a representative longitudinal profile because of the occurrence of karst in the drainage basin. The channel slope was calculated using elevation and distance over three cells. For the calculation of the concavity and steepness indices over the whole length of the rivers, the longitudinal profiles were smoothed by re-sampling to a constant vertical interval of 10 m, in order to avoid any bias related to the
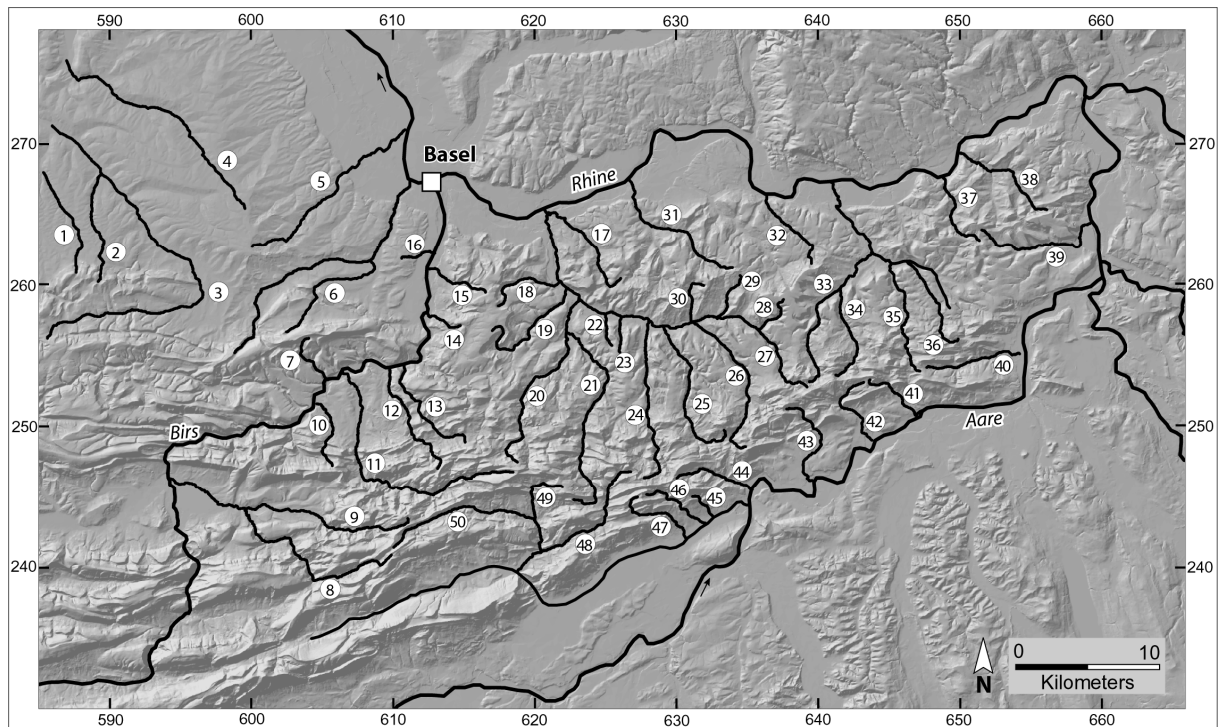
Figure 4: Overview of the studied rivers, with the 25 m DEM shaded relief as background. For river details see Table 1. Reproduced by permission of swisstopo (BA081777).

vertically irregular data point distribution, as well as to eliminate small errors in the digital elevation model and other minor discrepancies from the true river course (e.g., bridges). For a more extensive discussion of different smoothing methods, see Wobus et al. (2006a). The effect of DEM resolution on different drainage basin characteristics was analysed by Hancock (2005). His results suggest that while some detail in the slope-area relationship is lost with increasing cell size of the digital elevation model, the slope of the straight portion of the regression line essentially remains the same; however, the intercept seems to be systematically lower at larger cell sizes. This implies that for a purely comparative use of the indices, it is not necessary to work with higher-resolution data.

In a first step, we calculated the steepness index and the concavity index for each river in a linear regression, determining both variables at the same time, and we analysed their spatial distribution. In order to remove the scale dependence from the slope-area relation given in equation [1] (Sklar and Dietrich, 1998), we normalised the area data by the median catchment size A_r (=1.4×10^6 m^2), thus using the new equation

$$S = S_R * (A/A_r)^{-\theta} \tag{3}$$
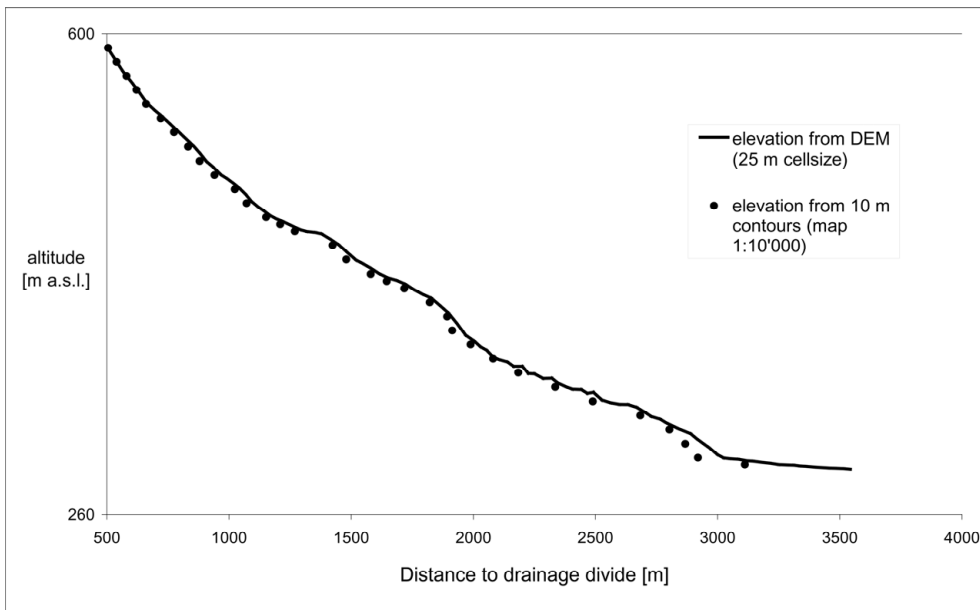
Figure 5: Comparison of the longitudinal profile of the Lolibach (river 14, Table 1) derived from the 25 m digital elevation model and a 1:10'000 topographic map (10 m contours). Note the generally excellent agreement, except for the lowermost reaches of the profile where the river flows through a narrow gorge.

and calculating S_R instead of k_s (S_R = increment of the straight line in this relation). Other studies have demonstrated that the results from this method are comparable to those obtained by calculating k_s using a fixed value for θ to remove the interdependence (e.g., Snyder et al., 2000; Kirby et al., 2003).

In a second step, the steepness and concavity index distributions were analysed in more detail. For that purpose, the rivers were divided into segments of 1 km length. In order to calculate the steepness index for such segments, the data could no longer be smoothed using constant vertical intervals because of the small number of data points within each segment. Hence, in this case, the data were subjected to a procedure that removed small-scale peaks in the longitudinal profile. Instead of normalising the area data by a common reference area we used a fixed θ, corresponding to the regional mean of the free regression; this makes the steepness indices k_s of the segments comparable. Note that the segments were arbitrarily defined as 1 km long, without previous analysis of the longitudinal profiles and the location of potential irregularities.

3.4 Results

Figures 6 and 7 show the steepness indices (S_R) and concavity indices (θ) resulting from the free-fit calculation using data over the entire length of the river courses. All values are listed in Table 1.
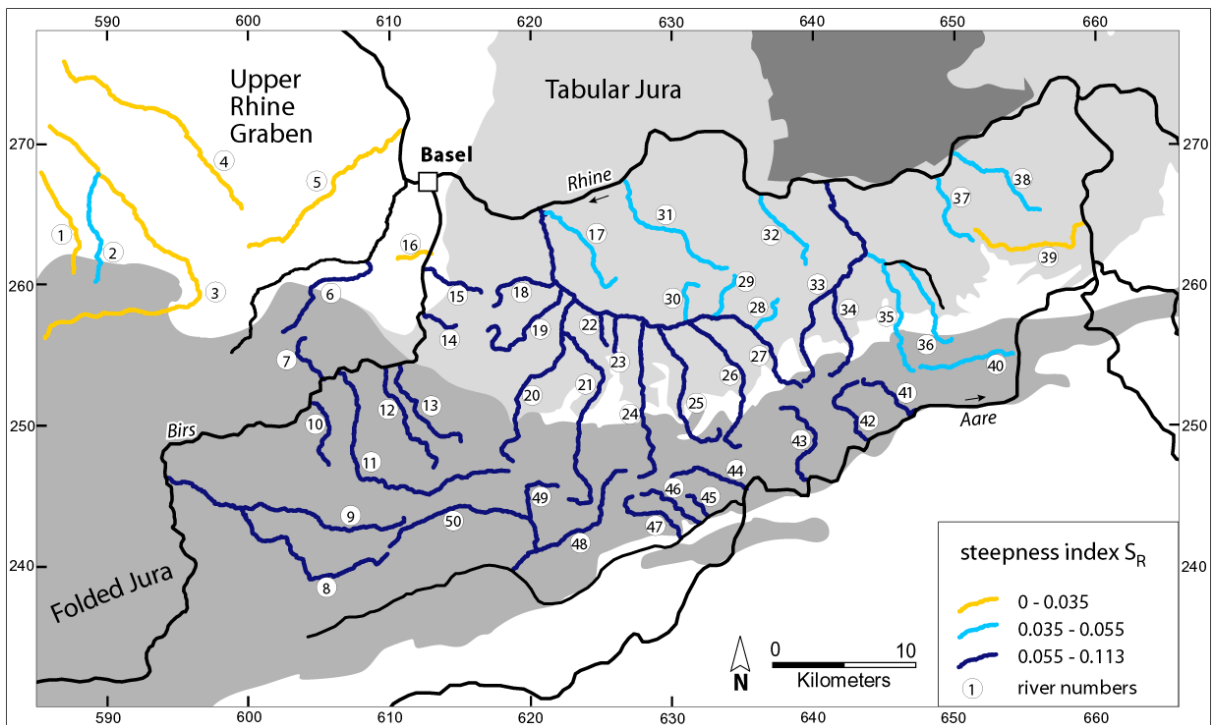
Figure 6: Map with steepness index S_R for entire river courses (yellow: 0-0.035, light blue: 0.035-0.055, dark blue: 0.055-0.113). High steepness indices are mainly found in rivers originating in the Jura fold-and-thrust belt, whereas low steepness indices concentrate in the Upper Rhine Graben. Numbers refer to Table 1.
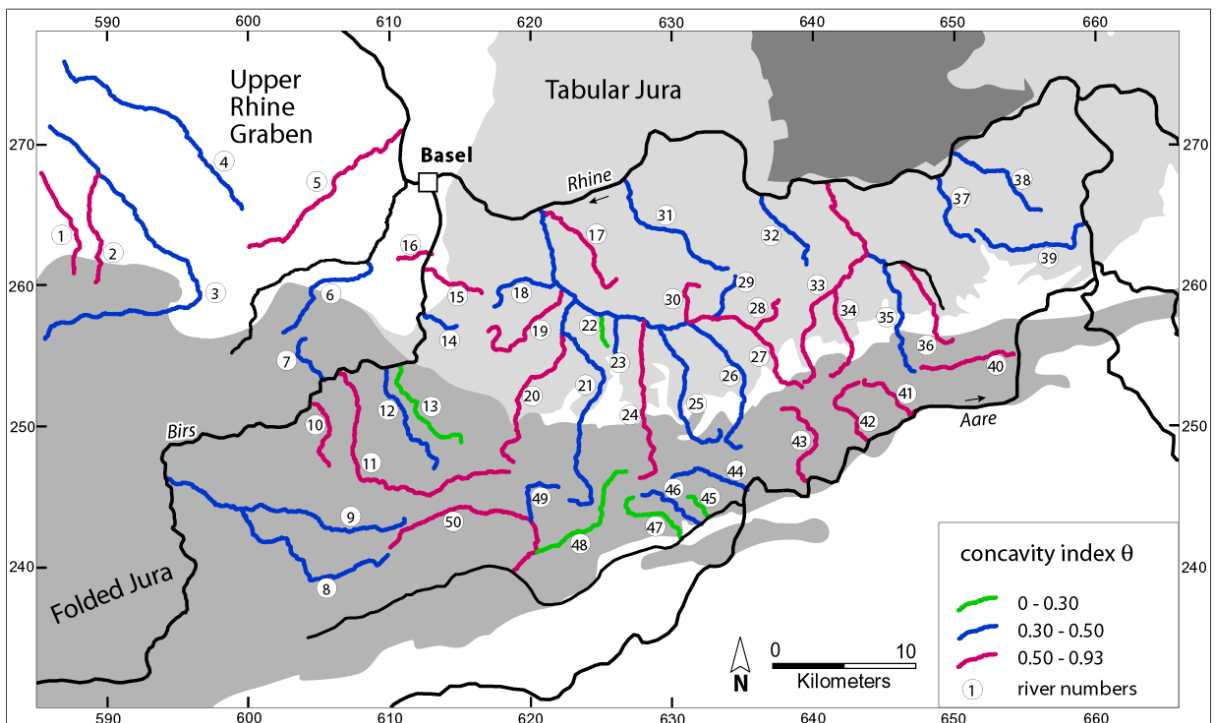
Figure 7: Map with concavity index θ for entire river courses (green: 0-0.3, blue: 0.3-0.5, purple: 0.5-0.9273). No systematic spatial distribution is found for the concavity indices in the study area. Numbers refer to Table 1.

ID	river name	concavity index (entire river)	steepness index (entire river)	variations of ks for segments	comments
1	Feldbach	0.567	0.031	small	
2	Geischbach	0.645	0.037	small	
3	Ill	0.372	0.025	small	
4	Thalbach	0.313	0.020	small	
5	Lertzbach	0.573	0.033	small	
6	Binnbach	0.469	0.058	large	variation can be explained by lithol. effects
7	Dittingerbach	0.412	0.078	small	
8	Gabiare	0.445	0.082	large	partly explained by lithological effects
9	Scheltenbach	0.421	0.083	small	
10	Wahle	0.584	0.066	small	
11	Lüssel	0.506	0.087	large	
12	Ibach	0.393	0.090	large	
13	Chastelbach	0.012	0.064	large	
14	Lolibach	0.325	0.084	small	
15	Arlesheimerbach	0.506	0.082	large	
16	Gretlibach	0.927	0.017	small	
17	Arisdörferbach	0.546	0.048	small	
18	Rösernbach	0.464	0.060	small	
19	Orisbach	0.797	0.098	large	karst in upper part of catchment
20	Hintere Frenke	0.704	0.113	large	
21	Vordere Frenke	0.432	0.067	large	
22	Buechhalden	0.155	0.059	small	
23	Talbächli	0.499	0.057	small	
24	Diegterbach	0.532	0.080	small	
25	Homburgerbach	0.460	0.057	small	
26	Eibach	0.436	0.059	large	
27	Ergolz	0.540	0.059	small	
28	Duebach	0.682	0.051	small	
29	Hemmiker	0.494	0.037	small	
30	Rickebächli	0.630	0.051	small	
31	Magdenerbach	0.368	0.044	large	
32	Fischingerbach	0.372	0.055	large	
33	Bruggbach	0.531	0.070	small	
34	Dorfbach (Sissle)	0.519	0.066	small	
35	No 35	0.396	0.044	small	
36	Zeiherbach	0.521	0.048	small	
37	Sulzerbach	0.393	0.047	small	
38	Etzgerbach	0.473	0.045	small	
39	Schmittenbach	0.415	0.035	small	
40	Talbach	0.513	0.054	small	
41	Aabach	0.515	0.075	large	artefact from dem
42	Erzbach	0.512	0.082	large	
43	Stüssliger	0.556	0.064	small	
44	Dorfbach	0.425	0.080	small	
45	No 45	0.255	0.102	small	
46	No 46	0.303	0.094	small	
47	Cholersbach	0.137	0.089	large	explained by lithological effects
48	Augstbach	0.273	0.064	large	explained by landslide effects
49	Limmerenbach	0.331	0.099	small	
50	Mümliswilerbach	0.548	0.088	large	explained by landslide effects
	range	0.012 – 0.927	0.017 – 0.130		
	arithmethic mean	0.464	0.064		

The S_R values vary from 0.017 to 0.113, around an arithmetic mean of 0.064. The geographic distribution shows that the rivers can be roughly divided into three groups (Figure 6). Rivers originating in the main part of the Folded Jura and from the Gempen Plateau (e.g. No 15) show the highest steepness values ($S_R > 0.055$). Rivers in the Tabular Jura and the easternmost Folded Jura have lower steepness values, mostly between 0.035 and 0.055, while rivers in the Upper Rhine Graben and the outermost Folded Jura have the lowest values ($S_R < 0.035$). Length and orientation of the river courses do not seem to have a significant effect on S_R (Figures 6 & 9).

The concavity values (θ) show a mean of 0.464 $\pm$0.157 (1 s.d.), which is in good agreement with the values determined in other studies (Snyder et al., 2000; Densmore et al., 2007), but display a very wide range from 0.012 to 0.927. This range reflects the occurrence of highly concave rivers as well as rivers with markedly convex reaches (ie, downstream increasing gradient; see Appendix). As Figure 7 demonstrates, their variations do not depend systematically on either the location or the orientation of the rivers, nor is there any correlation between concavity index and river length. However, the scatter around the arithmetic mean decreases with increasing river length (Figure 10).

The steepness indices k_s for river segments of 1 km length were calculated with a constant concavity index corresponding to the mean value of all rivers (0.46). k_s values for segments cover a range from 5.1 to 234.7. Each segment was assigned to one of the following classes of k_s: 0 – 30, 30 – 60, 60 – 90, and 90 – 235 (Figure 8). Grouping the rivers according to their geographic position as before, we see that the rivers in the Upper Rhine Graben group (rivers No 1, 2, 3, 4, 5, 16) show consistently low steepness values apart from some small irregularities (mean k_s of these rivers = 21). The rivers in the Tabular Jura group display slightly higher values, mostly up to k_s = 50 (mean k_s of these rivers = 30). Interestingly, the lowermost reaches of some of the rivers flowing into the Rhine have particularly high k_s values, the highest in this group (rivers No 31, 32, 37). The highest k_s values and also the highest variations along an individual river are found in the rivers of the Folded Jura group (mean k_s of these rivers = 45). Some of these rivers show very large variations along their course, covering all four k_s classes.

Large steepness index variations along a river may either be the result of (local or regional) tectonic acitivity, lithological changes inducing erodibility variations, or local base-level control. To investigate the effect of lithologic variations along the river courses, we performed a closer examination of all 16 rivers whose segments fall into at least three of the classes defined above

Table 1 (opposite): Concavity and steepness indices for the free-fit calculation of the entire rivers, and the variation of the segment-wise steepness index values (see text).

("large" variation of k_s in Tab. 1). This corresponds to a downstream variation in k_s of at least 30 over the length of a river and includes all rivers with very high-k_s segments (90 – 235). Lithological variations were studied using geological maps and field observations. The lithologies occurring in the study area show large differences in erodibility. Typical lithologies with high erosional resistivity are oolitic limestones, whereas marls have moderate resistivity and clays and evaporites have low resistivity.

The results of this analysis showed that the k_s variations of three rivers (No 6, 8, and 47) can easily be explained by erodibility contrasts and are therefore not interpreted as a sign for neotectonic activity (see Table 1). Two rivers are apparently affected by landslide processes that locally influence their longitudinal profiles (No 48 and 50). However, neither erodibility contrasts nor landslides were found to explain irregularities of the other 11 rivers in our analysis. Therefore, we assume that lithological variations play a minor role in determining the spatial pattern of k_s variations across the study area.

3.5 Discussion

The steepness index values (S_R) for the entire river lengths allow us to divide the study area into three distinct regions with relatively uniform S_R values (Figure 6). These three regions roughly correspond to the three main tectonic units in the area – the Upper Rhine Graben, the Folded Jura and the Tabular Jura. More specifically, the rivers from the Tabular Jura have higher S_R values than those from within the Upper Rhine Graben, and the S_R values of rivers in the Folded Jura are higher than those in the other two groups.

A changing steepness index S_R has been shown to correspond to changing uplift rates in a number of studies (Snyder et al., 2000; Kirby et al., 2003). However, at the basin scale S_R essentially describes the ratio of relief to river length, and hence different S_R values do not necessarily point to ongoing differential uplift. In the case of the rivers flowing from the Folded Jura into the Rhine, the high relief could be a feature inherited from the Miocene-Pliocene Jura folding activity and have nothing to do with recent uplift relative to the Tabular Jura; the higher S_R values in the Tabular Jura could simply be an effect of the relief resulting from earlier uplift/subsidence events and would now be at equilibrium.

However, arguments supporting the hypothesis of ongoing differential uplift are the long time period since the end of the main phase of detachment tectonics at ca. 5 Ma (Ustaszewski and Schmid, 2006) and the spatial pattern of the steepness index k_s, calculated over segments of 1 km (Figure 8). The k_s values are consistently higher in the Folded Jura compared to the Tabular Jura, where they are again higher compared to the Upper Rhine Graben. In particular, some of the
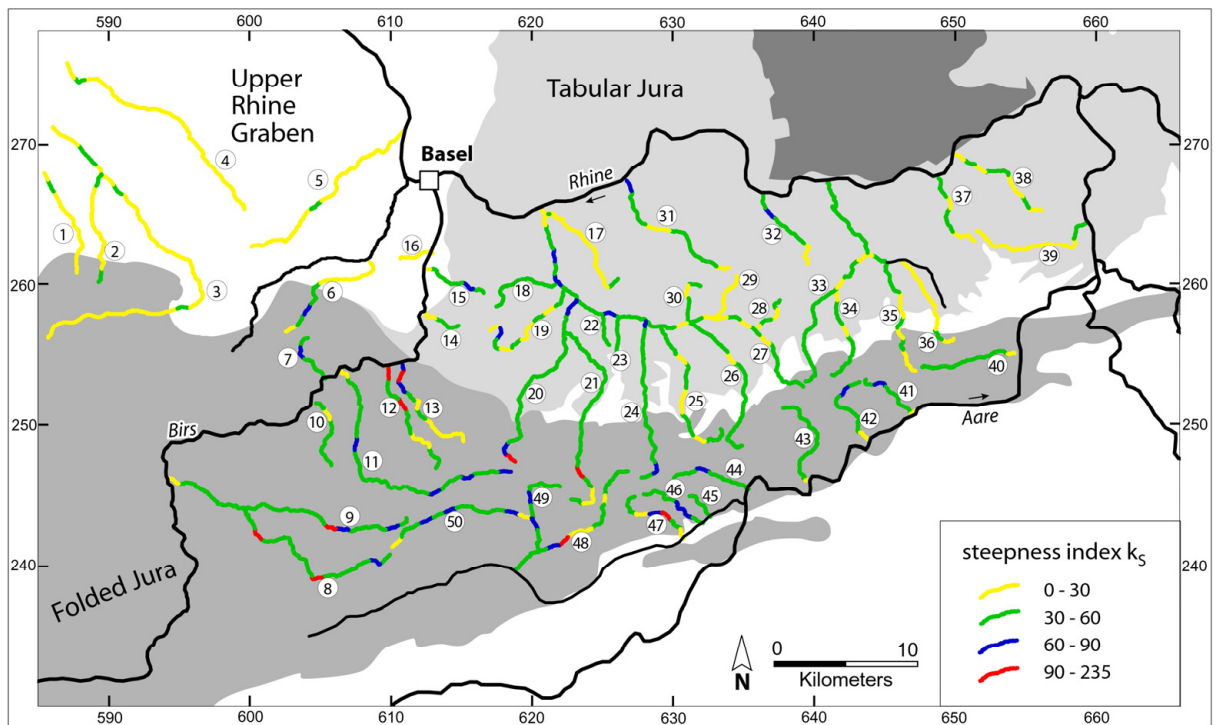
Figure 8: Map with steepness index k_s (constant θ) for segments of 1km length. The segments with the highest values (red) all lie within the Jura fold-and-thrust belt. Numbers refer to Table 1.

Rhine tributaries from the Tabular Jura steepen in their lowermost reaches before flowing into the Rhine, and have correspondingly high k_s values there (e.g., rivers No 31 and 32). We interpret this as a response to incision of the Rhine into the Tabular Jura due to recent subsidence of the Upper Rhine Graben. Incision of the Rhine and Aare upstream from the Upper Rhine Graben is also evidenced by 1) the system of erosional terraces formed in the past ca. 20 ka (Low Terrace Gravels, Bitterli et al. (2000)), and 2) the fact that bedrock is exposed at various places on the Rhine river bed between Basel and the Aare confluence (Isler et al., 1984). From this we conclude that the higher S_R values in the Tabular Jura and the Folded Jura, when compared to those in the Upper Rhine Graben, are at least partly an effect of ongoing subsidence of the Upper Rhine Graben and resulting incision of the Rhine and Aare.

The fact that the rivers from the Folded Jura have systematically higher steepness index values (S_R) than those from the Tabular Jura – despite the fact that they cross more or less the same lithologies – seems to imply that the Folded Jura is also being uplifted relative to the Tabular Jura. Again this is supported by the irregular distribution of the steepness index k_s, which indicates that these rivers are not in equilibrium, and that their high S_R values are not simply a result of the topography resulting from pre-Quaternary tectonic events. The reaches with the highest k_s values are located within the Folded Jura, suggesting recent uplift of the Folded Jura
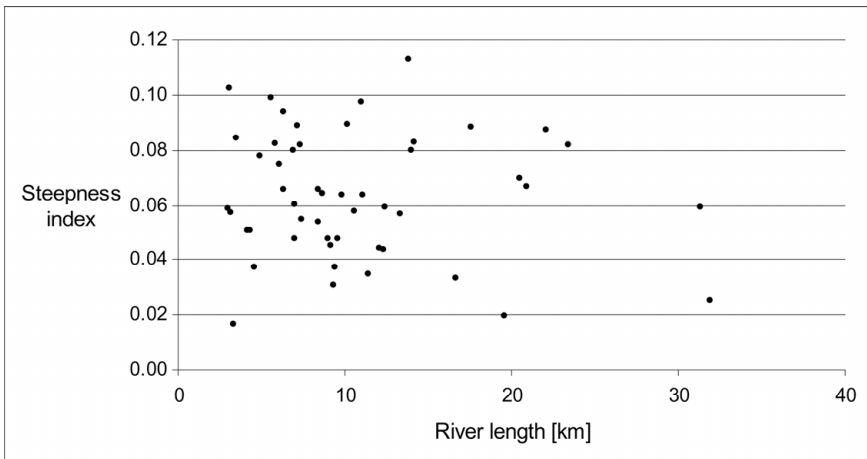
Figure 9: Steepness index S_R vs. river length. No correlation between steepness indices and the length of the studied rivers is observed.
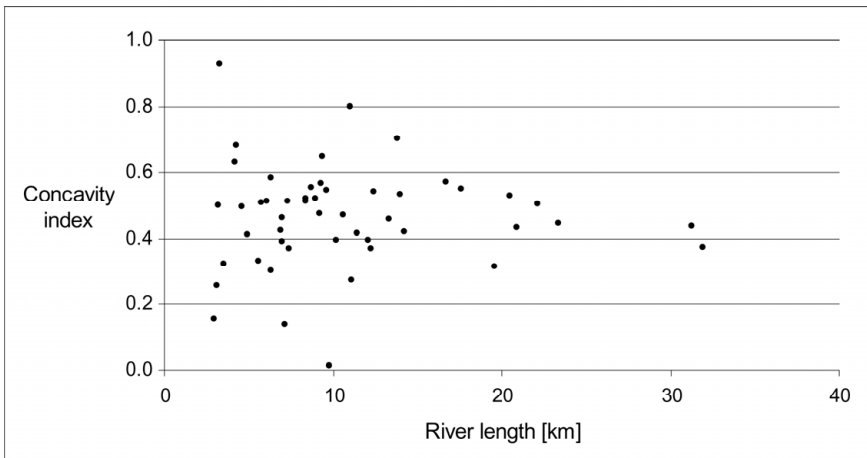
Figure 10: Concavity index θ vs. river length. Note larger θ values for short rivers.

area relative to the Tabular Jura.

This interpretation is compatible with the results of precision levelling measurements carried out over the past ca. 100 years (Schlatter, 2007; Zippelt and Dierks, 2007). These data indicate uplift in the Folded Jura relative to the Tabular Jura of ca. 0.25 mm/a as well as minor subsidence in the southern Upper Rhine Graben, although the values for the latter are not significant. Recent (post-Pliocene) subsidence in the southern Upper Rhine Graben is, however, also evidenced by the terrace systems of rivers flowing from the Sundgau area north into the Upper Rhine Graben (Giamboni et al., 2004b), thus supporting our interpretation. In addition, it is compatible with earthquake focal mechanisms, which point to pure and oblique normal faulting activity along Rhine Graben-related faults.

Geomorphological and geological studies at the front of the Jura fold-and-thrust belt have yielded relative uplift rates of ca. 0.05 mm/a (Ustaszewski and Schmid, 2007; Giamboni et al.,

2004b), comparable to the rates determined by geodetic measurements. Assuming that (long-term) relative uplift rates are in the same order of magnitude, and average erosion rates ca. 0.1 mm/a (Carretier et al., 2006), a tectonic signal should be visible in the river profiles after a few tens to hundreds of thousands of years, although tectonic deformation rates are probably not uniform, and erosion rates are expected to vary during climatic cycles. Estimating response times of rivers is, however, not straightforward (Whipple and Tucker, 1999), and in order to better constrain the time frame covered by the stream gradient analysis it would be necessary to model the erosion and tectonic influence on the river systems using varying parameter sets.

Interestingly, the concavity index θ shows a very irregular spatial distribution (Figure 7). Rivers with high and low concavities occur in all three groups defined by the steepness index S_R. The large scatter of both the steepness and concavity indices is also remarkable. While there seems to be no trend for the steepness index with river length, the scatter of the concavity index is largest for short rivers and decreases with river length (Figure 10). This indicates that the analysis of rivers below a certain length might not yield useful results. The fact that short rivers show a greater variability in the concavity index might be explained by the fact that these rivers are too small to average out changing lithologies.

Comparison of the resulting stream gradient pattern with field data revealed that it is difficult to assign the discussed irregularities of the river profiles to specific tectonic structures. In the west of the study area, where the structures of the Folded Jura and Upper Rhine Graben-related faults interfere more strongly, our data suggest that a boundary between two tectonic units with different uplift rates runs along the Rhine Valley flexure before turning west, following the Blauen anticline. In addition, the river Birs has a tendency to run at the eastern side of its valley south of Basel, compatible with ongoing normal faulting along the Rhine Valley flexure. But despite the distinct morphological expression of this structure, it does not seem to accommodate any substantial offset resulting from recent subsidence of the Upper Rhine Graben for a number of reasons. Whereas there is a concentration of earthquake epicentres along the eastern Main Border Fault north of Basel, no increased earthquake activity can be observed in its southern continuation (Bonjer, 1997). Although a drop in outcrop elevation of the Mid-Pleistocene Lower Cover Gravels across the Rhine Valley flexure is indicative of normal faulting, the well-preserved Late Quaternary terrace surfaces (Low Terrace Gravels) of the Rhine do not record a noticable change in gradient where they cross this structure (Kock et al., in prep.), as would be expected for an active normal fault. Moreover, the varying thickness of the Quaternary sediment fill in the Upper Rhine Graben indicates that subsidence has been largest to the southwest of the Kaiserstuhl volcanic complex, at some distance from the Graben boundary, in the Quaternary (Bartz, 1974).

The cut-and-fill terraces of the Rhine accordingly continue across the Rhine Valley flexure and into the Upper Rhine Graben before they end and give way to a normal sedimentary sequence (Wittmann, 1961). Significantly, the river Birs has also created a system of cut-and-fill terraces after the Würm glacial at ca. 10 ka (Bitterli-Brunner et al., 1984). It therefore seems more plausible that subsidence-related deformation is distributed on several tectonic structures and not necessarily on the exact prolongation of the eastern Main Border Fault of the Upper Rhine Graben. Normal faulting on the western side of the Birs valley (Basel-Reinach fault) is not supported by our results. However, only one short river could be analysed in this area due to the low-relief topography and the high population density.

In the eastern part of the study area, the boundary between the "Tabular Jura" rivers and the "Folded Jura" rivers, as determined from the S_R distribution, does not exactly follow the boundary between the autochthonous and the thrusted Mesozoic. For instance, three rivers from the Gempen Plateau, which is part of the Tabular Jura (Figure 4), fall into one category with the rivers from the Folded Jura with respect to their steepness index values (note that river No 45 is not included in the interpretation because of karst in its drainage basin). On the other hand, a few rivers that originate in the easternmost parts of the fold-and-thrust belt have S_R values corresponding to the majority of rivers from the Tabular Jura. This indicates that detachment tectonics, i.e. ongoing thin-skinned deformation of the Jura fold-and-thrust belt, cannot explain observed steepness index pattern. Moreover, according to fission track cooling ages in the Molasse Basin, at least 1 km of sediments was eroded in this area in the Pliocene-Pleistocene (Cederbom et al., 2004). We therefore suspect that compressive stresses might not be transmitted from the Alps to the Jura mountains anymore because of the missing sedimentary wedge in the Molasse Basin, and that the evaporitic detachment layer might be too shallow today to deform in a plastic style.

The differential uplift inferred from our data might instead be related to the (transpressional) reactivation of basement faults in the area of the Late Paleozoic Trough system, similarly to the observations at the front of the Folded Jura to the west of Basel. There, the ENE-WSW-trending faults of the Permo-Carboniferous troughs in the crystalline basement seem to have been transpressionally reactivated (Giamboni et al., 2004a; Madritsch et al., 2008). Further to the east, no such reactivation has been observed so far, but the trough system is known to continue to the east, passing underneath the easternmost Jura mountains (Diebold and Noack, 1996; Ustaszewski et al., 2005). A compressional reactivation of ENE-WSW trending basement faults would be in agreement with the NW-SE maximum principal stress direction in the basement, determined from earthquake focal mechanisms (Kastrup et al., 2004) and borehole breakouts (Becker, 2000). However, seismological data show that the predominant faulting mechanisms are normal and

strike-slip faulting; therefore, any appreciable thrust faulting along these ENE-WSW trending basement faults would have to be accommodated by an aseismic process.

3.6 Conclusions

It was the main motivation of this study to better characterise the recent tectonic deformation pattern in the eastern Jura fold-and-thrust belt and adjacent areas, which was hitherto poorly constrained. Calculating steepness and concavity indices for 50 rivers from a digital elevation model allowed us to divide the area into three parts, each subject to a different relative uplift rate. Based on the spatial pattern of the steepness index for the entire rivers, S_R, and the steepness index for segments of 1 km length, k_s, the following distribution of (vertical) tectonic deformation is suggested: One part of the study area that roughly corresponds to the Jura fold-and-thrust belt is uplifted relative to the Tabular Jura, probably as a result of the reactivation of faults in the underlying basement, which is, however, not visible in the available earthquake focal mechanisms. At the same time, ongoing subsidence of the Upper Rhine Graben causes incision and, partly, local steepening of upstream rivers. This interpretation is in agreement with the expected deformation style in a stress regime with a N-S to NW-SE oriented maximum principle stress axis, as indicated by earthquake focal mechanisms (Kastrup et al., 2004). It is also in accordance with the observed inversion of Late Paleozoic basement faults at the southern boundary of the Upper Rhine Graben (Giamboni et al., 2004a; Ustaszewski and Schmid, 2006), and at the north-western front of the Jura fold-and-thrust belt (Madritsch et al., 2008), in the Pliocene and Pleistocene. Our method does, however, not allow us to confidently determine any active faults or folds along which deformation is concentrated. As suggested by the results of geodetic measurements, the deformation rates in NW Switzerland appear to be very low (< 0.5 mm/a), which is probably one reason why active faulting is difficult to detect. In addition, our results suggest that vertical displacement in this area is distributed over many faults, which further impedes the identification of active structures, thus highlighting the importance of inherited fault systems on the present-day deformation pattern.

Furthermore, our results imply that short rivers should be used with caution in stream gradient analyses, as their stream power might be too low for them to adjust to alongstream lithological variations. The minimum length of rivers that should be included in the analysis will probably depend on the scale of the erodibility changes. We suggest that the steepness index for the entire river may be the best indicator to gain information about the recent tectonic history, since it is less likely to be affected by changing erodibilities along the river courses.

Acknowledgements

References

Bartz, J., 1974. Die Mächtigkeit des Quartärs im Oberrheingraben. Approaches to Taphrogenesis; The Rhinegraben; geologic history and neotectonic activity: 78-87.

Becker, A., 2000. The Jura Mountains - An active foreland fold-and-thrust belt? Tectonophysics, 321(4): 381-406.

Bitterli-Brunner, P., Fischer, H. and Herzog, P., 1984. Arlesheim (Blatt 1067), Geologischer Atlas der Schweiz, 1:25 000. Schweizerische Geologische Kommission, Switzerland.

Bitterli, T., Graf, H.R., Matousek, F. and Wanner, M., 2000. Geologischer Atlas der Schweiz: Zurzach (Blatt 1050), Erläuterungen. Bundesamt f. Wasser u. Geologie. Bern, Switzerland.

Bonjer, K.P., 1997. Seismicity pattern and style of seismic faulting at the eastern borderfault of the southern Rhine Graben. Tectonophysics, 275(1-3): 41-69.

Burbank, D.W. and Anderson, R.S., 2001. Tectonic Geomorphology. Blackwell Science.

Burkhard, M., 1990. Aspects of the large-scale Miocene deformation in the most external part of the Swiss Alps (Subalpine Molasse to Jura fold belt). Eclogae Geologicae Helvetiae, 83(3): 559-583.

Burkhard, M. and Sommaruga, A., 1998. Evolution of the western Swiss Molasse Basin; structural relations with the Alps and the Jura Belt. In: A. Mascle, C. Puigdefàbregas, H.P. Luterbacher and M. Fernàndez (Editors), Cenozoic foreland basins of Western Europe. Geological Society Special Publications.

Carretier, S., Niviere, B., Giamboni, M. and Winter, T., 2006. Do river profiles record along-stream variations of low uplift rate? Journal of Geophysical Research, 111.

Cederbom, C.E., Sinclair, H.D., Schlunegger, F. and Rahn, M.K., 2004. Climate-induced rebound and exhumation of the European Alps. Geology, 32(8): 709-712.

Chauve, P., Martin, J., Petitjean, E. and Sequeiros, F., 1988. Le chevauchement du Jura sur la Bresse. Données nouvelles et réinterpretation des sondages. Bull. Soc. géol. France, 8(4): 861-870.

Densmore, A.L., Gupta, S., Allen, P.A. and Dawers, N.H., 2007. Transient landscapes at fault tips. Journal of Geophysical Research, 112.

Dèzes, P., Schmid, S.M. and Ziegler, P.A., 2004. Evolution of the European Cenozoic rift system; interaction of the Alpine and Pyrenean orogens with their foreland lithosphere. Tectonophysics, 389(1-2): 1-33.

Diebold, P., Bitterli-Brunner, P. and Naef, H., 2006. Frick: Geologischer Atlas der Schweiz. Erläuterungen.

Diebold, P. and Noack, T., 1996. Late Palaeozoic troughs and Tertiary structures in the eastern Folded Jura. In: O.A. Pfiffner, P. Lehner, P. Heitzmann, S. Mueller and A. Steck (Editors), Deep structure of the Swiss Alps; results of NRP 20. Birkhäuser, Basel, Switzerland, pp. 59-63.

Dietrich, W.E., Wilson, C.J., Montgomery, D.R. and McKean, J., 1993. Analysis of erosion thresholds, channel networks, and landscape morphology using a digital terrain model. Journal of Geology, 101(2): 259-278.

Duvall, A., Kirby, E. and Burbank, D.W., 2004. Tectonic and lithologic controls on bedrock channel profiles and processes in coastal California. Journal of Geophysical Research, 109(3).

Fäh, D., Giardini, D., Bay, F., Bernardi, F., Braunmiller, J., Deichmann, N., Furrer, M., Gantner, L., Gisler, M., Isenegger, D., Jimenez, M.J., Kästli, P., Koglin, R., Masciadri, V., Rutz, M., Scheidegger, C.,

Schibler, R., Schorlemmer, D., Schwarz-Zanetti, G., Steimen, S., Sellami, S., Wiemer, S. and Wossner, J., 2003. Earthquake Catalogue Of Switzerland (ECOS) and the related macroseismic database. Eclogae Geologicae Helvetiae, 96(2): 219-236.

Ferry, M., Meghraoui, M., Delouis, B. and Giardini, D., 2005. Evidence for Holocene palaeoseismicity along the Basel-Reinach active normal fault (Switzerland); a seismic source for the 1356 earthquake in the Upper Rhine Graben. Geophysical Journal International, 160(2): 554-572.

Flint, J.J., 1974. Stream gradient as a function of order, magnitude, and discharge. Water Resources Research, 10(5): 969-973.

Giamboni, M., Ustaszewski, K., Schmid, S.M., Schumacher, M.E. and Wetzel, A., 2004a. Plio-Pleistocene transpressional reactivation of Paleozoic and Paleogene structures in the Rhine-Bresse transform zone (northern Switzerland and eastern France). International Journal of Earth Sciences, 93(2): 207-223.

Giamboni, M., Wetzel, A., Niviere, B. and Schumacher, M., 2004b. Plio-Pleistocene folding in the southern Rhinegraben recorded by the evolution of the drainage network (Sundgau area; northwestern Switzerland and France). Eclogae Geologicae Helvetiae, 97(1): 17-31.

Graf, H.R., 1993. Die Deckenschotter der zentralen Nordschweiz. PhD Thesis, ETH Zürich, Zürich.

Graul, H., 1962. Geomorphologische Studien zum Jungquartär des nördlichen Alpenvorlandes. Teil 1: Das Schweizer Mittelland. Heidelberger Geographische Arbeiten, Heft 9.

Hack, J.T., 1957. Studies of Longitudinal Stream Profiles in Virginia and Maryland. U.S. Geological Survey Professional Paper, 294-B: 45-97.

Hack, J.T., 1973. Stream-profile analysis and stream-gradient indices. United States Geological Survey Journal of Research, 1: 421-429.

Haldimann, P., Naef, H. and Schmassmann, H., 1984. Fluviatile Erosions- und Akkumulationsformen als Indizien jungpleistozäner und holozäner Bewegungen in der Nordschweiz und angrenzenden Gebieten. Nagra Technischer Bericht, 84-16.

Hancock, G.R., 2005. The use of digital elevation models in the identification and characterization of catchments over different grid scales. Hydrological Processes, 19(9): 1727-1749.

Hodges, K.V., Wobus, C., Ruhl, K., Schildgen, T. and Whipple, K., 2004. Quaternary deformation, river steepening, and heavy precipitation at the front of the Higher Himalayan ranges. Earth and Planetary Science Letters, 220(3-4): 379-389.

Howard, A.D. and Kerby, G., 1983. Channel changes in badlands. Geological Society of America Bulletin, 94(6).

Huang, X.J. and Niemann, J.D., 2006. An evaluation of the geomorphically effective event for fluvial processes over long periods. Journal of Geophysical Research-Earth Surface, 111(F3).

Isler, A., Pasquier, F. and Huber, M., 1984. Geologische Karte der zentralen Nordschweiz 1:100 000, mit angrenzenden Gebieten von Baden-Württemberg. Nagra und Schweiz Geol Kommission, Spezialkarte Nr. 131.

Jordan, P., 1992. Evidence for large-scale decoupling in the Triassic evaporites of northern Switzerland; an overview. Eclogae Geologicae Helvetiae, 85(3).

Kälin, D., 1997. Litho- und Biostratigraphie der mittel- bis obermiozänen Bois de Raube-Formation (Nordwestschweiz). Eclogae Geologicae Helvetiae, 90(1): 97-114.

Kastrup, U., Zoback, M.L., Deichmann, N., Evans, K.F., Giardini, D. and Michael, A.J., 2004. Stress field variations in the Swiss Alps and the northern Alpine foreland derived from inversion of fault plane solutions. Journal of Geophysical Research-Solid Earth, 109(B1).

Keller, E.A. and Pinter, N., 2002. Active Tectonics: Earthquakes, Uplift, and Landscape. Prentice Hall.

Kirby, E., Johnson, C., Furlong, K. and Heimsath, A., 2007. Transient channel incision along Bolinas Ridge, California: Evidence for differential rock uplift adjacent to the San Andreas fault. Journal of Geophysical Research-Earth Surface, 112(F3).

Kirby, E. and Whipple, K., 2001. Quantifying differential rock-uplift rates via stream profile analysis. Geology, 29(5): 415-418.

Kirby, E., Whipple, K.X., Tang, W.Q. and Chen, Z.L., 2003. Distribution of active rock uplift along the eastern margin of the Tibetan Plateau: Inferences from bedrock channel longitudinal profiles. Journal of Geophysical Research-Solid Earth, 108(B4).

Kock, S., Schmid, S.M., Fraefel, M. and Wetzel, A., in prep. Neotectonic activity in the area of Basel inferred from morphological analysis of fluvial terraces of the Rhine River.

Lacombe, O., Angelier, J., Byrne, D. and Dupin, J.M., 1993. Eocene-Oligocene Tectonics and Kinematics of the Rhine-Saone Continental Transform Zone (Eastern France). Tectonics, 12(4): 874-888.

Lague, D., Davy, P. and Crave, A., 2000. Estimating uplift rate and erodibility from the area-slope relationship; examples from Brittany (France) and numerical modelling. Physics and Chemistry of the Earth (A), 25(6-7): 543-548.

Lambert, J., Winter, T., Deweza, T.J.B. and Sabouraulta, P., 2004. New hypotheses on the maximum damage area of the 1356 Basel earthquake (Switzerland). Quaternary Science Reviews.

Laubscher, H., 1961. Die Fernschubhypothese der Jurafaltung. Eclogae geologicae Helvetiae, 54: 221-282.

Laubscher, H., 1986. The eastern Jura: relations between thin-skinned and basement tectonics, local and regional. Geologische Rundschau, 75: 535-553.

Laubscher, H., 2001. Plate interactions at the southern end of the Rhine graben. Tectonophysics, 343(1-2): 1-19.

Leopold, L.B., Wolman, M.G. and Miller, J.P., 1964. Fluvial Processes in Geomorphology. Freeman, San Francisco.

Mackin, J.H., 1948. Concept of the Graded River. Geological Society of America Bulletin, 59(5): 463-511.

Madritsch, H., Schmid, S.M. and Fabbri, O., 2008. Interactions of thin- and thick-skinned tectonics along the northwestern front of the Jura fold-and-thrust-belt (Eastern France). Tectonics, 27.

Marple, R.T. and Talwani, P., 2000. Evidence for a buried fault system in the Coastal Plain of the Carolinas and Virginia - Implications for neotectonics in the southeastern United States. Geological Society of America Bulletin, 112(2): 200-220.

Mayer-Rosa, D. and Cadiot, B., 1979. A review of the 1356 Basel earthquake: basic data. Tectonophysics, 53: 325-333.

Merritts, D. and Vincent, K.R., 1989. Geomorphic response of coastal streams to low, intermediate, and high rates of uplift, Mendocino triple junction region, Northern California. Geological Society of America Bulletin, 101(11): 1373-1388.

Meyer, B., Lacassin, R., Brulhet, J. and Mouroux, B., 1994. The Basel 1356 earthquake: which fault produced it? Terra Nova, 6: 54-63.

Meyer, M., 2001. Die Geologie des Adlertunnels. Bulletin für angewandte Geologie, 6(2): 199-208.

Montgomery, D.R. and Brandon, M.T., 2002. Topographic controls on erosion rates in tectonically active mountain ranges. Earth and Planetary Science Letters, 201: 481-489.

Müller, W.H., Blümling, P., Becker, A. and Clauss, B., 1987. Die Entkopplung des tektonischen Spannungsfeldes an der Jura-Ueberschiebung. Eclogae Geologicae Helvetiae, 80(2).

Müller, W.H., Naef, H. and Graf, H.R., 2002. Geologische Entwicklung der Nordschweiz, Neotektonik und Langzeitszenarien Zürcher Weinland. Nagra Technischer Bericht, 99-08.

Noack, T., 1995. Thrust development in the eastern Jura Mountains related to pre-existing extensional structures. Tectonophysics, 252(1-4): 419-431.

Oskin, M.E. and Burbank, D., 2007. Transient landscape evolution of basement-cored uplifts: Example of the Kyrgyz range, Tian shan. Journal of Geophysical Research-Earth Surface, 112(F3).

Ouchi, S., 1985. Response of alluvial rivers to slow active tectonic movement. Geol. Soc. of America Bull., 96(4).

Penck, A. and Brückner, E., 1909. Die Alpen im Eiszeitalter. Band 2: Die Eiszeiten in den nördlichen Westalpen.

Rózsa, S., Heck, B., Mayer, M., Seitz, K., Westerhaus, M. and Zippelt, K., 2005. Determination of displacements in the upper Rhine graben Area from GPS and leveling data. International Journal of Earth Sciences, 94(4): 538-549.

Schlatter, A., 2006. Das neue Landeshöhennetz der Schweiz LHN95. PhD Thesis, Diss Nr. 16840, ETH Zürich, Zürich.

Schlatter, A., 2007. Neotektonische Untersuchungen in der Nordschweiz und Süddeutschland: Kinematische Ausgleichung der Landesnivellementlinien CH/D. Nagra Arbeitsbericht NAB 07-12.

Schlatter, A., Schneider, D., Geiger, A. and Kahle, H.-G., 2005. Recent vertical movements from precise levelling in the vicinity of the city of Basel, Switzerland. Int Journ Earth Sciences, 94(4): 507-514.

Sklar, L. and Dietrich, W.E., 1998. River Longitudinal Profiles and Bedrock Incision Models: Stream Power and the Influence of Sediment Supply, Rivers over Rock.

Snyder, N.P., Whipple, K.X., Tucker, G.E. and Merritts, D.J., 2000. Landscape response to tectonic forcing: Digital elevation model analysis of stream profiles in the Mendocino triple junction region, northern California. Geol. Soc. of America Bull., 112(8).

Stock, J. and Dietrich, W.E., 2003. Valley incision by debris flows: Evidence of a topographic signature. Water Resources Research, 39(4).

Tucker, G.E. and Slingerland, R., 1996. Predicting sediment flux from fold and thrust belts. Basin Research, 8(3): 329-349.

Ustaszewski, K. and Schmid, S.M., 2006. Control of preexisting faults on geometry and kinematics in the northernmost part of the Jura fold-and-thrust belt. Tectonics, 25(5).

Ustaszewski, K. and Schmid, S.M., 2007. Latest Pliocene to recent thick-skinned tectonics at the Upper Rhine Graben - Jura Mountains junction. Swiss Journal of Geosciences, 100(2): 293-312.

Ustaszewski, K., Schumacher, M.E. and Schmid, S.M., 2005. Simultaneous normal faulting and extensional flexuring during rifting: an example from the southernmost Upper Rhine Graben. International Journal of Earth Sciences, 94(4): 680-696.

Verderber, R., 2003. Quartärgeologie im Hochrheingebiet zwischen Schaffhausen und Basel. Zeitschrift der Deutschen Gesellschaft für Geowissenschaften, 154(2-3): 369-406.

Whipple, K.X., 2004. Bedrock rivers and the geomorphology of active orogens. Annual Review of Earth and Planetary Sciences, 32: 151-185.

Whipple, K.X. and Tucker, G.E., 1999. Dynamics of the stream-power incision model: Implications for height limits of mountain ranges, landscape response timescales, and research needs. Journal of Geophysical Research, 104(B8).

Whipple, K.X. and Tucker, G.E., 2002. Implications of sediment-flux-dependent river incision models for landscape evolution. Journal of Geophysical Research-Solid Earth, 107(B2).

Wittmann, O., 1961. Die Niederterrassenfelder im Umkreis von Basel und ihre kartographische Darstellung. Basler Beiträge zur Geographie und Ethnologie, 3.

Wobus, C., Whipple, K.X., Kirby, E., Snyder, N., Johnson, J., Spyropolou, K., Crosby, B. and Sheehan, D., 2006a. Tectonics from topography: Procedures, promise, and pitfalls. GSA Special Paper - Tectonics, Climate, and Landscape Evolution. Penrose Conference Series, 398: 55-74.

Wobus, C.W., Whipple, K.X. and Hodges, K.V., 2006b. Neotectonics of the central Nepalese Himalaya: Constraints from geomorphology, detrital 40Ar/39Ar thermochronology, and thermal modeling. Tectonics, 25.

Ziegler, P.A., 1992. European Cenozoic rift system. Tectonophysics, 208(1-3): 91-111.

Zippelt, K. and Dierks, O., 2007. Auswertung von wiederholten Präzisionsnivellements im südlichen Schwarzwald, Bodenseeraum sowie in angrenzenden schweizerischen Landesteilen. Nagra Arbeitsbericht NAB 07-27.

Appendix

Longitudinal river profiles of all 50 rivers in this study (smoothed) and slope-area distribution (re-sampled). Coordinates are for the drainage system outlet.
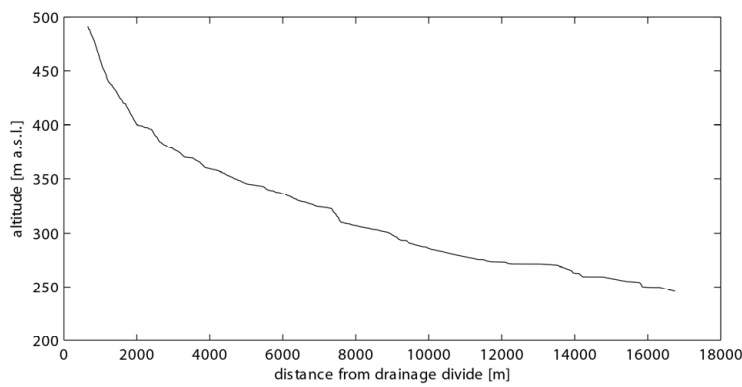
1 Feldbach (585 374 / 267 897)
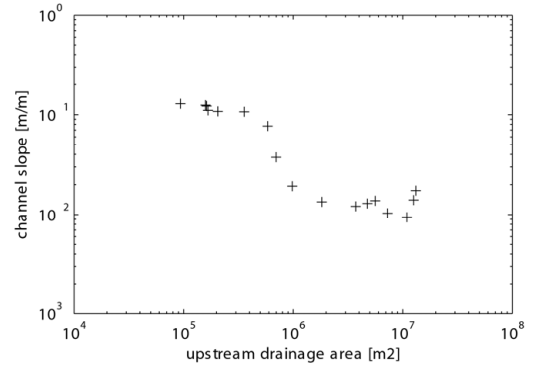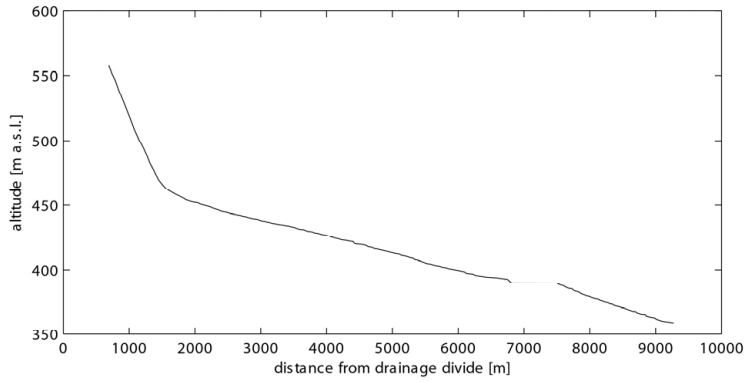
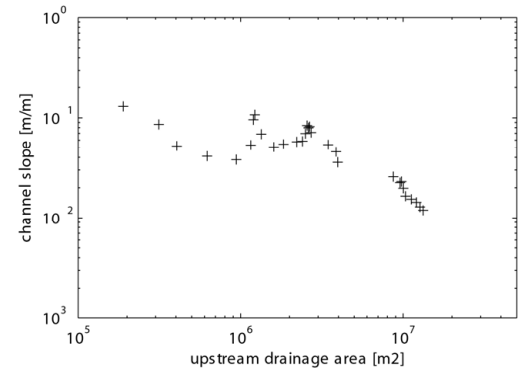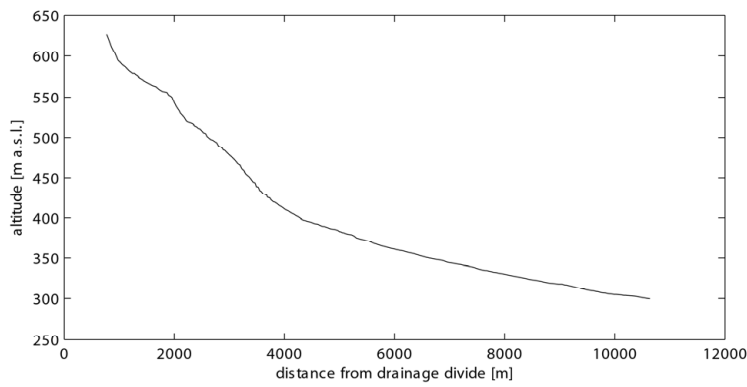2 Geischbach (589 445 / 267 827)
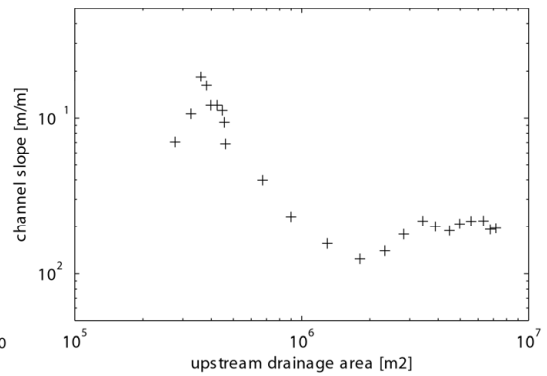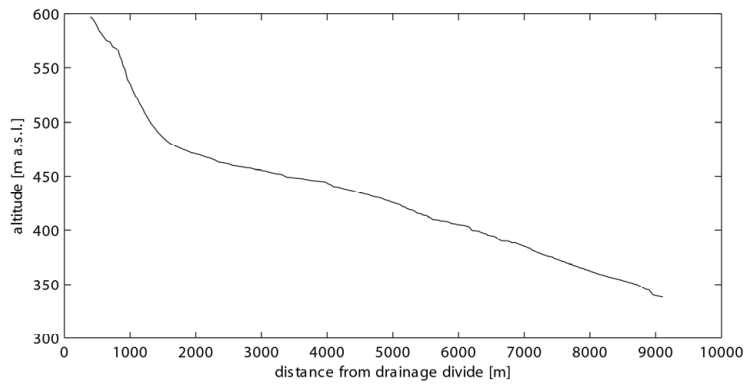
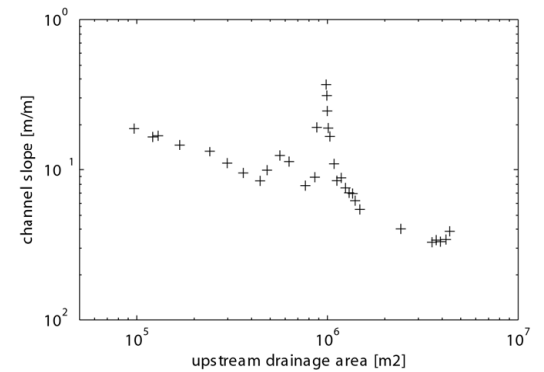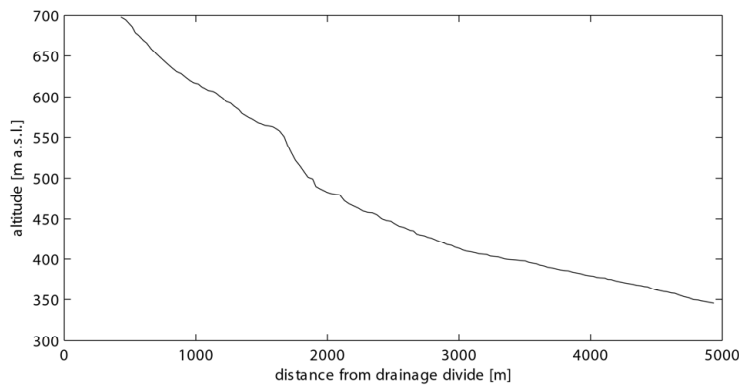3 Ill (585 993 / 271 206)
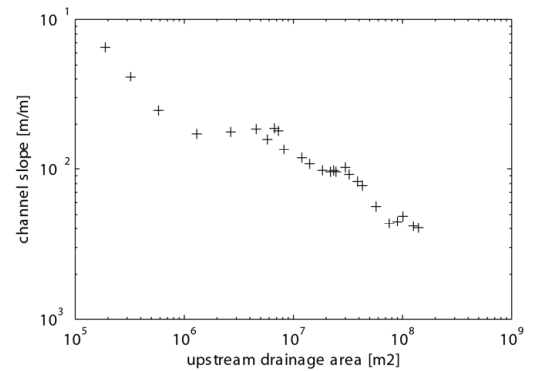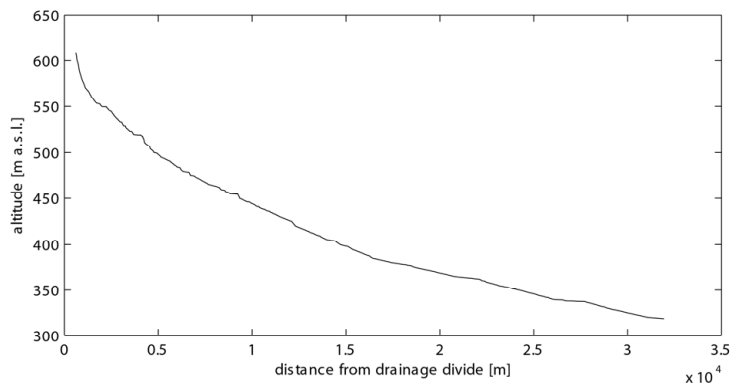
4 Thalbach (587 190 / 275 802)
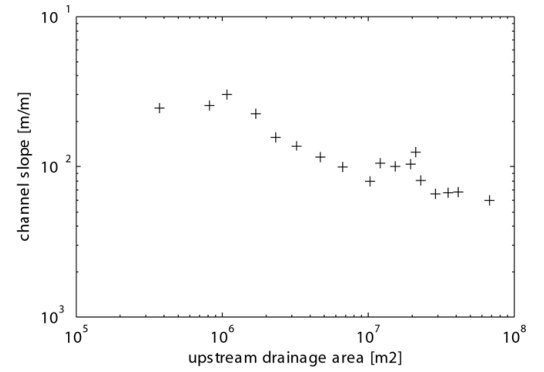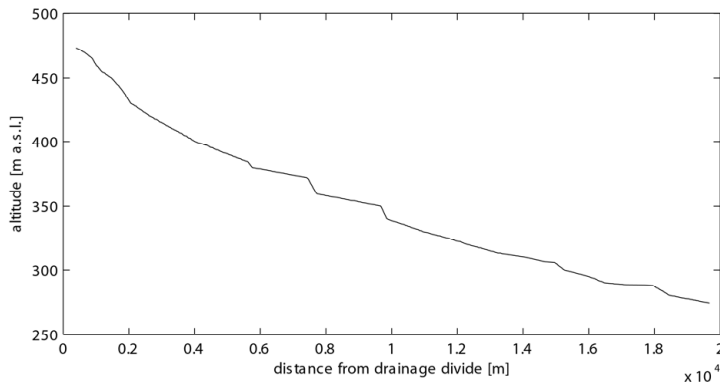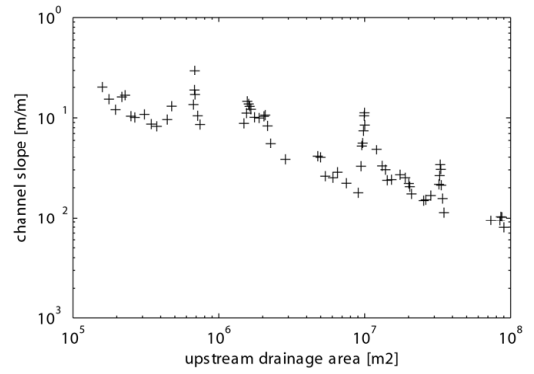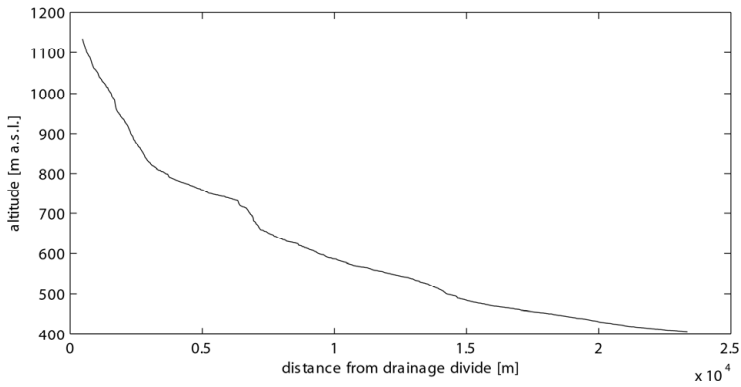

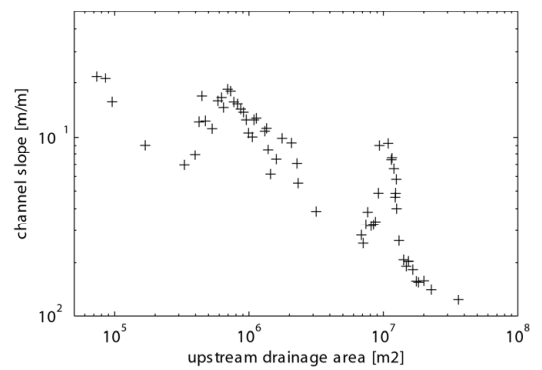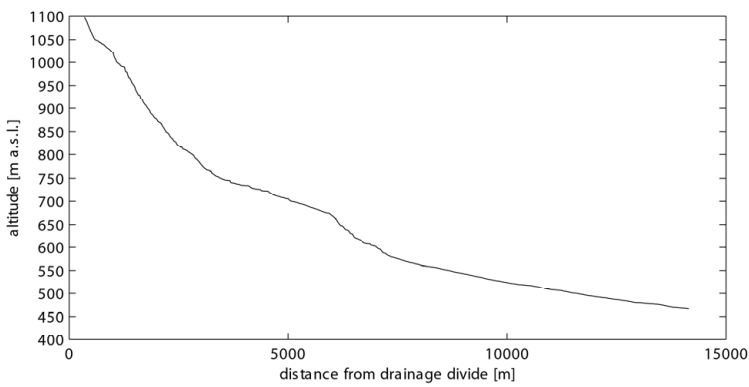## 5 Lertzbach (610 858 / 270 935)
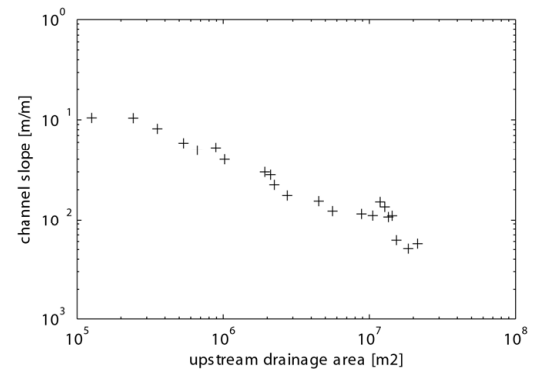
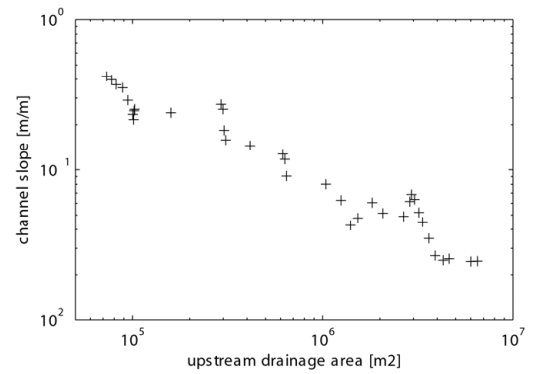## 6 Binnbach (608 518 / 261 557)
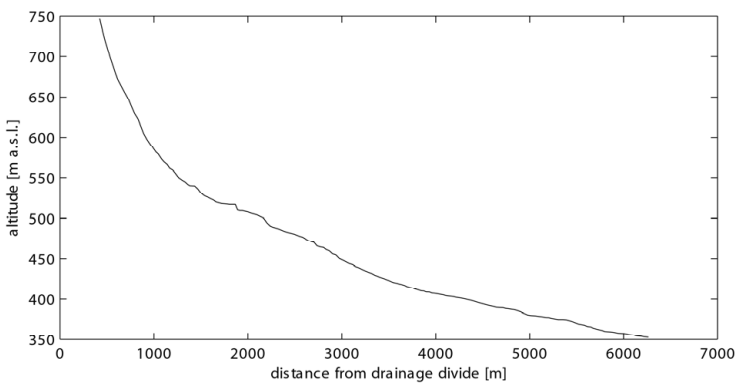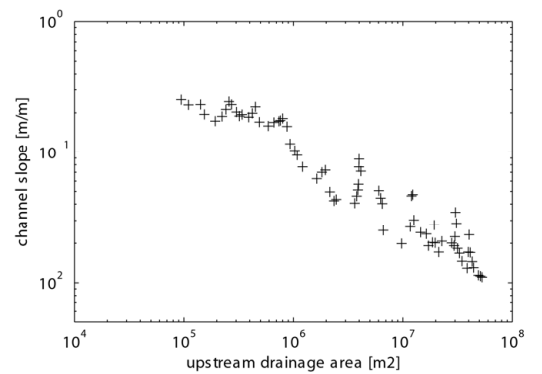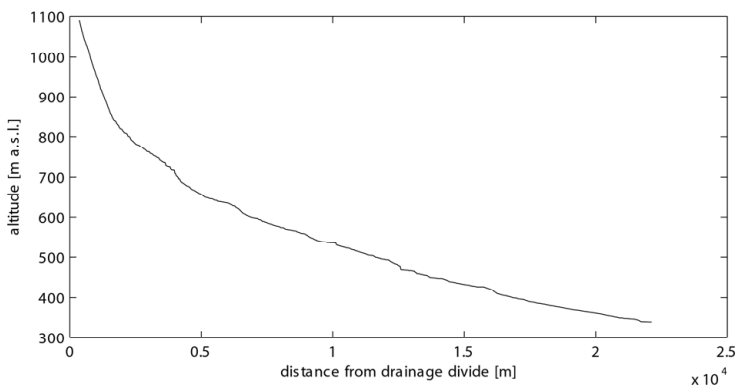

7 Dittingerbach (605 451 / 253 240)

8 Gabiare (594 243 / 246 285)

9 Scheltenbach (599 597 / 244 115)

10 Wahle (604 669 / 251 557)

11 Lüssel (606 499 / 253 830)

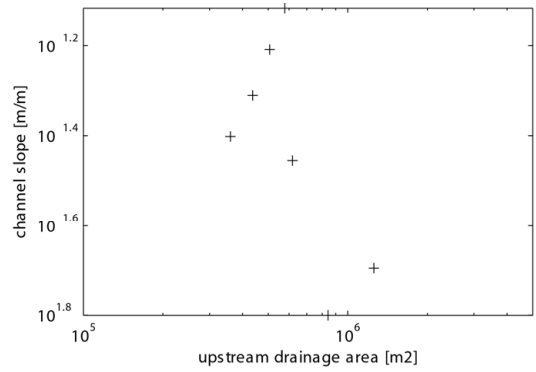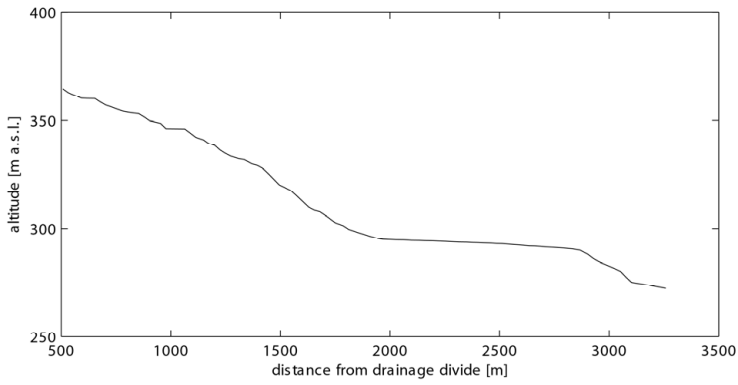12 Ibach (609 823 / 254 790)
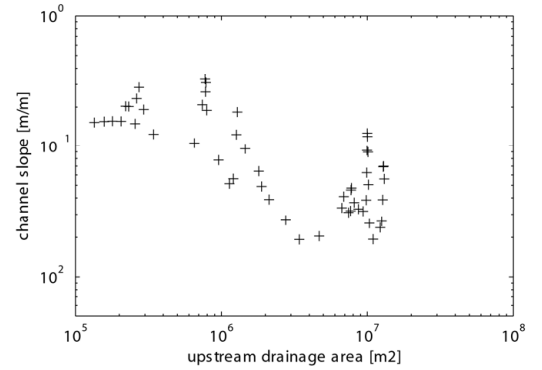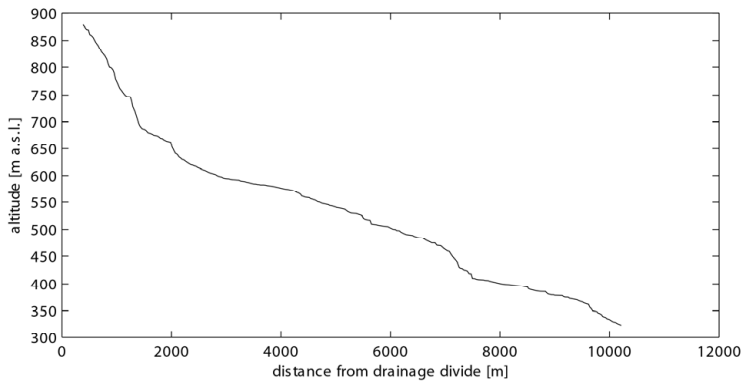
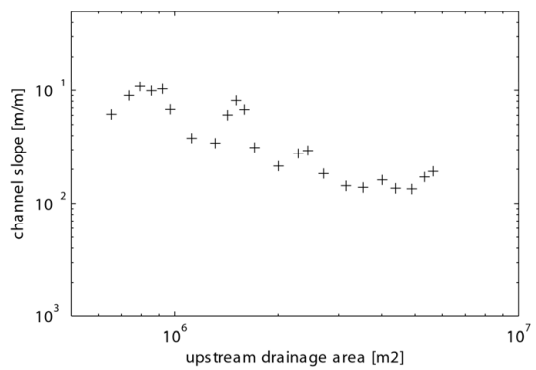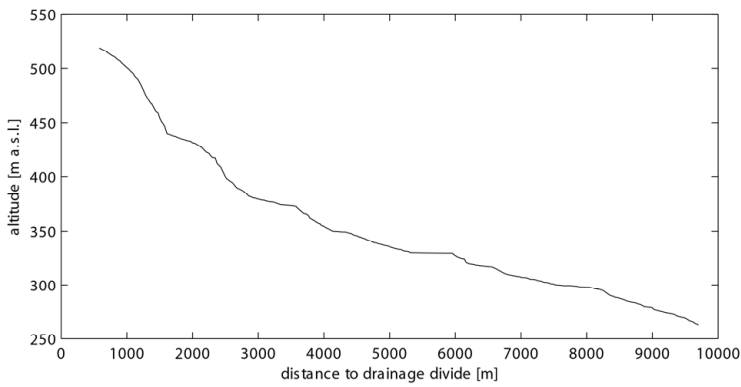13 Chastelbach (610 826 / 254 246)
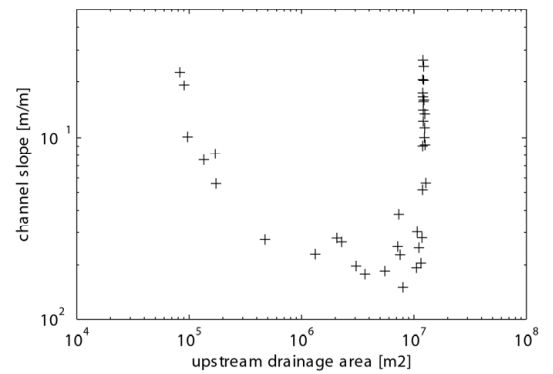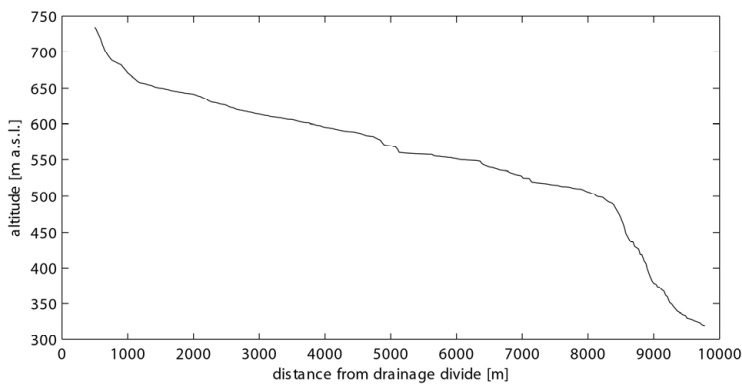
14 Lolibach (612 474 / 257 979)
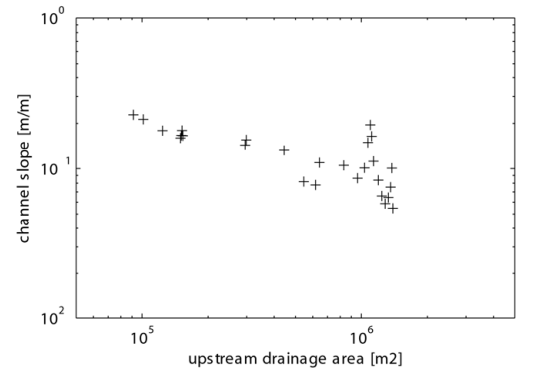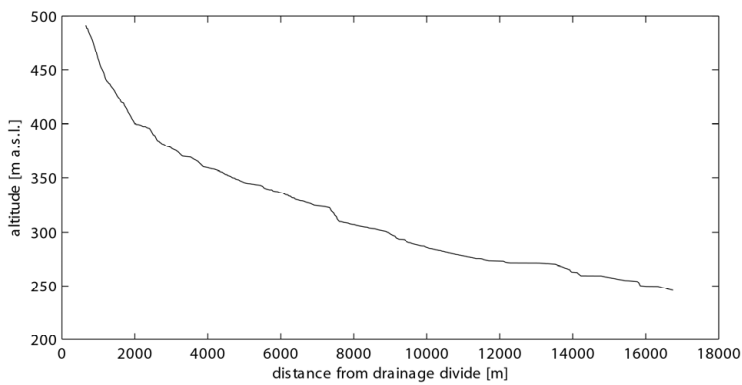
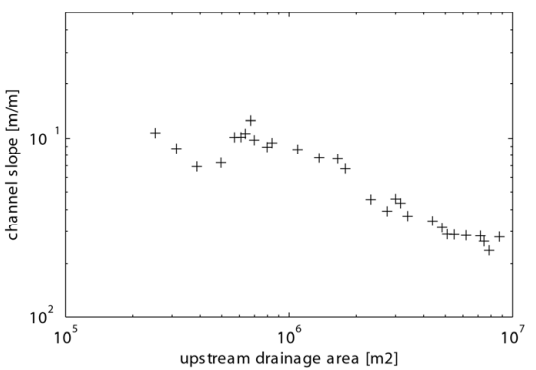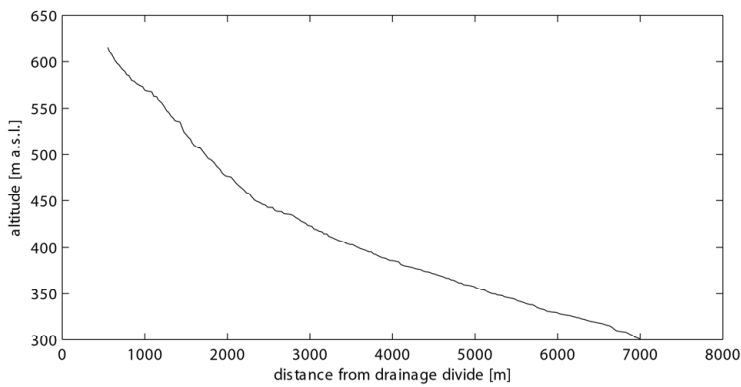15 Arlesheimerbach (612 624 / 261 550)
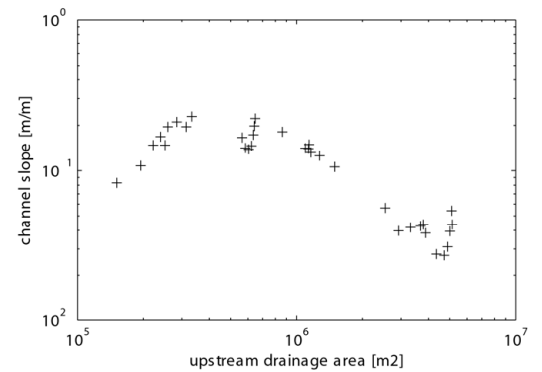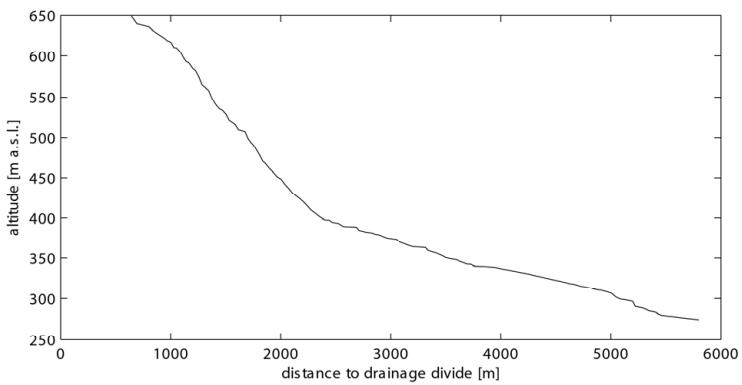
16 Gretlibach (613 520 / 262 148)

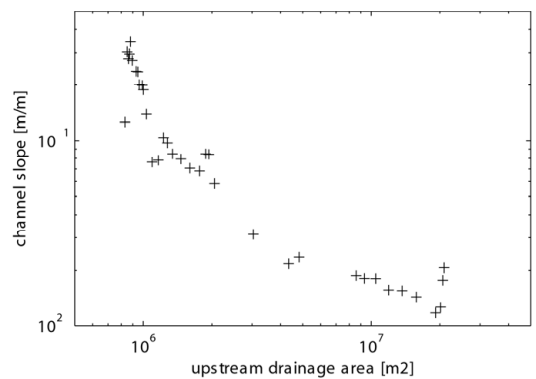

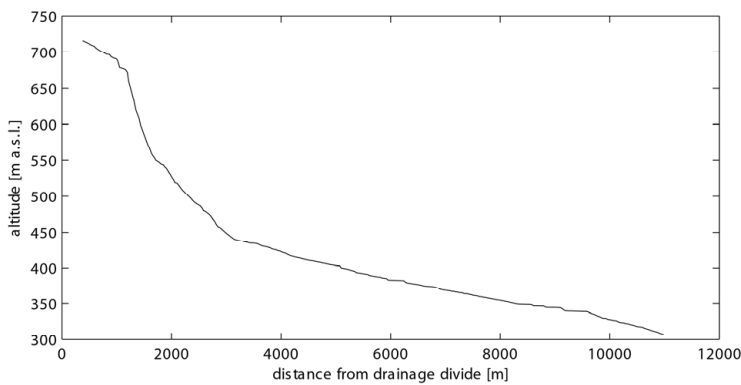17 Arisdörferbach (621 150 / 265 330)

18 Rösernbach (621 775 / 260 173)

19 Orisbach (622 325 / 259 704)

20 Hintere Frenke (622 300 / 256 551)
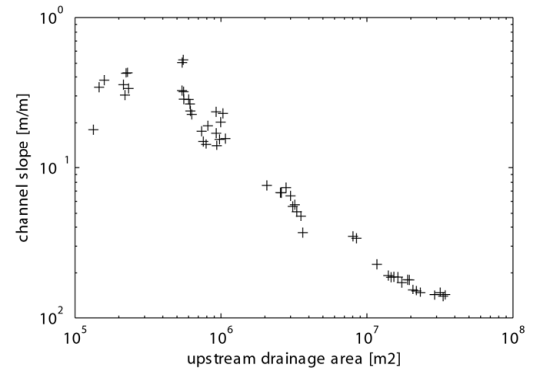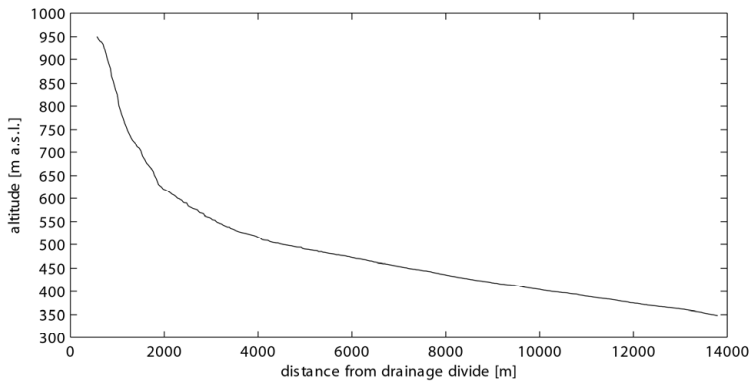
21 Vordere Frenke (623 176 / 258 897)
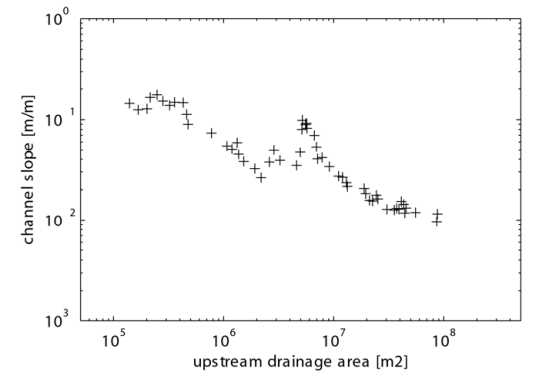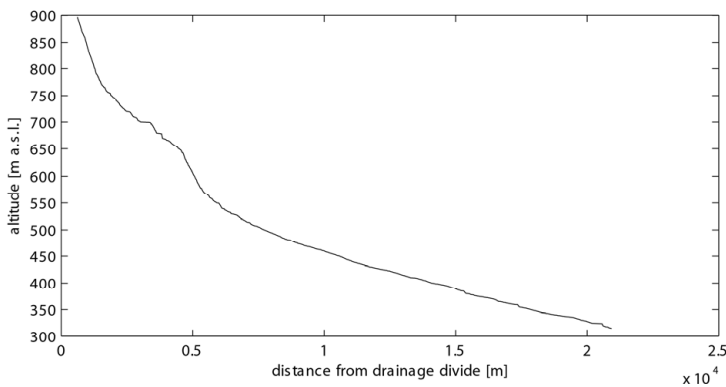
22 Buechhalden (625 480 / 257 830)
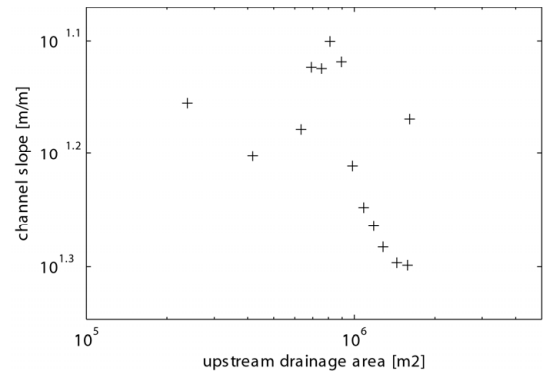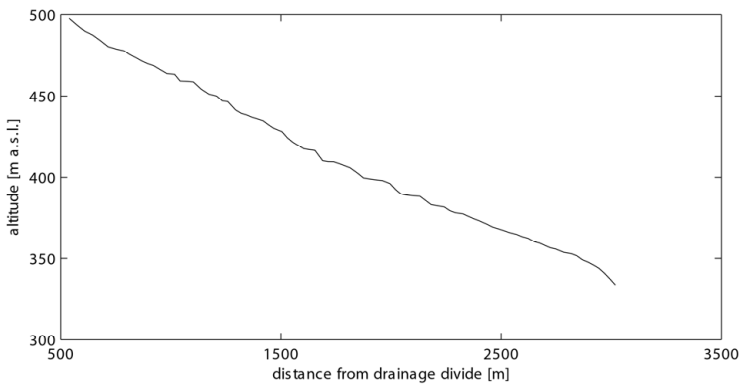
23 Talbächli (626 151 / 257 678)
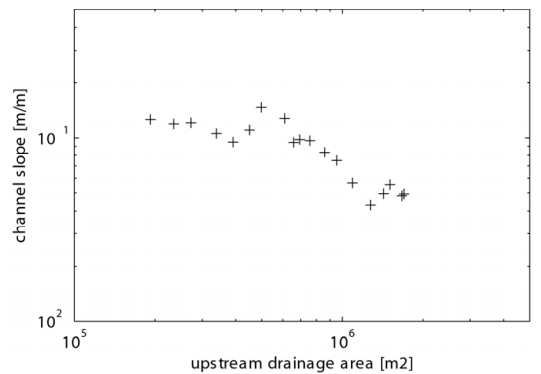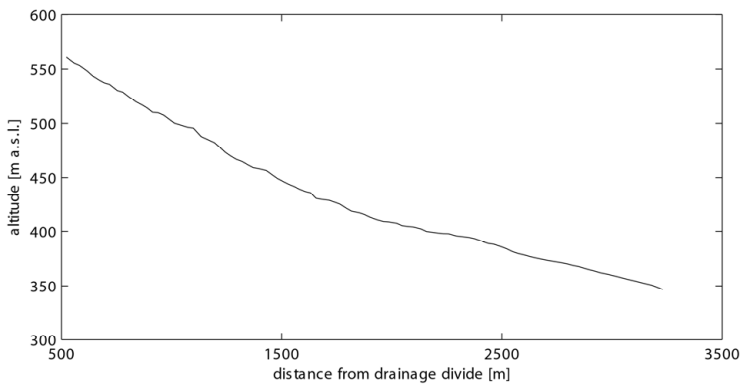
24 Diegterbach (628 990 / 257 394)
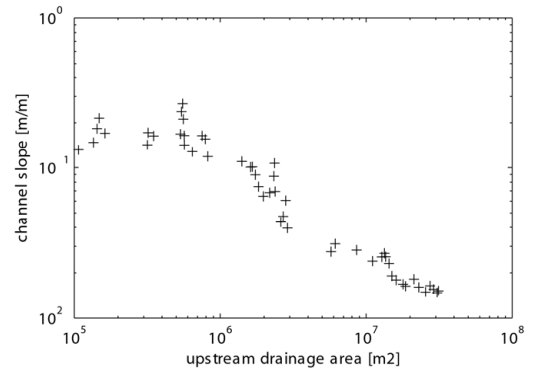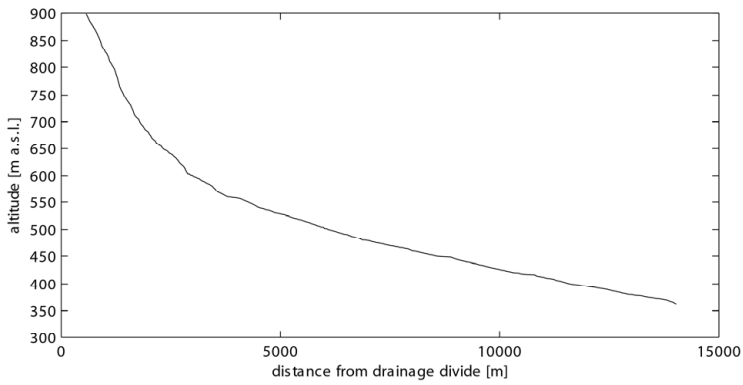
25 Homburgerbach (629 980 / 256 999)
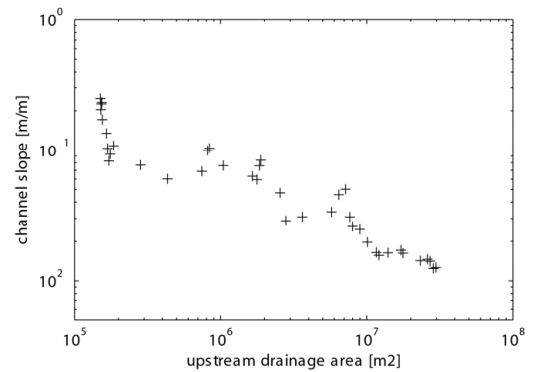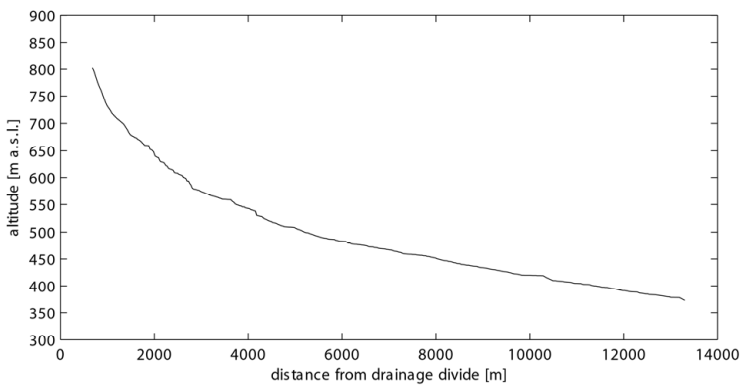
26 Eibach (620 650 / 265 384)
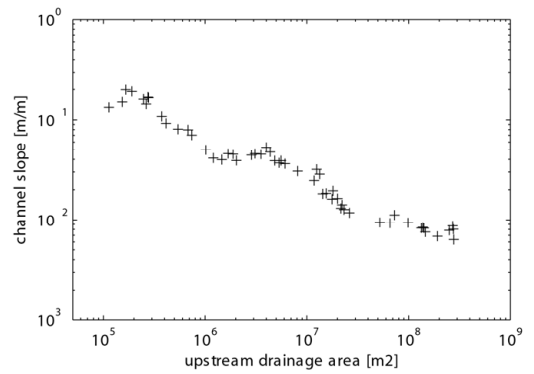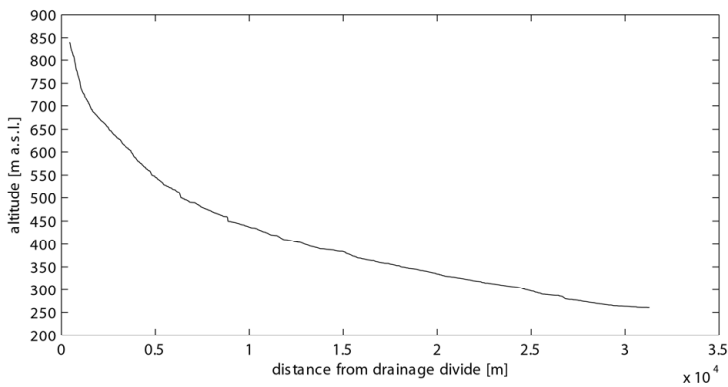
27 Ergolz (631 270 / 257 353)

_____
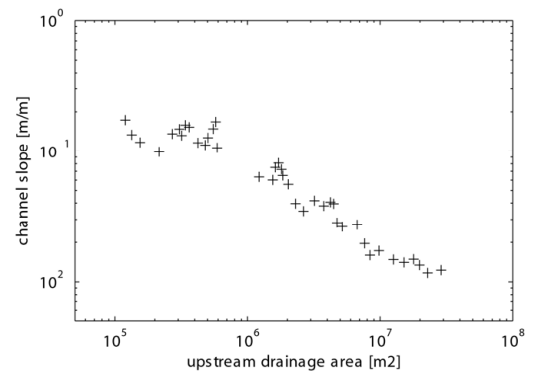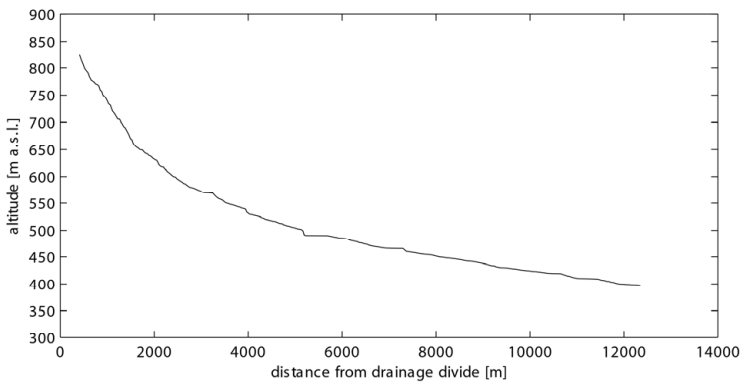
28 Duebach (635 779 / 256 826)
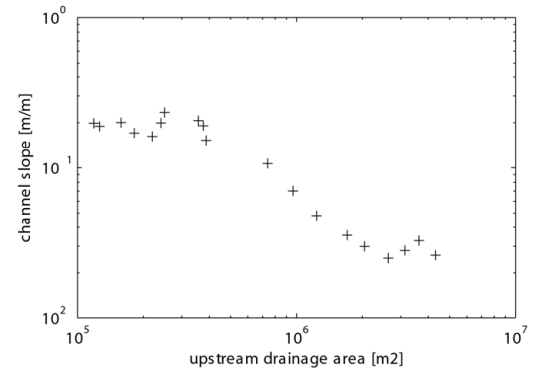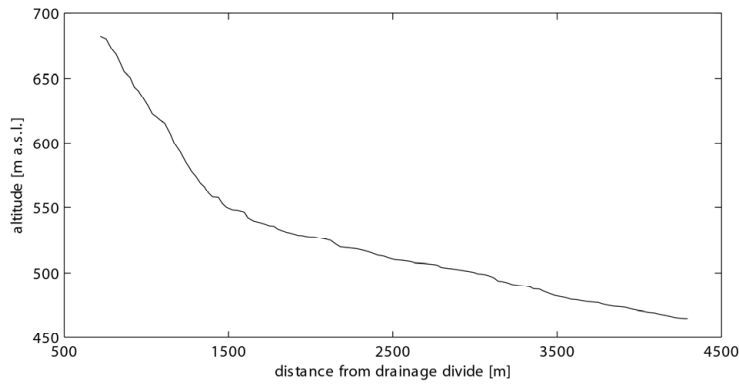
29 Hemmiker (632 890 / 257 626)
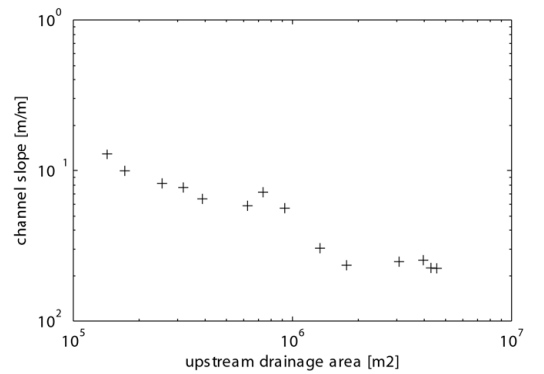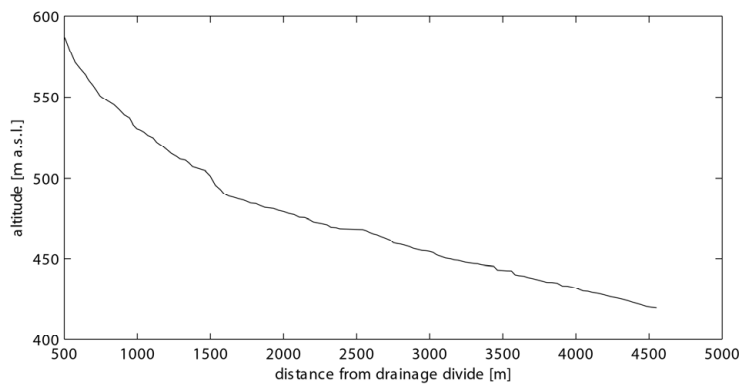
30 Rickebächli (631 920 / 257 299)
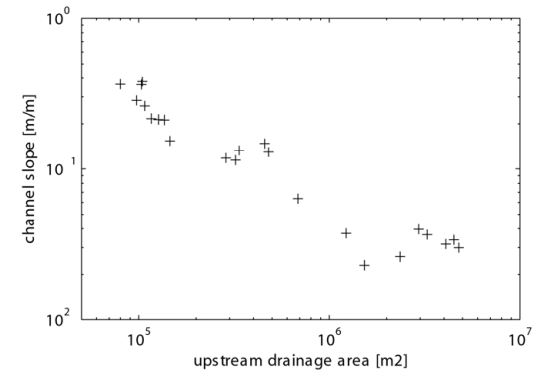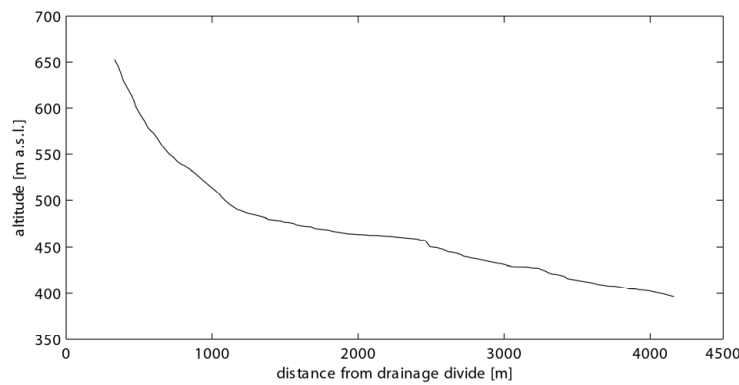
31 Magdenerbach (626 724 / 267 379)
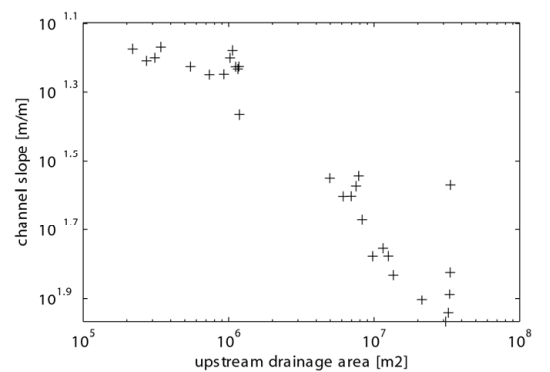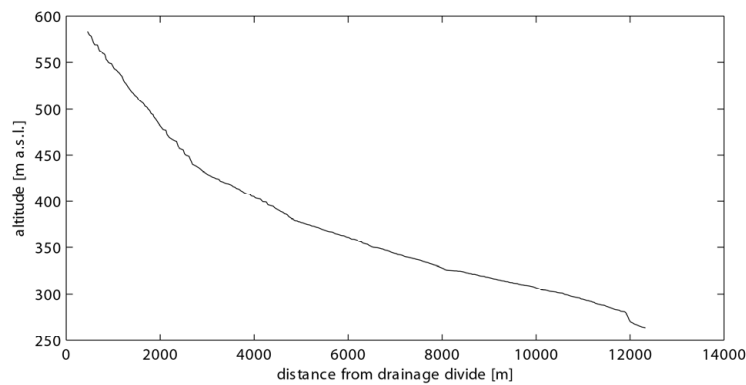
32 Fischingerbach (636 422 / 266 335)
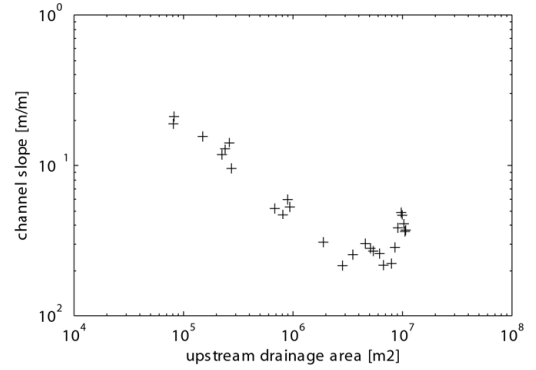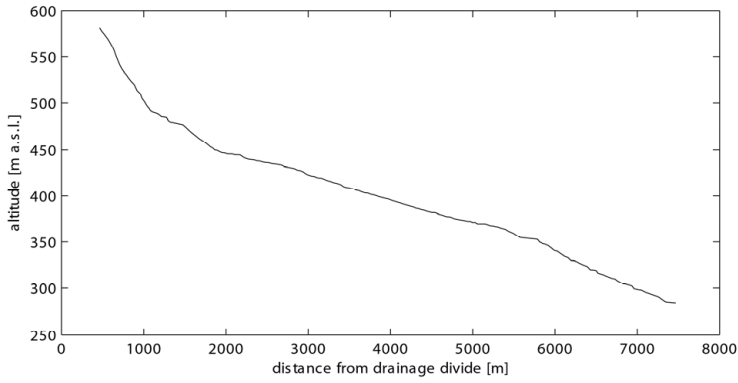
33 Bruggbach (640 990 / 267 202)
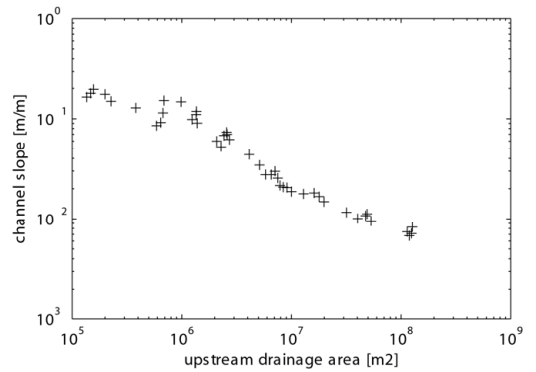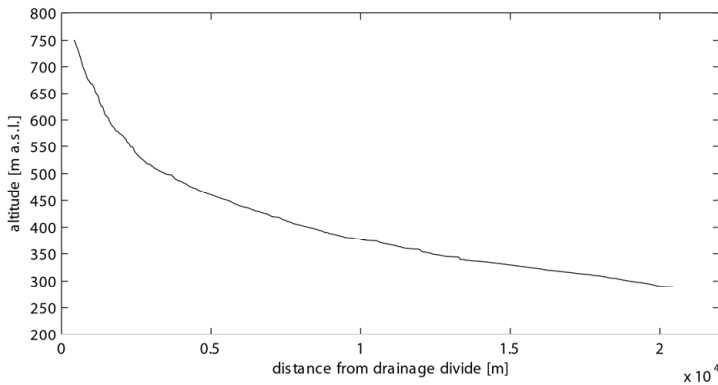
34 Dorfbach (Sissle) (641 573 / 259 625)
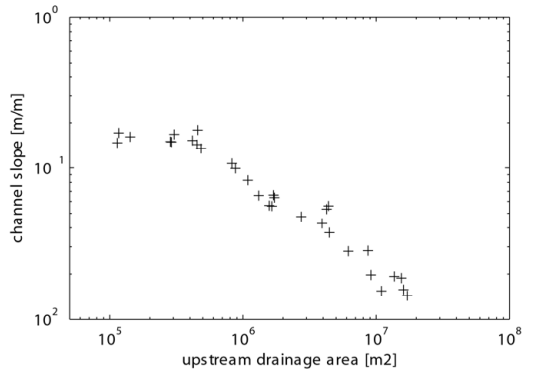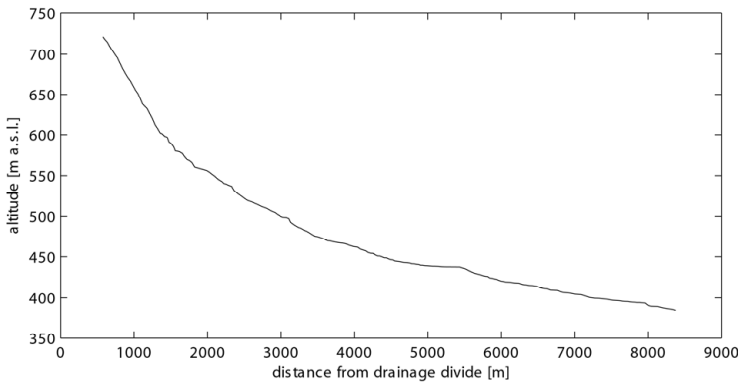
35 No 35 (643 844 / 262 251)

_____
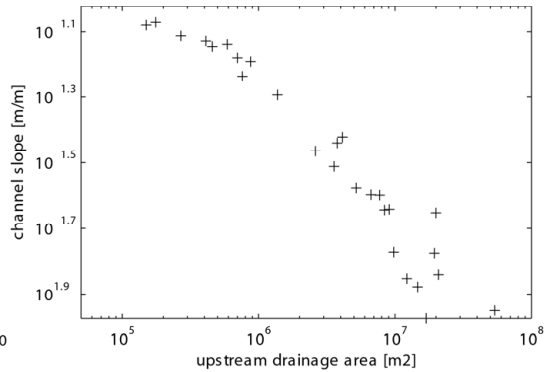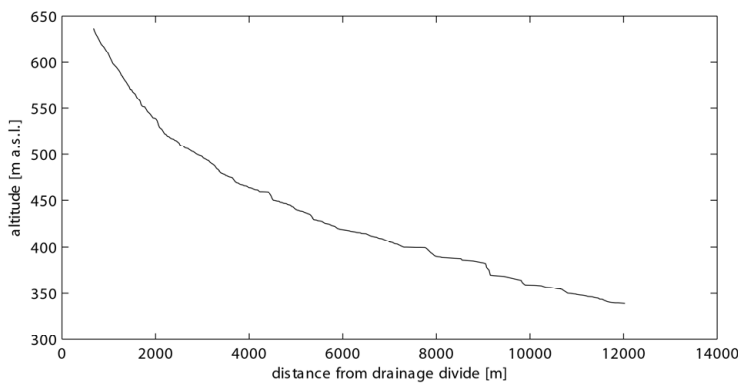
36 Zeiherbach (646 300 / 261 579)
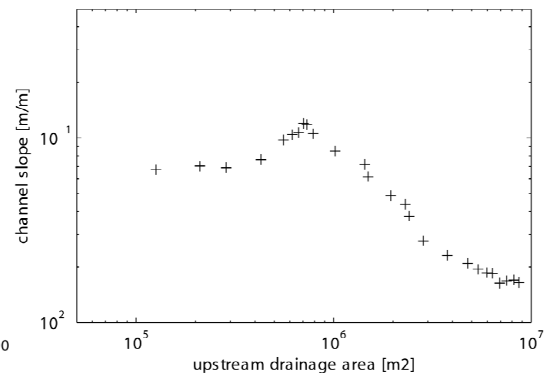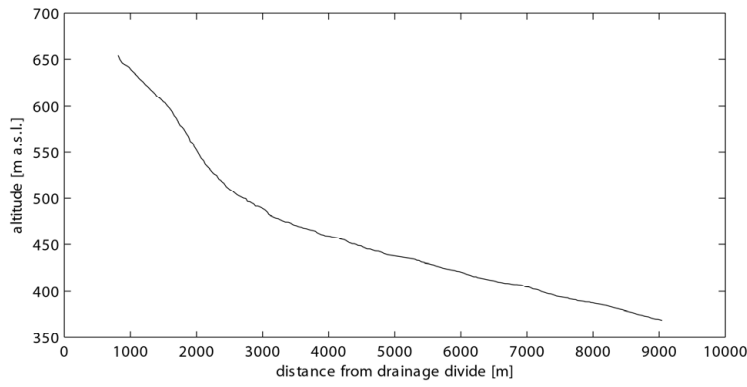
37 Sulzerbach (648 871 / 267 554)
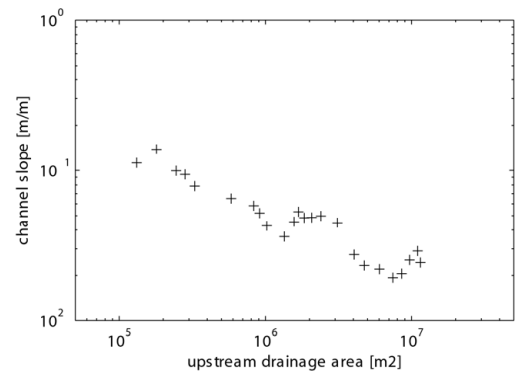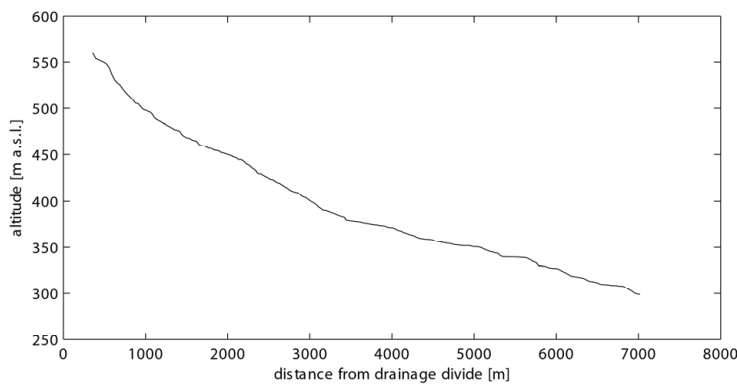
38 Etzgerbach (650 710 / 269 252)
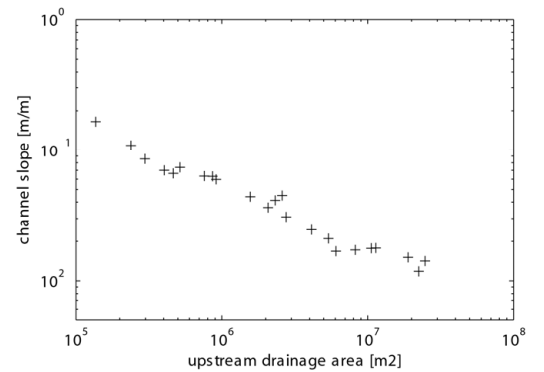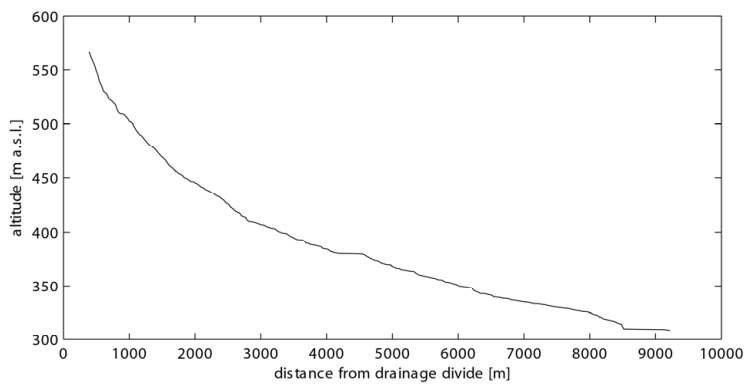
39 Schmittenbach (659 397 / 264 426)

_____
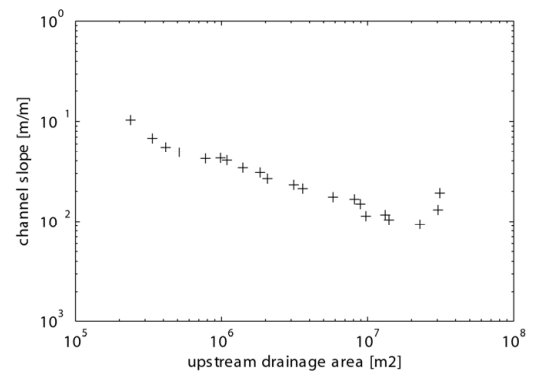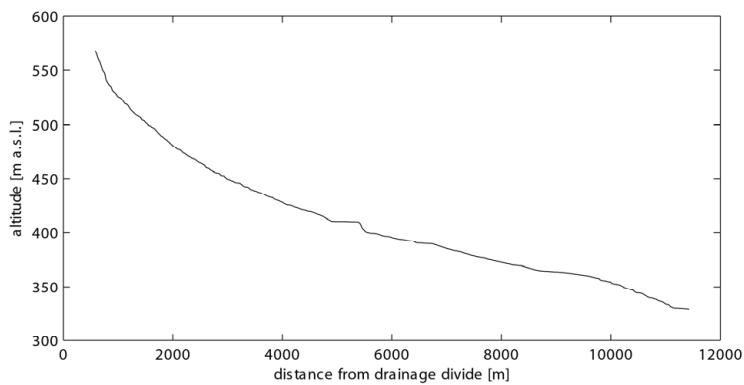
40 Talbach (654 263 / 255 810)
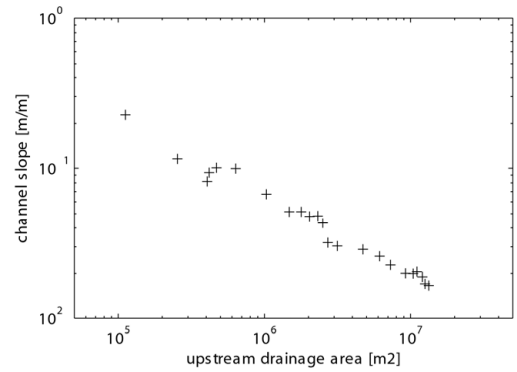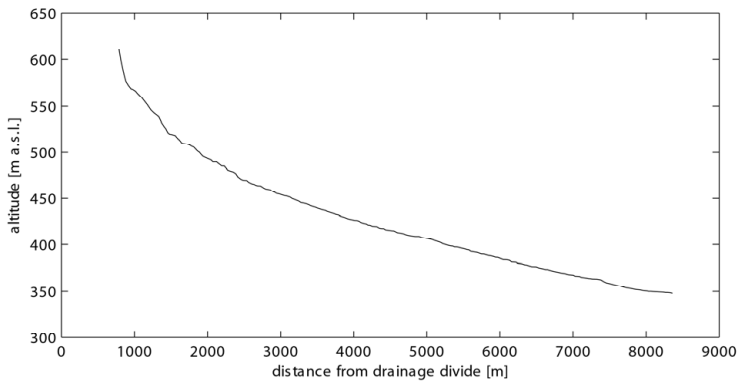
41 Aabach (647 399 / 251 720)
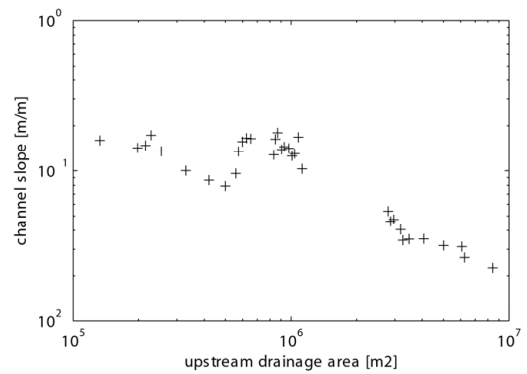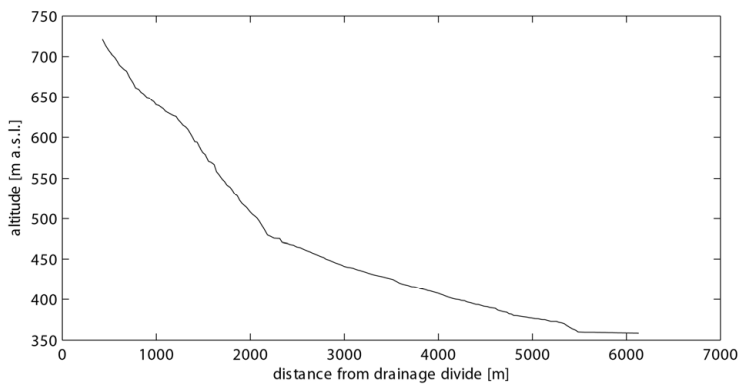
42 Erzbach (643 855 / 248 976)
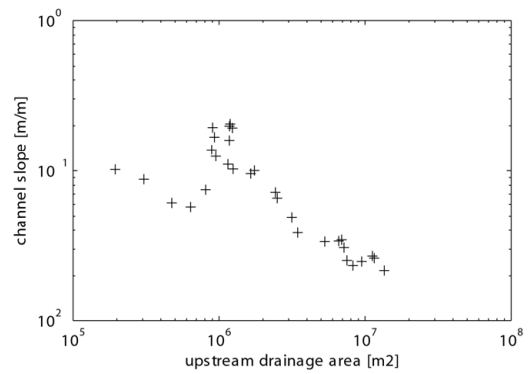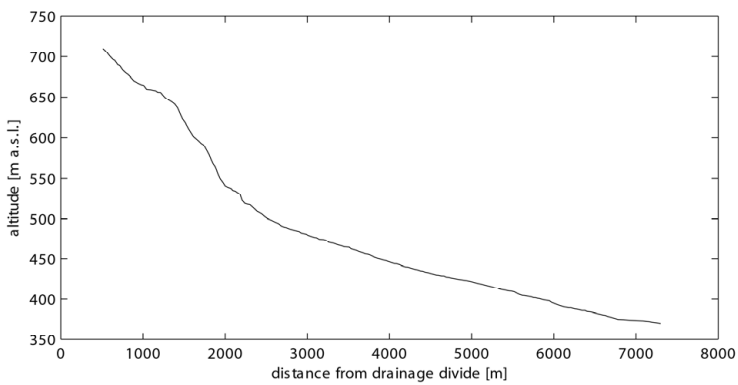
43 Stüssliger (639 626 / 246 154)
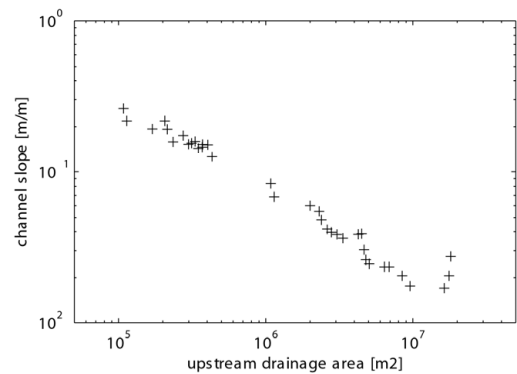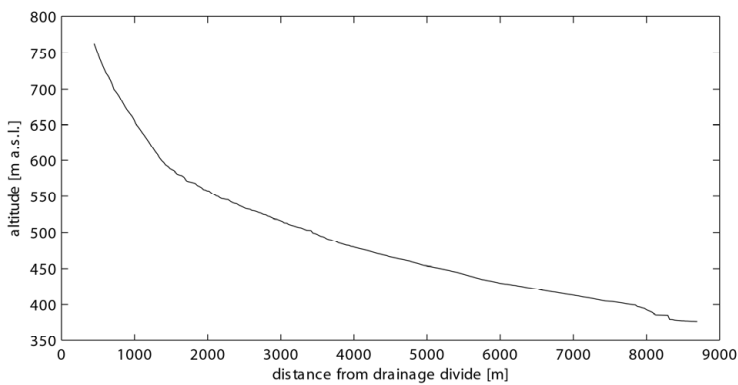
44 Dorfbach (635 404 / 245 473)
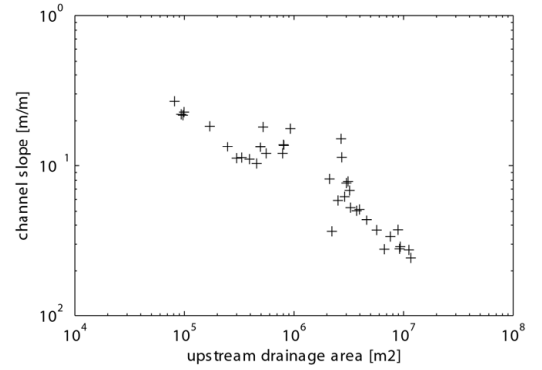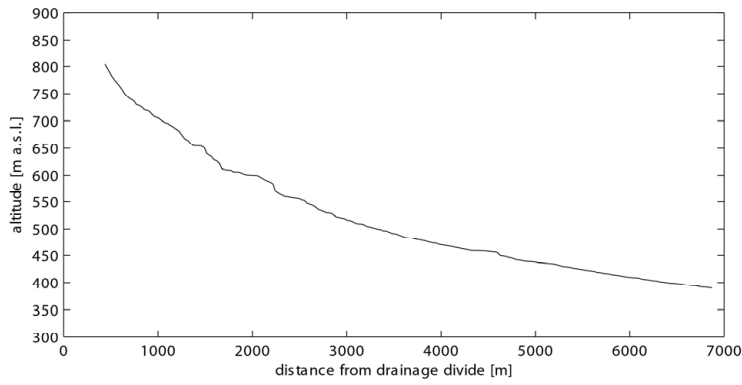
45 No 45 (632 668 / 243 503)
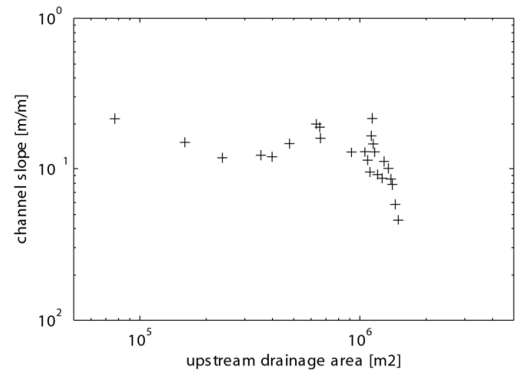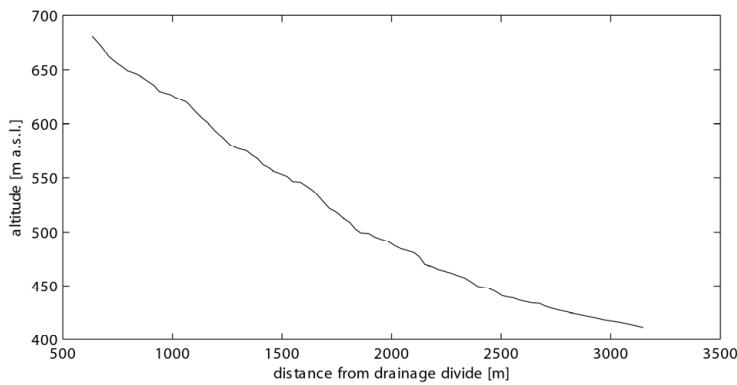
46 No 46 (632 151 / 243 510)
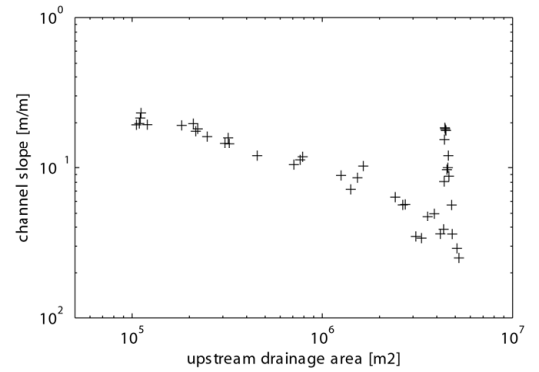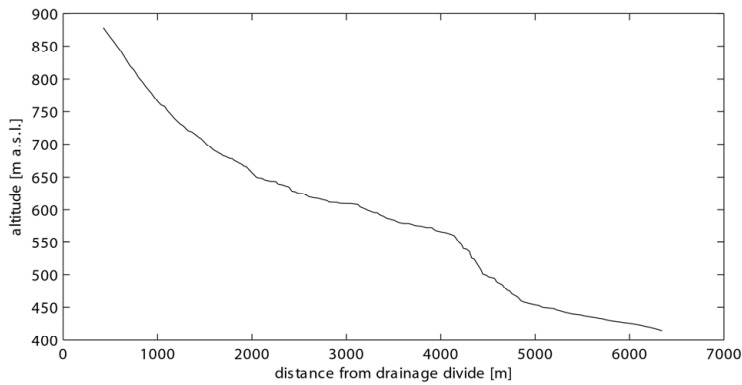
47 Cholersbach (630 775 / 241 972)
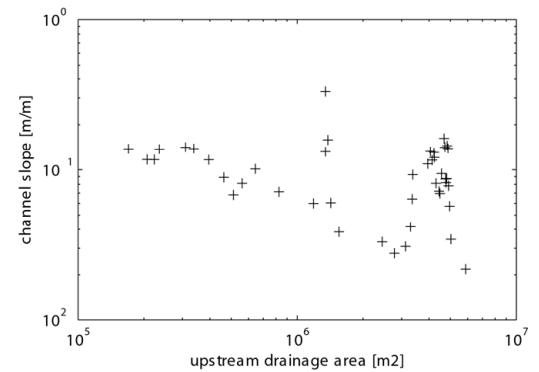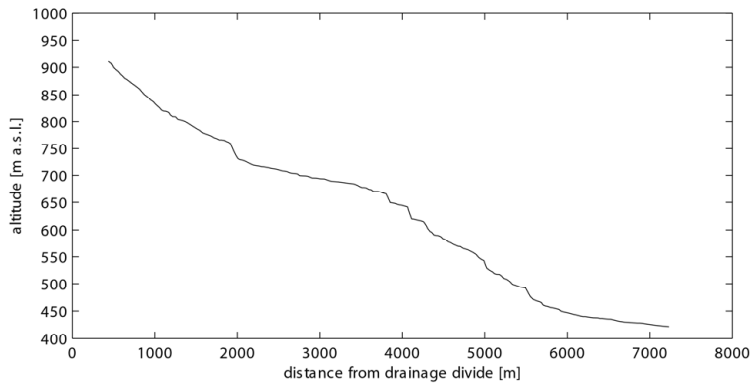
48 Augstbach (620 493 / 241 240)
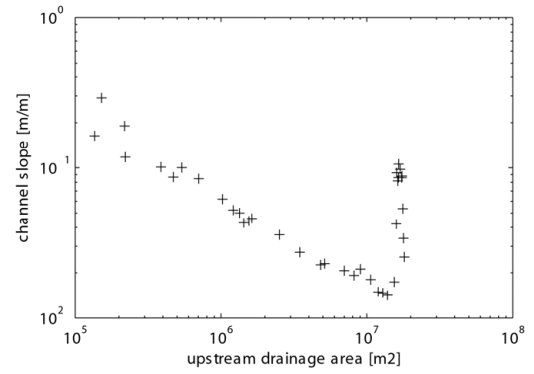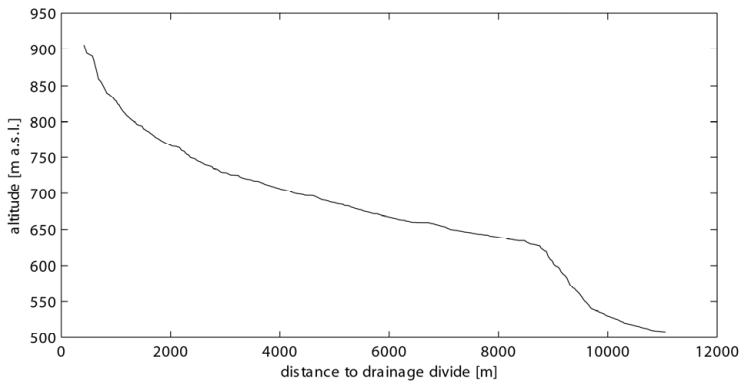
49 Limmerenbach (620 490 / 243 296)
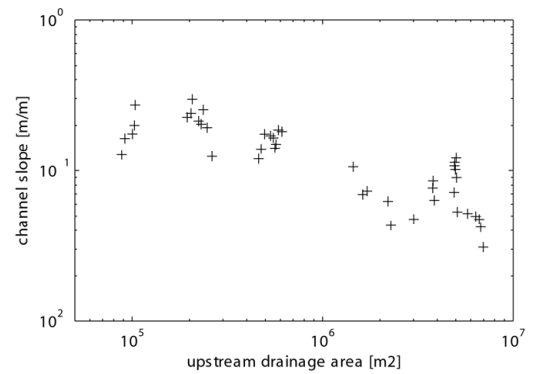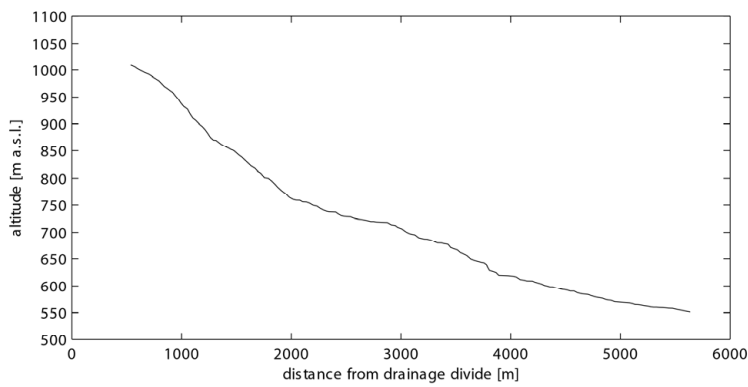
50 Mümliswilerbach (618 815 / 239 696)
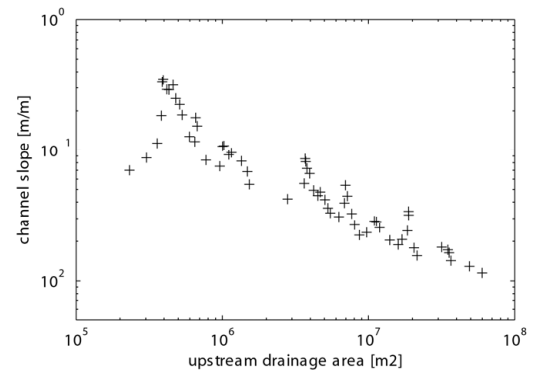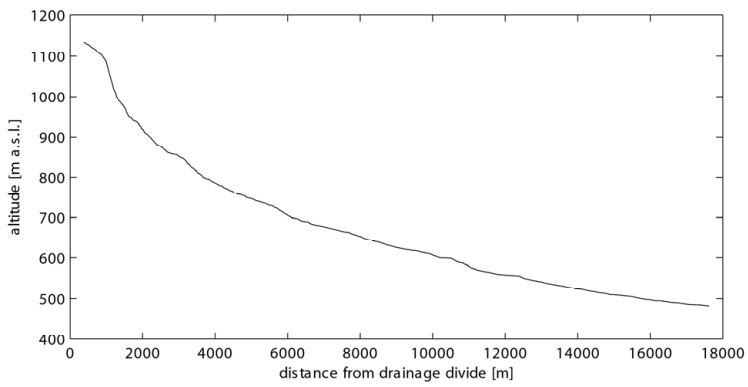
Chapter 4

Neotectonic activity in NW Switzerland: Evidence from the study of Late Quaternary alluvial terraces of the river Aare

4.1 Introduction

The geology of the subsurface of the Swiss Molasse basin in the northern Alpine foreland is being intensively studied as a potential site for the safe disposal of nuclear waste by Nagra (National Cooperative for the Disposal of Radioactive Waste). In particular, the Lower Jurassic Opalinuston formation appears to represent a suitable lithology due to its extremely low hydraulic conductivity (Croisé et al., 2004), and because it occurs at favourable depths for a nuclear-waste repository. Since the host rock of a waster repository should also be tectonically stable to minimise the hazard that the conatiners are exposed to, it is essential to know the tectonic activity in this area, in particular during the Quaternary (neotectonics) – quite aside from the immediate earthquake hazard this activity poses for the population.

Tectonically, the northern Alpine foreland is relatively stable today. The main tectonic events that have affected the region are, apart from the Alpine orogeny, the formation of the Upper Rhine Graben in the Paleogene (Ziegler, 1992) and the formation of the Jura fold-and-thrust belt in the Late Miocene (Burkhard, 1990) (Figure 1). Compressional deformation has been shown to be active in the southern Upper Rhine Graben west of Basel (Giamboni et al., 2004a), but the style of deformation seems to have changed from mostly thin-skinned (only affecting the sedimentary cover) to the reactivation of basement faults in the Late Pliocene (Ustaszewski and Schmid, 2007). The present-day stress field is consistent with ca. NW-SE oriented compression in the crystalline basement (Müller et al., 2002; Kastrup et al., 2004), and ca. N-S oriented compression in the sedimentary cover (Becker, 2000). In general, tectonic deformation rates are very low, and it is therefore difficult to detect active structures. Geodetic measurements suggest gentle uplift in the area of the Folded Jura relative to a reference point at Laufenburg (Müller et al., 2002; Schlatter, 2006). Recent tectonic activity in the easternmost Jura mountains has not yet been substantiated (Müller et al., 2002), even though moderate earthquake activity is recorded (Deichmann et al., 2000).
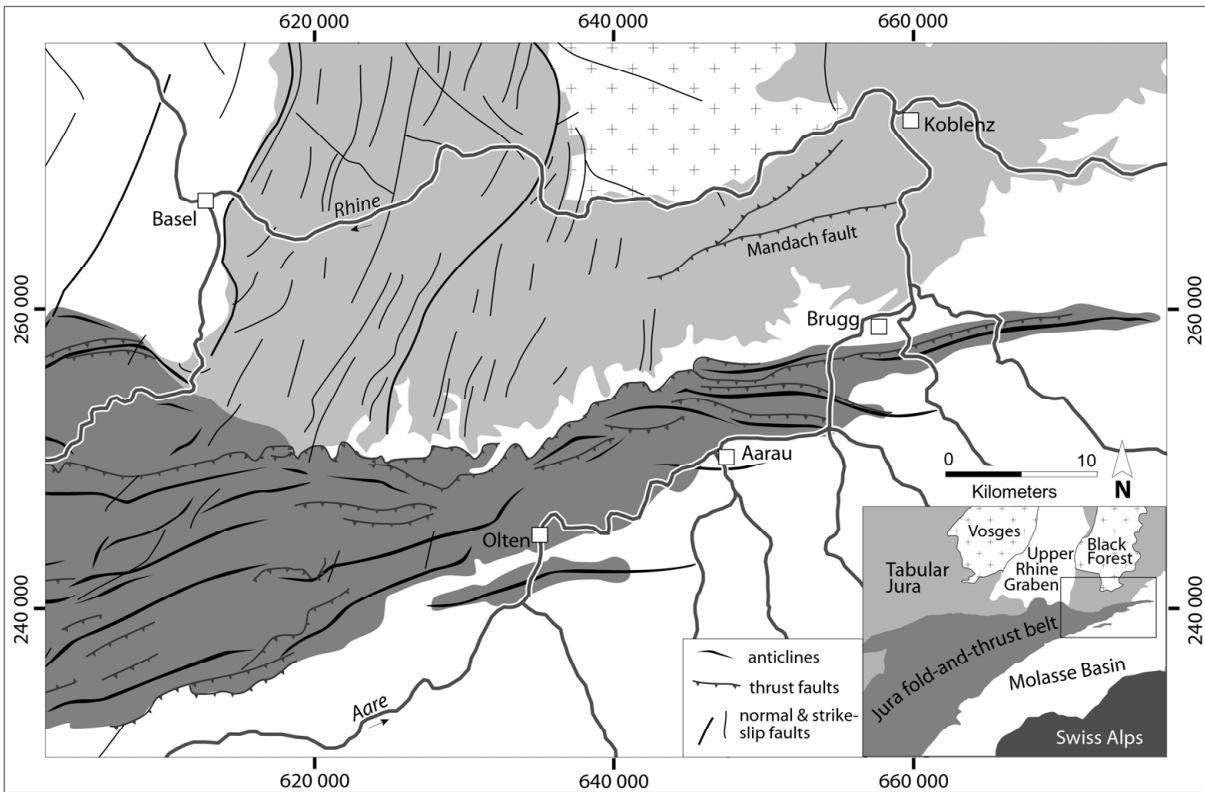
Figure 1: Main tectonic units and drainage system in the Aare valley area, central northern Switzerland.
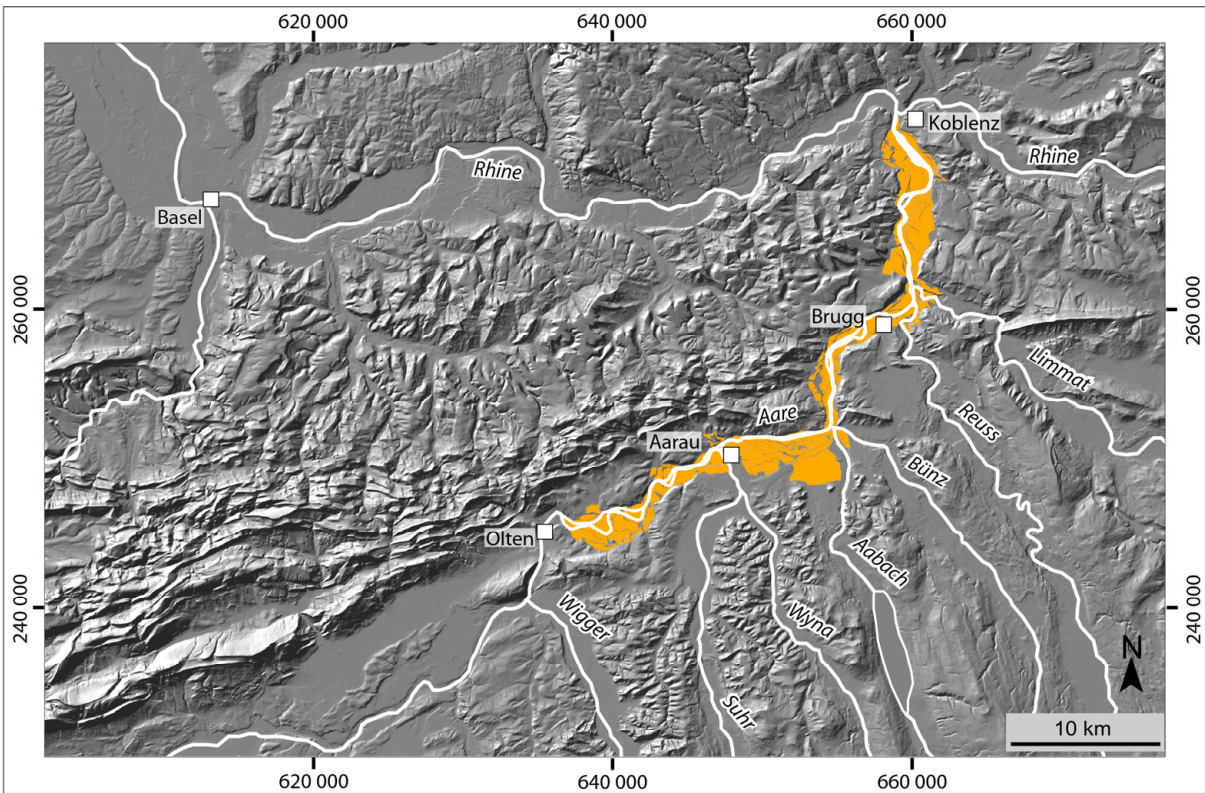
Figure 2: Shaded-relief map (DHM25, swisstopo) with occurrences of the Low Terrace gravels in the study area of the lower Aare valley, between Olten and Koblenz. Reproduced by permission of swisstopo (BA081622).

If the area of central northern Switzerland was tectonically active in the past 2 Ma, this should be visible in the deformation of the Quaternary fluvial terraces of the river Aare, which crosses the Jura fold-and-thrust belt in its lower reaches (Figure 2). A fluvial terrace forms when the aggradational river bed is abandoned due to incision of the river (Merritts et al., 1994). If this happens repeatedly, a terrace system with a series of abandoned surfaces develops, as is the case with the Aare river. These terraces, which are initially approximately planar features with submeter to meter scale topography, would be expected to represent ideal markers that record tectonic deformation within the Jura fold-and-thrust belt.

The lower Aare valley has already been studied by Haldimann et al. (1984), who focused on a longitudinal profile of the terraces and the analysis of the bedrock channel below the Quaternary valley fill to detect recent tectonic activity. In the meantime, a new high-resolution digital elevation model has been produced (Swisstopo, 2007), which obviously contains a large amount of additional morphological information. The aim of this study is to analyse these elevation data for the effects of tectonic deformation on the morphological terraces of the lower Aare valley between Aarau and Koblenz. In addition, the results are compared to those of the previous Nagra study by Haldimann et al. (1984), as well as to new precise levelling data (Zippelt and Dierks, 2007). Moreover, the usefulness of the additional topographic information in a high-resolution digital elevation model is evaluated.

4.2 Tectonic Geomorphology

The landscape in a tectonically active area is the result of the interaction of tectonic and surface processes (Burbank and Anderson, 2001). When tectonic activity causes vertical and horizontal rock movements, the resulting topography is subjected to erosional and depositional processes. In turn, erosion and deposition can also affect tectonic processes (e.g., enhanced uplift due to erosional unloading; Montgomery, 1994; Simpson, 2004) .

Tectonic geomorphology is the study of the interactions between tectonic and surface processes. A wide variety of geomorphic features, such as mountain front morphology, valley shapes, and drainage patterns, store information about past or ongoing tectonic movements (Burbank and Anderson, 2001; Keller and Pinter, 2002). Of particular interest are features that can be used as markers to track tectonic deformation, and quantify deformation rates provided their age is given. A marker can be any feature for which the original geometry is known. For instance, originally horizontal shorelines can evidence tectonic deformation if they are tilted or warped today (Adams et al., 1999). Similarly, river channels and terraces can be used as geomorphic markers, even though they are not originally horizontal. When a river is not affected by tectonic

_____

deformation, or other external influences (such as landslides, lithological changes or confluences), it tends to develop a typical gradient continuously decreasing downstream ("equilibrium profile", e.g., Hack, 1957). If only a relatively short part of the river far away from the source is analysed, the equilibrium profile can roughly be approximated as a straight line. A deviation from this shape can, therefore, be an indicator for tectonic activity (Burbank and Anderson, 2001; Kirby et al., 2007).

Apart from the active river channel, river terraces can also record tectonic deformation. Fluvial terraces represent a former river bed that has been abandoned due to downcutting of the river into its own sediments or a bedrock channel. Assuming that the river was in equilibrium at the time the terrace formed, the same considerations concerning river profiles can also be applied to river terraces. It has to be kept in mind that the formation of fluvial terraces itself can be an effect of tectonically induced base-level fall.

Since terraces above the active channel are no longer directly influenced by the river, they can accumulate tectonic deformation over time since they became abandoned (Merritts et al., 1994). Moreover, if a number of terrace levels have been preserved, systematic differences in terrace shape between these levels can point to progressive tectonic deformation.

Apart from the shape of the longitudinal profile, other characteristics of terrace morphology and river geometry can be used to infer tectonic activity, including stream pattern changes and lateral movement of the channel. Possible effects of different tectonic deformation styles on rivers and terraces are summarised in the following, based on the detailed descriptions by Burbank and Anderson (2001), Keller and Pinter (2002) and Holbrook and Schumm (1999).

A   Effects of vertical deformation (normal faulting, reverse faulting, folding)

Aggradation/Degradation: The vertical deformation associated with many tectonic processes causes the river gradient to increase or decrease in the vicinity of the fault or fold. This leads to locally enhanced erosion and deposition, respectively (Figure 3a).

Knickpoints: A knickpoint in a longitudinal river profile marks the sudden transition from a low gradient upstream to a higher gradient downstream. Knickpoints can propagate upstream due to continuous erosion.

Surface faulting of terraces: A fault that reaches the surface can be evident by offsetting terrace treads and risers. Continuous faulting leads to a larger offset on older terraces. Discontinuous terraces can be difficult to correlate without absolute surface ages. If, however, terrace surface ages are available, even slip rates on the fault can be determined.
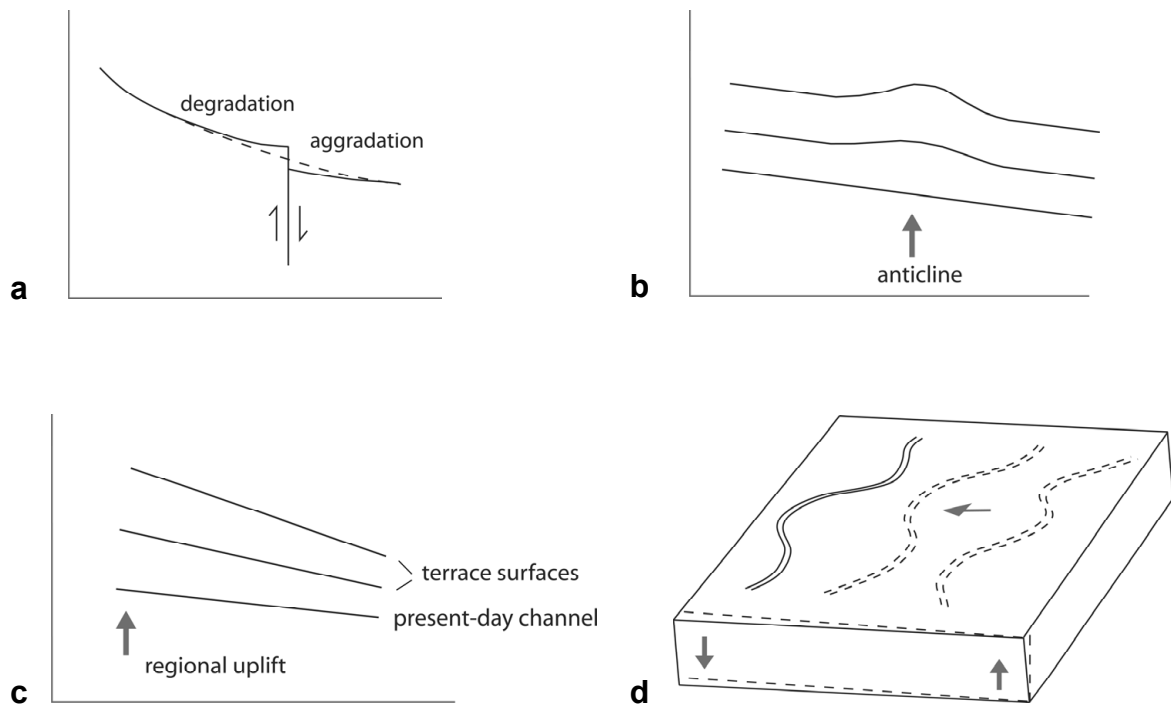
Figure 3: Possible effects of tectonic activity on river courses and terraces. a) Knickpoint generation at a fault, leading to aggradation and degradation. b) Warped terraces resulting from locally enhanced uplift. c) Tilting of terraces in the flow direction due to differential regional uplift. d) Lateral channel movement as an effect of regional tilting.

Warped terraces: If a terrace system crosses a fold or blind fault, the local deformation can cause warping of the terraces. Over time, continuing deformation is recorded by the terraces, with older terraces accumulating more deformation than younger ones (Figure 3b).

Changing river patterns: The differential vertical displacement associated with tectonic deformation sometimes leads to a change in sinuosity across the structure. This increases or decreases the channel length, compensating for the change in gradient. Similarly, the river pattern (braided, straight, meandering, or anastomosing) may change in the area of varying uplift.

Deflected river courses: If a stream encounters a zone of increased uplift and does not have sufficient erosional power to maintain its course, its path will be deflected around the structure, for instance, a propagating anticline (or into a zone of subsidence).

_____

B   Effects of strike-slip deformation

Surface faulting of terraces: Analogous to normal or thrust faults, terrace surfaces and risers can be used as markers recording offset by strike-slip faults. Again, surface (or deposition) ages may allow determination of deformation rates.

Offset river courses / beheaded rivers: When a stream crosses an active strike-slip fault, its downstream reaches are offset relative to the reaches upstream from the fault. This will result in increased lateral erosion and an asymmetric river cross-section, if the stream power is high, or an increasingly distinct deviation of the river course.

C   Effects of regional tilting

Tilted terraces (laterally or longitudinally): Regional tilting in the direction or opposite to the flow direction increases or decreases the longitudinal gradient of the terrace surfaces compared to the present-day river, assuming that the river itself is at equilibrium with the deformation. If deformation is continuous, higher (older) terrace surfaces will show a more pronounced difference than younger surfaces, resulting in downstream convergence or divergence (Figure 3c). Tilting perpendicular to the flow direction of the stream will result in a higher position of the terraces on one side of the river compared to the corresponding terrace treads on the other side. However, if the terraces are not continuous or incompletely preserved, it might not be possible to correctly correlate surfaces that formed at the same time.

Lateral channel movement: Regional lateral tilting cannot only affect the abandoned terrace surfaces, but also the active channel. Slow tilting will force an alluvial river to progressively shift to one side, eroding mainly on the down-thrown side (Figure 3d). Thus, channels and terraces on the uplifted side are more likely to be preserved. If the river is confined by valley sides, it may erode and undercut one side, resulting in an asymmetric valley cross-section.

All these features shoud be used with caution to infer past or ongoing tectonic processes, since most of them also occur in settings without tectonic activity. For instance, changing discharge or sediment load caused by climatic changes can force a river to incise or aggrade. The same accounts for base-level fall or rise, which itself might be a response to regional tectonics, but can also be a result of sea-level changes. Irregularities in the river longitudinal profile or pattern can be an effect of varying lithology (erodibility contrasts). Deflection of river courses can be caused by inactive faults, especially if the faulted rock is more easily eroded than the surrounding

material. Other factors contributing to stream deflection are tributaries with high sediment input and normal deposition processes on a floodplain that block the flow path. Moreover, also human modifications of the fluvial system have to be taken into account.

In specific tectonic environments, different scales of surface deformation are expected. A growing anticline is likely to influence the gradient of a river that crosses it on a width of several kilometres, depending on the wavelength of the fold. Surface rupture causes gradient changes within a few metres; if faulting does not reach the surface, however, deformation will have a longer wavelength comparable to that of folding. The response of the alluvial river can have an even larger extent upstream and downstream of the zone of deformation. Therefore, if differential uplift due to folding or faulting on blind faults is taking place, the expected gradient changes of the river terraces would have a scale of several kilometres. Low-rate regional tilting may be visible over tens of kilometres only.

4.3 Quaternary fluvial sediments in northern Switzerland

After the deposition of the youngest preserved Molasse units (Upper Freshwater Molasse, OSM) around 11-12 Ma ago (Bolliger, 1998; Rahn and Selbekk, 2007), an overall erosional regime largely prevented the deposition or preservation of younger sediments over wide areas in northern Switzerland. From the beginning of the Quaternary, repeated climatic changes with glacials and interglacials led to increased erosion in the Alps and the deposition of glacio-fluvial sediments in the northern Alpine foreland (Müller et al., 2002). Repeated incision caused the formation of new valleys and a system of alluvial terraces. This terrace system is usually divided into four main groups (Figure 4, from top to bottom): the Höhere Deckenschotter (Higher Cover Gravels), the Tiefere Deckenschotter (Lower Cover Gravels), the Hochterrassenschotter (High Terrace Gravels) and the Niederterrassenschotter (Low Terrace Gravels). They have traditionally been correlated with the four glacial stages recognized in SW Germany (Günz, Mindel, Riss, Würm), based on the classification by Penck and Brückner (1909). The highest terraces are the oldest, but radiometric or biostratigraphic ages are sparse. The classic morphostratigraphic concept applied to the northern Alpine foreland interprets the different sedimentary groups as deposits in front of the Alpine glaciers, based on alternating phases of accumulation and erosion. Increased sediment production at the end of each glacial is thought to have resulted in the accumulation of thick glacio-fluvial deposits. Continuous discharge combined with decreased sediment production, and general uplift relative to the base level in the Upper Rhine Graben caused incision into these sediments or into the underlying bedrock. This concept is probably adequate to describe the
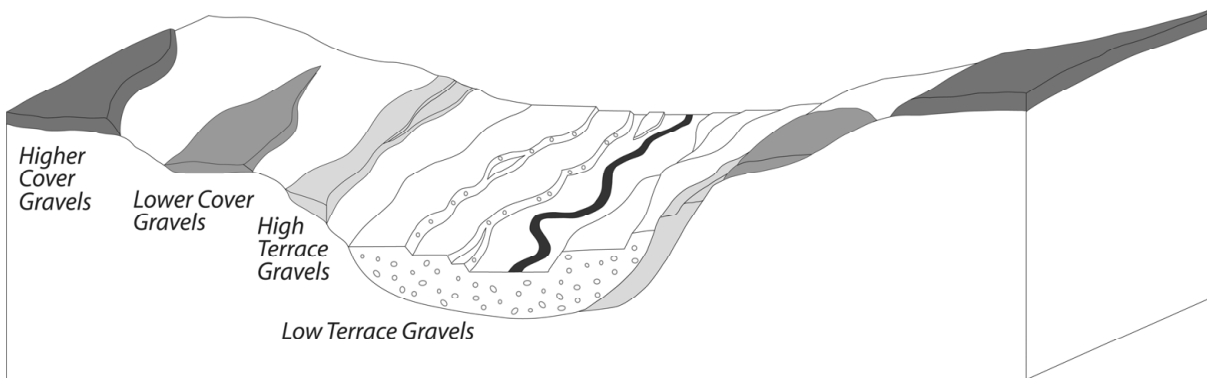
Figure 4: Schematic view of the terrace system in northern Switzerland.

general evolution of the present-day drainage system, and the assumption that the older deposits have a higher topographic position than the younger deposits appears to hold. However, it has been shown that a simple division into four groups does not capture the complex deposition and erosion history of the Quaternary gravels in northern Switzerland (Schlüchter, 1976; Graf, 1993). In the following, a short overview of the occurrence and the formation of the main gravel deposits is given.

The *Higher Cover Gravels*, a distal fluvio-glacial sediment, were deposited on a nearly planar surface after filling some pre-existing shallow valleys (Bitterli et al., 2000; Ivy-Ochs et al., 2006). Their age is uncertain. Graf (1993) discriminated the influence of a series of glaciations, and inferred from the normal polarity of the oldest sedimentary units that they were deposited during the Jaramillo reversal in the Matuyama chronozone, which corresponds to a minimum age of ca. 0.95 Ma. Bolliger (1996) determined an age between 1.8 and 2.1 Ma for the Higher Cover Gravels at the Irchel location, based on fossil mammals. Other ages vary between ca. 0.65 Ma (van Husen, 2004) and 2.35 (+1.08/-0.88) Ma (Häuselmann et al., 2007), determined using cosmogenic nuclide methods; these ages were, however, not determined in the Swiss Higher Cover Gravels, but equivalent sediments in Austria and Germany, respectively. The deposits of this unit are generally highly weathered and form isolated outcrops at relatively high altitudes (ca. 550-750 m a.s.l. compared to ca. 350 m a.s.l. of the present-day Aare river; Graf, 1993).

The following phase of incision initiated the formation of a new valley system in the Swiss Alpine foreland (Graf, 1993; Bitterli-Dreher et al., 2007), after which the *Lower Cover Gravels* were deposited. These, too, are difficult to correlate and date; proposed ages vary from ca. 0.45 Ma (marine isotope stage 12; van Husen, 2004) and 0.68 (+0.23/-0.24) Ma (Häuselmann et al., 2007).

This phase was again followed by a period of valley incision (ca. 150 m) before the deposition of the *High Terrace Gravels,* which can be roughly divided into three levels (Bitterli et al., 2000).

Apparently separated from the High Terrace Gravels by a glacier advance, the *Low Terrace Gravels* were deposited. In this unit, a series of accumulation and erosion episodes led to the formation of cut-and-fill terraces (Müller et al., 2002). They now consist of a large number of terrace levels; only segments of the highest level, the accumulation level, can be plausibly correlated at some places (Bitterli et al., 2000; Bitterli-Dreher et al., 2007). Due to the lack of age constraints it is not clear if the gravels were deposited in one accumulation period with subsequent incision, or whether erosion was followed by additional accumulation episodes. Downstream from the confluence of the Aare and the Rhine, deposition ages of 11-27 ka have been determined for different levels of the Low Terrace based on optically stimulated luminescence (OSL; Kock et al, submitted). In the lower Aare valley, however, dateable material has so far been limited to mammoth tusks and bones, which provided ages between ca. 19.7 ka and 32.6 ka (MBN-AG, 1998; Bitterli et al., 2000). In this reach the system of the Low Terrace Gravels was influenced by the water and sediment input from the Rhone, Aare, Reuss and Rhine-Linth glaciers (Graul, 1962). This further adds to the complexity of the terrace system.

4.4 Tectonic activity in Northern Switzerland in the Quaternary: different scenarios and their expected effects on fluvial terraces

The Neogene tectonic history of northern Switzerland was dominated by the main phase of the Alpine orogeny (late Eocene to Miocene) and the formation of the Upper Rhine Graben in the Paleogene (for a short overview, see Müller et al., 2002). During the latest stages of the Alpine orogeny, the Jura fold-and-thrust belt evolved as a result of decollement tectonics in the NE Alpine foreland. To the east of the Jura fold-and-thrust belt, the Molasse deposits remained generally undeformed.

The tectonic evolution after ca. 5 Ma is not very well resolved, due to low deformation rates and a generally erosive regime. Cederbom et al. (2004) have estimated that since ca. 5 Ma, at least 1 km has been eroded in the Swiss part of the Molasse basin based on fission-track data, which would imply some degree of isostatic rebound following this erosion. This isostatic uplift might still be responsible for a regional tilt towards the north in the study area.

Folding of the Pliocene Sundgau gravels west of Basel points to ongoing deformation at least until the Late Pliocene (Giamboni et al., 2004b). The interpretation of seismic lines indicates that this deformation was caused by the transpressional reactivation of basement faults, in contrast to

the thin-skinned decollement tectonics typical of the Jura fold-and-thrust belt (Ustaszewski and Schmid, 2006). These basement faults are probably related to a Permo-Carboniferous trough system that extends from the area of the Bresse Graben in the west to Lake Constance in the east (Diebold and Noack, 1996; Ustaszewski and Schmid, 2007).

As most of the preserved Quaternary sediments in northern Switzerland are very discontinuous, they are only of limited use for neotectonic analyses. Graf (1993) studied the Late Pliocene Cover gravels of Alpine origin that lie north of the topographic high formed by the Mandach thrust fault, suggesting that this north-vergent fault was active in the Pleistocene. Other studies have focused on the occurrence and distribution of the Low Terrace gravels, the youngest sedimentary unit, which has been preserved best (Penck and Brückner, 1909; Wittmann, 1961; Graul, 1962).

Here, special attention will be given to the work of Haldimann et al. (1984). These authors studied the river pattern and terrace systems, as well as the morphology of the bedrock channel below the Quaternary valley fill of the lower Aare reach between Aarau and the confluence with the Rhine. They suggested mainly three types of potential tectonic movements. First, from the upstream diverging terrace gradients, and the observation that the terraces were generally steeper in the N-S reaches, they deduced a regional tilt to the north (ca. 0.7 mm/a). Second, a gentle ridge in the bedrock channel, here consisting of soft Opalinuston clay, underneath the Quaternary valley fill along the eastern prolongation of the Mandach thrust near Böttstein, suggested thrusting activity on this fault (uplift rate of ca. 0.08 mm/a). This could also explain a suspicious terrace riser in this area. Third, activity on an anticlinal structure (uplift rate of ca. 0.04 mm/a) was inferred from an elevation in the bedrock channel surface near Klingnau, an area where the river course seems to be diverted. The rates of these movements were supposed to be in the order of 0.04 – 0.7 mm/a.

The present-day tectonic activity in the Swiss northern Alpine foreland is mainly constrained by seismotectonic and geodetic data. The seismicity in northern Switzerland has been described in detail by Deichmann et al. (2000); a summary of this report is given in Müller et al. (2002). In northern Switzerland, earthquake activity is concentrated in the area of the southern Upper Rhine Graben and the Dinkelberg on one hand and in the region of north-eastern Switzerland (Thurgau, Zürich, Central Switzerland) on the other hand. Seismicity is relatively low in the central part of northern Switzerland. The majority of the focal mechanisms show strike-slip deformation; pure and oblique normal faulting also occur (compare Chapter 5 in this thesis). In most cases the focal planes of the earthquakes seem to have a NW-SE or NNE-SSW strike. Faults related to the strike of the Permo-Carboniferous
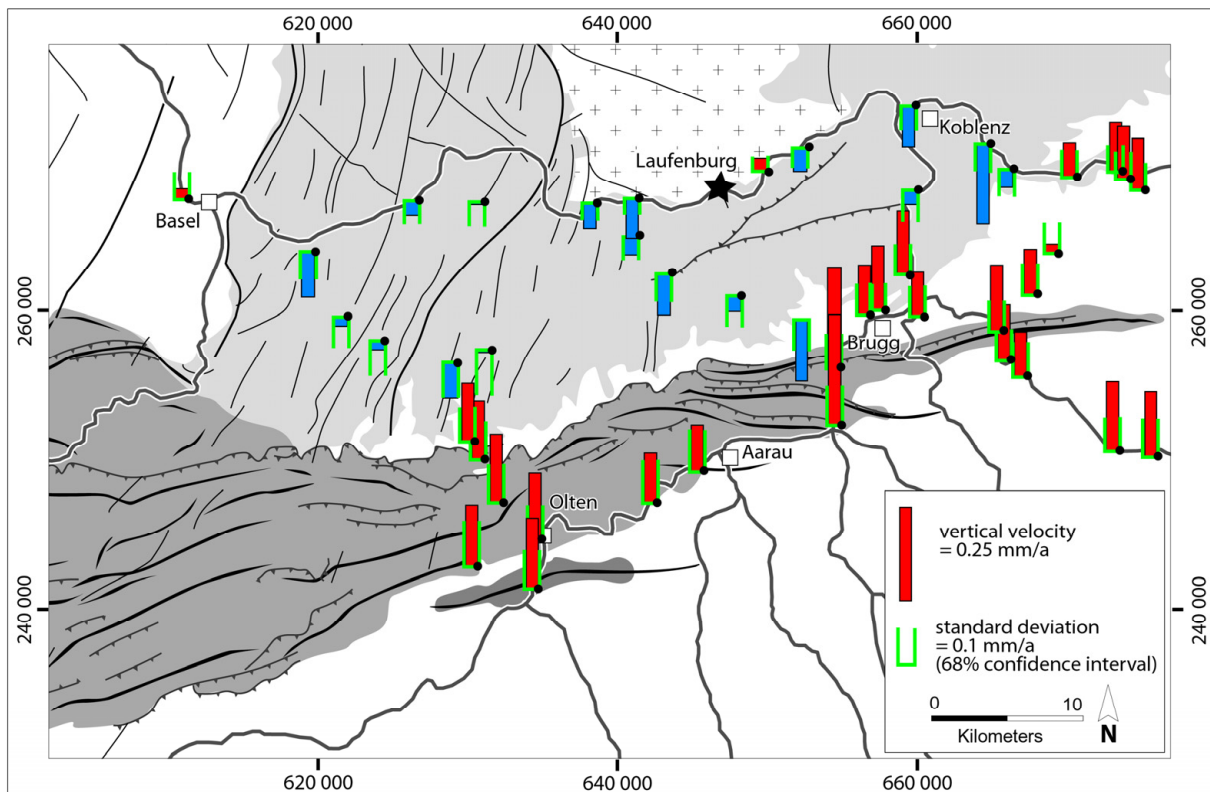
Figure 5: Selected vertical velocities in northern Switzerland, relative to a reference point near the Aare-Rhine confluence (Laufenburg, shown by the star) (after Schlatter (2007)).

trough system in the basement seem to be inactive, their orientation relative to the principal stress axes being unfavourable. The direction of maximum horizontal compression inferred from the analysis of focal mechanisms varies between 325° and 350° from west to east. Most hypocentres are located at a depth of > 2 km in the crystalline basement, but the occurrence of shallower earthquakes cannot be excluded completely. Due to the uncertainty of the hypocentre location and the large number of faults in the area, individual faults can usually not be identified. The earthquake record after 1999 generally confirms the findings by Deichmann et al. (2000).

In a newer study of the present-day stress field in northern Switzerland, Kastrup et al. (2004) inferred a regional NW-SE directed maximum horizontal stress axis in the crystalline basement, changing along the Alpine arc, from stress inversion using focal mechanisms. This does not, however, exclude local variations of the stress field. Becker (2000) analysed the stress field in the sedimentary cover of the Jura fold-and-thrust belt, using borehole breakout measurements, and derived a general maximum horizontal stress orientation (S_H) of NW-SE to N-S for the eastern and northwestern parts of the belt. Müller et al. (1987) observed an orientation change of borehole breakouts in a borehole that crosses the Triassic detachment horizon, implying a decoupling of the stress field at this boundary (S_H ca. 135° below, ca. 7°

above the boundary). However, this is no evidence of ongoing decollement tectonics. Morover, the detachment horizon may be too shallow today to deform in plastic style (Ustaszewski and Schmid, 2007).

Geodetic constraints on the recent deformation pattern mainly come from precise levelling campains, since the record of GPS measurements only covers ca. 20 years (Müller et al., 2002). In contrast, precise levelling measurements have been carried out in Switzerland for a period of ca. 100 years. The results suggest differential uplift in N Switzerland, in particular uplift in the area of the Folded Jura relative to the Tabular Jura, and a tendency to regional uplift of the southern parts of the Alpine foreland compared to the north (Schlatter, 2006; 2007; Zippelt and Dierks, 2007). However, the measurement uncertainties are still very large, and precise statements cannot be made. Maximum rates of relative vertical movements of the Folded Jura relative to a reference point in the Rhine valley (Laufenburg) are ca. 0.25 mm/a, very close to the level of uncertainty (Figure 5).

Despite in-depth analysis of evidence from different sources, the tectonic deformation pattern in northern Switzerland is still not very well constrained. In particular, the question as to whether the observed vertical deformations can be attributed to large-scale tectonic deformation (regional tilt) or local processes on descrete structures (Mandach thrust and its eastern continuation, Jura folds and thrusts, basement faults) remains open. Therefore, there exist several possible scenarios of tectonic processes that might currently affect the study area in northern Switzerland. These are given in Table 1, together with the expected effects on the Low Terrace Gravel system.

4.5 Key questions and objectives of this study

The focus of this study lies on the occurrence and morphological characteristics of the alluvial Low Terrace in the lower Aare valley between Aarau and Koblenz. The main objective is to analyse the terrace system with respect to neotectonic activity using the new 2 m-resolution digital elevation model DTM-AV (Swisstopo, 2007) and to compare the results to those of Haldimann et al. (1984). Therefore, the same transect lines as in the previous investigation are studied. This approach also allows evaluating the advantages of using high-resolution digital elevation data in a Geographic Information System (GIS).

The key research questions to be addressed are:

- What additional information about terrace morphology can be drawn from the new high-resolution digital elevation model?

Tectonic processes that might currently be affecting the study area in N Switzerland:	Expected effects of each of these scenarios on the Late Quaternary terraces in the lower Aare valley:
A: River incision, due to base-level fall in the Upper Rhine Graben / climate-driven (no tectonic activity)	A: Progressive lowering of the river bed, incision and terrace formation; younger terrace treads are lower and steeper at the same point along the river course
B: Large-scale regional tilt to the north, due to general differential uplift of the Alps and the nearby foreland (isostatic rebound)	B: Reaches in S-N direction: higher (older) terraces are steeper than lower (younger) terraces Reaches in W-E direction: terraces on S side are higher than corresponding terraces on N side; tilted terrace surfaces towards the river / away from the river; lateral movement of the river course (to the N); higher terrace risers in the S than in the N
C: Ongoing compression of the Alpine foreland, either thick-skinned or thin-skinned → folding, thrusting	C: Effects of individual folds or thrust faults: reduced gradient in front of, increased gradient behind the structure; more deformation on older terraces. Effects of entire fold-and-thrust belt: deflection; reduced and increased gradient as above
D: A combination of any of the above	D: Superposition of any of the above

Table 1: Different plausible neotectonic scenarios for northern Switzerland and expected corresponding effects on the terrace system.

- Can different terrace levels – corresponding to different ages – be correlated and followed alongstream? If so, how do these correlations relate to the interpretation of Haldimann et al. (1984)?
- Where can we find deviations from the "equilibrium" properties of a terrace system expected for an alluvial river in a tectonically stable environment? What kind of tectonic activity could explain these features? Are there alternative, non-tectonic explanations for them?

- If a tectonic influence seems probable, how does the proposed tectonic activity relate to other evidence or hypotheses about Quaternary tectonics in northern Switzerland?

To answer these questions, the morphological terraces are mapped and then analysed using longitudinal profiles as well as maps with terrace surface orientations.

4.6 Digital terrain model DTM-AV

In recent years, airborne laser scanning has become a well-established technique for topographic surveys (Ackermann, 1999; Pfeifer, 2003). The procedure is based on the emission of near-infrared waves from an airplane that are reflected from the ground (Figure 6). The travel times back to the airplane are recorded and converted to distance. Compared to other surveying methods (such as photogrammetry), it has several advantages (Baltsavias, 1999). The emitted signal (partly) penetrates ground-covering vegetation and, therefore, allows capture of the ground surface even in forested areas. The high point density leads to a very detailed description of the topography, reaching a vertical accuracy of 10 cm. Due to the high degree of automatisation in the data processing, the measured data points can efficiently be transferred into a surface model. This procedure includes filtering of the data cloud, removing objects (such as buildings or trees) that are not part of the ground surface.

To complement their contourline-derived digital elevation model with a cell size of 25 m (DHM25), swisstopo have created a new digital terrain model based on airborne laser scanning. The DTM-AV (Digitales Terrainmodell der Amtlichen Vermessung) covers the entire area of Switzerland lying below 2000 m a.s.l. (Swisstopo, 2007). The data acquisition was completed in 2007. The surveys yielded a data set with an average point density of 1 point / 2 m^2, which was then subjected to filtering to remove trees and other objects not belonging to the terrain surface. The measured points have a vertical accuracy of ca. 30 cm, whereas the accuracy of the model
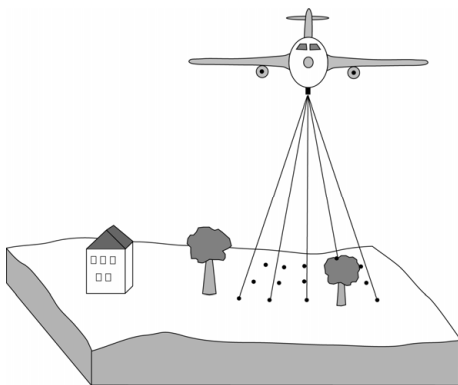
Figure 6: Principle of the laser scanning technique.
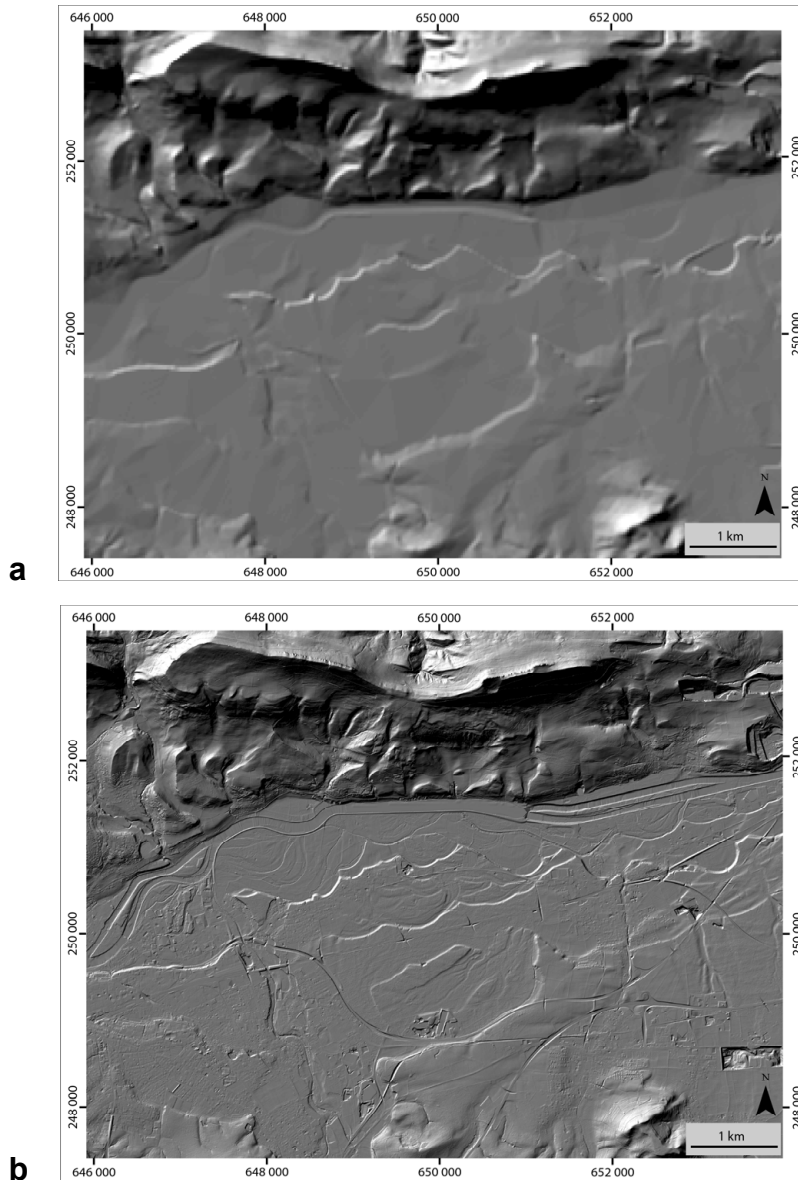
Figure 7: Comparison between the DHM25 digital elevation model (a) and the DTM-AV digital terrain model (b), showing terraces in the Rupperswil area. Reproduced by permission of swisstopo (BA081622).

amounts to ca. ± 50 cm (standard deviation) in open terrain. From the raw data, 2 m gridded terrain models were interpolated using Inverse Distance Weighting.

The comparison of the DTM-AV to the older 25 m cellsize digital elevation model shows that with the new terrain model, geomorphological features can be distinguished in much more detail, in particular in low-relief areas (Figure 7).

4.7 Methods

The first step in the morphological analysis of the Late Quaternary terraces in the lower Aare valley consists of the detailed mapping of all surfaces belonging to the Low Terrace gravels and

younger alluvial plains, using DTM-AV data and existing geological maps. These surfaces are then analysed in a longitudinal profile, following the transect line given by Haldimann et al. (1984), and compared to their results. Furthermore, the surfaces are approximated by individual "trend planes" to study the aspect and slope of the terraces to gain additional 3D morphological information. The terrace distribution, the alongstream correlations and gradient changes as well as the general orientation of the terraces are then analysed for deviations from the equilibrium trend and the results integrated into the context of other evidence of Quaternary tectonics in northern Switzerland.

4.7.1 Terrace surface mapping

The morphological terrace surfaces in this study are defined as planar areas within the mapped extent of the Low Terrace gravels. To map these areas as individual polygons using ArcGIS software (ESRI Inc.), information from the DTM-AV was used in different ways. First, the altitude distribution itself was displayed using different height intervals, displaying areas of one altitude in one colour. In order to include flat, but gently dipping surfaces, additional information was used from derivatives of the DTM-AV. The hillshade view calculated by ArcGIS highlighted the transitions from steep to flat areas, delineating terrace steps, but also abandoned channels on terrace surfaces, for example. Different light source positions (315/35 and 225/35) helped find steps of different orientations and eliminate steps caused by channels, roads or railway lines (Figure 8). In addition, the "Neighborhood Statistics" tool was used to determine the internal roughness of a surface, calculating for each cell the topographic relief (ie, the maximum altitude difference) within a window of 10 x 10 cells (Figure 9).

This information was combined with the extent of the Low Terrace deposits and alluvial plains given in the geological maps (Mühlberg, 1908; Bitterli et al., 2000; Graf, 2006). It is important to note that only the upper surface of a terrace was mapped, without the terrace risers. Also, colluvium and alluvial fans deposited on the terrace surfaces were excluded where distinguishable. Other deviations from the natural terrace surfaces, such as gravel pits or railroad embankments, were omitted if located at the edge of a polygon. Every polygon that was drawn using these criteria was given a unique number to make it easily identifiable in the course of the further data processing.

4.7.2 Longitudinal profiles

Once the terrace polygons were defined, their orientation along the longitudinal valley profile of Haldimann et al. (1984) was analysed. The profile line used by these authors was added to the

_____
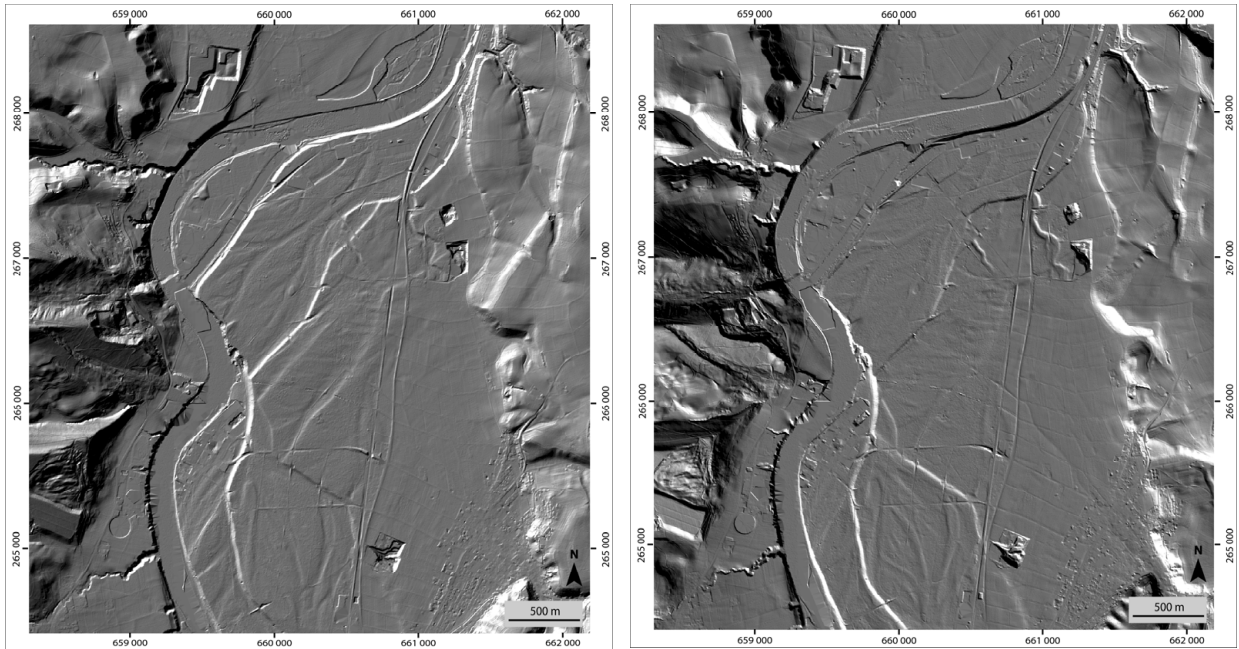
Figure 8: Hillshade view of a section of the Aare valley. Left: light source at 315/35, right: light source at 225/35. Coordinates are in metres (CH1903 LV95 national coordinate system). Reproduced by permission of swisstopo (BA081622).
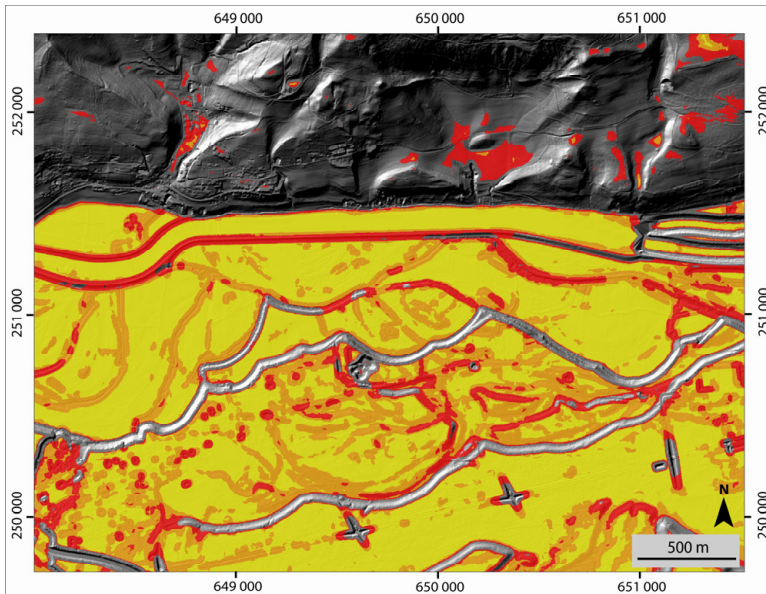
Figure 9: Topographic relief over a 10 cell (20 m) window of the DTM-AV data: no colour: ≥ 3 m, red: < 3 m, orange: < 2 m, yellow: < 1 m. Reproduced by permission of swisstopo (BA081622).

DTM-AV and converted into a "Route". This procedure assigns to every point of the line the upstream distance along the line (Figure 10). Rows of points were manually set within the polygons, roughly parallel to the profile line. This manual procedure allowed exclusion of man-made structures and erosional channels produced after the initial formation of the terrace
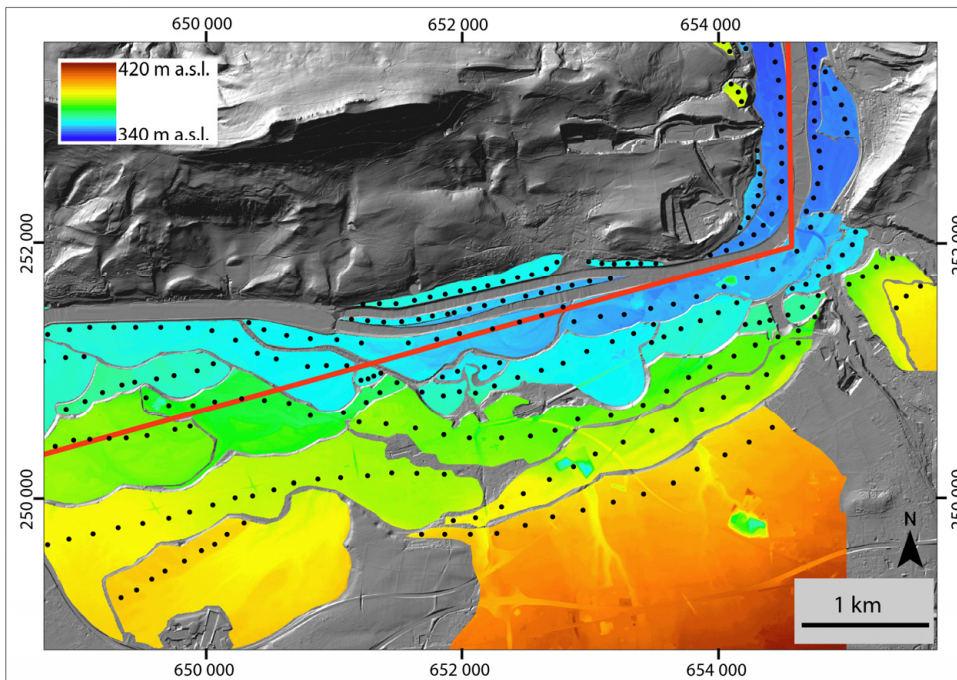
Figure 10: Points used to construct the longitudinal valley profile. The profile line, also used by Haldimann et al. (1984), is given in red. Background consists of a shaded relief image and a colour-coded extract of the DTM-AV altitude data. Reproduced by permission of swisstopo (BA081622).

surface.Each point was then attributed by the number of the polygon it falls into and the altitude value from the DTM-AV. By projecting the points perpendicularly onto the profile line, the altitude values of the terrace surfaces were related to the distance along the profile line. This allowed construction of the longitudinal valley profile in Excel and comparison of the trend of the along-valley terrace elevations for all terrace levels simultaneously. In addition, the terrace levels inferred from the DTM-AV could easily be compared to the results of Haldimann et al. (1984) by overlaying the longitudinal profiles.

4.7.3 Terrace aspect and slope

The profile view only provides information about the spatial orientation of the terrace surfaces in the direction of the main valley. However, the projection to the profile can sometimes introduce artefacts, due to the distortion where the orientation of the profile changes (profile "kinks") as well as the fact that the river that formed a terrace did not necessarily flow parallel to the profile. Therefore, the 3D orientation of the terrace surfaces, as well as their slope, were also analysed. To this aim, extracts from the DTM-AV were produced using each polygon as a mask (Figure 11, above). The surface of each of these partial DTMs was then approximated by a plane, using the "Trend" function in ArcGIS to calculate a 1st order regression surface (Figure 11,

_____
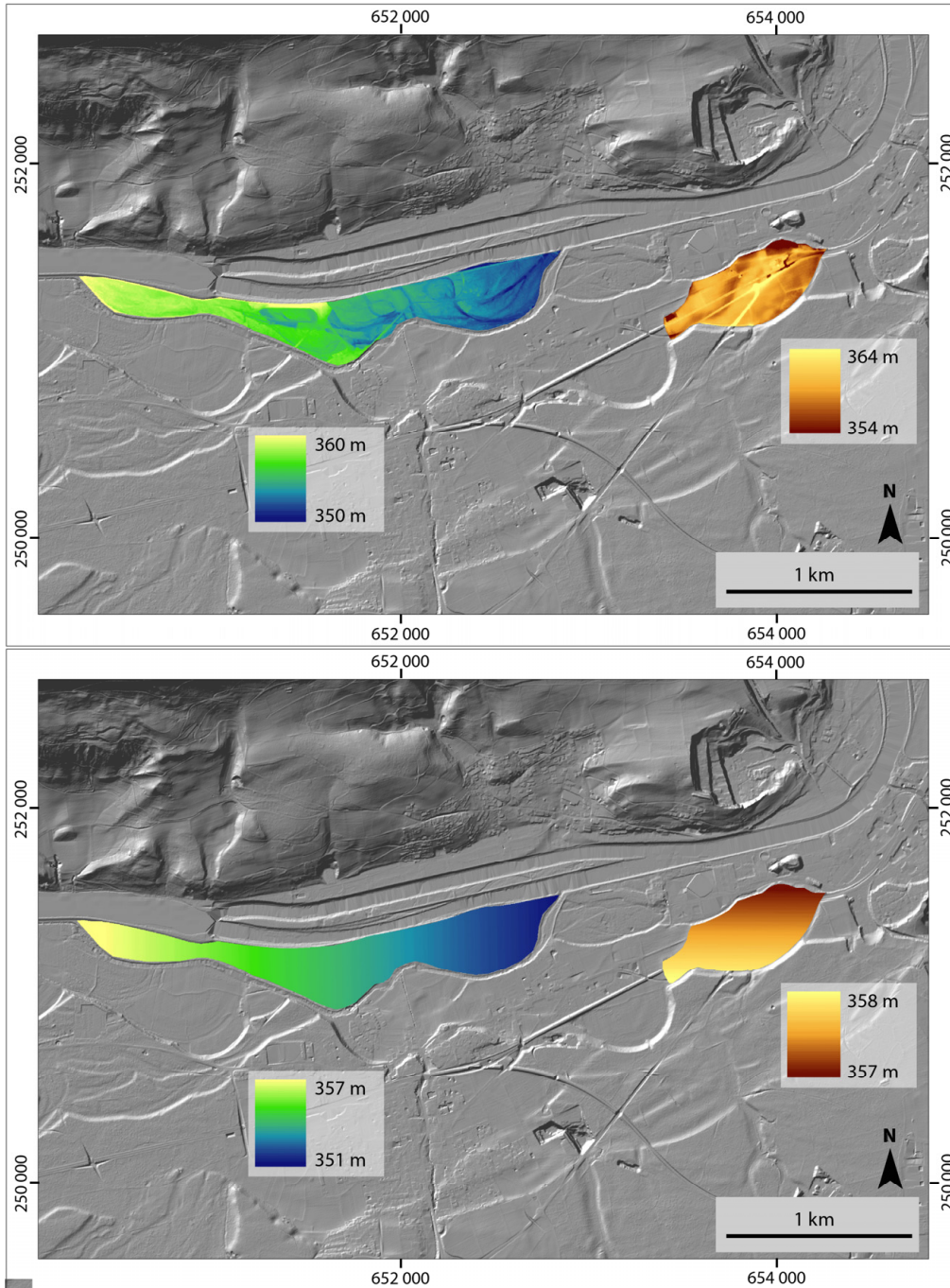
Figure 11: Above: Extracts from the DTM-AV altitude data for two terrace polygons. Below: TIN planes representing the general trend (dip) of the terrace surfaces (1st order regression). Altitude is given by colour code. Reproduced by permission of swisstopo (BA081622).

below). For these planes, the aspect and slope could then be determined and displayed in map view.

To account for the disturbances introduced by man-made structures and erosional / depositional features, for each polygon the resulting regression plane was compared to the DTM-AV by eye to confirm that a meaningful trend was calculated.An automatic procedure to define

the aspect of the terrace surfaces, such as averaging the aspect, did not prove successful. Due to the high internal roughness of the surfaces, the dominant aspect of the individual cells (if such a dominant aspect existed) did not necessarily represent the general aspect of the whole surface. The same applies to the definition of the general slope of the surface.

4.8 Results

4.8.1 Terrace surface mapping

The mapped surfaces of the Low Terrace of the Aare river are shown in Figure 12. The Low Terrace and the lower levels of the High Terrace (if present at all) could usually be distinguished without difficulty. However, sometimes the Aare terraces could not be clearly differentiated from those of the tributaries, in particular, those of the Bünz and Limmat. Terrace surfaces at tributary junctions were included in the map, even if a fan was visible, because this could also be taken into account at a later stage of the analysis. If a part of the Low Terrace did not clearly belong to one or the other of two terrace surfaces (e.g., near Rupperswil), or if intensive human modification made it impossible to identify the original morphology (e.g., in the area of Aarau), no terrace surface was mapped.

In general, the use of the DTM-AV and its derivatives (e.g., shaded relief) allowed reliable mapping of the terrace surfaces. Problems arose where the modification of the terrain by roads, railroads, and building is strong, but also where many of the original fluvial structures are still visible, which in some cases made it difficult to discern the braided river system from an abandoned surface.

Extensive terraces are mainly found in the area between Olten (Dulliken) and Wildegg and between Stilli and Koblenz. In the reach between Wildegg and Stilli the Aare valley is narrower, and terraces are small and confined to the immediate neighbourhood of the river (Figure 12). Between Aarau and Wildegg, terraces occur almost exclusively on the southern side of the present-day Aare river. On the northern side, the river course follows the edge of the Jura fold-and-thrust belt.

4.8.2 Longitudinal profiles

The longitudinal valley profile (Figure 13) demonstrates the difficulty of correlating specific terrace levels alongstream. The lowermost terraces (or the recent alluvial plain, respectively) can be followed relatively easily between Aarau and the Limmat confluence (Stilli), and again in the area around Klingnau. The higher Low Terrace levels are highly discontinuous, and the along-
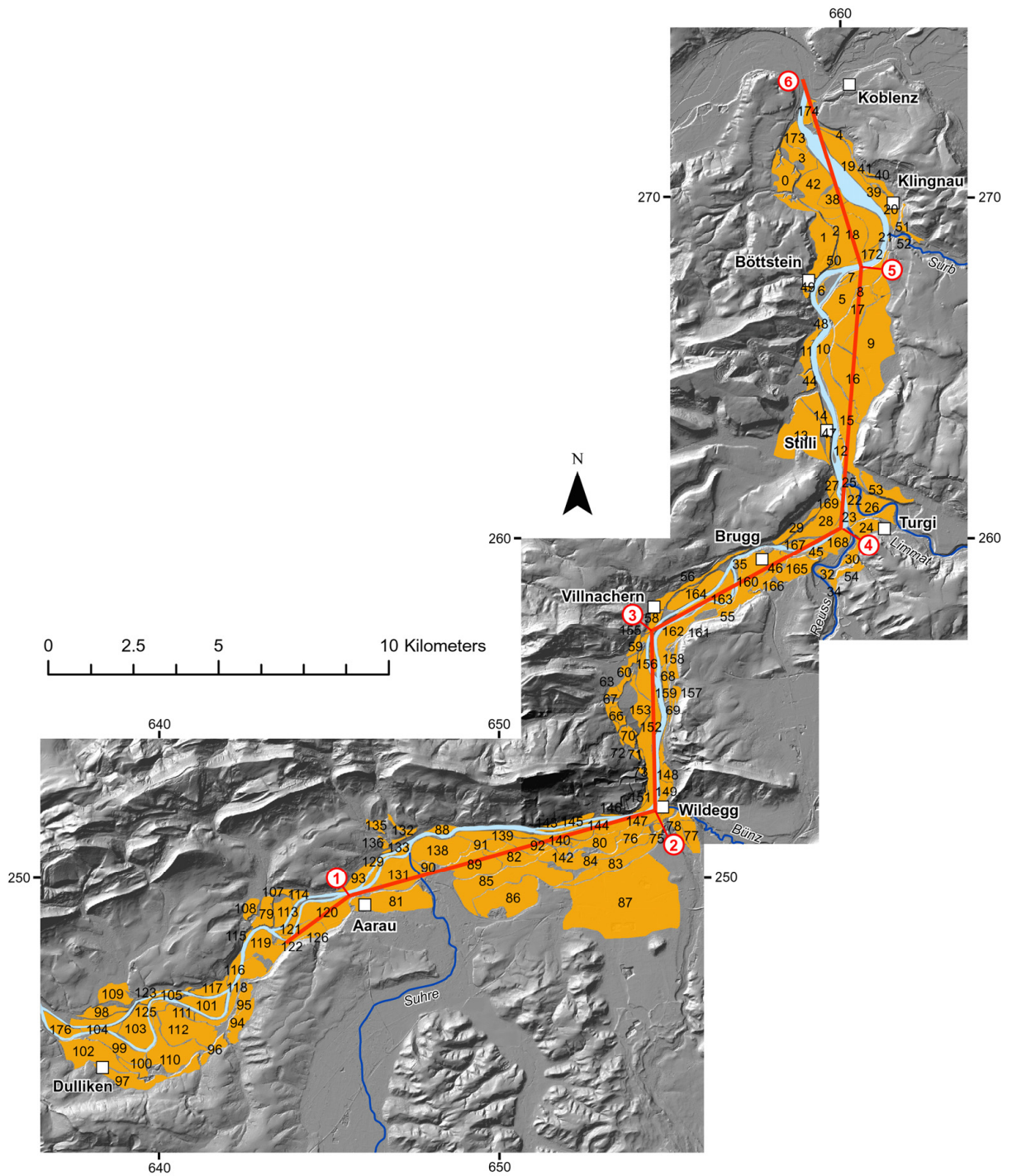
Figure 12: Terrace surfaces mapped as polygons in ArcGIS, Low Terrace gravels, Aare valley. Red line: profile line used for the longitudinal valley profile. Reproduced by permission of swisstopo (BA081622).

profile gradient varies strongly between the different terraces as well as within individual terraces. A correlation of left- and right-bank terraces is for the most part impossible. There seems to be a continuous upper terrace level between Stilli and the Rhine confluence, which might be interpreted as the accumulation surface of the Low Terrace. Further upstream, however, such a
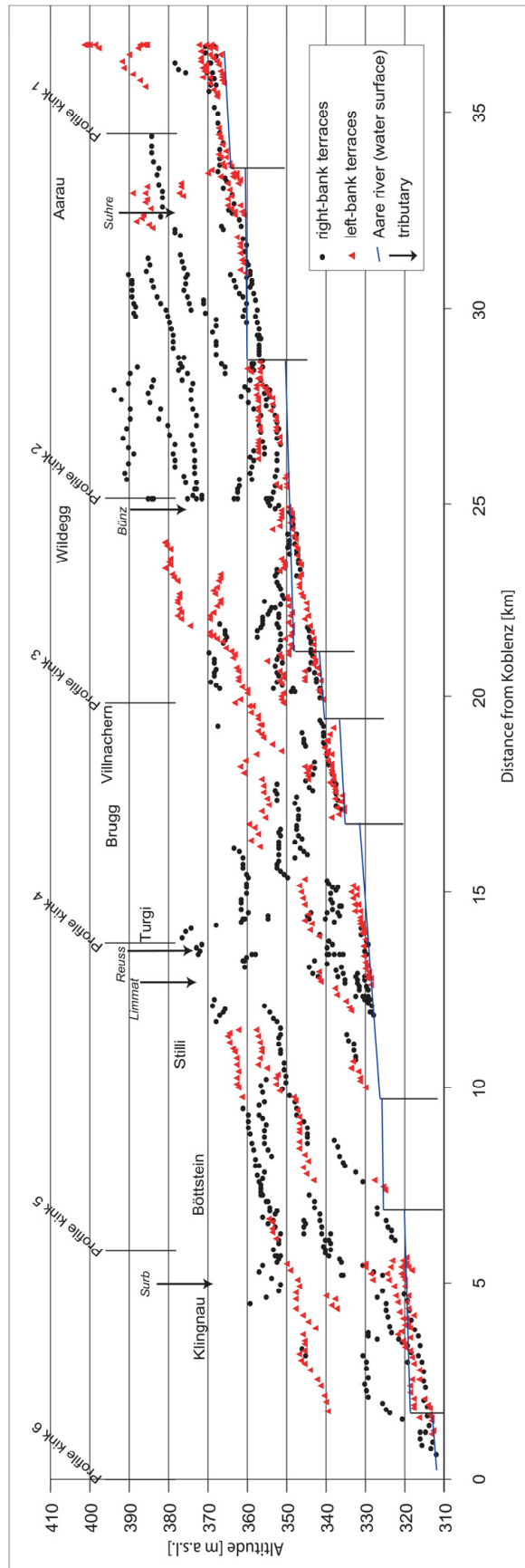
Figure 13: Longitudinal valley profile along the line given by Haldimann et al. (1984) (Figure 12), with different signatures for the terraces on the left and right side of the river.

distinction is not possible, since from their surface morphology, aggradational terraces cannot be distinguished from degradational terraces.

In Figures 14 to 16, the longitudinal profile is divided into three parts. The slope of individual terraces is manually approximated by a line, linking only points that fall into the same terrace polygon (see Figure 12). This interpretation considers the fact that the terrace slope as it appears in the longitudinal profile can be affected in different ways. First, artefacts in the digital elevation model, such as inaccurate removal of buildings, lead to irregular gradients within individual terraces. A similar effect is produced by small-scale erosional features on the terrace surface, which cannot always be avoided when the points are chosen. Apart from this, terrace slopes may be controlled by tributary fans; in this case the terraces do no longer represent the fluvial system of the Aare. In addition, the orientation of the terrace-forming river may have been perpendicular to the profile line at a certain place, making this terrace appear steeper in the profile than a terrace formed where the river flowed parallel to the profile line. Finally, the point lines could not always be set strictly parallel to the profile line, which may introduce a similar bias (steepening or flattening) if a terrace dips towards the river. Where these effects are recognised (by comparison of the longitudinal profile and the map view of the elevation points), they are highlighted in Figures 14 – 16.

The level of the lowermost terrace surfaces can be approximated by a straight line between Aarau and Stilli (Figure 13). However, this line cannot be continued across the gap where low terrace levels are missing to the Rhine confluence, because the lowest terraces downstream lie at higher levels than the extrapolation of the line would suggest. The lowest terraces between profile kinks 5 and 6 allow two different interpretations. If a uniform gradient for the entire Aare reach is assumed, there is an offset between the lowest terrace levels upstream and those downstream from Böttstein, the latter appearing at a higher altitude than expected. Alternatively, the relatively high position of the terraces below profile kink 5 might be due to a gradient decrease downstream from the confluences of the Reuss and Limmat.

Interestingly, the intermediate terrace levels seem to follow the gradient of the present-day river Aare in the region between Aarau and Wildegg, but many of the terraces between Wildegg and Turgi have a very low along-stream gradient, appearing almost horizontal in the profile (Figure 15). Downstream from Turgi, the gradients increase again. This results in a general trend of the terrace gradients to decrease in the area of Wildegg, and increase again after the confluences of Reuss and Limmat.

Figure 16 shows that the gradient of some of the low and intermediate terraces changes
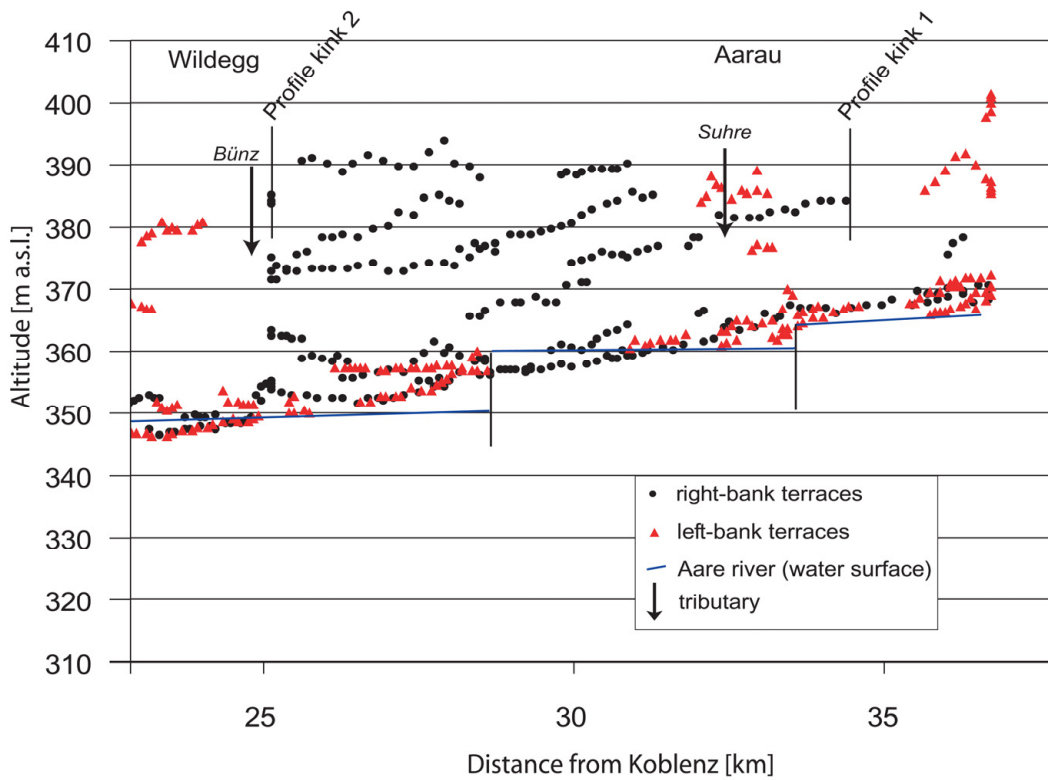
Figure 14 (a): Close-up of the first part of the longitudinal profile (Aarau to Wildegg).
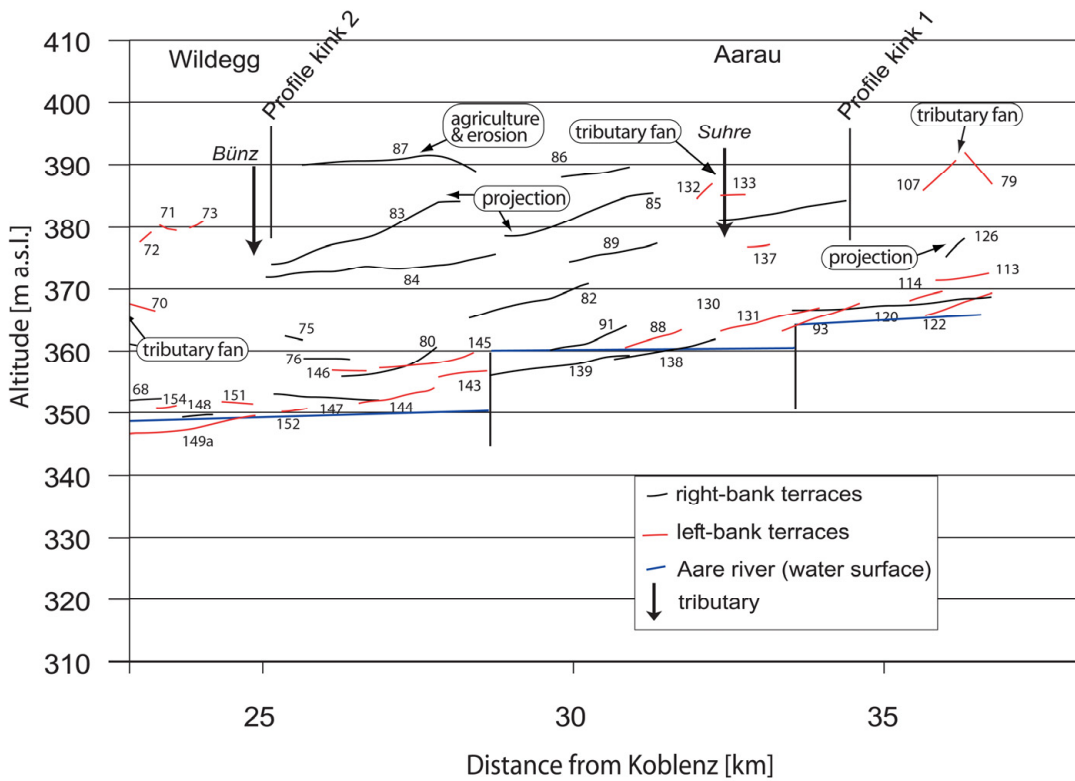
Figure 14 (b): Same extract as Figure 14 (a), with terrace surfaces belonging to the same polygon approximated by a line. Influences on the (apparent) gradient as mentioned in the text are indicated.
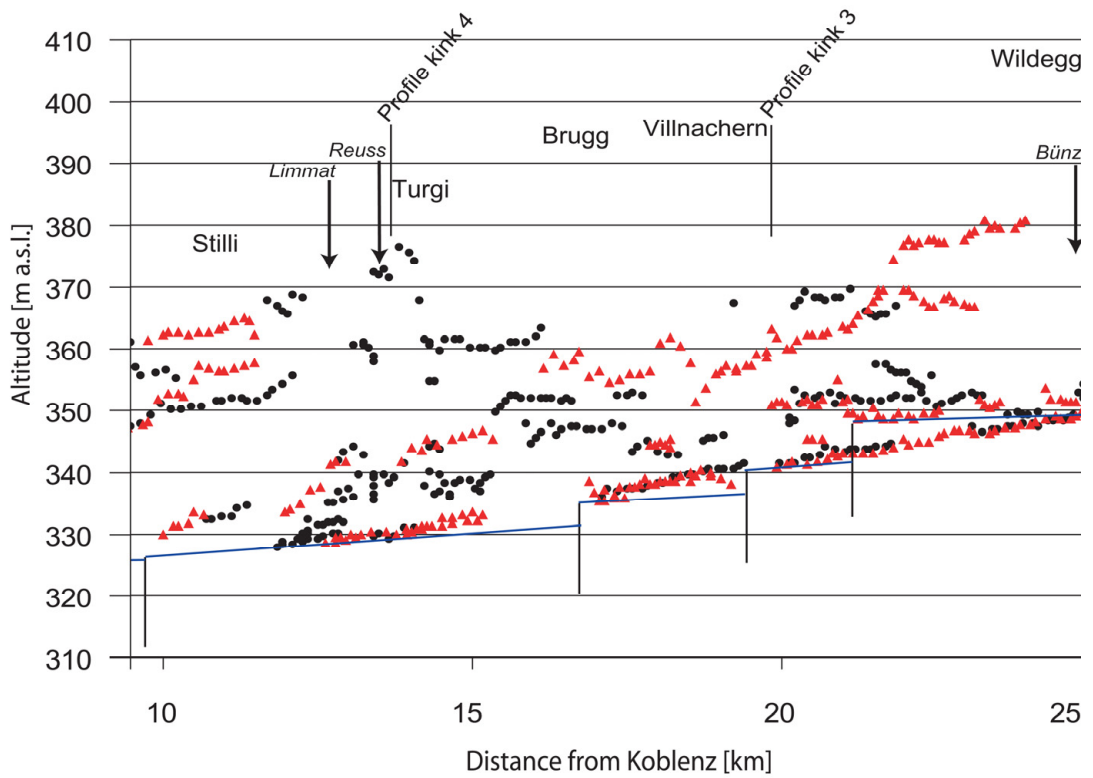
Figure 15 (a): Close-up of the central part of the longitudinal profile (Wildegg to Stilli).
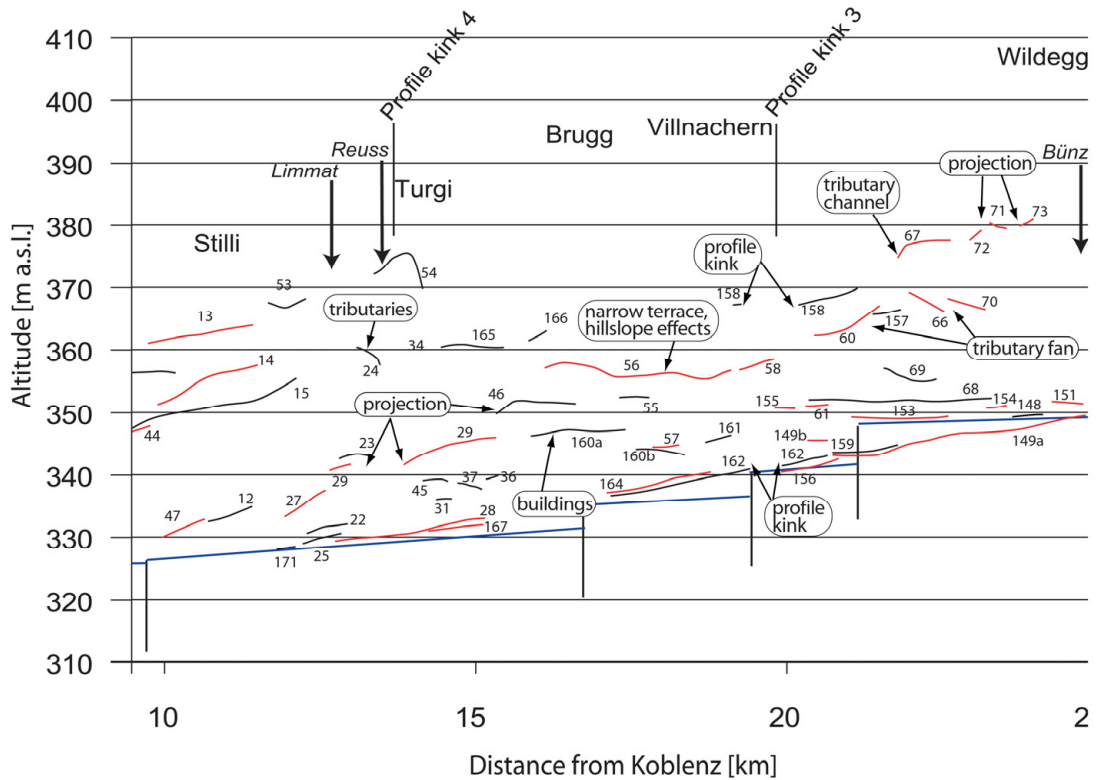
Figure 15 (b): Same extract as Figure 15 (a), with terrace surfaces belonging to the same polygon approximated by a line.
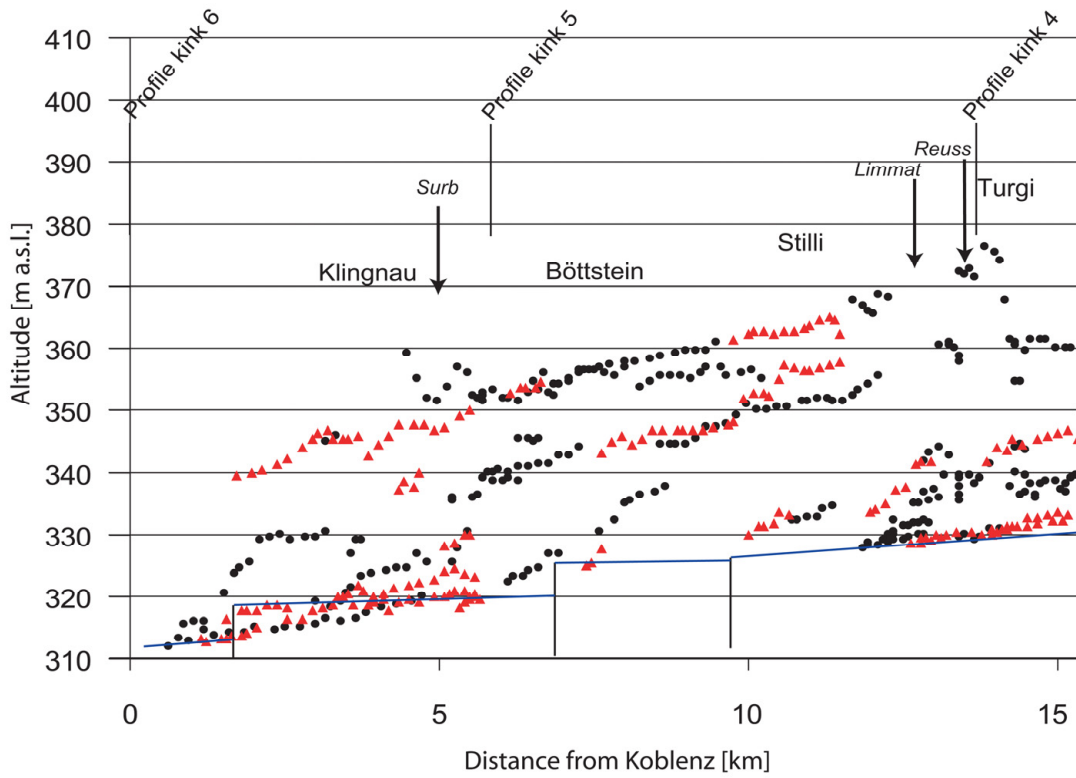
Figure 16 (a): Close-up of the last part of the longitudinal profile (Stilli to Klingnau).
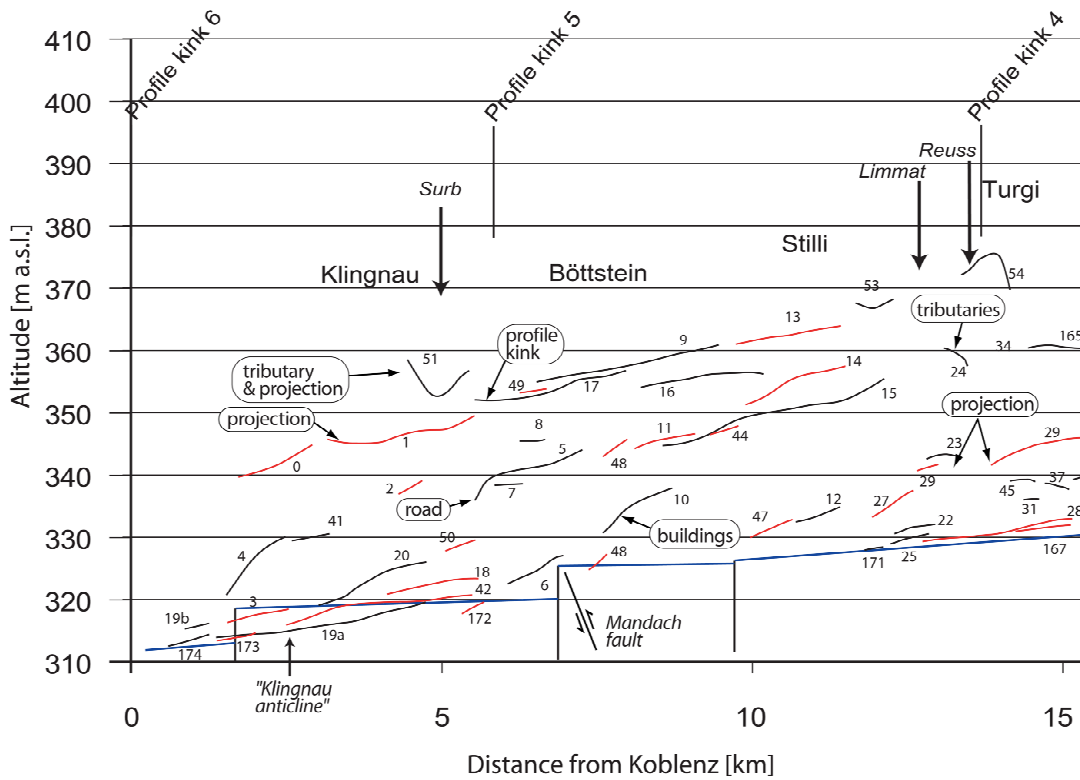
Figure 16 (b): Same extract as Figure 16 (a), with terrace surfaces belonging to the same polygon approximated by a line.

downstream, resulting in a warped line in the longitudinal profile (e.g., terraces no. 14 and 20). However, these irregularities cannot be seen in the gradients of higher terraces at the same point along the river, which would be expected (even in an enhanced form) if the warping were due to progressive tectonic deformation. This is particularly true for the reach between Stilli and Klingnau, where the highest terrace levels are well-preserved and display a uniform gradient.

4.8.3 Comparison of the longitudinal profile with the results of Haldimann et al. (1984)

The match between the terrace points resulting from our dtm study and the profile drawn by Haldimann et al. (1984) is generally good (Figure 17). Although some differences in altitude exist, most of the terraces defined by Haldimann et al. (1984) were also identified from the DTM-AV. A comparison of the results from both studies is impeded by the different method used by Haldimann et al. (1984) to define the terraces, namely describing each terrace by one straight line. Because of this, the interpretation of their data basis could not always be followed.

Agreement between the profiles is quite good between the Rhine confluence and Brugg. Between Brugg and Wildegg, a lot of terraces were found using the DTM-AV which were not reported by Haldimann et al. (1984). The reach upstream from Wildegg shows mainly a good match; however, some terraces could be followed over a longer distance using the DTM-AV, in a few cases resulting in different correlations and, correspondingly, different gradients (e.g., Oberfeld – Suret between Wildegg and Aarau, and terraces 84 and 85, respectively).

4.8.4 Terrace aspect and slope

Figure 18 shows the results from the analysis of the terrace slope and aspect in map view. Terrace slope is given by the colour of the polygon, whereas the aspect (dip direction) of the terrace surface is given by an arrow. A comparison to the original digital elevation model showed that in a few cases (7 out of 177 polygons), the "Trend" plane was strongly influenced by man-made structures such as road embankments or underbridges. These polygons were not included in the analysis and are not shown on the map in Figure 18.

Generally, the terrace surface aspect follows the direction of the present-day river, or the main direction of the valley. This direction can, however, vary by as much as 90°; i.e., most terraces have an aspect between parallel to the present-day river course and perpendicular to it, dipping towards the river. Most terrace surfaces are very flat, with a dip of not more than 1 ‰, similar to the present-day river, which has a gradient of ca. 1-1.5 ‰. Steeper terraces, usually dipping towards the valley, are often observed at higher altitudes, e.g., between Dulliken and Aarau (both sides of the river) and on the left-bank side between Wildegg and Brugg.
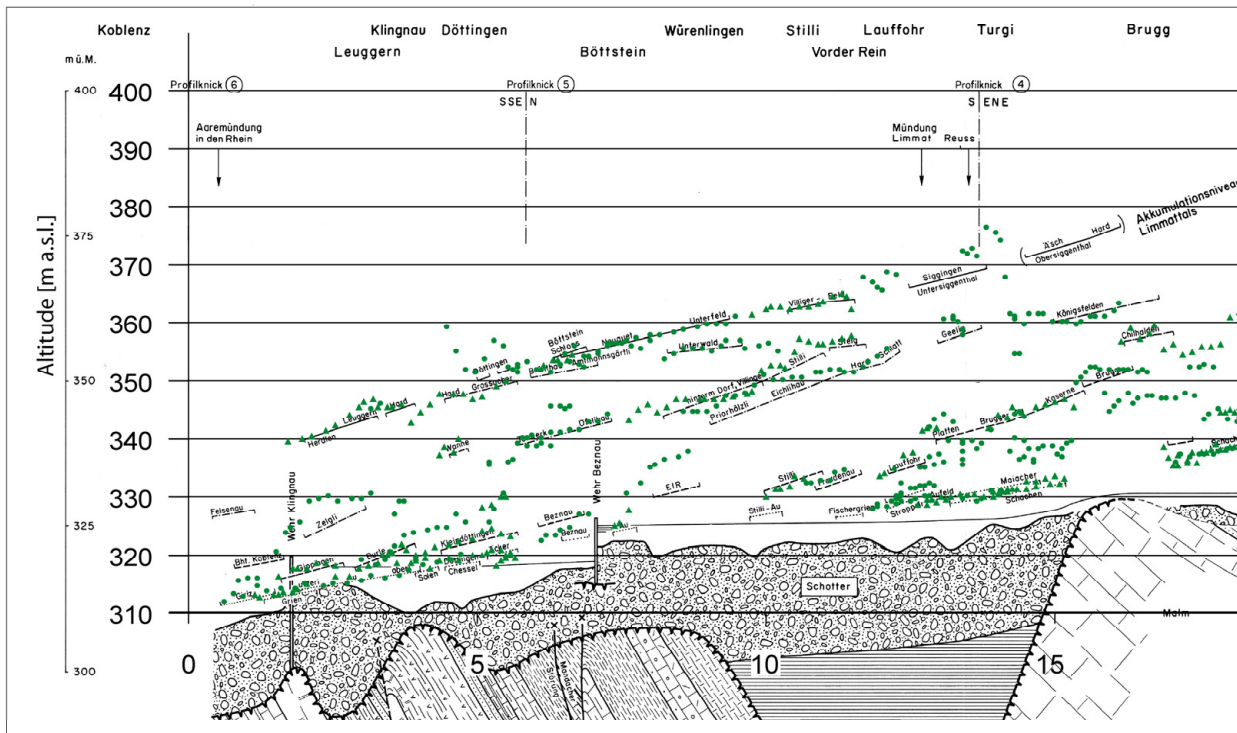
Figure 17: Comparison of terraces defined using the digital elevation model in this study (points) with the interpretation by Haldimann et al. (1984) (thin lines).

Interestingly, between Turgi and Böttstein relatively steep terraces are found at the lowermost levels. In the narrow valley between Wildegg and Villnachern, the main dip direction of the terrace surfaces is towards the present-day Aare.

As was to be expected by the effect of tributary fans visible in the longitudinal profile, the aspect (and to a lesser degree, the slope) also differs from the general trend where tributaries, even small ones, join the Aare (e.g., terraces 60/63/66, between Wildegg and Villnachern, or 79/107, upstream from Aarau). However, the aspect of the "Trend" planes does not always exactly represent the gradient observed in the longitudinal profile, pointing to differences due to the different data processing techniques (single points vs. trend function).

4.9 Discussion: Sedimentologic and tectonic effects on the morphology of the Low Terrace system in the lower Aare valley

The terrace surfaces of the lower Aare valley cannot be correlated over long distances, nor between the sides of the present-day river, due to their relictic occurrence (Figure 13). This is typical for a terrace system that was formed by a river with frequently shifting channel(s), which eroded laterally during incision. The alongstream correlation of specific terrace treads would be facilitated if different levels of aggradation and degradation within the Low Terrace Gravels could
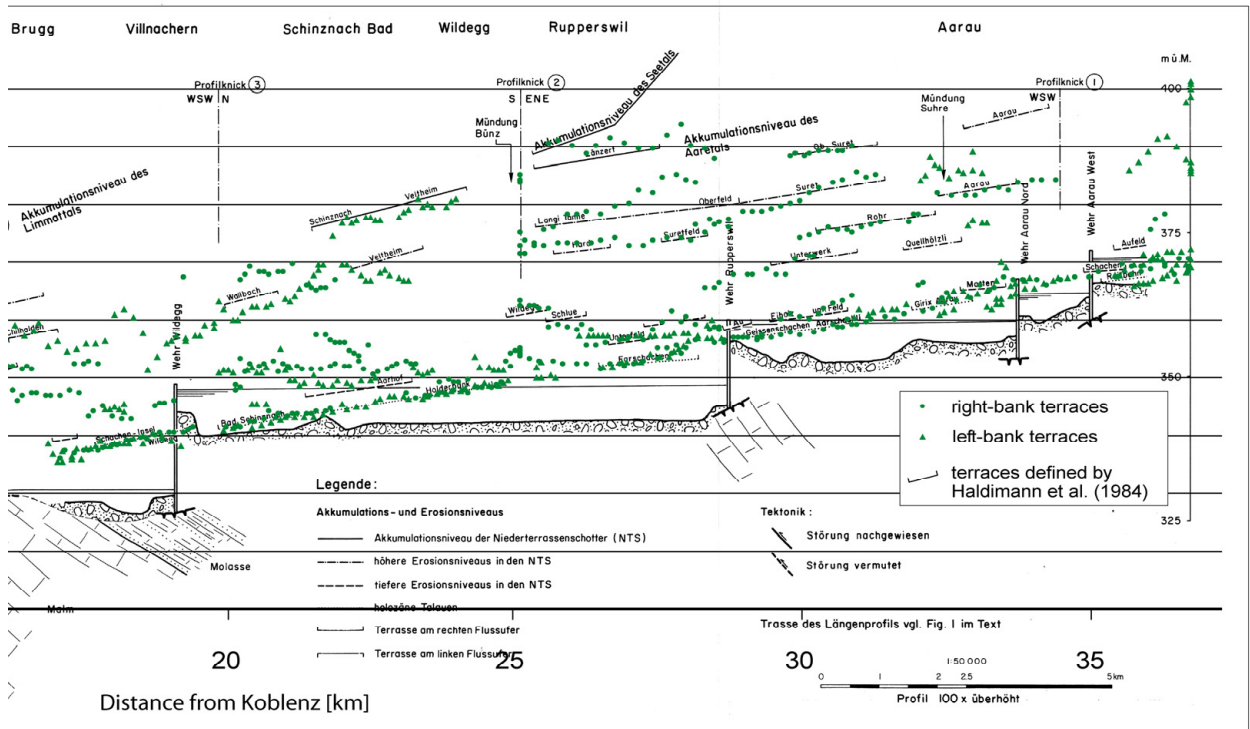
Figure 17 (continued).

be distinguished. In the case of the Aare river, the morphology of the terrace treads did not allow differentiation of aggradational and erosional surfaces. This is not surprising because both types represent the (vertical) position of the river bed at a certain time, either the highest level reached by the river during a phase of aggradation, or an interval of relative stability during a phase of general downcutting. Which of the two possibilities applies to each terrace surface could only be determined if the terrace materials showed clear compositional differences, or if deposition ages of the terraces could be defined.

In the longitudinal profile (Figure 13), the terrace surfaces generally show an alongstream gradient decrease at Wildegg. Downstream from Turgi, the general gradient goes back to values similar to those upstream from Wildegg, or even slightly higher. This could be explained by uplift in the area of the Jura fold-and-thrust belt (Figure 1), which would be expected to introduce a southward tilt to the terraces south of the main uplift zone, thus decreasing their downstream gradient. Accordingly, the terraces downstream of the main uplift zone would be tilted in the flow direction and thus steepened. A similar observation was made by Haldimann et al. (1984), namely a lower gradient of the terraces across the area of the Jura fold-and-thrust belt, suggestive of local uplift. The main uplift zone would be located in the area of Turgi, where the gradient increases again. However, this is where the tributaries Limmat and Reuss join the Aare river. Both have a discharge comparable to that of the Aare, and probably did so during the main deposition of the
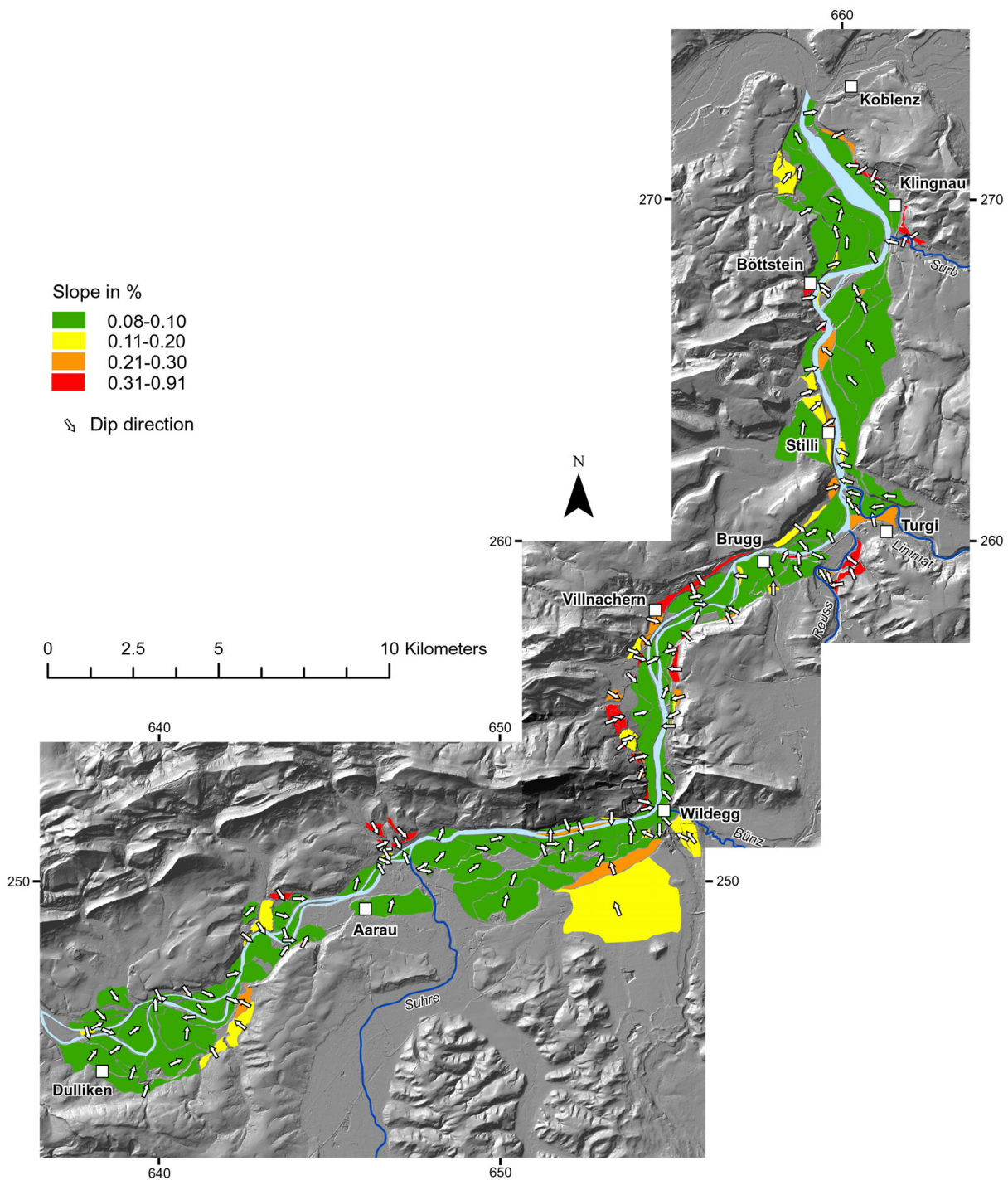
Figure 18: Slope and aspect (dip direction) of the terrace surfaces in the lower Aare valley. Slopes are given by colour code (green: flat, red: steep), arrows show the aspect of the terraces.

Low Terrace Gravels, considering their position in front of the Rhine and Reuss glaciers, respectively. This implies that their sediment input might have been high enough to significantly influence the Aare system. Therefore, it seems plausible that the changing gradients of the Low Terrace across the Jura fold-and-thrust belt are the effect of a very large fan-like structure, formed

by the sediment input of the Reuss and Limmat rivers. In addition, low gradients also predominatein the Aare reach between Villnachern and Turgi, even though the river runs parallel to the Jura fold-and-thrust belt here.

Processes related to the deposition of the gravels also have to be considered when looking at the discontinuity in the lowest terrace levels upstream and downstream from Stilli. If these terraces are approximated by straight lines of the same gradient, an offset results that implies uplift of the area downstream from Stilli relative to the upstream area. However, no structure is presently known in this area that would have such an effect. Alternatively, since the discontinuity is located where the rivers Reuss and Limmat join the Aare, it also seems plausible to interpret the discontinuity of the lowest Aare terrace surfaces across this area as a gradient change due to an increased discharge (and sediment input), with no relation to tectonic activity.

The varying orientations of the terrace surfaces can partly be explained by the effect of a main river channel that followed different flow paths on a wide valley floor. In other words, a terrace surface might have formed at a time when the river locally flowed perpendicularly to the strike of the valley, as can be observed today in the area between Dulliken and Aarau, or downstream of Böttstein. Consequently, this terrace will have a different aspect, and possibly a different slope, in relation to the longitudinal valley profile or the general strike of the valley, compared to terraces that formed when the river flowed in a direction closer to that of the valley. It is important to note, however, that the terrace surfaces generally do not have dip directions opposite to the valley trend, which could be interpreted as a clear sign of recent tectonic activity.

Some of the steeper terrace surfaces are very narrow. This suggests that erosional and depositional surface processes – colluvium accumulation at the upslope side and erosion at the downslope side – have affected the terrace surface since its formation, which has a stronger effect on the general slope of narrow terraces, because no part of the terrace showing the original surface may remain.

The terrace polygon map (Figure 12) illustrates the pronounced asymmetry in the terrace distribution between Aarau and Wildegg. Terraces occur almost exlusively on the southern, right-hand side of the present-day river. Since the elevation of the terrace surfaces continuously decreases towards the river, the Aare must have laterally shifted to the north during the incision that followed the main (highest) Low Terrace accumulation. Whether this trend of incision was interrupted by aggradational phases or not is irrelevant in this regard. A significant amount of sediment may have been delivered by tributaries from the south, as the wide alluvial tributary valleys imply. However, this cannot have been the cause for the lateral shift of the river Aare, because the highest, southernmost terrace risers must have formed after the main sediment
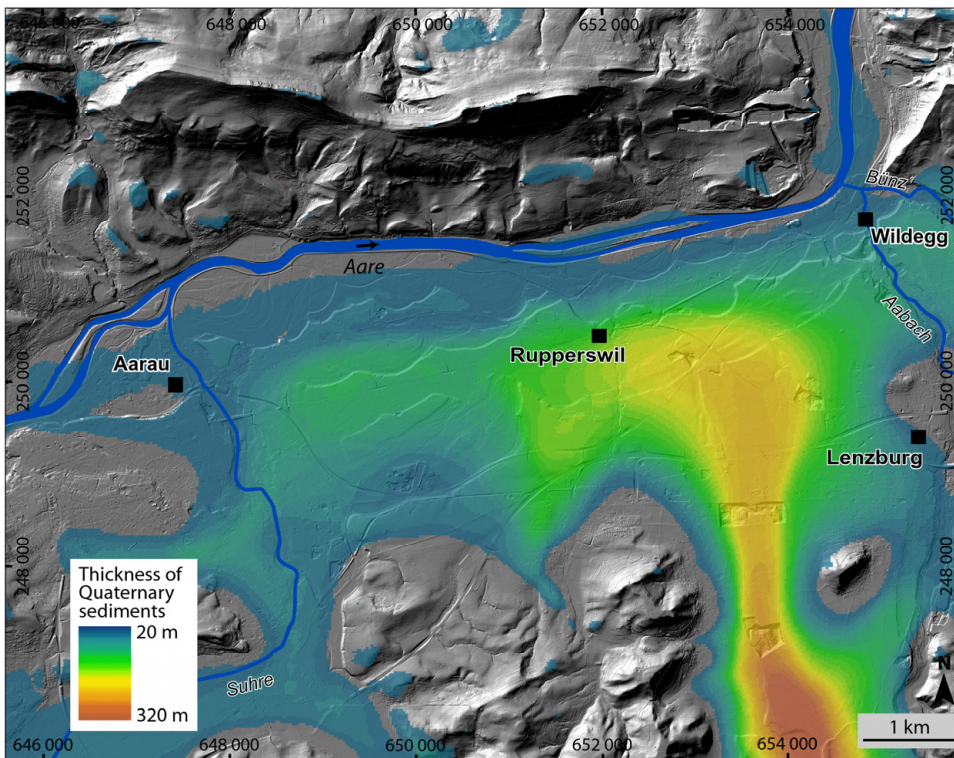
Figure 19: Map of the thickness of the Quaternary sediments (Jordan, 2007), showing a lower bedrock–sediment boundary on the southern side of the Aare valley. Reproduced by permission of swisstopo (BA081622).

deposition from the tributaries. The comparison of the position of the Aare and its terraces with a map of the thickness of the Quaternary sediments (Figure 19; Jordan, 2007) shows that the sediment thickness is actually lower on the northern side of the valley, where the Aare flows today. This makes it improbable that the lateral migration of the river course was an effect of differential compaction of the sedimentary valley fill. Therefore, it is suggested that the northward shift of the river Aare is a result of tectonic activity, either a regional tilt to the north as proposed by Cederbom et al. (2004), or localised uplift to the south of Aarau, possibly caused by a gentle anticlinal structure between Aarau and Lenzburg. The lateral displacement of the river Aare amounts to ca. 1500 m in the time span since the deposition of the hightest Low Terrace gravels at ca. 11 ka (Kock et al., submitted). The altitude difference between the highest Low Terrace levels and the present-day position of the river is ca. 38 m. However, to determine a tilt rate it would be necessary to know which part of this altitude difference is due to incision. Without this knowledge, only a maximum tilt rate can be calculated assuming that the entire altitude difference is a result of tilting. This maximum tilt rate amounts to ca. 0.013° / 100 a, or relative uplift of 23 cm / 100 a over a distance of 1 km. This value, however, is much higher than what can be deduced from geodetic measurements and not plausible in the tectonic setting the the study area.

_____
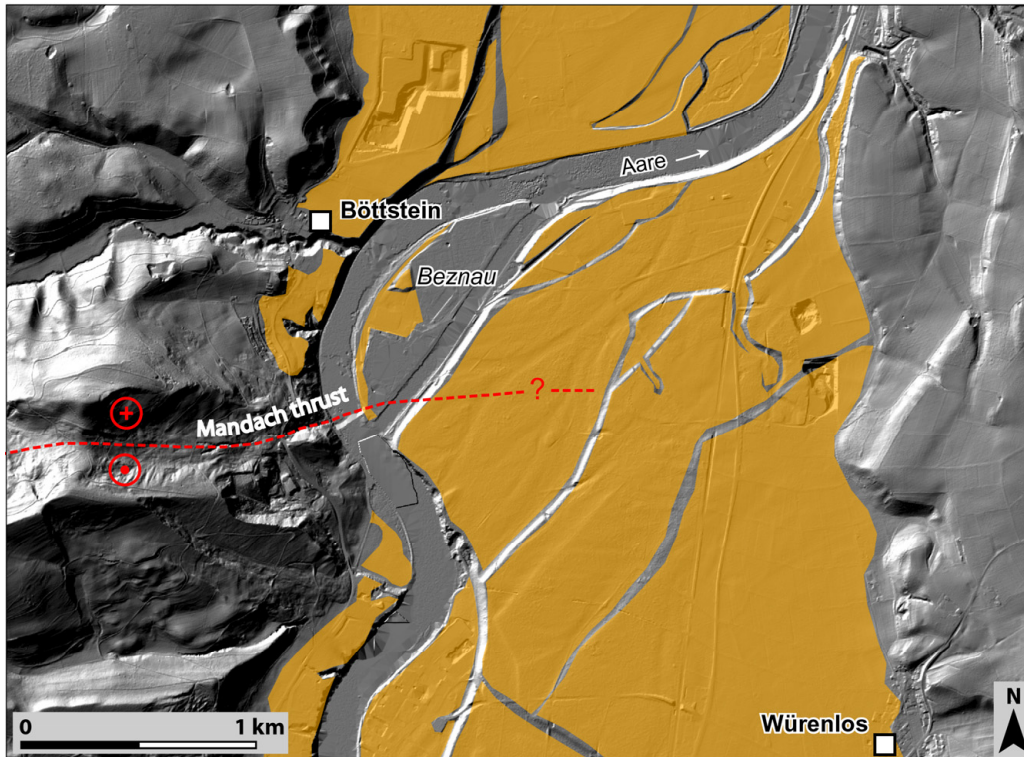
Figure 20: Detail of the DTM-AV with mapped terraces in the Beznau area. Low Terrace is given in orange; Mandach thrust after Bitterli et al. (2000). Reproduced by permission of swisstopo (BA081622).

The comparison of the results with the interpretation by Haldimann et al. (1984) shows that a large part of the terraces in the longitudinal profile coincide (Figure 17). The DTM-AV allowed definition of additional surfaces, sometimes of very narrow terraces, especially at intermediate elevations in the central part of the profile. In the following, the main interpretations from the previous study are re-evaluated using the new altitude information.

In the previous study, a gradient difference was described between the higher and the lower terraces in the area between Brugg and Koblenz. No pronounced trend of this kind could be observed in the DTM-AV data. However, if the interpretation of a regional tilt to the north is correct, higher gradients of the older, topographically higher terraces in the S-N oriented reaches would indeed be expected. The precise levelling results (Schlatter, 2007) indicate that the station at Wildegg is vertically displaced by ca. 0.4 mm/a relative to the station at Koblenz. Extrapolation of this value over an estimated age of the Low Terrace Gravels of ca. 20 ka would result in a vertical displacement of ca. 4 m, and a gradient increase of ca. 0.02° (or 0.35 ‰) along the river course for the oldest terrace surfaces. Thus, the highest terraces would be steeper by ca. a third compared to the lowest terraces. This does not seem to be the case from the analysis of the present data set.

A series of small terraces in the Stilli area, which have similar gradients and occur at similar altitudes, give the impression of several offsets, but can easily be explained by the formation process of the terraces, as explained above, as abandoned former river plains that were only partly preserved. The same accounts for a suspicious terrace riser that forms the extension of the Mandach thrust to the east (Figure 20). It can be interpreted as the right-hand bank of the river flowing E-W here before incising down to its present-day elevation. In the longitudinal profile, no activity is evident above the Mandach thrust. However, hardly any terraces can be followed across this structure (Fig. 16b). Similarly, only very few terraces cross the proposed anticlinal structure at Klingnau, most of them at low elevations and therefore probably very young. Terrace No. 4 significantly steepens across this area, however, it is very narrow and not very well defined, as this region is highly used for agriculture and building activity.

In summary, from the analysis of the Low Terrace system of the lower Aare valley using the DTM-AV digital terrain model no active tectonic structure which is crossed by the Aare can reliably be inferred. Tectonic activity could be deduced from a possible vertical offset of the lowest terraces in the Stilli area; however, this cannot be said with certainty, because of the influence of the Reuss and Limmat confluences upstream from this reach. It seems likely, though, that the Aare river has been affected by a regional tilt to the north in the past 20 ka, resulting in a lateral shift in the area between Aarau and Wildegg, or possibly by a local compressional structure south of this Aare reach.

According to their relatively young age, the Low Terrace Gravels have recorded only little deformation. But while the higher units of the Quaternary terrace system in this region have been exposed to tectonic processes for longer, they have also been more strongly affected by erosional and depositional processes. The Higher and Lower Cover Gravels are only preserved in fragmentary outcrops, and their eroded surfaces do not offer a traceable landscape feature. The High Terrace Gravels are more completely preserved; however, they are often covered by moraine or loess deposits, and aggradational or erosional surfaces can generally not be identified.

4.10 Conclusions

The results from the analysis of the high-resolution digital terrain model DTM-AV indicate that the terrace system of the Low Terrace Gravels in the lower Aare valley formed by the dynamics of a braided river and was heavily influenced by the sediment input from its tributaries. No clear evidence of tectonic influence can be found in the longitudinal valley profile. This may partly be due to the difficulty in the downstream correlation of different terrace levels, which in turn results from the lack of surface (or deposition) ages. The distribution of terrace slope and aspect values

seems to reflect the changing flow directions of the incising river and erosional processes that have affected the terraces after their formation.

The asymmetric distribution of terraces between Aarau and Wildegg suggests that here, the river Aare was deflected to the north after the main deposition of the Low Terrace Gravels. This can be explained by a regional northward tilt, which would be in agreement with a general, northward decreasing uplift in the Alpine foreland as described by Müller et al. (2002), and suggested by precise-levelling data (Zippelt and Dierks, 2007). Alternatively, a more localised zone of active uplift to the south of this area would have a similar effect, but has not been reported so far.

The analysis of the DTM-AV in a GIS permitted to map terrace surfaces in detail, even if they are defined only by very small differences in altitude. The interpretation of the data was greatly facilitated by the use of a GIS, which allowed viewing, analysing and presenting different types of data simultaneously. In addition, some of the necessary calculations could be automatised using the GIS utilities, significantly reducing the time required (e.g., extraction of parts of the digital elevation model, or aspect calculation). However, the high resolution of the DTM leads to a large amount of noise in the topographic surface; therefore, some essential steps were found to be best done by hand, such as the terrace mapping itself and the choice of the points used for the longitudinal profile. The high roughness also required a smoothing procedure before general trends and expositions could be systematically analysed. As another effect of the high resolution, many objects unrelated to the terrace system are visible (e.g., roads) and complicate the interpretation of geomorphologic features.

The comparison of the results from this study with the longitudinal profile by Haldimann et al. (1984) shows a generally good match of the terraces. Nevertheless, the use of the digital terrain model DTM-AV allowed including additional terrace levels and to draw a more complete picture of the terrace system of the lower Aare valley. The systematic and reproducible approach makes it possible to follow the procedure and can easily be transferred from this study to other terrace systems.

References

Ackermann, F., 1999. Airborne laser scanning – present status and future expectations. ISPRS Journal of Photogrammetry & Remote Sensing 54: 64-67.

Adams, K.D., Wesnousky, S.G. and Bills, B.G., 1999. Isostatic rebound, active faulting, and potential geomorphic effects in the Lake Lahontan basin, Nevada and California. Geological Society of America Bulletin, 111(12): 1739-1756.

Baltsavias, E.P., 1999. A comparison between photogrammetry and laser scanning. ISPRS Journal of Photogrammetry & Remote Sensing, 54: 83-94.

Becker, A., 2000. The Jura Mountains - An active foreland fold-and-thrust belt? Tectonophysics, 321(4): 381-406.

Bitterli-Dreher, P. et al., 2007. Geologischer Atlas der Schweiz: Baden (Blatt 1070), Erläuterungen. Bundesamt f. Wasser u. Geologie. Bern, Switzerland.

Bitterli, T., Graf, H.R., Matousek, F. and Wanner, M., 2000. Geologischer Atlas der Schweiz: Zurzach (Blatt 1050), Erläuterungen. Bundesamt f. Wasser u. Geologie. Bern, Switzerland.

Bolliger, T., 1998. Age and geographic distribution of the youngest Upper Freshwater Molasse (OSM) of eastern Switzerland. Eclogae Geologicae Helvetiae, 91: 321-332.

Bolliger, T., Fejfar, O., Graf, H.R. and Kälin, D., 1996. Vorläufige Mitteilung über Funde von pliozänen Kleinsäugern aus den höheren Deckenschottern. Eclogae Geologicae Helvetiae, 89(3): 1043-1048.

Burbank, D.W. and Anderson, R.S., 2001. Tectonic Geomorphology. Blackwell Science.

Burkhard, M., 1990. Aspects of the large-scale Miocene deformation in the most external part of the Swiss Alps (Subalpine Molasse to Jura fold belt). Eclogae Geologicae Helvetiae, 83(3): 559-583.

Cederbom, C.E., Sinclair, H.D., Schlunegger, F. and Rahn, M.K., 2004. Climate-induced rebound and exhumation of the European Alps. Geology, 32(8): 709-712.

Croisé, J. et al., 2004. Hydrogeological investigations in a low permeability claystone formation: the Mont Terri Rock Laboratory. Physics and Chemistry of the Earth, Parts A/B/C, 29(1): 3-15.

Deichmann, N., Dolfin, D.B. and Kastrup, U., 2000. Seismizität der Nord- und Zentralschweiz. Nagra Technischer Bericht, 00-05.

Diebold, P. and Noack, T., 1996. Late Palaeozoic troughs and Tertiary structures in the eastern Folded Jura. In: O.A. Pfiffner, P. Lehner, P. Heitzmann, S. Mueller and A. Steck (Editors), Deep structure of the Swiss Alps; results of NRP 20. Birkhäuser, Basel, Switzerland, pp. 59-63.

Giamboni, M., Ustaszewski, K., Schmid, S.M., Schumacher, M.E. and Wetzel, A., 2004a. Plio-Pleistocene transpressional reactivation of Paleozoic and Paleogene structures in the Rhine-Bresse transform zone (northern Switzerland and eastern France). International Journal of Earth Sciences, 93(2): 207-223.

Giamboni, M., Wetzel, A., Niviere, B. and Schumacher, M., 2004b. Plio-Pleistocene folding in the southern Rhinegraben recorded by the evolution of the drainage network (Sundgau area; northwestern Switzerland and France). Eclogae Geologicae Helvetiae, 97(1): 17-31.

Graf, H.R., 1993. Die Deckenschotter der zentralen Nordschweiz. PhD Thesis, ETH Zürich, Zürich.

Graf, H.R., 2006. Baden (Blatt 1070), Geologischer Atlas der Schweiz 1:25000. Bundesamt f. Wasser u. Geologie. Bern, Switzerland.

Graul, H., 1962. Geomorphologische Studien zum Jungquartär des nördlichen Alpenvorlandes. Teil 1: Das Schweizer Mittelland. Heidelberger Geographische Arbeiten, Heft 9.

Hack, J.T., 1957. Studies of Longitudinal Stream Profiles in Virginia and Maryland. U.S. Geological Survey Professional Paper, 294-B: 45-97.

Haldimann, P., Naef, H. and Schmassmann, H., 1984. Fluviatile Erosions- und Akkumulationsformen als Indizien jungpleistozäner und holozäner Bewegungen in der Nordschweiz und angrenzenden Gebieten. Nagra Technischer Bericht, 84-16.

Häuselmann, P., Fiebig, M., Kubik, P.W. and Adrian, H., 2007. A first attempt to date the original "Deckenschotter" of Penck and Brückner with cosmogenic nuclides. Quaternary International, 164-165: 33-42.

Holbrook, J. and Schumm, S.A., 1999. Geomorphic and sedimentary response of rivers to tectonic deformation: a brief review and critique of a tool for recognizing subtle epeirogenic deformation in modern and ancient settings. Tectonophysics, 305: 287-306.

Ivy-Ochs, S. et al., 2006. The timing of glacier advances in the northern European Alps based on surface exposure dating with cosmogenic 10Be, 26Al, 36Cl, and 21Ne. Geological Society of America (GSA) Bulletin Special Paper, 415: 43-60.

Jordan, P., 2007. Digitales Höhenmodell Basis Quartär (DHM B_QU, "Felsmodell") - Grundlagen, Erarbeitung, Ergebnisse, Stand Juni 2007. Nagra Arbeitsbericht NAB 07-12.

Kastrup, U. et al., 2004. Stress field variations in the Swiss Alps and the northern Alpine foreland derived from inversion of fault plane solutions. Journal of Geophysical Research-Solid Earth, 109(B1).

Keller, E.A. and Pinter, N., 2002. Active Tectonics: Earthquakes, Uplift, and Landscape. Prentice Hall.

Kirby, E., Johnson, C., Furlong, K. and Heimsath, A., 2007. Transient channel incision along Bolinas Ridge, California: Evidence for differential rock uplift adjacent to the San Andreas fault. Journal of Geophysical Research-Earth Surface, 112(F3).

Kock, S., Kramers, J.D., Preusser, F. and Wetzel, A., submitted. Dating of Late Pleistocene terrace deposits of the River Rhine using uranium series and luminescence methods: potential and limitations. Quaternary Geochronology.

MBN-AG, 1998. Zur Stratigraphie des jüngeren Pleistozäns im Gebiet des Zusammenflusses von Aare, Surb, Rhein und Wutach. Ber. z. Hd. Landeshydrologie und -geologie, Bern.

Merritts, D.J., Vincent, K.R. and Wohl, E.E., 1994. Long river profiles, tectonicsm, and eustasy: a guide to interpreting fluvial terraces. Journal of Geophysical Research, 99(B7): 14031-14050.

Montgomery, D.R., 1994. Valley incision and the uplift of mountain peaks. Journal of Geophysical Research, B, Solid Earth and Planets, 99(7): 13913-13921.

Mühlberg, F., 1908. Geologische Karte der Umgebung von Aarau / Spezialkarte No 45, Geologische Karte der Schweiz.

Müller, W.H., Blümling, P., Becker, A. and Clauss, B., 1987. Die Entkopplung des tektonischen Spannungsfeldes an der Jura-Ueberschiebung. Eclogae Geologicae Helvetiae, 80(2).

Müller, W.H., Naef, H. and Graf, H.R., 2002. Geologische Entwicklung der Nordschweiz, Neotektonik und Langzeitszenarien Zürcher Weinland. Nagra Technischer Bericht, 99-08.

Penck, A. and Brückner, E., 1909. Die Alpen im Eiszeitalter. Band 2: Die Eiszeiten in den nördlichen Westalpen.

Pfeifer, N., 2003. Oberflächenmodelle aus Laserdaten. Österreichische Zeitschrift für Vermessung und Geoinformation, 4.

Rahn, M.K. and Selbekk, R., 2007. Absolute dating of the youngest sediments of the Swiss Molasse basin by apatite fission track analysis. Swiss Journal of Geosciences, 100(3): 371-381.

Schlatter, A., 2006. Das neue Landeshöhennetz der Schweiz LHN95. Diss ETH Nr. 16840 Thesis, ETH Zürich, Zürich.

Schlatter, A., 2007. Neotektonische Untersuchungen in der Nordschweiz und Süddeutschland: Kinematische Ausgleichung der Landesnivellementlinien CH/D. Nagra Arbeitsbericht NAB 07-12.

Schlüchter, C., 1976. Geologische Untersuchungen im Quartär des Aaretals südlich von Bern. Beiträge zur Geologischen Karte der Schweiz, 148.

Simpson, G., 2004. Role of river incision in enhancing deformation. Geology, 32(4): 341-344.

Swisstopo, 2007. DTM-AV. geodata-news, 14: http://www.swisstopo.admin.ch/internet/swisstopo/de/home/products/height/dom_dtm-av.parsysrelated1.19059.downloadList.63245.DownloadFile.tmp/gn142007defr.pdf (accessed 07 April 2008).

Ustaszewski, K. and Schmid, S.M., 2006. Control of preexisting faults on geometry and kinematics in the northernmost part of the Jura fold-and-thrust belt. Tectonics, 25(5).

Ustaszewski, K. and Schmid, S.M., 2007. Latest Pliocene to recent thick-skinned tectonics at the Upper Rhine Graben - Jura Mountains junction. Swiss Journal of Geosciences, 100(2): 293-312.

van Husen, D., 2004. Quaternary glaciations in Austria. In: J. Ehlers and P.L. Gibbard (Editors), Developments in Quaternary Science. Elsevier, pp. 1-13.

Wittmann, O., 1961. Die Niederterrassenfelder im Umkreis von Basel und ihre kartographische Darstellung. Basler Beiträge zur Geographie und Ethnologie, 3.

Ziegler, P.A., 1992. European Cenozoic rift system. Tectonophysics, 208(1-3): 91-111.

Zippelt, K. and Dierks, O., 2007. Auswertung von wiederholten Präzisionsnivellements im südlichen Schwarzwald, Bodenseeraum sowie in angrenzenden schweizerischen Landesteilen. Nagra Arbeitsbericht NAB 07-27.

Chapter 5

Seismotectonics and state of stress in north-western Switzerland: Analysis of natural and induced earthquake focal mechanisms

5.1 Introduction

The occurrence of earthquakes reflects the location of active brittle deformation in the lithosphere. This makes the seismologic record an important source of information for the characterisation of the current deformation pattern of a region, especially when no surface faulting can be observed. However, for the assessment of the seismic hazard not only the location of faulting is relevant, but also the deformation style – thrust, normal or strike-slip faulting – that is to be expected. In addition, it is critical to know the orientation of faults that are most likely reactivated. These questions can be answered if the state of stress in the lithosphere is known, or, in other words, the regional tectonic regime, which determines the predominant faulting style.

The key to this information is the analysis of earthquake faulting mechanisms. These are determined by constructing a fault plane solution, a stereographic projection of the deformation caused by the earthquake. This information has been used in a variety of tectonic settings to analyse the regional deformation pattern, and to determine the orientation of the principal stress axes (e.g., Harmsen, 1994; Plenefisch and Bonjer, 1997; Baroux et al., 2001; Clark and Leonard, 2003). This allows putting constraints on the orientation of faults that are likely reactivated and is crucial for the assessment of the seismic hazard, for the safety of above-ground infrastructure as well as of subsurface structures like tunnels or nuclear waste disposal sites.

In this chapter, the spatial distribution of earthquakes that occurred in the Basel area between 1961 and 2006 is analysed in the tectonic context. The associated focal mechanisms are used to characterise the current state of stress and the deformation regime(s) related to it. Data from previous seismotectonic studies (e.g., Kastrup et al., 2004) are combined and complemented with the focal mechanisms of recent earthquakes (e.g., Deichmann et al., 2006; Baer et al., 2007). The principal aim of this study is to determine if the analysis of focal mechanisms with the Right Dihedra method allows lining out regions with contrasting tectonic regimes and determining on which fault set(s) seismic deformation most probably occurs. These data are supplemented by and

compared to the focal mechanisms of a series of earthquakes that were triggered by the injection of fluids during the stimulation phase of a geothermal-energy project in Basel (Häring et al., in press). The results from these analyses are then discussed in the context of the regional (neo-)tectonic situation and other evidence of the present-day deformation pattern.

5.1.1 Determining the regional state of stress from earthquake focal mechanisms

Earthquakes occur when deviatoric stresses build up and are released in the crust. In a pre-fractured rock body, this stress release is usually located on pre-existing fault planes, because they form zones of weakness in the crust, and the forces required to generate a new fault are higher than those required to reactivate an existing fault. Whether a given deviatoric stress tensor can cause slip on a specific plane depends on the orientation of the fault (and the frictional forces opposing slip). Conversely, possible orientations of the stress tensor can therefore be determined from the fault-plane orientations (McKenzie, 1969).

In the ideal case of a planar fault plane and a 1D slip vector (double-couple assumption), the radiation pattern that is observed at the earth surface allows remote determination of the faulting mechanism (Lay and Wallace, 1995). To achieve this, the initial motion that reaches the surface is recorded, i.e. whether the first movement arriving at a point from the source is "up" or "down" (Figure 1). The position of the corresponding receiver station relative to the orientation of the ray path from the source is projected in a stereogram. The resulting pattern reflects the orientation of the compressional and dilatational quadrants around the source. The compressional and dilatational quadrants are separated by great circles, which are orthogonal and represent the two nodal planes of the focal mechanism. One of these two planes is the fault plane on which slip occurred, the other one is an auxiliary plane with no physical significance. Which of the two nodal
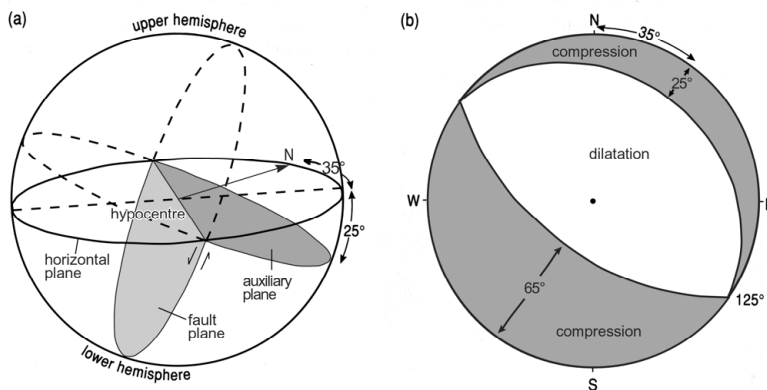
Figure 1: (a) Illustration of the focal sphere and the motion recorded on the earth surface resulting from slip on the fault plane. (b) Projected quadrants of compression and dilatation (focal mechanism) (after Mussett and Khan, 2000).

planes is the fault plane, and which one the auxiliary plane, can only be determined with additional information, such as the hypocentre locations of aftershocks or surface rupture.

The maximum deformation is localised in the centre of each quadrant. The bisectors of the nodal plane orientations represent the principal strain axes (directions of maximum shortening and extension, respectively) and are called T axis (for the compressional quadrant) and P axis (for the dilatational quadrant). The P and T axes are often used to approximate the σ_1 and σ_3 directions.

5.1.2 The Right Dihedra Method

In the last decades, a number of methods have been developed to determine the regional state of stress in the lithosphere from fault-slip data (Etchecopar et al., 1981; Gephart and Forsyth, 1984; Carey-Gailhardis and Mercier, 1987; Michael, 1987). One of the most straightforward approaches is the Right-Dihedra method (Angelier and Mechler, 1977; Angelier, 1984). It corresponds to a simple graphic procedure and, in contrast to some of the other methods, allows testing if all fault-slip data are compatible with a single stress tensor. In general, these data can come from fault striation analysis, earthquake focal mechanisms or calcite twins (Pfiffner and Burkhard, 1987).

The Right Dihedra Method has been applied to earthquake focal mechanisms in various settings (Galindo-Zaldivar et al., 1993; González-Casado et al., 2000; Baroux et al., 2001). It is based on the concept that the two nodal planes of a focal mechanism – the actual fault and the auxiliary plane – define four quadrants (or dihedra), two with compressional and two with tensional deformation around the source. For an individual earthquake, the only restriction on σ_1 is that it must lie somewhere in the dilatational quadrant, and σ_3 accordingly somewhere in the compressional quadrant, assuming that the slip on the plane was parallel to the direction of the maximum resolved shear stress (Bott, 1959). Note that σ_1 and σ_3 are not identical to the P and T axis commonly used in seismology, which represent the strain tensor and are located at the centre of each quadrant.

If all studied earthquakes occurred in one homogeneous stress field, and provided the different fault planes are mechanically independent, the σ_1 direction must fall into the dilatational dihedron of all focal mechanisms. The direction of σ_1 (and σ_3, respectively) can thus be confined to the common area of all dilatational dihedra in the stereogram by superposing the stereographic projections of all focal mechanisms. Conversely, if such a common area does not exist, this means that no stress field can be found that is compatible with all the earthquake focal mechanisms in the analysis (Carey-Gailhardis and Vergely, 1992).

Because σ_1 and σ_3 can lie anywhere in the dilatational or compressional dihedra, respectively, this method takes into account that earthquakes usually do not occur on ideally oriented, newly

created faults but reactivate existing fault planes, if they are favourably oriented. No assumption as to which of the two nodal planes was the actual fault plane is made.

The orientation of the stress tensor then indicates the tectonic regime, i.e., whether the deformation corresponds to an environment of compressive, extensive or strike-slip deformation. Moreover, if a common stress tensor is found, and if the principal stress axes are well-defined, their orientation may be used to determine on which one of the two nodal planes slip occurred. However, well-constrained σ_1 and σ_3 directions can only be determined if the strike directions of the fault planes vary strongly.

5.2 Earthquake activity and state of stress in the Basel area

5.2.1 The earthquake record in NW Switzerland and surrounding areas

The earthquake record in Switzerland covers a time span of almost 1800 years (Fäh et al., 2003). For the time period before the beginning of the 20th century, the record largely relies on historical accounts of earthquake shocks and caused damage. The most prominent of the historical earthquakes in Switzerland is the Basel earthquake of 1356 (Meyer, 2006). With an estimated magnitude between 6.2 (Lambert et al., 2004) and 6.9 (Fäh et al., 2003), it is the largest known historical earthquake in central western Europe.

The operation of a national instrumental measurement network started in 1975 (Deichmann et al., 2000; Swiss Seismological Service, 2002). For seismological investigations in NW Switzerland, also the national earthquake records of bordering countries play an important role (the German Seismological Service of the Landesamt für Geologie, Rohstoffe und Bergbau Baden-Württemberg and the French RéNaSS (Réseau National de Surveillance Sismique)).

The instrumental and historical records are complemented by paleoseismological studies. However, because not many active faults (surface or sub-surface) are known in the area, the possibilities of investigating surface faults (trenching) are limited. One example for trench analyses of a suspected seismogenic fault is a study south of Basel, from which a NNE-SSW trending, east-dipping normal fault was inferred (Ferry et al., 2005). Together with sediment dating, the trenching results suggested the occurrence of five events during the past 13.2 ka. Limnogeological studies in two lakes near Basel (Becker et al., 2002), using reflection seismics and dated drill cores, indicate that five earthquakes large enough to trigger mass movement of lake sediments occurred in the past 12 ka (M $\geq$ 5.5).

Generally, the highest seismicity in Switzerland is recorded in the Valais, Central Switzerland, the Alpine Rhine Valley and the Basel area. Near Basel, seismic activity is concentrated in the area of the eastern Main Border Fault, which separates the Upper Rhine
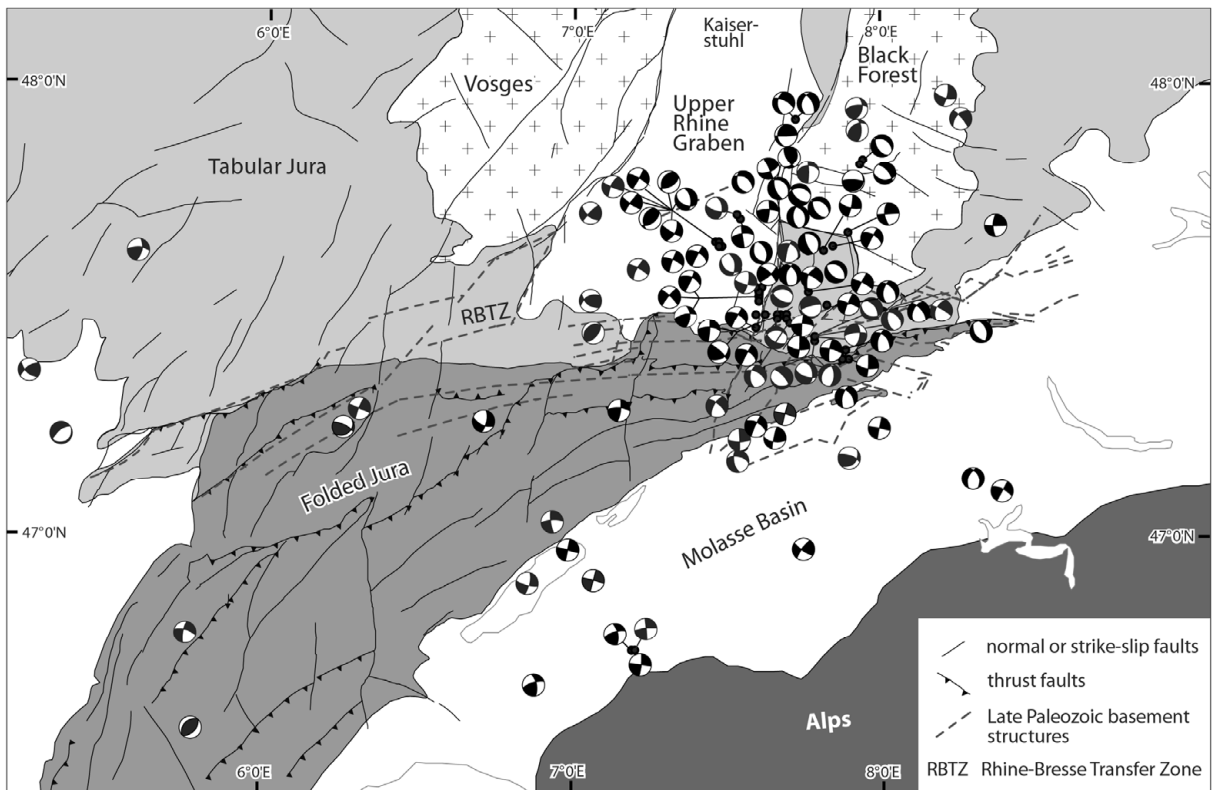
Figure 2: Location of earthquakes with available fault-plane solutions 1961-2006, and the main tectonic units in the study area.

Graben from the Black Forest crystalline massif (Figure 2). At the southern border of the Upper Rhine Graben, the earthquake occurrence is more diffuse. Potentially active fault systems include faults related to the Rhine Graben in its southward continuation, ca. ENE-WSW striking faults related to Late Paleozoic basement troughs, and ca. NE-SW to E-W striking faults related to the Neogene Jura fold-and-thrust belt. West of Basel, in particular, the dominant fault system is that of the Rhine-Bresse Transfer Zone, which trends mainly ENE-WSW and is linked to the underlying basement trough system (Diebold and Noack, 1996; Ustaszewski and Schmid, 2007).

5.2.2 Previous studies of the stress field

The hypocentre distribution as well as the style of seismic faulting and the related stress field in the Basel area have been investigated in a number of studies. Bonjer (1997) analysed earthquakes in the area of the eastern Main Border Fault of the Upper Rhine Graben. They show a variety of faulting mechanisms, but most of them indicate oblique normal faulting. The nodal planes include the general direction of Rhine-Graben faults that are visible at the surface (NNE-SSW), but the earthquakes cannot easily be attributed to individual faults because the hypocentre locations have an accuracy of 2-3 km. The stress tensor deduced from all focal mechanisms in the area of the

southern Upper Rhine Graben represents a regime intermediate between normal and strike-slip faulting. Plenefisch and Bonjer (1997) investigated earthquakes in northern Switzerland and derived a horizontal SSE-NNW direction for σ_1, a horizontal WSW-ENE direction for σ_3, and a vertical σ_2. These authors also pointed out a change of the stress tensor with depth for the southern Rhine Graben area, a strike-slip regime dominating in the upper crust (<15 km) and an extensional regime prevailing in the lower crust. They suggested that this change with depth was caused either by the increasing overburden with depth or by different effects of subduction and collision of the European and African crust at different depth levels. Using data from a temporary seismometer network, Lopes Cardozo and Granet (2003) calculated 15 focal mechanisms for earthquakes in the southern Upper Rhine Graben and adjacent areas. From the analysis of these focal mechanisms they deduced mainly left-lateral faulting on the eastern Boundary Faults and underneath the Jura Mountains. Kastrup et al. (2004) analysed 138 focal mechanisms in the northern Alpine foreland and the Alps. Their stress inversion yielded a general NE-SW direction for S_H (max. horizontal stress); however, S_H exhibits a counter-clockwise rotation from east to west, following the strike of the Alpine chain. This indicates that the NW-SE stress field of Western Europe (Reinecker et al., 2005) may be locally perturbed by the Alpine chain. For the area of the eastern Upper Rhine Graben, Kastrup et al. (2004) defined a tectonic regime of strike slip, whereas the faulting style in the Basel area to the south of it varies from strike-slip to normal.

In addition to stress inversion from focal mechanisms, evidence of the principal stress directions can be obtained from the deformation in boreholes. Müller et al. (1987) describe a change in the maximum horizontal stress directions across the Triassic detachment horizon in a study of borehole breakout measurements in northern Switzerland. From this, they inferred a decoupling of the stress field at this boundary and ongoing decollement tectonics. Becker (2000) compiled results from different down-hole stress measurement methods to analyse the stress field in the sedimentary cover of the Jura fold-and-thrust belt, and found a general maximum horizontal stress orientation (S_H) of NW-SE to N-S for the eastern and northwestern parts of the belt. From the fact that the stress orientations do not change at tectonic boundaries within the fold belt, nor between the fold belt and the rest of the northern Alpine foreland, this author deduced that thin-skinned decollement tectonics are no longer active in the Jura area. This view is shared by Bossart and Wermeille (2003), who also pointed out the difficulties in measuring principal stress directions in the anisotropic rocks of the Jura Mountains.

5.2.3 The stress field in the Basel area from the analysis of fault-plane solutions

For this study, a set of 115 focal mechanisms was compiled for earthquakes that occurred between 1961 and 2006 in the northern Alpine foreland (46.5 to 48.0 northern latitude and 5.2 to 8.5 eastern longitude). A complete list of these events, together with the literature sources, is given in the Appendix (p 119).

The magnitudes of these events range from 1.1 to 5.2. The majority of the focal mechanisms in this area show strike-slip or oblique normal faulting (Figure 2). However, some pure normal faulting as well as (oblique) thrust faulting also occurs. The dominant nodal-plane strike orientations are NW-SE and NNE-SSW. The uncertainty of the hypocentre location usually does not allow the identification of individual active faults, considering the large number of pre-existing faults of various orientations in the study area.

The distribution of the P axes orientations of all 115 earthquakes is shown in Figure 3a. The directions vary between horizontal in a NW-SE direction and vertical, showing a distinct girdle distribution. The T axes directions are better confined, being mostly subhorizontal in a NE-SW direction (Figure 3b). This points to an overall tectonic regime of strike-slip to normal faulting. Figure 3b shows that a number of T axes deviates from this simple pattern, having a subvertical or ca. NW-SE orientation. This points to local thrust faulting, or a component of SE-NW extension, respectively, incompatible with the regional state of stress. The location of the corresponding earthquakes (eight events, highlighted in Figure 4) shows that they do not concentrate in a distinct region. Therefore, they cannot be interpreted as belonging to a different tectonic unit or deformation regime than the rest of the earthquakes.
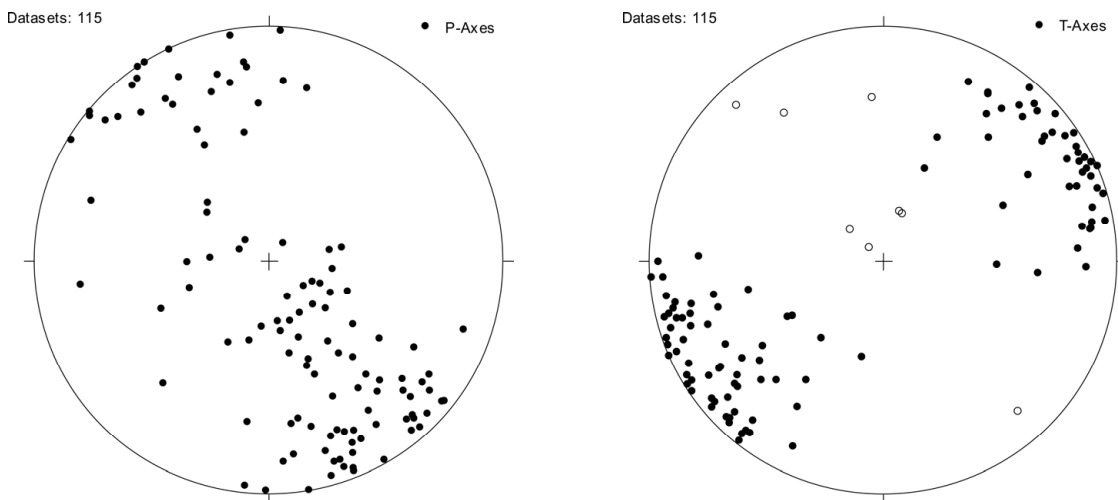
Figure 3: Equal-area lower-hemisphere plots of the P axes (a) and T axes (b) of all 115 earthquakes in the study area for which a focal mechanism could be obtained. In (b), open circles are T axes of eight events that were omitted in the second Right-Dihedra analysis. Sources see text.
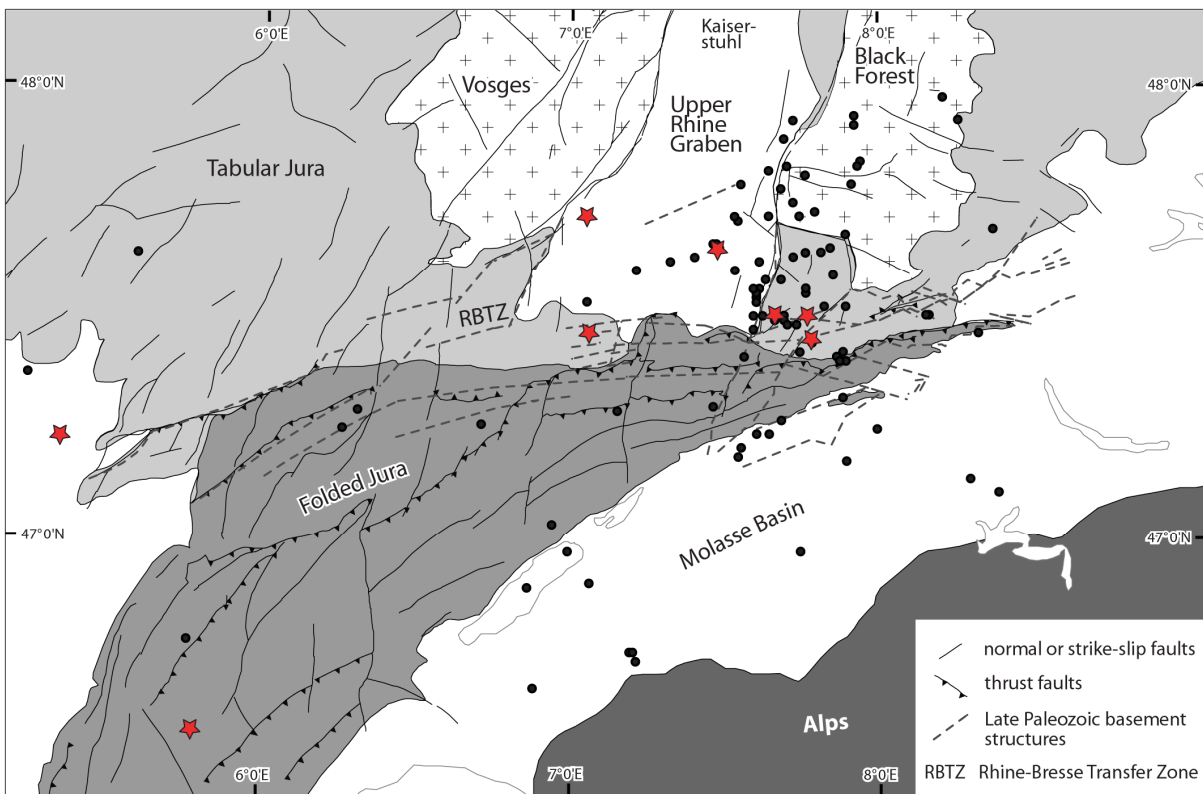
Figure 4: Epicentre locations (red stars) of earthquakes with a subvertical, SE or NW orientation of their T axis (see Figure 3b).

The focal mechanism data of these earthquakes were analysed using the Right-Dihedra method in the TectonicsFP program (Reiter and Acs, 1996-2003). For a small number of earthquakes (15), the nodal plane orientations first had to be computed from the P / T axes information. The result of the Right-Dihedra analysis is shown in Figure 5 and yields directions of 148/13 for σ_1, 336/77 for σ_2 and 239/02 for σ_3. Note that this result is a best-fit solution, and not necessarily compatible with all focal mechanism data. Therefore, it cannot be used to determine the active fault plane of individual focal mechanisms.

Because of the irregular distribution of the P / T axes (Figure 3), which points to an inhomogeneous regional stress field, the data set was divided into different sub-sets, for which separate Right-Dihedra analyses were performed. A distinct difference in the resulting principal stress axis orientations was found for a subdivision into two sub-sets along a ~N-S trending line separating the Rhine-Bresse Transfer Zone and the central/western Jura Mountains from the main part of the Upper Rhine Graben and the region to the east of it (Figure 6). For the western part, the result points to a strike-slip regime with a tendency to transpression, σ_1 being horizontal at 148/02 and σ_2 nearly vertical at 048/77 (Figure 7a). In contrast, the eastern part of the study area seems to be dominated by a stress regime with a stronger normal-faulting component (19° dip of σ_1, Figure 7b).

```
115.cor                          Max. value: 0.15%
Datasets: 115                    at : 146 / 31
```

```
Contours at:
0.01  0.03  0.06  0.09  0.12
```

```
Eigenval.
Sig1  150/14  0.46
Sig2  341/76  0.35
Sig3  240/02  0.19
```
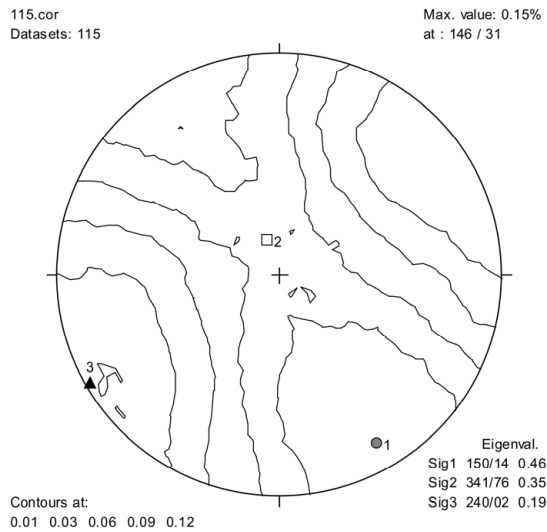
Figure 5: Best-fit stress tensor from the Right Dihedra analysis of all 115 events.

For comparison, an additional subdivision in the area of the eastern Border Fault of the Upper Rhine Graben was performed following the groupings by Kastrup et al. (2004) (Figure 8). It shows that the transtensional regime applies predominantly to the area of the eastern Jura fold-and-thrust belt and the adjacent Tabular Jura, south of the Black Forest crystalline massiv. The events in the Black Forest and the interior of the Upper Rhine Graben show a mixture of strike-slip, normal and thrust faulting and do not represent a clear tectonic regime.

5.2.4 Interpretation of the FPS data set

The analysis of 115 focal mechanisms in the area of the southern Upper Rhine Graben and the eastern Jura fold-and-thrust belt yields a P- and T-axes distribution that is best compatible with a general tectonic regime between normal faulting and strike-slip faulting. The fact that the earthquakes with focal mechanisms that do not conform to this mean stress field did not occur geographically separated from the rest of the earthquakes (Figure 4) implies that they do not belong to a distinct tectonic unit with a different deformation regime. Also, these earthquakes with different focal mechanisms are not concentrated at a certain depth, but occurred at depths between 6 and 21 km. However, the analysis of different data sub-sets using the Right-Dihedra method suggests that a certain change in tectonic regime exists between the eastern and western part of the study area, with a tendency towards transpression in the west, although this result is based on a relatively small number of earthquakes.

An explanation for this difference might be found in the depth distribution of the studied earthquakes. This question was addressed by Plenefisch and Bonjer (1997) for earthquakes in the
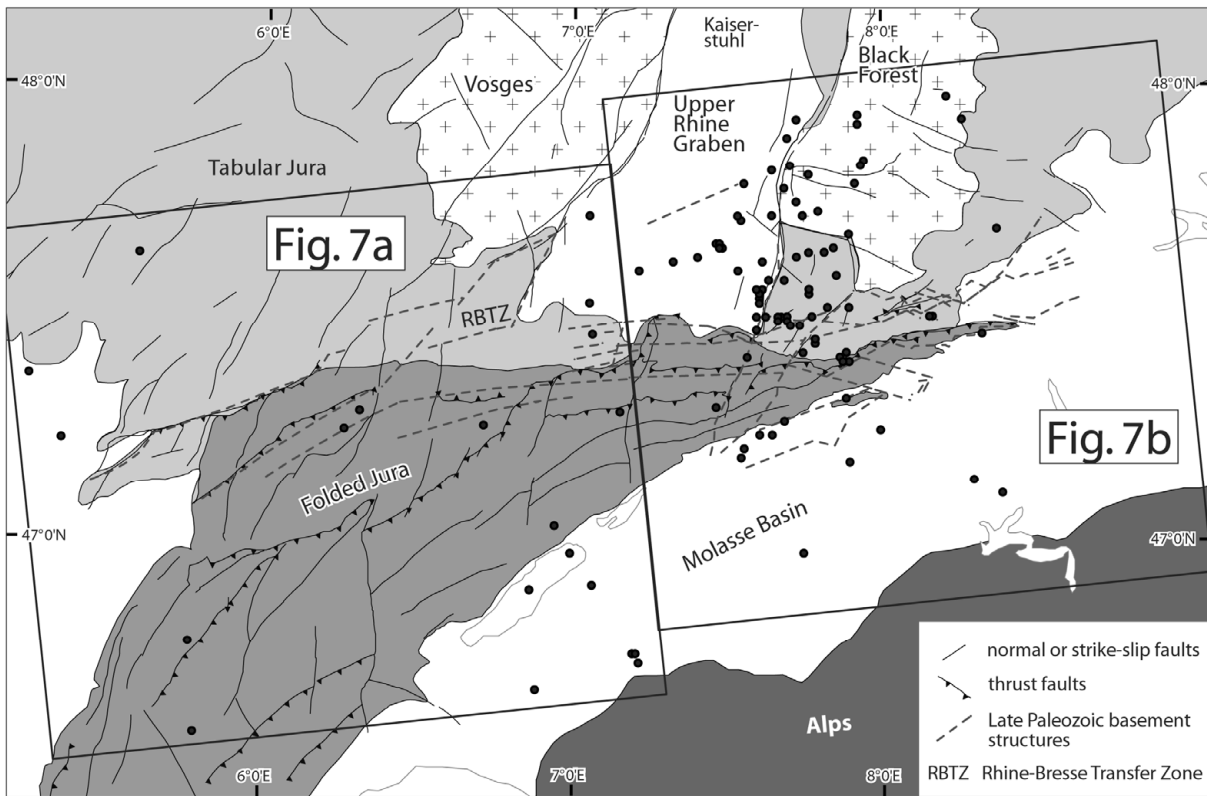
Figure 6: Division of the studied earthquakes into two sub-sets, an eastern and a western part. The results of the respective Right-Dihedra analyses are given in Figure 7.
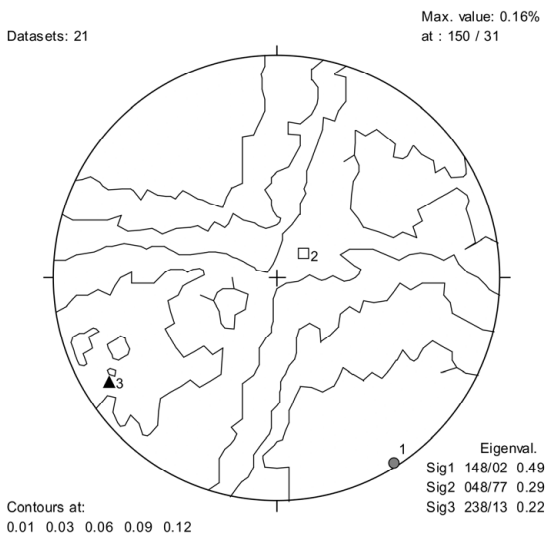
Figure 7a: Best-fit stress tensor from the Right Dihedra analysis of events in the western part of the study area, see Figure 6.
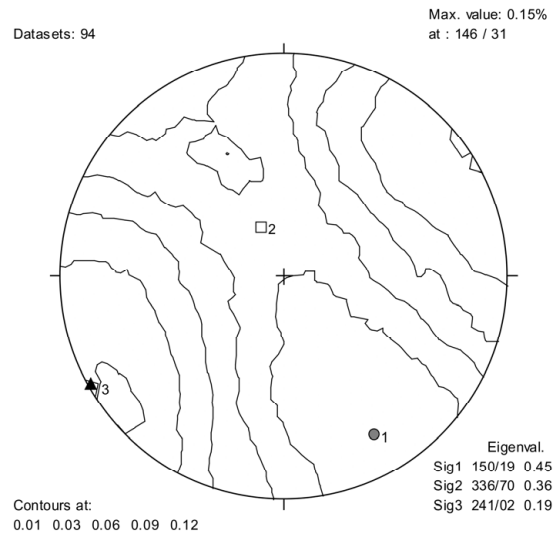
Figure 7b: Best-fit stress tensor from the Right Dihedra analysis of events in the eastern part of the study area, see Figure 6.
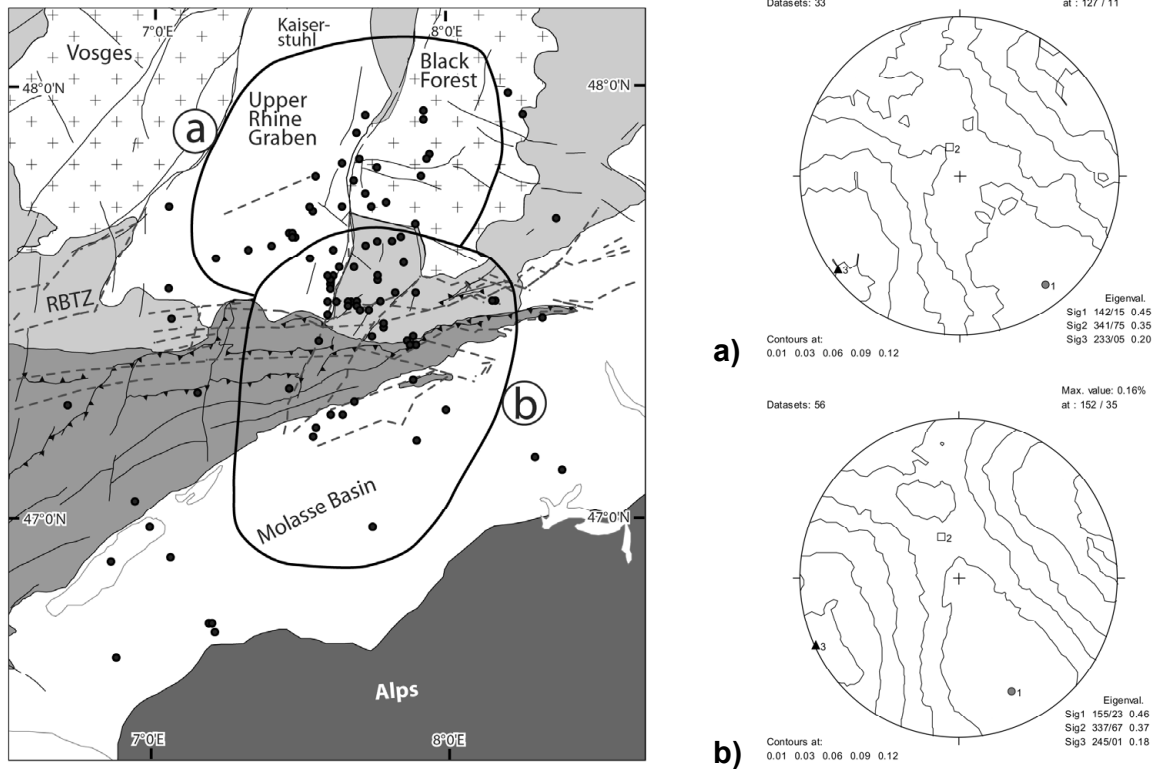
Figure 8: Subdivision of the earthquake dataset in the eastern part of the study area according to the F4 (a) and F3 (b) groups by Kastrup et al. (2004) (p. 9), and corresponding Right-Dihedra results.

Upper Rhine Graben area, who found a stress regime of predominantly strike-slip deformation in the upper crust (z<15 km) and mainly normal faulting in the lower crust (z >15 km). Because the average hypocentre depth of the earthquakes in the eastern group (15 km) is lower than the mean depth of the western group (10 km), this might have an effect on the general tectonic regime found in the Right-Dihedra analysis.

However, there are other possible explanations for ambiguities of the focal mechanisms. The presence of active faults might locally modify the stress field, leading to a deviation of the principal stress tensor and, accordingly, earthquakes with focal mechanisms different from the regional trend. A similar effect would be caused by the movement of rigid blocks, which may locally change the stress field and cause slip on fault planes that would not be activated by the regional stress field (Carey-Gailhardis and Mercier, 1992). In this case the different activated fault planes would not be mechanically independent. Finally, some earthquakes may be the result of displacement on a fault that overcompensates the accumulated stress, thus causing an earthquake on the same fault, but with a faulting style opposite to the first shock. Further studies to solve these questions are hindered by the limited number of earthquakes of a sufficient magnitude in the Jura fold-and-thrust belt and the Rhine-Bresse Transfer Zone.

5.3 Induced earthquake activity and state of stress in Basel

5.3.1 Enhanced Geothermal Systems and induced seismicity

The heat stored in the earth's interior is an almost unlimited source of energy. In recent decades, this potential has been increasingly recognised, and several attempts have been made to exploit it on a large scale (Majer et al., 2007). In contrast to the heat extraction on a small scale (e.g., to heat individual buildings), power generation from geothermal resources requires a high flow rate of very hot water to be economic. This is only the case at locations where a) hot rock is found not too far from the surface and b) the flow rate of water through the rock volume is high enough. In this case, water can be pumped into the hot rock, circulates in the pores and fractures and is heated, and can then be pumped back to the surface where the heat is transformed into electric energy. At many places, hot rock is found close to the surface, but the natural permeability is too low to economically exploit the heat. Therefore, techniques have been developed to increase the permeability of the rock by injecting water under high pressure (stimulation). The fractured rock body is called an Enhanced Geothermal System.

This method relies on the fact that increased pore pressure reduces the effective stress on existing fault planes; thus, friction is reduced and slip can occur on planes that would not be activated in the natural stress field. The injection pressure is usually not high enough to create new fractures. This is in contrast to the hydraulic fracturing method, which uses water pressure for the dilatational opening of new fractures. In the case of Enhanced Geothermal Systems, new tensile fractures are not desired because they would simply close again after the stimulation injection has been stopped. It is lateral slip on existing fault planes with their asperities that creates a permanent increase of the fracture volume.

The stress release related to the movement on pre-existing fault planes leads to the emission of seismic waves, which are perceived as earthquakes at the earth surface. In order to determine where in the rock body slip has occurred and, consequently, new pore space has been created, these earthquakes are monitored and their hypocentres are calculated. At the same time, these induced earthquakes can potentially cause damage, depending on their magnitude and the vulnerability of the infrastructure near the site.

5.3.2 The Basel Deep Heat Mining project

In the Basel area, rocks with an estimated temperature of 195°C are found in the crystalline basement at a depth of 5 km (Häring et al., in press). The high temperature gradient is due to the situation at the edge of the Rhine Graben rift system, where the crust has been thinned and mantle heat is more easily transported to the surface. However, permeability of the granitoid rock found at this depth is low. Therefore, stimulation of the reservoir was started on 02 December 2006 with the aim of increasing the fracture volume in the rock. Injection rates reached a maximum of 3300 l/min, and the well-head pressure reached 296 bar (Häring et al., in press). The injection was stopped on 08 December 2006 after an earthquake with $M_L = 2.7$ had occurred (Schanz et al., 2007).

5.3.3 Induced seismicity and earthquake focal mechanisms

A microseimic network, consisting of 6 borehole geophones, was installed to monitor the induced seismicity and to precisely locate the hypocentres within a limited volume around the open hole section of well Basel 1 (Häring et al., in press). As expected, seismicity increased few hours after the onset of injection. A maximum of ca. 200 seismic events per hour were monitored on 08 December, shortly before the well was shut in. During the phase of pressure release the earthquake with the highest magnitude was recorded ($M_L = 3.4$, 08 December), and a few more shocks with a magnitude > 3 occurred after the pressure release was completed (January and February 2007). Seismicity then continuously decreased but had not reached the background level by May 2008.

The spatial distribution of the hypocentres shows that they are located predominantly along an oblate ellipsoid structure trending ca. NNW-SSE, and a minor branch trending ESE-WNW. For the 27 largest events that occurred in the Basel 1 reservoir during and after the stimulation, single-event focal mechanisms were calculated by the Swiss Seismological Service, using P-wave first motion observations (Deichmann et al., 2007). The nodal planes of all earthquakes have very similar strike orientations (Figure 9). In most cases, the faulting mechanism was almost pure strike slip. Some fault plane solutions indicate oblique normal faulting. Magnitudes of the earthquakes with an interpreted focal mechanism range from 1.7 to 3.4.

The P axes (circles) and T axes (triangles) are shown in Figure 10a. The T axes show consistent subhorizontal SW-NE orientations. The P axes have a SE-NW orientation; their plunges vary between horizontal and ca. 60°.
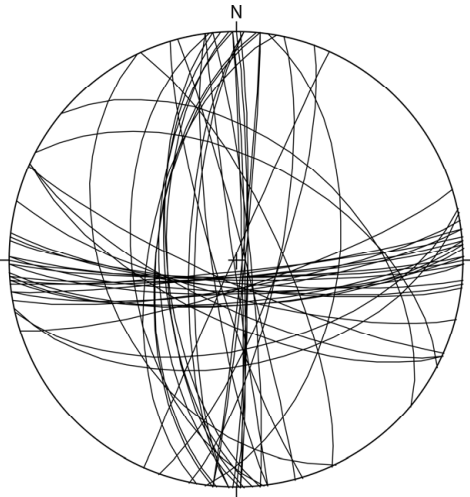
Figure 9: Orientation of the nodal planes of all triggered earthquakes in Basel.

5.3.4 Results of the Right Dihedra Analysis

The Right Dihedra method was applied to the whole dataset of 27 earthquakes for which a fault plane solution could be obtained. The earthquakes that were triggered by the stimulation injection in Basel are assumed to have been caused by the same stress field, since they all occurred within a rock volume of ca. 1 km^3 (Häring et al., in press). The result of the analysis is given in Figure 10b and reflects the similarity of the fault plane solutions. The best-fit orientations of the principal stress axes are NW-SE for σ_1 (316/01), SW-NE for σ_3 (046/11), and subvertical for σ_2 (222/79). However, due to the uniform orientation of the nodal planes the field into which σ_1 can fall is relatively big. Therefore, the precise orientations of the principal stress axes remain ill-constrained.

5.3.5 Discussion

The result of the Right Dihedra analysis suggests that the tectonic regime at the drilling site in Basel is one of almost pure strike-slip deformation. The occurrence of two normal-faulting events seems to be responsible for a slight asymmetry in the Right Dihedra plot, suggesting a more girdle-like distribution for σ1 and a slightly more constrained orientation for σ_3. This behaviour is consistent with the assumption that all earthquakes occurred in a rock volume that is subjected to a homogeneous stress field. However, it cannot be excluded that some of the smaller earthquakes, for which no focal mechanism could be determined, had faulting styles different from those analysed here, and accommodated local (and temporal) stress field variations.

If a well-constrained stress tensor can be calculated from a set of focal mechanisms, it might in some cases be possible to distinguish the (favourably oriented) fault plane from the auxiliary
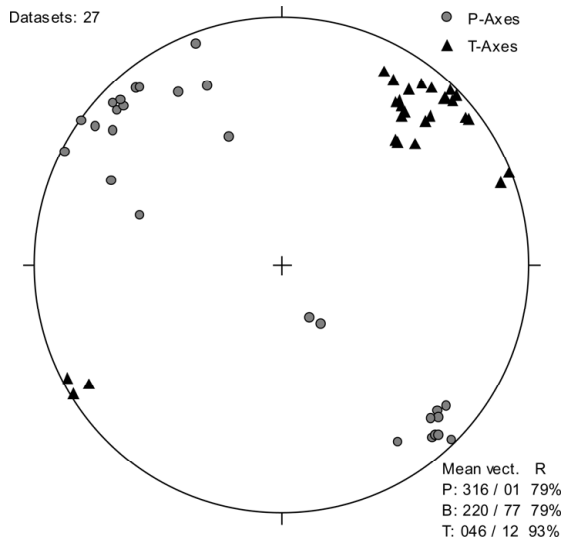
Figure 10a: Equal area plot of the P axes (circles) and T axes (triangles) of 27 earthquakes associated with hydraulic stimulation in Basel.
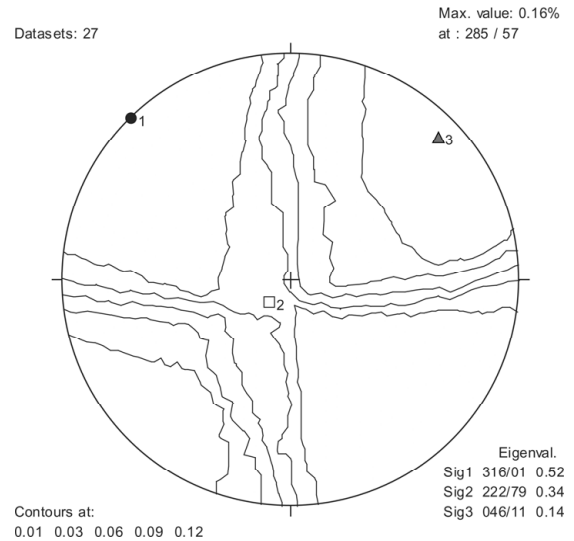
Figure 10b: Result of the Right-Dihedra analysis for the focal mechanisms of the same 27 earthquakes as in Figure 9, showing the orientations of the best-fit solutions for σ_1, σ_2 and σ_3. Contour lines show percentages.

plane. In the case of the Basel earthquakes, the similarity of the nodal-plane orientations prevented determining a well-confined stress tensor and did not allow the definition of the actual fault plane.

The orientation of the nodal planes – predominantly N-S and E-W – does not correspond to any of the main fault systems in this region. Most of the hypocentres are aligned within two steep conjugate planes striking ca. NNW-SSE and WNW-ESE, each about 30° from the maximum horizontal stress direction of 315° from the Right-Dihedra analysis. This suggests that earthquake foci concentrated on planes of shear stress concentration caused by the regional stress field and activated small-scale fault planes with a N-S or E-W strike. Alternatively, and especially if the S_{Hmax} value of ca. 144° from borehole breakouts in the well Basel 1 is considered (Häring et al., in press), the activation of N-S trending fault planes seems more plausible than slip on E-W trending structures.

5.4 Conclusions

The Right Dihedra method allows the use of focal mechanism data for the determination of the predominant regional stress field. This method has been applied to a data set of 115 earthquakes that occurred in the area of the southern Upper Rhine Graben, the Jura Mountains, the Rhine-Bresse Transfer Zone and the Swiss Molasse basin. The principal stress directions resulting from

the analysis of the entire data set are 148/13 for σ_1, 336/77 for σ_2 and 239/02 for σ_3 and agree well with the regional stress field determined by in-situ measurements. The tectonic regime is characterised by normal to strike-slip faulting, as found in earlier studies. A number of earthquakes with a thrust component cannot be explained by this general tectonic regime and seem to represent a transition to a more transpressive regime in the western part of the study area (Rhine-Bresse Transfer Zone and and northwestern Jura fold-and-thrust belt), as well as some effects of local stress field disturbances.

In comparison, the focal mechanisms of the earthquakes that were induced by fluid injection are much more homogeneous. This is probably due to the fact that they all occurred in a very limited volume of rock (ca. 1 km^3). The Right-Dihedra analysis gives principal stress axes orientations (σ_1: 316/01, σ_2: 222/79, σ_3: 046/11) that do not differ strongly from the orientations determined for the "natural" earthquakes. Therefore, the faulting mechanisms of the induced earthquakes in Basel seem to reflect the regional stress field.

Under this stress regime, the general faulting mechanisms to be expected are mainly left-lateral normal faulting on the west-dipping faults of the Rhine-Graben system and right-lateral thrust faulting on the faults related to the Late Paleozoic basement trough system. This is in agreement with the results from geological studies by Giamboni et al. (2004) and Ustaszewski and Schmid (2007) in the Rhine-Bresse Transfer Zone. To gain an improved understanding of deformation patterns and, hence, seismic hazard in the Basel area, improved hypocentre localisation on one hand and more earthquake recordings (e.g., using temporary networks) on the other hand would be necessary, in particular in the low seismicity areas of the Jura Mountains and the Rhine-Bresse Transfer Zone.

Appendix

Fault plane solution data for 115 earthquakes in the study area (1961-2006)

Date	Latitude	Longitude	Depth (km)	Magnitude (M_L)	Strike1/dip1/rake1	Strike2/dip2/rake2	P axis (azimuth/dip)	T axis (azimuth/dip)	Source
28.04.1961	47.700	7.900	0	4.9	176/64/000	086/90/154	134/18	038/18	Kastrup et al. (2004)
19.09.1965	47.950	8.267	18	4.1	223/54/-011	319/81/-143	187/32	086/18	Ahorner & Schneider (1974)
16.07.1967	47.380	5.250	0	4.1	133/65/156	234/68/027	003/02	094/34	Dorel et al. (1983)
05.02.1968	46.600	5.800	6	4.4	224/38/090	44/52/090	134/07	314/83	Kastrup et al. (2004)
08.03.1968	47.240	5.363	10	3.8	070/21/-072	231/70/-097	130/64	326/25	Dorel et al. (1983)
26.04.1974	47.200	7.900	0	3.0	044/40/031	289/71/125	354/18	240/51	Mayer-Rosa & Pavoni (1977)
21.05.1974	47.650	7.730	14	4.4	300/35/-162	195/80/-057	138/45	259/27	Bonjer et al. (1984)
08.01.1975	46.800	5.780	5	3.7	285/70/-165	190/76/-021	146/24	238/04	Dorel et al. (1983)
03.01.1976	48.000	8.220	10	2.1	107/70/-167	013/78/-021	328/23	062/05	Bonjer et al. (1984)
22.03.1976	47.000	7.000	0	2.7	013/90/000	283/90/180	148/00	058/00	Kastrup et al. (2004)
06.01.1977	47.310	6.320	5	3.0	203/84/000	113/90/174	158/04	068/04	Dorel et al. (1983)
11.02.1978	47.550	7.060	8	2.4	242/54/038	128/60/137	186/04	092/50	Bonjer et al. (1984)
07.04.1978	47.060	6.950	8	2.9	265/76/-169	172/79/-014	128/18	219/02	Pavoni (1984)
13.08.1978	47.290	7.690	24	3.4	121/66/-168	26/79/-024	341/25	075/08	Kastrup et al. (2004)
03.07.1979	46.925	7.072	30	3.8	285/86/179	015/89/004	150/02	240/04	Kastrup et al. (2004)
15.07.1980	47.673	7.475	12	4.7	125/80/174	216/84/010	350/03	081/11	Kastrup et al. (2004)
15.07.1980	47.674	7.485	10	3.7	117/46/-132	349/58/-055	314/60	055/06	Kastrup et al. (2004)
16.07.1980	47.671	7.481	13	3.8	201/42/064	054/53/111	129/06	021/72	Kastrup et al. (2004)
22.07.1980	47.680	7.470	12	3.9	205/74/007	113/84/164	160/07	068/16	Rouland et al. (1980)
25.03.1982	47.487	7.601	7	2.5	110/79/-172	018/82/-011	334/13	064/02	Kastrup et al. (2004)
03.09.1982	47.420	7.900	11	2.5	097/70/-175	005/85/-020	319/18	053/10	Kastrup et al. (2004)
04.10.1982	47.674	7.852	23	2.9	036/74/-006	128/84/-164	353/15	261/07	Kastrup et al. (2004)
10.04.1984	47.432	7.565	22	2.6	300/62/-176	208/87/-028	160/22	257/17	Kastrup et al. (2004)
12.04.1984	47.435	7.748	21	2.5	162/42/-030	275/71/-128	143/49	032/17	Kastrup et al. (2004)
16.06.1984	47.750	7.800	9	2.7	295/41/-118	150/55/-068	113/70	225/08	Kastrup et al. (2004)
07.01.1985	47.162	8.303	27	2.1	336/46/-125	201/54/-059	170/65	270/04	Kastrup et al. (2004)
28.02.1985	47.650	7.413	10	3.4	292/49/-169	195/82/-041	145/34	250/21	Kastrup et al. (2004)
07.07.1985	47.003	7.753	30	2.7	124/80/169	216/79/010	170/01	080/15	Kastrup et al. (2004)
18.07.1985	47.620	7.215	11	2.9	207/77/-010	299/80/-167	163/16	073/02	Bonjer & Apopei (1986)

Date	Latitude	Longitude	Depth (km)	Magnitude (M_L)	Strike1/dip1/rake1	Strike2/dip2/rake2	P axis (azimuth/dip)	T axis (azimuth/dip)	Source
15.09.1985	47.954	7.733	14	2.0	180/44/-033	295/68/-129	160/51	052/14	Kastrup et al. (2004)
05.11.1985	47.650	5.600	12	3.4	013/64/021	273/71/152	324/05	231/33	Nicolas et al. (1990)
20.01.1986	47.945	7.726	12	1.4	200/40/-048	330/61/-119	193/62	081/12	Kastrup et al. (2004)
07.10.1986	47.860	7.954	18	2.1	297/42/-114	148/52/-070	116/74	224/05	Kastrup et al. (2004)
01.11.1986	47.565	7.770	19	1.2	296/81/-174	205/84/-009	160/11	251/02	Kastrup et al. (2004)
08.01.1987	47.255	7.605	6	2.6	298/62/-174	205/85/-028	158/23	255/16	Kastrup et al. (2004)
11.04.1987	47.428	7.870	7	3.4	190/76/-011	282/79/-166	146/18	056/02	Kastrup et al. (2004)
18.07.1987	47.673	7.476	12	2.8	299/80/177	030/87/010	164/05	255/09	Kastrup et al. (2004)
20.09.1987	46.756	7.220	7	3.9	007/81/000	277/90/171	323/06	232/06	Kastrup et al. (2004)
21.11.1987	47.679	7.476	12	2.8	209/38/064	061/56/109	138/09	018/72	Kastrup et al. (2004)
11.12.1987	47.313	7.161	9	3.7	274/70/168	008/79/020	140/06	232/22	Kastrup et al. (2004)
16.12.1987	47.521	7.675	9	2.7	006/86/036	273/54/175	134/21	236/28	Kastrup et al. (2004)
31.12.1987	47.518	7.676	12	1.1	053/40/014	312/81/129	013/26	258/41	Kastrup et al. (2004)
23.03.1988	47.675	7.474	11	1.6	007/30/-013	108/84/-119	350/44	222/33	Kastrup et al. (2004)
16.04.1988	47.436	7.889	9	1.9	310/63/-108	165/32/-059	187/67	053/16	Kastrup et al. (2004)
11.05.1988	47.515	7.677	10	1.5	199/75/-016	293/75/-164	156/22	066/00	Kastrup et al. (2004)
26.08.1988	47.804	7.688	19	3.3	307/30/-118	158/64/-075	097/67	237/18	Kastrup et al. (2004)
28.08.1988	47.803	7.694	20	1.5	296/33/-134	165/67/-066	111/61	237/19	Kastrup et al. (2004)
03.09.1988	47.740	7.060	6.6	3.0	130/65	224/82	089.6/23.5	354.5/11.5	Plenefisch & Bonjer (1997)
11.09.1988	47.130	8.390	29	2.5	298/74/180	028/90/016	162/11	254/11	Kastrup et al. (2004)
14.10.1988	46.698	6.889	2	3.3	350/69/020	253/71/158	302/02	211/29	Kastrup et al. (2004)
18.10.1988	47.738	7.648	12	2.0	272/73/170	005/80/017	138/05	229/19	Kastrup et al. (2004)
27.10.1988	47.500	7.741	12	1.6	275/77/-177	184/87/-013	139/11	230/07	Kastrup et al. (2004)
20.11.1988	47.730	7.548	17	1.9	263/68/-177	172/87/-022	125/17	220/13	Kastrup et al. (2004)
18.03.1989	47.909	7.698	14	3.0	184/27/007	088/87/117	154/36	023/42	Kastrup et al. (2004)
30.04.1989	47.282	6.715	19	2.9	115/61/-156	013/69/-031	332/36	066/05	Kastrup et al. (2004)
05.05.1989	47.559	7.609	10	2.2	312/79/-170	220/80/-011	176/15	266/01	Kastrup et al. (2004)
09.06.1989	47.478	8.331	18	1.3	142/42/-105	342/50/-077	311/79	063/04	Kastrup et al. (2004)
12.08.1989	47.767	7.726	19	2.7	275/35/-120	130/60/-071	080/69	206/13	Kastrup et al. (2004)

Date	Latitude	Longitude	Depth (km)	Magnitude (M$_L$)	Strike1/dip1/rake1	Strike2/dip2/rake2	P axis (azimuth/dip)	T axis (azimuth/dip)	Source
11.05.1990	47.808	7.924	20	2.0	058/14/056	273/78/098	356/33	193/56	Kastrup et al. (2004)
16.06.1990	47.576	7.619	18	2.0	293/80/177	024/87/010	158/05	249/09	Kastrup et al. (2004)
20.06.1990	47.848	7.713	17	2.0	031/35/145	151/71/060	263/20	024/54	Kastrup et al. (2004)
25.07.1990	47.516	7.672	10	2.0	180/86/-032	272/58/-176	131/25	231/19	Kastrup et al. (2004)
31.07.1990	47.659	7.770	19	2.0	318/21/-109	158/70/-083	080/64	243/25	Kastrup et al. (2004)
11.08.1990	47.274	8.000	15	2.8	011/90/000	281/90/180	326/00	236/00	Kastrup et al. (2004)
16.08.1990	47.523	7.599	11	2.1	282/61/-167	186/79/-030	140/29	237/12	Kastrup et al. (2004)
08.11.1990	47.524	7.698	11	2.0	282/50/-141	164/61/-047	127/53	225/06	Kastrup et al. (2004)
28.11.1990	47.539	7.830	18	2.0	319/48/-130	190/55/-055	159/61	256/04	Kastrup et al. (2004)
11.12.1990	47.853	7.941	13	1.5	092/35/-132	320/65/-065	269/62	032/16	Kastrup et al. (2004)
01.01.1991	47.836	7.654	12	2.0	068/63/-176	336/87/-027	288/21	025/16	Kastrup et al. (2004)
20.05.1991	47.664	7.823	17	1.5	105/73/-170	012/80/-017	328/19	059/05	Kastrup et al. (2004)
04.06.1991	47.552	7.614	7	1.7	360/56/024	256/70/144	311/09	213/39	Kastrup et al. (2004)
25.08.1991	47.638	7.330	12	2.0	292/76/-172	200/82/-014	155/16	247/04	Kastrup et al. (2004)
05.11.1991	47.599	7.692	17	1.8	334/43/-122	194/55/-064	160/68	266/07	Kastrup et al. (2004)
12.11.1991	47.679	7.475	12	1.8	175/59/-022	277/71/-147	139/36	044/08	Kastrup et al. (2004)
25.03.1992	47.515	7.633	8	2.6	278/65/-160	179/72/-026	137/31	230/05	Kastrup et al. (2004)
30.12.1992	47.710	8.380	22	4.0	181/71/003	090/87/161	137/11	044/15	Kastrup et al. (2004)
10.01.1995	47.744	7.748	14	2.7	336/36/-108	178/56/-077	126/75	259/10	Kastrup et al. (2004)
17.09.1995	46.782	7.200	7	3.8	175/88/003	085/87/178	310/01	040/04	Kastrup et al. (2004)
24.04.1996	47.565	7.607	12	2.7	292/55/174	025/85/035	153/20	254/28	Kastrup et al. (2004)
15.06.1996	47.602	7.642	21	2.4	314/73/165	048/76/017	180/02	271/23	Kastrup et al. (2004)
15.12.1996	47.341	7.886	20	3.0	313/50/-141	195/61/-047	158/53	256/06	Kastrup et al. (2004)
01.02.1997	47.67	7.48	10	3.6	028/63/-007	121/84/-153	348/23	252/14	LGRB (2008)
20.02.1997	47.81	7.56	21	3.1	160/45/-060	301/52/-117	149/69	049/04	LGRB (2008)
21.02.1997	47.422	7.875	8	1.8	316/55/-114	174/42/-060	171/69	063/07	Kastrup et al. (2004)
02.09.1997	47.606	7.861	23	2.6	128/53/-090	308/37/-090	038/82	218/08	Kastrup et al. (2004)
17.11.1997	47.64	7.62	17	3.5	147/38/-103	343/53/-080	292/79	066/08	LGRB (2008)
17.12.1998	47.58	7.77	18	3.0	204/61/-012	300/80/-150	166/28	069/13	LGRB (2008)

137

Date	Latitude	Longitude	Depth (km)	Magnitude (M_L)	Strike1/dip1/rake1	Strike2/dip2/rake2	P axis (azimuth/dip)	T axis (azimuth/dip)	Source
14.02.1999	46.782	7.212	7	4.3	354/88/009	264/81/178	129/05	219/08	Kastrup et al. (2007)
13.07.1999	47.514	7.696	19	2.7	215/70/-005	307/85/-160	173/17	079/11	Kastrup et al. (2004)
04.04.2000	47.48	7.07	9	2.3	250/29.9	058.4/60.5	152.7/15.3	313.8/73.9	Lopes Cardozo & Granet (2003)
19.04.2000	47.32	7.47	19	2.6	309.9/72	211.3/65.4	172.2/30.9	079.6/4.4	Lopes Cardozo & Granet (2003)
28.05.2000	47.74	7.54	14	2.3	106.6/71	359.9/50	331.4/43.1	228.9/13.0	Lopes Cardozo & Granet (2003)
15.06.2000	47.96	7.93	17	2.6	264.2/60.5	359.9/79.9	128.9/13.0	226.0/28.1	Lopes Cardozo & Granet (2003)
15.06.2000	47.94	7.93	15	2.1	233.8/42	354.9/64.9	109.6/13.1	219.3/55.5	Lopes Cardozo & Granet (2003)
20.06.2000	47.471	7.787	18	2.9	111/35/-118	324/60/-072	273/70	041/13	Baer et al. (2001)
20.06.2000	47.47	7.79	16	1.8	170/55	310.7/42	134.7/68.5	242.5/6.9	Lopes Cardozo & Granet (2003)
20.06.2000	47.46	7.79	16	3.0	317.7/71	094.8/25	252.1/60.4	034.9/24.3	Lopes Cardozo & Granet (2003)
20.06.2000	47.46	7.79	16	2.9	339.9/64.9	213.7/38.3	207.2/58.6	091.5/14.8	Lopes Cardozo & Granet (2003)
20.06.2000	47.46	7.79	17	2.0	172.2/48.2	324.9/45	152.1/75.9	249.0/1.7	Lopes Cardozo & Granet (2003)
20.06.2000	47.47	7.79	16	1.9	264.9/75	003.3/61.2	221.0/31.6	316.7/9.1	Lopes Cardozo & Granet (2003)
10.07.2000	47.21	7.55	6	3.0	168.1/69.9	281.1/55.7	130.9/47.5	225.5/4.2	Lopes Cardozo & Granet (2003)
13.07.2000	47.52	7.67	10	1.6	019.8/69.9	267.7/43.9	246.5/48.7	138.1/15.5	Lopes Cardozo & Granet (2003)
13.07.2000	47.51	7.67	11	2.4	149.9/54.7	284.9/44.7	117.2/65.1	219.2/5.5	Lopes Cardozo & Granet (2003)
23.07.2000	47.83	7.77	14	1.7	359.8/85	264/40.2	121.2/28.6	235.3/37.0	Lopes Cardozo & Granet (2003)
28.07.2000	47.52	7.78	21	2.5	253.1/77.2	124.9/20	143.9/55.1	356.0/30.6	Lopes Cardozo & Granet (2003)
13.11.2000	47.225	7.560	10	3.4	090/75/-178	359/88/-015	313/12	045/09	Baer et al. (2001)
13.04.2001	47.620	7.543	8	2.9	123/40/-130	351/61/-062	308/63	061/11	Deichmann et al. (2002)
31.08.2003	47.542	7.898	17	2.9	292/82/-172	201/82/-008	156/11	246/00	Deichmann et al. (2004)
23.02.2004	47.278	6.270	15	4.8	296/74/119	053/32/031	004/24	240/53	Baer et al. (2005)
21.06.2004	47.503	7.711	21	3.8	199/66/-043	309/51/-149	158/47	257/09	Baer et al. (2005)
28.06.2004	47.523	8.165	21	4.0	295/88/-134	202/44/-004	169/33	059/28	Baer et al. (2005)
12.05.2005	47.264	7.651	24	4.1	101/61/147	208/61/033	155/00	065/43	Deichmann et al. (2006)
11.12.2005	47.520	8.160	18	4.1	314/57/-130	191/50/-045	167/57	071/04	Deichmann et al. (2006)
29.03.2006	46.920	6.869	4	3.2	179/70/025	080/67/158	309/02	040/31	Baer et al. (2007)
08.12.2006	47.582	7.600	6	3.4	013/72/-013	107/78/-162	331/22	239/04	Baer et al. (2007)

References

Ahorner, L. and Schneider, G., 1974. Herdmechanismen von Erdbeben im Oberrhein-Graben und in seinen Randgebirgen. Approaches to Taphrogenesis; The Rhinegraben; geologic history and neotectonic activity: 104-117.

Angelier, J., 1984. Tectonic analysis of fault slip data sets. Journal of Geophysical Research 89(B7): 5835–5848

Angelier, J. and Mechler, P., 1977. Sur une méthode graphique de recherche des contraintes principales également utilisable en tectonique et en séismologie: la méthode des dièdres droits. Bulletin de la Société Géologique de France, 7(6): 1309-1318.

Baer, M., Deichmann, N., Braunmiller, J., Bernardi, F., Cornou, C., Fäh, D., Giardini, D., Huber, S., Kästli, P., Kind, F., Kradolfer, U., Mai, M., Maraini, S., Oprsal, I., Schler, T., Schorlemmer, D., Sellami, S., Steimen, S., Wiemer, S., Wossner, J. and Wyss, A., 2003. Earthquakes in Switzerland and surrounding regions during 2002. Eclogae Geologicae Helvetiae, 96(2): 313-324.

Baer, M., Deichmann, N., Braunmiller, J., Clinton, J., Husen, S., Fäh, D., Giardini, D., Kästli, P., Kradolfer, U. and Wiemer, S., 2007. Earthquakes in Switzerland and surrounding regions during 2006. Swiss Journal of Geosciences, 100(3): 517-528.

Baer, M., Deichmann, N., Braunmiller, J., Dolfin, D.B., Bay, F., Bernardi, F., Delouis, B., Fäh, D., Gerstenberger, M., Giardini, D., Huber, S., Kastrup, U., Kind, F., Kradolfer, U., Maraini, S., Mattle, B., Schler, T., Salichon, J., Sellami, S., Steimen, S. and Weimer, S., 2001. Earthquakes in Switzerland and surrounding regions during 2000. Eclogae Geologicae Helvetiae, 94(2): 253-264.

Baer, M., Deichmann, N., Braunmiller, J., Husen, S., Fäh, D., Giardini, D., Kästli, P., Kradolfer, U. and Wiemer, S., 2005. Earthquakes in Switzerland and surrounding regions during 2004. Eclogae Geologicae Helvetiae, 98(3): 407-418.

Baroux, E., Bethoux, N. and Bellier, O., 2001. Analyses of the stress field in southeastern France from earthquake focal mechanisms. Geophysical Journal International, 145(2): 336-348.

Becker, A., 2000. The Jura Mountains - An active foreland fold-and-thrust belt? Tectonophysics, 321(4): 381-406.

Becker, A., Davenport, C.A. and Giardini, D., 2002. Palaeoseismicity studies on end-Pleistocene and Holocene lake deposits around Basle, Switzerland. Geophysical Journal International, 149(3): 659-678.

Bonjer, K.P., 1997. Seismicity pattern and style of seismic faulting at the eastern borderfault of the southern Rhine Graben. Tectonophysics, 275(1-3): 41-69.

Bonjer, K.P. and Apopei, I., 1986. The complexity of the seismogenetic energy release in the southernmost Rhine Graben and Dinkelberg area; first results obtained by the new digital seismic network. Jahrestagung der Deutschen Geophysikalischen Gesellschaft e.V., 46: 141.

Bonjer, K.P., Gelbke, C., Gilg, B., Rouland, D., Mayer-Rosa, D. and Massinon, B., 1984. Seismicity and dynamics of the Upper Rhine Graben. Journal of Geophysics, 55: 1-12.

Bossart, P. and Wermeille, S., 2003. The stress field in the Mont Terri Region - Data Compilation. In: P. Heitzmann and J.-P. Tripet (Editors), Mont Terri Project - Geology, Paleohydrology and Stress Field of the Mont Terri Region. Reports of the Federal Office for Water and Geology, Geology Series 4.

Bott, M.H.P., 1959. The mechanics of oblique slip faulting. Geological Magazine, 96(2): 109-117.

Carey-Gailhardis, E. and Mercier, J.L., 1987. A numerical method for determining the state of stress using focal mechanisms of earthquake populations: application to Tibetan teleseisms and microseismicity of Southern Peru. Earth and Planetary Science Letters, 82(1-2): 165-179.

Carey-Gailhardis, E. and Mercier, J.L., 1992. Regional state of stress, fault kinematics and adjustments of blocks in a fractured body of rock: application to the microseismicity of the Rhine graben. Journal of Structural Geology, 14(8/9): 1007-1017.

Carey-Gailhardis, E. and Vergely, P., 1992. Graphical analysis of fault kinematics and focal mechanisms of earthquakes in terms of stress; the right dihedra method, use and pitfalls. Annales Tectonicae, 6(1): 3-9.

Clark, D. and Leonard, M., 2003. Principal stress orientations from multiple focal-plane solutions: new insight into the Australian intraplate stress field. Geological Society of America (GSA) Bulletin Special Paper, 372: 91-105.

Deichmann, N., Baer, M., Braunmiller, J., Cornou, C., Fäh, D., Giardini, D., Gisler, M., Huber, S., Husen, S., Kästli, P., Kradolfer, U., Mai, M., Maraini, S., Oprsal, I., Schler, T., Schorlemmer, D., Wiemer, S., Wossner, J. and Wyss, A., 2004. Earthquakes in Switzerland and surrounding regions during 2003. Eclogae Geologicae Helvetiae, 97(3): 447-458.

Deichmann, N., Baer, M., Braunmiller, J., Dolfin, D.B., Bay, F., Bernardi, F., Delouis, B., Fäh, D., Gerstenberger, M., Giardini, D., Huber, S., Kradolfer, U., Maraini, S., Oprsal, I., Schibler, R., Schler, T., Sellami, S., Steimen, S., Wiemer, S., Wossner, J. and Wyss, A., 2002. Earthquakes in Switzerland and surrounding regions during 2001. Eclogae Geologicae Helvetiae, 95(2): 249-262.

Deichmann, N., Baer, M., Braunmiller, J., Husen, S., Fäh, D., Giardini, D., Kästli, P., Kradolfer, U. and Wiemer, S., 2006. Earthquakes in Switzerland and surrounding regions during 2005. Eclogae Geologicae Helvetiae, 99(3): 443-452.

Deichmann, N., Dolfin, D.B. and Kastrup, U., 2000. Seismizität der Nord- und Zentralschweiz. Nagra Technischer Bericht, 00-05.

Deichmann, N., Ernst, J. and Wöhlbier, S., 2007. Data Analysis. In: Evaluation of the induced seismicity in Basel 2006/2007: locations, magnitudes, focal mechanisms, statistical forecasts and earthquake scenarios, Report of the Swiss Seismological Service to Geopower Basel AG, Basel, Switzerland, 152 pp.

Diebold, P. and Noack, T., 1996. Late Palaeozoic troughs and Tertiary structures in the eastern Folded Jura. In: O.A. Pfiffner, P. Lehner, P. Heitzmann, S. Mueller and A. Steck (Editors), Deep structure of the Swiss Alps; results of NRP 20. Birkhäuser, Basel, Switzerland, pp. 59-63.

Dorel, J., Frechet, J., Gagnepain-Benex, J., Haessler, H., Lachaize, M., Madariaga, R., Modiano, T., Pascal, G., Perrier, G., Philip, H., Rouland, D. and Wittlinger, G., 1983. Focal mechanism in metropolitan France and the lesser Antilles. Annales Geophysicae, 1(4-5): 299-305.

Etchecopar, A., Vasseur, G. and Daignieres, M., 1981. An inverse problem in microtectonics for the determination of stress tensors from fault striation analysis. Journal of Structural Geology, 3(1): 51-65.

Fäh, D., Giardini, D., Bay, F., Bernardi, F., Braunmiller, J., Deichmann, N., Furrer, M., Gantner, L., Gisler, M., Isenegger, D., Jimenez, M.J., Kästli, P., Koglin, R., Masciadri, V., Rutz, M., Scheidegger, C., Schibler, R., Schorlemmer, D., Schwarz-Zanetti, G., Steimen, S., Sellami, S., Wiemer, S. and Wossner, J., 2003. Earthquake Catalogue Of Switzerland (ECOS) and the related macroseismic database. Eclogae Geologicae Helvetiae, 96(2): 219-236.

Ferry, M., Meghraoui, M., Delouis, B. and Giardini, D., 2005. Evidence for Holocene palaeoseismicity along the Basel-Reinach active normal fault (Switzerland); a seismic source for the 1356 earthquake in the Upper Rhine Graben. Geophysical Journal International, 160(2): 554-572.

Galindo-Zaldivar, J., González-Lodeiro, F. and Jabaloy, A., 1993. Stress and Paleostress in the Betic-Rif Cordilleras (Miocene to the Present). Tectonophysics, 227(1-4): 105-126.

Gephart, J.W. and Forsyth, D.W., 1984. An improved method for determining the regional stress tensor using earthquake focal mechanism data - application to the San-Fernando earthquake sequence. Journal of Geophysical Research, 89(NB11): 9305-9320.

Giamboni, M., Ustaszewski, K., Schmid, S.M., Schumacher, M.E. and Wetzel, A., 2004. Plio-Pleistocene transpressional reactivation of Paleozoic and Paleogene structures in the Rhine-Bresse transform zone (northern Switzerland and eastern France). International Journal of Earth Sciences, 93(2): 207-223.

González-Casado, J.M., Giner-Robles, J.L. and López-Martínez, J., 2000. Bransfield Basin, Antarctic Peninsula: Not a normal backarc basin. Geology, 28(11): 1043-1046.

Häring, M.O., Schanz, U., Ladner, F. and Dyer, B., in press. Characterisation of the Basel 1 Enhanced Geothermal System. Geothermics.

Harmsen, S.C., 1994. The Little-Skull-Mountain, Nevada, Earthquake of 29-June-1992 - Aftershock Focal Mechanisms and Tectonic Stress-Field Implications. Bulletin of the Seismological Society of America, 84(5): 1484-1505.

Kastrup, U., Deichmann, N., Fröhlich, A. and Giardini, D., 2007. Evidence for an active fault below the northwestern Alpine foreland of Switzerland. Geophysical Journal International, 169(3): 1273-1288.

Kastrup, U., Zoback, M.L., Deichmann, N., Evans, K.F., Giardini, D. and Michael, A.J., 2004. Stress field variations in the Swiss Alps and the northern Alpine foreland derived from inversion of fault plane solutions. Journal of Geophysical Research-Solid Earth, 109(B1).

Lambert, J., Winter, T., Deweza, T.J.B. and Sabouraulta, P., 2004. New hypotheses on the maximum damage area of the 1356 Basel earthquake (Switzerland). Quaternary Science Reviews.

Lay, T. and Wallace, T.C., 1995. Modern Global Seismology. Academic Press, 521 pp.

LGRB, 2008. http://www.lgrb.uni-freiburg.de/lgrb/Fachbereiche/erdbebendienst/jahresbulletins. Accessed on 23.05.2008.

Lopes Cardozo, G.G.O. and Granet, M., 2003. New insight in the tectonics of the southern Rhine Graben-Jura region using local earthquake seismology. Tectonics, 22(6).

Majer, E.L., Baria, R., Stark, M., Oates, S., Bommer, J., Smith, B. and Asanumag, H., 2007. Induced seismicity associated with Enhanced Geothermal Systems. Geothermics 36: 185-222.

Mayer-Rosa, D. and Pavoni, N., 1977. Fault-plane solutions of earthquakes in Switzerland from 1971 to 1976. Publ. Inst. Geophys. Pol. Acad. Sci., A-5(116): 321–326.

McKenzie, D.P., 1969. Relation between fault plane solutions for earthquakes and directions of principal stresses. Bulletin of the Seismological Society of America, 59(2): 591-601.

Meyer, W., 2006. Da verfiele Basel überall. Schwabe, Basel.

Michael, A.J., 1987. Use of Focal Mechanisms to Determine Stress - a Control Study. Journal of Geophysical Research-Solid Earth and Planets, 92(B1): 357-368.

Müller, W.H., Blümling, P., Becker, A. and Clauss, B., 1987. Die Entkopplung des tektonischen Spannungsfeldes an der Jura-Ueberschiebung. Eclogae Geologicae Helvetiae, 80(2).

Mussett, A. and Khan, M., 2000. Looking into the Earth - An Introduction to Geological Geophysics. Cambridge University Press, 470 pp.

Nicolas, M., Santoire, J.P. and Delpech, P.Y., 1990. Intraplate seismicity; new seismotectonic data in Western Europe. Tectonophysics, 179(1-2): 27-53.

Pavoni, N., 1984. Seismotektonik Nordschweiz. Nagra Technischer Bericht 84-45, Baden.

Pfiffner, O.A. and Burkhard, M., 1987. Determination of paleo-stress axes orientations from fault, twin and earthquake data. Annales Tectonicae, 1(1): 48-57.

Plenefisch, T. and Bonjer, K.P., 1997. The stress field in the Rhine Graben area inferred from earthquake focal mechanisms and estimation of frictional parameters. Tectonophysics, 275(1-3): 71-97.

Reinecker, J., Heidbach, O., Tingay, M., Sperner, B. and Mueller, B., 2005. The 2005 release of the World Stress Map (available online at www.world-stress-map.org).

Reiter, F. and Acs, P., 1996-2003. TectonicsFP. Software for structural geology. Innsbruck University, Austria. http://go.to/TectonicsFP.

Rouland, D., Haessler, H., Bonjer, K.P., Gilg, B., Mayer-Rosa, D. and Pavoni, N., 1980. The Sierentz southern Rhinegraben earthquake of July 15, 1980; preliminary results. Proceedings of the Seventeenth assembly of the European Seismological Commission.

Schanz, U., Dyer, B., Ladner, F. and Häring, M.O., 2007. Microseismic aspects of the Basel 1 geothermal reservoir, 5th Swiss Geoscience Meeting, Geneva.

Swiss Seismological Service, 2002. ECOS - Earthquake Catalog of Switzerland, http://histserver.ethz.ch/download/ECOS.pdf (accessed on 05.05.2008).

Ustaszewski, K. and Schmid, S.M., 2007. Latest Pliocene to recent thick-skinned tectonics at the Upper Rhine Graben - Jura Mountains junction. Swiss Journal of Geosciences, 100(2): 293-312.

Chapter 6

Synthesis and conclusions

This thesis addresses the recent tectonic history of the eastern Jura fold-and-thrust belt and the southern Upper Rhine Graben. While the tectonic evolution of this region up to ca. 5 Ma ago is relatively well resolved, the younger history is less well defined, due to the combined effect of low deformation rates (less than 1 mm/a, vertical as well as horizontal) and a lack of datable sediments younger than ca. 5 Ma. However, improved understanding of the tectonic processes in the recent geological past is essential for the assessment of the seismic hazard in this densely populated area, and in order to arrive at a concept of the future evolution of the study area indispensable for the search of a suitable repository for nuclear waste. In an attempt to bridge this gap, the focus of this thesis is laid on a combination of geomorphological and seismotectonic analyses, with the aim of better defining the recent deformation history in north-western Switzerland. The approaches chosen cover different time scales and concentrate on different regions within the larger study area. The results and conclusions of this study are summarised in the following.

On the largest temporal and spatial scale, the response of the drainage system in the northern Alpine foreland to tectonic processes between the Oligocene and the Quaternary was examined (Chapter 2). Geomorphic and sedimentary evidence of former river courses allows reconstructing the drainage system evolution to a large extent. This drainage system evolution primarily reflects the formation of the thin-skinned Jura fold-and-thrust belt, which introduced a new watershed between areas draining into the Black Sea (Danube) and into the Mediterranean (Doubs), respectively, in the Miocene. The transitions between different stages of drainage organisation are reflected in the widespread occurrence of water and wind gaps in Jura anticlines. These gaps allow for the reconstruction of river courses in the area of the Jura fold-and-thrust belt at the beginning of folding, and for the tracking of the folding process through time. The observed stages in the development of the drainage system suggest a general fold-belt propagation to the north and west that was, however, not entirely in sequence. Apart from the effects of the Jura fold-and-thrust belt, the drainage system was significantly affected by larger-scale tectonic processes leading to differential vertical deformation in the Rhine and Bresse grabens, the Vosges-Black Forest Arch, and the Molasse basin.

The geomorphic response of rivers in the eastern Jura mountains (Jura fold-and-thrust belt and Tabular Jura) and the southernmost Upper Rhine Graben to tectonic activity following the main decollement phase in the Miocene was investigated in a stream gradient analysis (Chapter 3). From the topographic information in a 25 m cell size digital elevation model, slope and drainage area data were calculated, and steepness and concavity indices determined for rivers as well as river segments. In the Upper Rhine Graben, steepness index values are found to be relatively low; intermediate values characterise rivers from the Tabular Jura, whereas the highest values are found in the Folded Jura. This suggests that subsidence of the southern Upper Rhine Graben (relative to the Tabular Jura) has continued after 5 Ma, and is probably still ongoing. The complete sedimentary sequence that was deposited in the Upper Rhine Graben in the Quaternary (Bartz, 1974) supports this interpretation, as does the occurrence of the Lower Cover Gravel terraces along the river Rhine, indicating an alongstream gradient increase across the eastern Main Boundary Fault of the Upper Rhine Graben (Kock et al., in prep.). Postulated ongoing graben subsidence is also in agreement with the predominant normal faulting mechanism for earthquakes in the area of the SE Upper Rhine Graben (Chapter 5), and with the present-day tectonic stress regime of strike-slip to normal faulting in north-western Switzerland, determined by focal mechanism stress inversion (Kastrup et al., 2004).

The steepness index distribution further suggests that relative to the Tabular Jura, an area that roughly corresponds to the Jura fold-and-thrust belt has been uplifted in the Latest Quaternary (after ca. 100 ka). This observation confirms a trend in geodetic data that indicate slightly higher uplift rates in the Jura fold-and-thrust belt compared to a reference point at the border of the Tabular Jura and the Black Forest crystalline massif (Schlatter, 2007; Zippelt and Dierks, 2007). Two different tectonic mechanisms can in principle be invoked to explain this uplift: ongoing detachment tectonics, i.e. continuing shortening activity of the thin-skinned Jura fold-and-thrust belt, as opposed to the differential vertical movement induced by reactivation of faults in the crystalline basement. Basement faults related to the Late Paleozoic Trough system that crosses the area of the eastern Jura mountains underneath the Mesozoic sediments have a favourable orientation (ENE-WSW) for transpressive reactivation in the present-day stress field, which is characterised by a SE-NW oriented maximum principal stress axis, especially since the intermediate principal stress axis is not exactly vertical, as determined in the seismotectonic analysis (Chapter 5). At the north-western front of the Jura fold-and-thrust belt, Madritsch et al. (2008) report transpressional inversion of basement faults after the Early Pliocene as well as active thrust faulting evident from earthquake fault plane solutions. In the eastern Jura mountains, however, thrust faulting plays only a marginal role in the seismotectonic record of the area. This

apparent contradiction might be explained by a) an aseismic faulting process in this part of the Jura mountains, or b) the fact that elastic deformation is presently accumulating in the lithosphere.

Alternatively, if differential relative uplift rates are caused by ongoing thin-skinned thrusting, and thus deformation along the evaporitic detachment layer, this would imply that the evaporites – mainly anhydrite – behave in a plastic way today, despite their shallow position at depths of less than 1 km. Madritsch et al. (2008) suggest that this mechanism might still be at work at the north-western front of the Jura fold-and-thrust belt (France), causing anticline growth after the Middle Pliocene. GPS measurements in the eastern Jura mountains neither give evidence of the horizontal movements corresponding to detachment tectonics, nor do they rule them out, due to the higher measurement uncertainty of this technique compared to precise levelling (Brockmann et al., 2005). However, the fact that a large amount of material has been eroded in the Molasse Basin between the Alps and the Jura fold-and-thrust belt in the Pliocene-Pleistocene (Cederbom et al., 2004) raises the question of how the horizontal stresses that might lead to detachment in the Jura mountains could be transmitted across the Molasse Basin today. Therefore, it seems more probable that processes in the crystalline basement underneath the detachment horizon are responsible for the observed differential uplift in the area of the eastern Jura mountains.

Additional information about the most recent part of the Quaternary tectonic history in north-western Switzerland is provided by a geomorphologic study of Late Quaternary fluvial terraces in the lower Aare valley (Chapter 4). After the accumulation of the Low Terrace Gravels at ca. 20 ka, a system of erosional terraces developed due to incision of the Aare, possibly interrupted by additional aggradational phases. Based on a high-resolution (2 m cell size) digital elevation model, the occurrence and morphology of these terraces were studied, including the analysis of a longitudinal profile along the lower Aare valley and the 3D orientation of the terrace treads. Although the longitudinal profile of the terraces does not yield any conclusive evidence of localised tectonic activity or active faults – in part also due to the very fragmentary preservation of the terrace surfaces –, asymmetries in the terrace distribution suggest a regional tilt to the north in this area during the past 20 ka. Such a tilt might be caused by differential uplift in the northern Alpine foreland due to erosional unloading of the Molasse basin in the Quaternary, as proposed by Cederbom et al. (2004). This tilt would be expected to decrease to the north, thus explaining why the Low Terrace along the river Rhine does not show any pronounced asymmetry along reaches in E-W direction (Kock et al., in prep.). However, the observed terrace asymmetry downstream from Aarau might also be a more local effect, caused by a gentle anticlinal structure to the south of the valley. Alternatively, it could be the result of a rotating basement block underneath the Quaternary valley fill. This is, however, highly hypothetical and not supported by the seismological record.

In summary, the observations made in the stream gradient analysis and the terrace study can most plausibly be explained by a combination of ongoing, largely aseismic, basement-related transpressive tectonic deformation, and an elastic rebound effect of the central northern Alpine foreland due to massive erosional unloading in the Quaternary. Considering the apparent tilt along an ~E-W axis, systematic analyses of terrace geomorphology in differently oriented tributary valleys might provide additional information on the tilting mechanism and deformation pattern in this region.

The regional present-day stress tensor derived from an analysis of an updated compilation of earthquake focal mechanisms in the southern Upper Rhine Graben, Rhine-Bresse Transfer Zone, Jura fold-and-thrust belt, and Tabular Jura indicates a NW-SE oriented maximum stress axis (Chapter 5). Focal mechanisms from a series of induced earthquakes in Basel point to a strike-slip stress regime with a weak tendency to transtension, and are hence consistent with the regional stress field in this area. This is in agreement with the results from focal mechanism inversions in previous studies (Plenefisch and Bonjer, 1997; Kastrup et al., 2004). However, the results presented in this thesis demonstrate substantial small-scale stress variations, which are expressed by the fact that earthquakes with faulting mechanisms indicating different stress fields occur close to each other. This implies that the large number of faults of different age lead to stress perturbations and a heterogeneous deformation pattern in this area. In addition, the seismologic data show a tendency of the stress regime to change from transtension in northern and north-western Switzerland and along the eastern Main Boundary Fault of the Upper Rhine Graben, to transpression to the west and north-west (western Switzerland and Rhine-Bresse Transfer Zone), thus confirming the observations made by Madritsch et al. (2008). In the light of the geomorphologic investigations, however, this variation might also be due to different deformation mechanisms in the east and west, i.e. that a larger component of convergence is accommodated by aseismic movement in the area of the eastern Jura mountains compared to the region west of the southern Upper Rhine Graben.

In summary, this thesis provides new evidence for continuing tectonic activity in the Alpine foreland in the vicinity of the Upper Rhine Graben since Pliocene times. Distinct faults or folds along which tectonic deformation is focused could not be conclusively identified, which indicates that the near-surface deformation takes place in poorly constrained deformation zones today, rather than concentrating on distinct faults. In particular, along the eastern boundary of the Upper Rhine Graben, deformation appears to be distributed on a set of normal faults of limited length. Field observations of deformed Quaternary sediments within the southern Upper Rhine Graben, indicating active normal faulting on several faults, are reported by Kock et al. (in prep.) and support this interpretation.

Focal mechanism data show that the faulting style of a majority of earthquakes in this region has a predominant strike-slip component. This deformation at depth, if it is transferred to the surface, is expected to have a minor effect on the gradients of rivers and terraces, and is therefore difficult to detect by the geomorphological methods used in this thesis. To monitor lateral deformation, the systematic analysis of GPS measurements promises some success; however, the low strain rates in the study area necessitate data from a longer time interval than the period covered today, if detailed knowledge of the deformation field is needed. Considering the deformation rates in the study area and the error of this measurement technique, relative movement of several mm (since the beginning of GPS measurements) would be required for significant results, which can be expected to be reached in about 20 years from now (Brockmann et al., 2005). Continued precise levelling, and possibly also the comparison of INSAR images, may allow delineating active structures more precisely. In addition, a possible approach would be the operation of temporary high-resolution seismometer networks to achieve a more complete earthquake record (including weak events), and a better definition of their hypocentre locations to delineate the location of active structures.

Additional terrace studies in the Low Terrace Gravels across the whole Jura region would complement the results from this study and provide more extended insight into the tectonic activity of the study area. For these investigations, better age constraints on the surfaces that are investigated are critical, which will be difficult to obtain considering the coarse-grained nature of most of the young, well-preserved sediments in this area. While radiocarbon dating on organic material (wood) found in the gravels, as well as Optically Stimulated Luminescence dating on fine-grained sediments that may occur within the terrace deposits, may provide more information about the deposition ages of the terrace material, more detailed knowledge of the erosion history would be equally crucial to allow for the correct correlation of terrace surfaces alongstream as well as on both sides of the river. Exposure dating of the terrace surfaces (e.g., using cosmogenic isotopes) is, however, difficult on the coarse fluvial sediments covered by soil and vegetation that prevail in the study area.

The digital elevation models used in this thesis have been demonstrated to be a valuable data source for systematic analyses of river gradients and terrace morphology at a very detailed level. This type of data, combined with appropriate software and geological methods, opens a promising avenue for the study of tectonic activity in areas of low deformation rates. Without doubt, in these settings the combination of different methods constitutes a prerequisite to gain further insight into the tectonic activity in the recent past, which is fundamental for the understanding of the present-day tectonic activity and its consequences for society.

References

Bartz, J., 1974. Die Mächtigkeit des Quartärs im Oberrheingraben. Approaches to Taphrogenesis; The Rhinegraben; geologic history and neotectonic activity: 78-87.

Brockmann, E., Ineichen, D., Marti, U. and Schlatter, H., 2005. Results of the 3rd observation of the Swiss GPS Reference Network LV95 and status of the Swiss Combined Geodetic Network CH-CGN. In: J.A. Torres and H. Hornik (Editors), Subcommission of the European Reference Frame (EUREF), Vienna 2005. EUREF Publ. 15 (in prep.).

Cederbom, C.E., Sinclair, H.D., Schlunegger, F. and Rahn, M.K., 2004. Climate-induced rebound and exhumation of the European Alps. Geology, 32(8): 709-712.

Kastrup, U., Zoback, M.L., Deichmann, N., Evans, K.F., Giardini, D. and Michael, A.J., 2004. Stress field variations in the Swiss Alps and the northern Alpine foreland derived from inversion of fault plane solutions. Journal of Geophysical Research-Solid Earth, 109(B1).

Kock, S., Schmid, S.M., Fraefel, M. and Wetzel, A., in prep. Neotectonic activity in the area of Basel inferred from morphological analysis of fluvial terraces of the Rhine River.

Madritsch, H., Schmid, S.M. and Fabbri, O., 2008. Interactions of thin- and thick-skinned tectonics along the northwestern front of the Jura fold-and-thrust-belt (Eastern France). Tectonics, 27.

Plenefisch, T. and Bonjer, K.P., 1997. The stress field in the Rhine Graben area inferred from earthquake focal mechanisms and estimation of frictional parameters. Tectonophysics, 275(1-3): 71-97.

Schlatter, A., 2007. Neotektonische Untersuchungen in der Nordschweiz und Süddeutschland: Kinematische Ausgleichung der Landesnivellementlinien CH/D. Nagra Arbeitsbericht NAB 07-12.

Zippelt, K. and Dierks, O., 2007. Auswertung von wiederholten Präzisionsnivellements im südlichen Schwarzwald, Bodenseeraum sowie in angrenzenden schweizerischen Landesteilen. Nagra Arbeitsbericht NAB 07-27.

Reference list

Ackermann, F., 1999. Airborne laser scanning – present status and future expectations. ISPRS Journal of Photogrammetry & Remote Sensing 54: 64-67.

Adams, K.D., Wesnousky, S.G. and Bills, B.G., 1999. Isostatic rebound, active faulting, and potential geomorphic effects in the Lake Lahontan basin, Nevada and California. Geological Society of America Bulletin, 111(12): 1739-1756.

Affolter, T. and Gratier, J.P., 2004. Map view retrodeformation of an arcuate fold-and-thrust belt: The Jura case. Journal of Geophysical Research-Solid Earth, 109(B3).

Angelier, J., 1984. Tectonic analysis of fault slip data sets. Journal of Geophysical Research 89(B7): 5835–5848

Angelier, J. and Mechler, P., 1977. Sur une méthode graphique de recherche des contraintes principales également utilisable en tectonique et en séismologie: la méthode des dièdres droits. Bulletin de la Société Géologique de France, 7(6): 1309-1318.

Baer, M. et al., 2003. Earthquakes in Switzerland and surrounding regions during 2002. Eclogae Geologicae Helvetiae, 96(2): 313-324.

Baer, M. et al., 2007. Earthquakes in Switzerland and surrounding regions during 2006. Swiss Journal of Geosciences, 100(3): 517-528.

Baer, M. et al., 2001. Earthquakes in Switzerland and surrounding regions during 2000. Eclogae Geologicae Helvetiae, 94(2): 253-264.

Baer, M. et al., 2005. Earthquakes in Switzerland and surrounding regions during 2004. Eclogae Geologicae Helvetiae, 98(3): 407-418.

Baltsavias, E.P., 1999. A comparison between photogrammetry and laser scanning. ISPRS Journal of Photogrammetry & Remote Sensing, 54: 83-94.

Baroux, E., Bethoux, N. and Bellier, O., 2001. Analyses of the stress field in southeastern France from earthquake focal mechanisms. Geophysical Journal International, 145(2): 336-348.

Bartz, J., 1974. Die Mächtigkeit des Quartärs im Oberrheingraben. Approaches to Taphrogenesis; The Rhinegraben; geologic history and neotectonic activity: 78-87.

Becker, A., 2000. The Jura Mountains - An active foreland fold-and-thrust belt? Tectonophysics, 321(4): 381-406.

Becker, A., Davenport, C.A. and Giardini, D., 2002. Palaeoseismicity studies on end-Pleistocene and Holocene lake deposits around Basle, Switzerland. Geophysical Journal International, 149(3): 659-678.

Behrmann, J.H., Hermann, O., Horstmann, M., Tanner, D.C. and Bertrand, G., 2003. Anatomy and kinematics of oblique continental rifting revealed: A three-dimensional case study of the southeast Upper Rhine graben (Germany). AAPG Bulletin, 87(7): 1105-1121.

Berger, J.-P. et al., 2005a. Paleogeography of the Upper Rhine Graben (URG) and the Swiss Molasse Basin (SMB) from Eocene to Pliocene. International Journal of Earth Sciences, 94(4): 697-710.

Berger, J.-P. et al., 2005b. Eocene-Pliocene time scale and stratigraphy of the Upper Rhine Graben (URG) and the Swiss Molasse Basin (SMB). International Journal of Earth Sciences, 94(4): 771-731.

Bieg, U., 2005. Palaeooceanographic modelling in global and regional scale: An example from the Burdigalian Seaway Upper Marine Molasse (Early Miocene). PhD Thesis, University of Tübingen.

Bitterli-Brunner, P., Fischer, H. and Herzog, P., 1984. Arlesheim (Blatt 1067), Geologischer Atlas der Schweiz, 1:25 000. Schweizerische Geologische Kommission, Switzerland.

Bitterli-Dreher, P. et al., 2007. Geologischer Atlas der Schweiz: Baden (Blatt 1070), Erläuterungen. Bundesamt f. Wasser u. Geologie. Bern, Switzerland.

Bitterli, T., Graf, H.R., Matousek, F. and Wanner, M., 2000. Geologischer Atlas der Schweiz: Zurzach (Blatt 1050), Erläuterungen. Bundesamt f. Wasser u. Geologie. Bern, Switzerland.

Bitterli, T. and Matousek, F., 1991. Die Tektonik des östlichen Aargauer Tafeljuras. Mitteilungen der Aargauischen Naturforschenden Gesellschaft, 33: 5-30.

Bolliger, T., 1998. Age and geographic distribution of the youngest Upper Freshwater Molasse (OSM) of eastern Switzerland. Eclogae Geologicae Helvetiae, 91: 321-332.

Bolliger, T., Engesser, B. and Weidmann, M., 1993. Première découverte de mammifères pliocènes dans le Jura neuchâtelois. Eclogae geologicae Helvetiae, 86(3): 1031-1068.

Bolliger, T., Fejfar, O., Graf, H.R. and Kälin, D., 1996. Vorläufige Mitteilung über Funde von pliozänen Kleinsäugern aus den höheren Deckenschottern. Eclogae Geologicae Helvetiae, 89(3): 1043-1048.

Bonjer, K.P., 1997. Seismicity pattern and style of seismic faulting at the eastern borderfault of the southern Rhine Graben. Tectonophysics, 275(1-3): 41-69.

Bossart, P. and Wermeille, S., 2003. The stress field in the Mont Terri Region - Data Compilation. In: P. Heitzmann and J.-P. Tripet (Editors), Mont Terri Project - Geology, Paleohydrology and Stress Field of the Mont Terri Region. Reports of the Federal Office for Water and Geology, Geology Series 4.

Bott, M.H.P., 1959. The mechanics of oblique slip faulting. Geological Magazine, 96(2): 109-117.

Braillard, L., 2006. Morphogenèse des vallées sèches du Jura tabulaire d'Ajoie (Suisse): rôle de la fracturation et étude des remplissages quaternaires. PhD Thesis, University of Fribourg (GeoFocus 14).

Brockmann, E., Ineichen, D., Marti, U. and Schlatter, H., 2005. Results of the 3rd observation of the Swiss GPS Reference Network LV95 and status of the Swiss Combined Geodetic Network CH-CGN. In: J.A. Torres and H. Hornik (Editors), Subcommission of the European Reference Frame (EUREF), Vienna 2005. EUREF Publ. 15 (in prep.).

Burbank, D.W. and Anderson, R.S., 2001. Tectonic Geomorphology. Blackwell Science.

Burkhard, M., 1990. Aspects of the large-scale Miocene deformation in the most external part of the Swiss Alps (Subalpine Molasse to Jura fold belt). Eclogae Geologicae Helvetiae, 83(3): 559-583.

Burkhard, M. and Sommaruga, A., 1998. Evolution of the western Swiss Molasse Basin; structural relations with the Alps and the Jura Belt. In: A. Mascle, C. Puigdefàbregas, H.P. Luterbacher and M. Fernàndez (Editors), Cenozoic foreland basins of Western Europe. Geological Society Special Publications.

Carey-Gailhardis, E. and Mercier, J.L., 1987. A numerical method for determining the state of stress using focal mechanisms of earthquake populations: application to Tibetan teleseisms and microseismicity of Southern Peru. Earth and Planetary Science Letters, 82(1-2): 165-179.

Carey-Gailhardis, E. and Mercier, J.L., 1992. Regional state of stress, fault kinematics and adjustments of blocks in a fractured body of rock: application to the microseismicity of the Rhine graben. Journal of Structural Geology, 14(8/9): 1007-1017.

Carey-Gailhardis, E. and Vergely, P., 1992. Graphical analysis of fault kinematics and focal mechanisms of earthquakes in terms of stress; the right dihedra method, use and pitfalls. Annales Tectonicae, 6(1): 3-9.

Carretier, S., Nivière, B., Giamboni, M. and Winter, T., 2006a. Do river profiles record along-stream variations of low uplift rate? Journal of Geophysical Research-Earth Surface, 111(F2).

Cederbom, C.E., Sinclair, H.D., Schlunegger, F. and Rahn, M.K., 2004. Climate-induced rebound and exhumation of the European Alps. Geology, 32(8): 709-712.

Chauve, P., Enay, R., Fluck, P. and Sittler, C., 1980. L'Est de la France (Vosges, Fossé Rhénan, Bresse, Jura). Annales scientifiques de l'Université de Besançon, Géologie, 4(1): 3-80.

Chauve, P., Martin, J., Petitjean, E. and Sequeiros, F., 1988. Le chevauchement du Jura sur la Bresse. Données nouvelles et réinterpretation des sondages. Bull. Soc. géol. France, 8(4): 861-870.

Clark, D. and Leonard, M., 2003. Principal stress orientations from multiple focal-plane solutions: new insight into the Australian intraplate stress field. Geological Society of America (GSA) Bulletin Special Paper, 372: 91-105.

Croisé, J. et al., 2004. Hydrogeological investigations in a low permeability claystone formation: the Mont Terri Rock Laboratory. Physics and Chemistry of the Earth, Parts A/B/C, 29(1): 3-15.

Deichmann, N. et al., 2004. Earthquakes in Switzerland and surrounding regions during 2003. Eclogae Geologicae Helvetiae, 97(3): 447-458.

Deichmann, N. et al., 2002. Earthquakes in Switzerland and surrounding regions during 2001. Eclogae Geologicae Helvetiae, 95(2): 249-262.

Deichmann, N. et al., 2006. Earthquakes in Switzerland and surrounding regions during 2005. Eclogae Geologicae Helvetiae, 99(3): 443-452.

Deichmann, N., Dolfin, D.B. and Kastrup, U., 2000. Seismizität der Nord- und Zentralschweiz. Nagra Technischer Bericht, 00-05.

Deichmann, N., Ernst, J. and Wöhlbier, S., 2007. Data Analysis. In: Evaluation of the induced seismicity in Basel 2006/2007: locations, magnitudes, focal mechanisms, statistical forecasts and earthquake scenarios, Report of the Swiss Seismological Service to Geopower Basel AG, Basel, Switzerland, 152 pp.

Densmore, A.L., Gupta, S., Allen, P.A. and Dawers, N.H., 2007. Transient landscapes at fault tips. Journal of Geophysical Research, 112.

Deville, E. et al., 1994. Thrust propagation and syntectonic sedimentation in the Savoy Tertiary Molasse Basin (Alpine Foreland). In: A. Mascle (Editor), Hydrocarbon and Petroleum Geology of France. European Association of Petroleum Geoscientists Special Publication 4, pp. 269-280.

Dèzes, P., Schmid, S.M. and Ziegler, P.A., 2004. Evolution of the European Cenozoic rift system; interaction of the Alpine and Pyrenean orogens with their foreland lithosphere. Tectonophysics, 389(1-2): 1-33.

Diebold, P., Bitterli-Brunner, P. and Naef, H., 2006. Frick: Geologischer Atlas der Schweiz. Erläuterungen.

Diebold, P. and Noack, T., 1996. Late Palaeozoic troughs and Tertiary structures in the eastern Folded Jura. In: O.A. Pfiffner, P. Lehner, P. Heitzmann, S. Mueller and A. Steck (Editors), Deep structure of the Swiss Alps; results of NRP 20. Birkhäuser, Basel, Switzerland, pp. 59-63.

Dietrich, W.E., Wilson, C.J., Montgomery, D.R. and McKean, J., 1993. Analysis of erosion thresholds, channel networks, and landscape morphology using a digital terrain model. Journal of Geology, 101(2): 259-278.

Duvall, A., Kirby, E. and Burbank, D.W., 2004. Tectonic and lithologic controls on bedrock channel profiles and processes in coastal California. Journal of Geophysical Research, 109(3).

Edel, J.-B., Whitechurch, H. and Diraison, M., 2006. Seismicity wedge beneath the Upper Rhine Graben due to backwards Alpine push? Tectonophysics, 428(1-4): 49-64.

Etchecopar, A., Vasseur, G. and Daignieres, M., 1981. An inverse problem in microtectonics for the determination of stress tensors from fault striation analysis. Journal of Structural Geology, 3(1): 51-65.

Fäh, D. et al., 2003. Earthquake Catalogue Of Switzerland (ECOS) and the related macroseismic database. Eclogae Geologicae Helvetiae, 96(2): 219-236.

Fejfar, O., Heinrich, W.-D. and Lindsay, E.H., 1998. Updating the Neogene rodent biochronology in Europe. Mededelingen Nederlands Instituut voor Toegepaste Geowetenschappen TNO, 60: 533-553.

Ferry, M., Meghraoui, M., Delouis, B. and Giardini, D., 2005. Evidence for Holocene palaeoseismicity along the Basel-Reinach active normal fault (Switzerland); a seismic source for the 1356 earthquake in the Upper Rhine Graben. Geophysical Journal International, 160(2): 554-572.

Flint, J.J., 1974. Stream gradient as a function of order, magnitude, and discharge. Water Resources Research, 10(5): 969-973.

Fromm, K., 1989. Paläomagnetische Untersuchungen zur Quartärstratigraphie im Südschwarzwald bei Schadenbirndorf. Geowissenschaftliche Gemeinschaftsaufgaben, Niedersächsisches Landesamt für Bodenforschung, Hannover: 16 p.

Fügenschuh, B. and Schmid, S.M., 2003. Late stages of deformation and exhumation of an orogen constrained by fission-track data; a case study in the Western Alps. Geological Society of America Bulletin, 115(11): 1425-1440.

Galindo-Zaldivar, J., González-Lodeiro, F. and Jabaloy, A., 1993. Stress and Paleostress in the Betic-Rif Cordilleras (Miocene to the Present). Tectonophysics, 227(1-4): 105-126.

Gephart, J.W. and Forsyth, D.W., 1984. An improved method for determining the regional stress tensor using earthquake focal mechanism data - application to the San-Fernando earthquake sequence. Journal of Geophysical Research, 89(NB11): 9305-9320.

Giamboni, M., Ustaszewski, K., Schmid, S.M., Schumacher, M.E. and Wetzel, A., 2004a. Plio-Pleistocene transpressional reactivation of Paleozoic and Paleogene structures in the Rhine-Bresse transform zone (northern Switzerland and eastern France). International Journal of Earth Sciences, 93(2): 207-223.

Giamboni, M., Wetzel, A., Niviere, B. and Schumacher, M., 2004b. Plio-Pleistocene folding in the southern Rhinegraben recorded by the evolution of the drainage network (Sundgau area; northwestern Switzerland and France). Eclogae Geologicae Helvetiae, 97(1): 17-31.

González-Casado, J.M., Giner-Robles, J.L. and López-Martínez, J., 2000. Bransfield Basin, Antarctic Peninsula: Not a normal backarc basin. Geology, 28(11): 1043-1046.

Graf, H.R., 1993. Die Deckenschotter der zentralen Nordschweiz. PhD Thesis, ETH Zürich, Zürich.

Graf, H.R., 2006. Baden (Blatt 1070), Geologischer Atlas der Schweiz 1:25000. Bundesamt f. Wasser u. Geologie. Bern, Switzerland.

Graul, H., 1962. Geomorphologische Studien zum Jungquartär des nördlichen Alpenvorlandes. Teil 1: Das Schweizer Mittelland. Heidelberger Geographische Arbeiten, Heft 9.

Guellec, S., Mugnier, J.-L., Tardy, M. and Roure, F., 1990. Neogene evolution of the western Alpine Foreland in the light of ECORS data and balanced cross-section. Mémoires de la Société Géologique de France, Nouvelle Serie, 156: 165-184.

Gupta, H.K. et al., 2001. Bhuj earthquake of 26 January, 2001. Journal of the Geological Society of India, 57(3): 275-278.

Hack, J.T., 1957. Studies of Longitudinal Stream Profiles in Virginia and Maryland. U.S. Geological Survey Professional Paper, 294-B: 45-97.

Hack, J.T., 1973. Stream-profile analysis and stream-gradient indices. United States Geological Survey Journal of Research, 1: 421-429.

Haering, M.O., Schanz, U., Ladner, F. and Dyer, B., submitted. Characterisation of the Basel 1 Enhanced Geothermal System. Geothermics.

Hagedorn, E.-M., 2004. Sedimentpetrographie und Lithofazies der jungtertiären und quartären Sedimente im Oberrheingebiet. PhD Thesis, University of Cologne.

Hagedorn, E.-M. and Boenigk, W., 2008. The Pliocene and Quaternary sedimentary and fluvial history in the Upper Rhine Graben based on heavy mineral analyses. Netherlands Journal of Geosciences (Geologie en Mijnbouw), 87(1).

Haimberger, R., Hoppe, A. and Schäfer, A., 2005. High-resolution seismic survey on the Rhine River in the northern Upper Rhine Graben. International Journal of Earth Sciences, 94(4): 657-668.

Haldimann, P., Naef, H. and Schmassmann, H., 1984. Fluviatile Erosions- und Akkumulationsformen als Indizien jungpleistozäner und holozäner Bewegungen in der Nordschweiz und angrenzenden Gebieten. Nagra Technischer Bericht, 84-16.

Hancock, G.R., 2005. The use of digital elevation models in the identification and characterization of catchments over different grid scales. Hydrological Processes, 19(9): 1727-1749.

Harmsen, S.C., 1994. The Little-Skull-Mountain, Nevada, Earthquake of 29-June-1992 - Aftershock Focal Mechanisms and Tectonic Stress-Field Implications. Bulletin of the Seismological Society of America, 84(5): 1484-1505.

Häuselmann, P., Fiebig, M., Kubik, P.W. and Adrian, H., 2007. A first attempt to date the original "Deckenschotter" of Penck and Brückner with cosmogenic nuclides. Quaternary International, 164-165: 33-42.

Heim, A., 1919. Geologie der Schweiz. Band 1, Molasseland und Juragebirge. C.H. Tauchnitz, Leipzig, 704 pp.

Hinsken, S., Ustaszewski, K. and Wetzel, A., 2007. Graben width controlling syn-rift sedimentation: the Palaeogene southern Upper Rhine Graben as an example. International Journal of Earth Sciences, 96(6): 979-1002.

Hodges, K.V., Wobus, C., Ruhl, K., Schildgen, T. and Whipple, K., 2004. Quaternary deformation, river steepening, and heavy precipitation at the front of the Higher Himalayan ranges. Earth and Planetary Science Letters, 220(3-4): 379-389.

Hofmann, F., 1960. Beitrag zur Kenntnis der Glimmersandsedimentation in der oberen Süsswassermolasse der Nord- und Nordostschweiz. Eclogae Geologicae Helvetiae, 53(1): 1-25.

Hofmann, F., 1969. Neue Befunde über die westliche Fortsetzung des beckenaxialen Glimmersand-Stromsystems in der oberen Süsswassermolasse des schweizerischen Alpenvorlandes. Eclogae Geologicae Helvetiae, 62(1): 279-284.

Hofmann, F., 1996. Zur plio-pleistozänen Landschaftsgeschichte im Gebiet Hochrhein-Wutach-Randen-Donau: Geomorphologische Überlegungen und sedimentpetrographische Befunde. Eclogae geologicae Helvetiae, 89(3): 1023-1041.

Holbrook, J. and Schumm, S.A., 1999. Geomorphic and sedimentary response of rivers to tectonic deformation: a brief review and critique of a tool for recognizing subtle epeirogenic deformation in modern and ancient settings. Tectonophysics, 305: 287-306.

Howard, A.D. and Kerby, G., 1983. Channel changes in badlands. Geological Society of America Bulletin, 94(6).

Huang, X.J. and Niemann, J.D., 2006. An evaluation of the geomorphically effective event for fluvial processes over long periods. Journal of Geophysical Research-Earth Surface, 111(F3).

Isler, A., Pasquier, F. and Huber, M., 1984. Geologische Karte der zentralen Nordschweiz 1:100 000, mit angrenzenden Gebieten von Baden-Württemberg. Nagra und Schweiz Geol Kommission, Spezialkarte Nr. 131.

Ivy-Ochs, S. et al., 2006. The timing of glacier advances in the northern European Alps based on surface exposure dating with cosmogenic 10Be, 26Al, 36Cl, and 21Ne. Geological Society of America (GSA) Bulletin Special Paper, 415: 43-60.

Johnston, A.C. and Schweig, E.S., 1996. The enigma of the New Madrid earthquakes of 1811-1812. Annual Review of Earth and Planetary Sciences, 24: 339-384.

Jordan, P., 1992. Evidence for large-scale decoupling in the Triassic evaporites of northern Switzerland; an overview. Eclogae Geologicae Helvetiae, 85(3).

Jordan, P., 2007. Digitales Höhenmodell Basis Quartär (DHM B_QU, "Felsmodell") - Grundlagen, Erarbeitung, Ergebnisse, Stand Juni 2007. Nagra Arbeitsbericht NAB 07-12.

Kälin, D., 1997. Litho- und Biostratigraphie der mittel- bis obermiozänen Bois de Raube-Formation (Nordwestschweiz). Eclogae Geologicae Helvetiae, 90(1): 97-114.

Kastrup, U. et al., 2004. Stress field variations in the Swiss Alps and the northern Alpine foreland derived from inversion of fault plane solutions. Journal of Geophysical Research-Solid Earth, 109(B1).

Keller, E.A. and Pinter, N., 2002. Active Tectonics: Earthquakes, Uplift, and Landscape. Prentice Hall.

Kemna, H.A., 2008. A Revised Stratigraphy for the Pliocene and Lower Pleistocene Deposits of the Lower Rhine Embayment. Netherlands Journal of Geosciences (Geologie en Mijnbouw), 87(1): 91-105.

Kemna, H.A. and Becker-Haumann, R., 2003. Die Wanderblock-Bildungen im Schweizer Juragebirge südlich von Basel: Neue Daten zu einem alten Problem. Eclogae geologicae Helvetiae, 96(1): 71-83.

Kempf, O., Matter, A., Burbank, D.W. and Mange, M., 1999. Depositional and structural evolution of a foreland basin margin in a magnetostratigraphic framework: the eastern Swiss Molasse Basin. International Journal of Earth Sciences, 88(2): 253–275.

Kirby, E., Johnson, C., Furlong, K. and Heimsath, A., 2007. Transient channel incision along Bolinas Ridge, California: Evidence for differential rock uplift adjacent to the San Andreas fault. Journal of Geophysical Research-Earth Surface, 112(F3).

Kirby, E. and Whipple, K., 2001. Quantifying differential rock-uplift rates via stream profile analysis. Geology, 29(5): 415-418.

Kirby, E., Whipple, K.X., Tang, W.Q. and Chen, Z.L., 2003. Distribution of active rock uplift along the eastern margin of the Tibetan Plateau: Inferences from bedrock channel longitudinal profiles. Journal of Geophysical Research-Solid Earth, 108(B4).

Kock, S., Kramers, J.D., Preusser, F. and Wetzel, A., submitted. Dating of Late Pleistocene terrace deposits of the River Rhine using uranium series and luminescence methods: potential and limitations. Quaternary Geochronology.

Kock, S., Schmid, S.M., Fraefel, M. and Wetzel, A., in prep. Neotectonic activity in the area of Basel inferred from morphological analysis of fluvial terraces of the Rhine River.

Kuhlemann, J. and Kempf, O., 2002. Post-Eocene evolution of the North Alpine foreland basin and its response to Alpine tectonics. Sedimentary Geology, 152(1-2): 45-78.

Lacombe, O., Angelier, J., Byrne, D. and Dupin, J.M., 1993. Eocene-Oligocene Tectonics and Kinematics of the Rhine-Saone Continental Transform Zone (Eastern France). Tectonics, 12(4): 874-888.

Lacombe, O. and Mouthereau, F., 2002. Basement-involved shortening and deep detachment tectonics in forelands of orogens: Insights from recent collision belts (Taiwan, Western Alps, Pyrenees). Tectonics, 21(4).

Lague, D., Davy, P. and Crave, A., 2000. Estimating uplift rate and erodibility from the area-slope relationship; examples from Brittany (France) and numerical modelling. Physics and Chemistry of the Earth (A), 25(6-7): 543-548.

Lambert, J., Winter, T., Deweza, T.J.B. and Sabouraulta, P., 2004. New hypotheses on the maximum damage area of the 1356 Basel earthquake (Switzerland). Quaternary Science Reviews.

Lang, U., Gudera, T., Elsass, P. and Wirsing, G., 2005. Numerical modelling of chloride propagation in the quaternary aquifer of the southern Upper Rhine Graben. International Journal of Earth Sciences, 94(4): 550-564.

Laubscher, H., 1961. Die Fernschubhypothese der Jurafaltung. Eclogae geologicae Helvetiae, 54: 221-282.

Laubscher, H., 1967. Exkursion Nr. 14, Basel-Delémont-Biel. Geologischer Führer der Schweiz.

Laubscher, H., 1981. The 3D propagation of decollement in the Jura. In: K.R. McClay and N.J. Price (Editors), Thrust and nappe tectonics; International conference. Special Publication - Geological Society of London, pp. 311-318.

Laubscher, H., 1986. The eastern Jura: relations between thin-skinned and basement tectonics, local and regional. Geologische Rundschau, 75: 535-553.

Laubscher, H., 1992. Jura kinematics and the Molasse Basin. Eclogae geologicae Helvetiae, 85(3): 653-675.

Laubscher, H., 1998. Der Ostrand des Laufenbeckens und der Knoten von Grellingen; die verwickelte Begegnung von Rheingraben und Jura. Eclogae Geologicae Helvetiae, 91(2): 275-291.

Laubscher, H., 2001. Plate interactions at the southern end of the Rhine graben. Tectonophysics, 343(1-2): 1-19.

Laubscher, H., 2003. The Miocene dislocations in the northern foreland of the Alps: Oblique subduction and its consequences (Basel area, Switzerland-Germany). Jahresberichte und Mitteilungen des Oberrheinischen Geologischen Vereins, Neue Folge, 85: 423-439.

Lay, T. and Wallace, T.C., 1995. Modern Global Seismology. Academic Press, 521 pp.

Le Carlier de Veslud, C., Bourgeois, O., Diraison, M. and Ford, M., 2005. 3D stratigraphic and structural synthesis of the Dannemarie basin (Upper Rhine Graben). Bulletin de la Société Géologique de France, 176: 433-442.

Leopold, L.B., Wolman, M.G. and Miller, J.P., 1964. Fluvial Processes in Geomorphology. Freeman, San Francisco.

LGRB, 2008. http://www.lgrb.uni-freiburg.de/lgrb/Fachbereiche/erdbebendienst/jahresbulletins. Accessed on 23.05.2008.

Liniger, H., 1953. Zur Geschichte und Geomorphologie des nordschweizerischen Juragebirges. Geographica Helvetica, 8(4): 289-303.

Liniger, H., 1966. Das Plio-Altpleistozäne Flussnetz der Nordschweiz. Regio Basiliensis, 7(2).

Liniger, H., 1967. Pliozän und Tektonik des Juragebirges. Eclogae geologicae Helvetiae, 60(2): 407-490.

Lopes Cardozo, G.G.O. and Behrmann, J.H., 2006. Kinematic analysis of the Upper Rhine Graben boundary fault system. Journal of Structural Geology, 28(6): 1028-1039.

Lopes Cardozo, G.G.O. and Granet, M., 2003. New insight in the tectonics of the southern Rhine Graben-Jura region using local earthquake seismology. Tectonics, 22(6).

Mackin, J.H., 1948. Concept of the Graded River. Geological Society of America Bulletin, 59(5): 463-511.

Madritsch, H., Schmid, S.M. and Fabbri, O., 2008. Interactions of thin- and thick-skinned tectonics along the northwestern front of the Jura fold-and-thrust-belt (Eastern France). Tectonics, 27.

Majer, E.L. et al., 2007. Induced seismicity associated with Enhanced Geothermal Systems. Geothermics 36: 185-222.

Marple, R.T. and Talwani, P., 2000. Evidence for a buried fault system in the Coastal Plain of the Carolinas and Virginia - Implications for neotectonics in the southeastern United States. Geological Society of America Bulletin, 112(2): 200-220.

Mayer-Rosa, D. and Cadiot, B., 1979. A review of the 1356 Basel earthquake: basic data. Tectonophysics, 53: 325-333.

MBN-AG, 1998. Zur Stratigraphie des jüngeren Pleistozäns im Gebiet des Zusammenflusses von Aare, Surb, Rhein und Wutach. Ber. z. Hd. Landeshydrologie und -geologie, Bern.

McKenzie, D.P., 1969. Relation between fault plane solutions for earthquakes and directions of principal stresses. Bulletin of the Seismological Society of America, 59(2): 591-601.

Merritts, D. and Vincent, K.R., 1989. Geomorphic response of coastal streams to low, intermediate, and high rates of uplift, Mendocino triple junction region, Northern California. Geological Society of America Bulletin, 101(11): 1373-1388.

Merritts, D.J., Vincent, K.R. and Wohl, E.E., 1994. Long river profiles, tectonicsm, and eustasy: a guide to interpreting fluvial terraces. Journal of Geophysical Research, 99(B7): 14031-14050.

Meyer, B., Lacassin, R., Brulhet, J. and Mouroux, B., 1994. The Basel 1356 earthquake: which fault produced it? Terra Nova, 6: 54-63.

Meyer, M., 2001. Die Geologie des Adlertunnels. Bulletin für angewandte Geologie, 6(2): 199-208.

Meyer, W., 2006. Da verfiele Basel überall. Schwabe, Basel.

Michael, A.J., 1987. Use of Focal Mechanisms to Determine Stress - a Control Study. Journal of Geophysical Research-Solid Earth and Planets, 92(B1): 357-368.

Montgomery, D.R., 1994. Valley incision and the uplift of mountain peaks. Journal of Geophysical Research, B, Solid Earth and Planets, 99(7): 13913-13921.

Montgomery, D.R. and Brandon, M.T., 2002. Topographic controls on erosion rates in tectonically active mountain ranges. Earth and Planetary Science Letters, 201: 481-489.

Mosar, J., 1999. Present-day and future tectonic underplating in the western Swiss Alps: reconciliation of basement/wrench-faulting and decollement folding of the Jura and Molasse basin in the Alpine foreland. Earth and Planetary Science Letters, 173(3): 143-155.

Mühlberg, F., 1908. Geologische Karte der Umgebung von Aarau / Spezialkarte No 45, Geologische Karte der Schweiz.

Müller, W.H., Blümling, P., Becker, A. and Clauss, B., 1987. Die Entkopplung des tektonischen Spannungsfeldes an der Jura-Ueberschiebung. Eclogae Geologicae Helvetiae, 80(2).

Müller, W.H., Naef, H. and Graf, H.R., 2002. Geologische Entwicklung der Nordschweiz, Neotektonik und Langzeitszenarien Zürcher Weinland. Nagra Technischer Bericht, 99-08.

Mussett, A. and Khan, M., 2000. Looking into the Earth - An Introduction to Geological Geophysics. Cambridge University Press, 470 pp.

Nivière, B. et al., 2008. Active tectonics of the southeastern Upper Rhine graben, Freiburg area (Germany). Quaternary Science Reviews, 27(5-6): 541-555.

Nivière, B. and Winter, T., 2000. Pleistocene northwards fold propagation of the Jura within the southern Upper Rhine Graben: seismotectonic implications. Global and Planetary Change, 27(1-4): 263-288.

Noack, T., 1995. Thrust development in the eastern Jura Mountains related to pre-existing extensional structures. Tectonophysics, 252(1-4): 419-431.

Oskin, M.E. and Burbank, D., 2007. Transient landscape evolution of basement-cored uplifts: Example of the Kyrgyz range, Tian shan. Journal of Geophysical Research-Earth Surface, 112(F3).

Ouchi, S., 1985. Response of alluvial rivers to slow active tectonic movement. Geol. Soc. of America Bull., 96(4).

Penck, A. and Brückner, E., 1909. Die Alpen im Eiszeitalter. Band 2: Die Eiszeiten in den nördlichen Westalpen.

Petit, C., Campy, M., Chaline, J. and Bonvalot, J., 1996. Major palaeohydrographic changes in Alpine foreland during the Pliocene - Pleistocene, pp. 131-143.

Pfeifer, N., 2003. Oberflächenmodelle aus Laserdaten. Österreichische Zeitschrift für Vermessung und Geoinformation, 4.

Pfiffner, O.A., 2006. Thick-skinned and thin-skinned styles of continental contraction. Special Paper - Geological Society of America, 414: 153-177.

Pfiffner, O.A. and Burkhard, M., 1987. Determination of paleo-stress axes orientations from fault, twin and earthquake data. Annales Tectonicae, 1(1): 48-57.

Philippe, Y., Colletta, B., Deville, E. and Mascle, A., 1996. The Jura fold-and-thrust belt: a kinematic model based on map-balancing. In: Peri-Tethys memoir 2; Structure and prospects of Alpine basins and forelands, Eds: Ziegler, Horvath / Memoires du Museum National d'Histoire Naturelle, 170: 235-261.

Plenefisch, T. and Bonjer, K.P., 1997. The stress field in the Rhine Graben area inferred from earthquake focal mechanisms and estimation of frictional parameters. Tectonophysics, 275(1-3): 71-97.

Rahn, M.K. and Selbekk, R., 2007. Absolute dating of the youngest sediments of the Swiss Molasse basin by apatite fission track analysis. Swiss Journal of Geosciences, 100(3): 371-381.

Reinecker, J., Heidbach, O., Tingay, M., Sperner, B. and Mueller, B., 2005. The 2005 release of the World Stress Map (available online at www.world-stress-map.org).

Reiter, F. and Acs, P., 1996-2003. TectonicsFP. Software for structural geology. Innsbruck University, Austria. http://go.to/TectonicsFP.

Rolf, C., Hambach, U. and Weidenfeller, M., 2008. Rock and palaeomagnetic evidence for the Plio-Pleistocene palaeoclimatic change recorded in Upper Rhine Graben sediments (Core Ludwigshafen-Parkinsel) Netherlands Journal of Geosciences (Geologie en Mijnbouw), 87(1): 41-50.

Rotstein, Y., Behrmann, J.H., Lutz, M., Wirsing, G. and Luz, A., 2005a. Tectonic implications of transpression and transtension: Upper Rhine Graben. Tectonics, 24(6).

Rotstein, Y., Schaming, M. and Rousse, S., 2005b. Structure and Tertiary tectonic history of the Mulhouse High, Upper Rhine Graben: Block faulting modified by changes in the Alpine stress regime. Tectonics, 24(1).

Roure, F., Brun, J.-P., Colletta, B. and Vially, R., 1994. Multiphase extensional structures, fault reactivation, and petroleum plays in the Alpine foreland Basin of southeastern France. In: Mascle, A (Ed.), Hydrocarbon and Petroleum Geology of France, Europ. Assoc. Petrol. Geosci., Spec. Publ., 4: 245-268.

Rózsa, S. et al., 2005. Determination of displacements in the upper Rhine graben Area from GPS and leveling data. International Journal of Earth Sciences, 94(4): 538-549.

Schanz, U., Dyer, B., Ladner, F. and Häring, M.O., 2007. Microseismic aspects of the Basel 1 geothermal reservoir, 5th Swiss Geoscience Meeting, Geneva.

Schlatter, A., 2006. Das neue Landeshöhennetz der Schweiz LHN95. PhD Thesis, Diss Nr. 16840, ETH Zürich, Zürich.

Schlatter, A., 2007. Neotektonische Untersuchungen in der Nordschweiz und Süddeutschland: Kinematische Ausgleichung der Landesnivellementlinien CH/D. Nagra Arbeitsbericht NAB 07-12.

Schlatter, A., Schneider, D., Geiger, A. and Kahle, H.-G., 2005. Recent vertical movements from precise levelling in the vicinity of the city of Basel, Switzerland. Int Journ Earth Sciences, 94(4): 507-514.

Schlüchter, C., 1976. Geologische Untersuchungen im Quartär des Aaretals südlich von Bern. Beiträge zur Geologischen Karte der Schweiz, 148.

Schreiner, A., 1965. Die Juranagelfluh im Hegau. Jahresheft Geologisches Landesamt Baden-Württemberg, 7(303-354).

Simpson, G., 2004a. A dynamic model to investigate coupling between erosion, deposition, and three-dimensional (thin-plate) deformation. Journal of Geophysical Research-Earth Surface, 109(F2).

Simpson, G., 2004b. Role of river incision in enhancing deformation. Geology, 32(4): 341-344.

Sissingh, W., 2006. Syn-kinematic palaeogeographic evolution of the West European Platform: correlation with Alpine plate collision and foreland deformation. Netherlands Journal of Geosciences-Geologie En Mijnbouw, 85(2): 131-180.

Skinner, B.J. and Porter, S.C., 1995. The Dynamic Earth, An Introduction to Physical Geology, New York, 567 pp.

Sklar, L. and Dietrich, W.E., 1998. River Longitudinal Profiles and Bedrock Incision Models: Stream Power and the Influence of Sediment Supply, Rivers over Rock.

Snyder, N.P., Whipple, K.X., Tucker, G.E. and Merritts, D.J., 2000. Landscape response to tectonic forcing: Digital elevation model analysis of stream profiles in the Mendocino triple junction region, northern California. Geol. Soc. of America Bull., 112(8).

Stock, J. and Dietrich, W.E., 2003. Valley incision by debris flows: Evidence of a topographic signature. Water Resources Research, 39(4).

Swiss Seismological Service, 2002. ECOS - Earthquake Catalog of Switzerland, http://histserver.ethz.ch/download/ECOS.pdf (accessed on 05.05.2008).

Swisstopo, 2007. DTM-AV. geodata-news, 14: http://www.swisstopo.admin.ch/internet/swisstopo/de/home/products/height/dom_dtm-av.parsysrelated1.19059.downloadList.63245.DownloadFile.tmp/gn142007defr.pdf (accessed 07 April 2008).

Tesauro, M., Hollenstein, C., Egli, R., Geiger, A. and Kahle, H.G., 2005. Continuous GPS and broad-scale deformation across the Rhine Graben and the Alps. International Journal of Earth Sciences, 94(4): 525-537.

Tucker, G.E. and Slingerland, R., 1996. Predicting sediment flux from fold and thrust belts. Basin Research, 8(3): 329-349.

Twidale, C.R., 2004. River patterns and their meaning. Earth-Science Reviews, 67(3-4): 159-218.

Ustaszewski, K. and Schmid, S.M., 2006. Control of preexisting faults on geometry and kinematics in the northernmost part of the Jura fold-and-thrust belt. Tectonics, 25(5).

Ustaszewski, K. and Schmid, S.M., 2007. Latest Pliocene to recent thick-skinned tectonics at the Upper Rhine Graben - Jura Mountains junction. Swiss Journal of Geosciences, 100(2): 293-312.

Ustaszewski, K., Schumacher, M.E. and Schmid, S.M., 2005a. Simultaneous normal faulting and extensional flexuring during rifting: an example from the southernmost Upper Rhine Graben. International Journal of Earth Sciences, 94(4): 680-696.

Ustaszewski, K., Schumacher, M.E., Schmid, S.M. and Nieuwland, D., 2005b. Fault reactivation in brittle-viscous wrench systems - Dynamically scaled analogue models and application to the Rhine-Bresse transfer zone. Quaternary Science Reviews, 24: 365-382.

Ustaszewski, K.M., 2004. Reactivation of pre-existing crustal discontinuities: the southern Upper Rhine Graben and the northern Jura Mountains: a natural laboratory PhD Thesis, University of Basel.

van Husen, D., 2004. Quaternary glaciations in Austria. In: J. Ehlers and P.L. Gibbard (Editors), Quaternary Glaciations - Extent and Chronology. Elsevier, pp. 1-13.

Verderber, R., 1992. Quartärgeologische Untersuchungen im Hochrheingebiet zwischen Schaffhausen und Basel. PhD Thesis, University of Freiburg i.Br.

Verderber, R., 2003. Quartärgeologie im Hochrheingebiet zwischen Schaffhausen und Basel. Zeitschrift der Deutschen Gesellschaft für Geowissenschaften, 154(2-3): 369-406.

Villinger, E., 1998. Zur Flussgeschichte von Rhein und Donau in Südwestdeutschland. Jahresberichte und Mitteilungen des Oberrheinischen Geologischen Vereins, Neue Folge, 80: 361-398.

Villinger, E., 1999. Freiburg im Breisgau - Geologie und Stadtgeschichte. Informationen LGRB, 12.

Villinger, E., 2003. Zur Paläogeographie von Alpenrhein und oberer Donau. Zeitschrift der Deutschen Gesellschaft für Geowissenschaften, 154(2-3): 193-253.

Westerhoff, W.E., Kemna, H.A. and Boenigk, W., 2008. The confluence area of Rhine, Meuse, and Belgian rivers: Late Pliocene and Early Pleistocene fluvial history of the northern Lower Rhine Embayment Netherlands Journal of Geosciences (Geologie en Mijnbouw), 87(1): 107-125.

Whipple, K.X., 2004. Bedrock rivers and the geomorphology of active orogens. Annual Review of Earth and Planetary Sciences, 32: 151-185.

Whipple, K.X. and Tucker, G.E., 1999. Dynamics of the stream-power incision model: Implications for height limits of mountain ranges, landscape response timescales, and research needs. Journal of Geophysical Research, 104(B8).

Whipple, K.X. and Tucker, G.E., 2002. Implications of sediment-flux-dependent river incision models for landscape evolution. Journal of Geophysical Research-Solid Earth, 107(B2).

Wittmann, O., 1961. Die Niederterrassenfelder im Umkreis von Basel und ihre kartographische Darstellung. Basler Beiträge zur Geographie und Ethnologie, 3.

Wobus, C. et al., 2006a. Tectonics from topography: Procedures, promise, and pitfalls. GSA Special Paper - Tectonics, Climate, and Landscape Evolution. Penrose Conference Series, 398: 55-74.

Wobus, C.W., Whipple, K.X. and Hodges, K.V., 2006b. Neotectonics of the central Nepalese Himalaya: Constraints from geomorphology, detrital 40Ar/39Ar thermochronology, and thermal modeling. Tectonics, 25.

Ziegler, P.A., 1992. European Cenozoic rift system. Tectonophysics, 208(1-3): 91-111.

Ziegler, P.A. and Dèzes, P., 2007. Cenozoic uplift of Variscan Massifs in the Alpine foreland: Timing and controlling mechanisms. Global and Planetary Change, 58: 237-269.

Zippelt, K. and Dierks, O., 2007. Auswertung von wiederholten Präzisionsnivellements im südlichen Schwarzwald, Bodenseeraum sowie in angrenzenden schweizerischen Landesteilen. Nagra Arbeitsbericht NAB 07-27.

_____

Acknowledgements

First of all, I would like to thank Stefan Schmid for giving me the opportunity to do my PhD research in the tectonics group at the University of Basel. He gave me a lot of freedom to focus on the topics and methods that I found most fascinating, and was always willing to discuss any new ideas that came up.

My profound thanks go to Alex Densmore for introducing me to the field of tectonic (and quantitative) geomorphology and for taking the time to help me, in spite of being busy with his new job in England. The discussions with him always made everything look logical and feasible.

I sincerely thank Peter Ziegler for his constant interest and support and for initiating the drainage evolution study. His efforts to keep the Eucor-Urgent project alive are very much appreciated.

Michael Schnellmann, Peter Jordan and Tim Vietor made the study on the Aare terraces possible. Thanks for your ideas, your help and our discussions!
Of course, I also benefited from the discussions on various topics with many other people. Among them, I would like to specifically mention Kamil Ustaszewski, Andreas Wetzel, Nico Deichmann and the "geothermal explorers".

I enjoyed working with a team of PhD students who provided the cheerful atmosphere and the network of support without which creative and efficient work is not possible. In particular, I would like to mention my colleagues Herfried Madritsch and Stéphane Kock, who created a good balance of calmness and excitement at Room 020, and our fellow tectonicians Michael Wiederkehr and Senecio Schefer.

I also thank various members of the Eucor-Urgent network, and in particular the organisers of the yearly workshops, which provided an invaluable opportunity to discuss my work at different stages, in an informal and friendly atmosphere.

The whole administrative and technical team at the institute deserves my gratitude for their support, which makes research possible in the first place. There are many other people who contributed to the completion of this thesis in various ways, at the institute and elsewhere, and I wish to thank all of them.

Finally, I am greatly indebted to my family for their constant support, and to Thomas for his patience and encouragement.

Curriculum Vitae of Marielle Fraefel

Personal Details

Date of birth: 10.09.1976
Citizenship: Swiss

Education

02/2005 to 07/2008:	PhD thesis at the Institute of Geology, University of Basel, Switzerland Thesis topic: *Geomorphologic and seismological evidence of neotectonic activity in the Jura – Upper Rhine Graben area, NW Switzerland.* Supervisors: Prof. Stefan Schmid & Prof. Alexander L. Densmore
10/1997 – 04/2002:	MSc degree in Earth Sciences at ETH Zurich, Switzerland Major: Engineering Geology and Hydrogeology Minors: Seismology / Seismotectonics; Geomorphodynamics; Metamorphic and Magmatic Petrology Thesis topic: *Fracture network analysis and rockfall hazard assessment in a crystalline Alpine region; geological mapping*
08/1991 – 01/1996:	Gymnasium Kantonsschule Sargans; Maturity type B (Latin)

Professional experience

02/2005 – 03/2008:	Lecture assistant of geology and GIS courses at the University of Basel; field assistant on geological excursions
10/2002 – 02/2005:	Research geoscientist at the Swiss Federal Institute for Forest, Snow and Landscape Research WSL, Natural Hazards Department
06/2002 – 08/2002:	Internship at WSL
10/2001 – 02/2002:	Teaching assistant of undergraduate geology lectures at ETH, Zürich
06/2001 – 07/2001:	Internship at the National Geological Institute of Hungary, Budapest

Complementary Education

Short course "Geology and geomorphology of tectonically active regions" at the Geologische Vereinigung International Conference, Potsdam, Germany (2006)

Courses in Academic Writing and Presentations (University of Basel, 2005 – 2007)

Various GIS courses (ArcGIS) at the University of Zurich and ETH
Self-directed learning (2001 – present)

Master courses in Pedagogy and Didactics for high-school level at ETH Zurich (2001 – 2002)

CAE - Certificate in Advanced English (1996)